THE INTERACTION OF ELECTRIC AND MAGNETIC FIELDS WITH BIOLOGICAL MATERIALS

BY

ABDOLHOSSEIN JAFARY-ASL

A THESIS SUBMITTED FOR THE DEGREE OF DOCTOR OF PHILOSOPHY IN THE DEPARTMENT OF ELECTRONIC AND ELECTRICAL ENGINEERING AT THE UNIVERSITY OF SALFORD

OCTOBER 1983

TO MY PARENTS

ACKNOWLEDGEMENTS

The author would like to express his sincere gratitude and appreciation to Dr. C.W. Smith, for his advice and encouragement during the supervision of the work presented in this thesis.

My thanks to Professor G. Carter in whose Department the experiments were conducted.

The continued interest of, and lively discussions with Professor H. Fröhlich F.R.S. throughout the course of these studies are gratefully acknowledged.

Special thanks are also conveyed to Mr. L. Preston, for his friendly discussions.

Thanks also go to Dr. H. Foster for his supervision with biological methods.

Also I would like to thank the workshop staffs and all of the Electrical Engineering Department.

Finally, I would like to thank Mrs. D.M. Scott for devoting much of her spare time to typing this thesis.

ABSTRACT

In the course of the work on the interactions of electric and magnetic fields with biological materials both living and dead, it was noticed that published dielectrophoretic yield curves for biological cells showed unexplained deviations in the region of 2kHz which is the proton magnetic resonance frequency in a typical laboratory ambient magnetic field. The exact value is 2.13 kHz for a field of 50 μT.

The results of preliminary dielectrophoretic and dielectric measurements show features at frequencies which correspond to the NMR condition for that value of steady magnetic field in which the measurements were made. Very sharp dielectric loss peaks were found corresponding to ^{1}H, ^{31}P, ^{23}Na, ^{35}Cl amd ^{39}K resonances. The electron spin resonance also showed up in the dielectric loss.

The onset plus NMR conditions of these resonances commences at the value of the steady magnetic field strength such that one quantum of magnetic flux (2.07×10^{-15} Wb) would link the cross-sectional area of a single biological cell or pair of cells. Approximately 1.0 gauss or 0.5 gauss (100μT or 50μT) respectively in the case of 5μm diameter yeast cell.

Growing cultures of the yeast cells in fields which satisfy the proton NMR conditions as a function of temperature results in a slight reduction in the mean generation time (MGT). Comparison of this with the dielectric constant and loss increments at the corresponding temperatures showed that when the MGT is least, the cells are dividing most rapidly

and the dielectric increments are greatest.

Steps in the voltage-current characteristic of a pearl-chain of yeast cells were found to occur for a few minutes around the time of cytokinesis as they were observed under phase contrast microscope. The cells prepared for synchronous division were collected by dielectrophoresis into a one micron gap between two point electrodes mounted on a microscope slide. Steps were observed about 3 to 4 hours later at ambient temperature. The mean generation time is 4 hours.

An emission of a radio frequency signal from yeast cells in the region of 7 MHz and in the range of 50 MHz - 80 MHz were found to occur about a mean generation time after starting the incubation of the cells for synchronous growth.

All these effects were only observed on the live yeast cells and never observed in experiments using killed yeast cells under the conditions otherwise same in all aspects.

CONTENTS

CONTENTS CONTINUED

CONTENTS CONTINUED

CONTENTS CONTINUED

Published Papers

1. Jafary-Asl, A.H., Solanki, S., Aarholt, E. and Smith, C.W., J. Biol. Phys. 11, 15-22 (1983)
2. Jafary-Asl, and Smith, C.W., Biological Dielectrics in Electric and Magnetic Fields (in print) 1983.
3. Jafary-Asl , A.H., Solank, S., Aarholt, E., and Smith, C.W., Dielectrics Society 1982 Meeting, Pembroke

College, Cambridge.

4. Jafary-Asl, A.H. Solanki, S., and Smith, C.W., Gordon Conference on Dielectric Phenomena 1982.

LIST OF ILLUSTRATIONS

PAGE

PAGE

LIST OF TABLES

CHAPTER 1 INTRODUCTION

In recent years living organisms, especially microorganisms, have become the subject for study by a large and diverse segment of the scientific community. They are no longer the private domain of the life scientists but are now being investigated by chemists, physicists, and engineers. This influx of the physical sciences has resulted in the development of many new approaches to biological problems.

As biological systems use the same atoms and molecules as the physical sciences, it is therefore reasonable that extent physical processes should be capable of giving a quantitative account of the interactions between electromagnetic fields and biological dielectrics, from zero frequency upwards.

Fröhlich (1980) suggested that biological materials might possess a metastable state with high electric dipole moment. The experimental evidence produced by some workers, for example Mascarenhas (1975), Neumann and Katchalsky (1972) and Ahmed et al (1976) seems to support these suggestions.

The membranes of the biological materials function through their composites structure of lipid and protein, in which the protein could exceed the lipid. The proteins in the membrane are lipid soluble and not water soluble (Petrov, 1979). The sub-molecular electronic properties of this type of protein has interested many investigators

especially those seeking to establish the relevance of solid state physical concepts to biological phenomena. The lipid soluble proteins contribute to the most sensitive part of the biological processes of living systems. On the other hand water soluble proteins serve as catalyzers of chemical reactions and transporters of ions and molecules through biological compartment fluids.

The diffusion of protons and ions across the membrane considered as the main factor for the establishment of electrical phenomena associated with the membranes. The possibility that electron conduction processes may play a role in the functioning of some of the membrane proteins is made the more reasonable when it is remembered that biological membranes in their normal physiological state are subjected to electric field gradients of $10^{7} Vm^{-1}$ and greater.

Ionic conduction through the biological membrane is achieved by "hopping conduction" (Pethig, 1979). If the cations are the only mobile ions within the biological membrane such as protons that have dissociated from protein molecules for example. These cations migrate through the membrane by a series of jumps from one position to the next over a coulombic potential energy barrier as shown in Figure 1.1a. Before hopping conduction takes place the cations will be in thermal equilibrium with the surrounding molecular structure and will vibrate in the potential well at a characteristic frequency f_o , which have a value of the

order of 10^{12}Hz at room temperature. The probability per second that the cation will pass over the barrier into a neighbouring equilibrium position in each vibration is given by

$$p = f_o \exp\left(-\frac{\Delta W}{kT}\right) \qquad 1.1$$

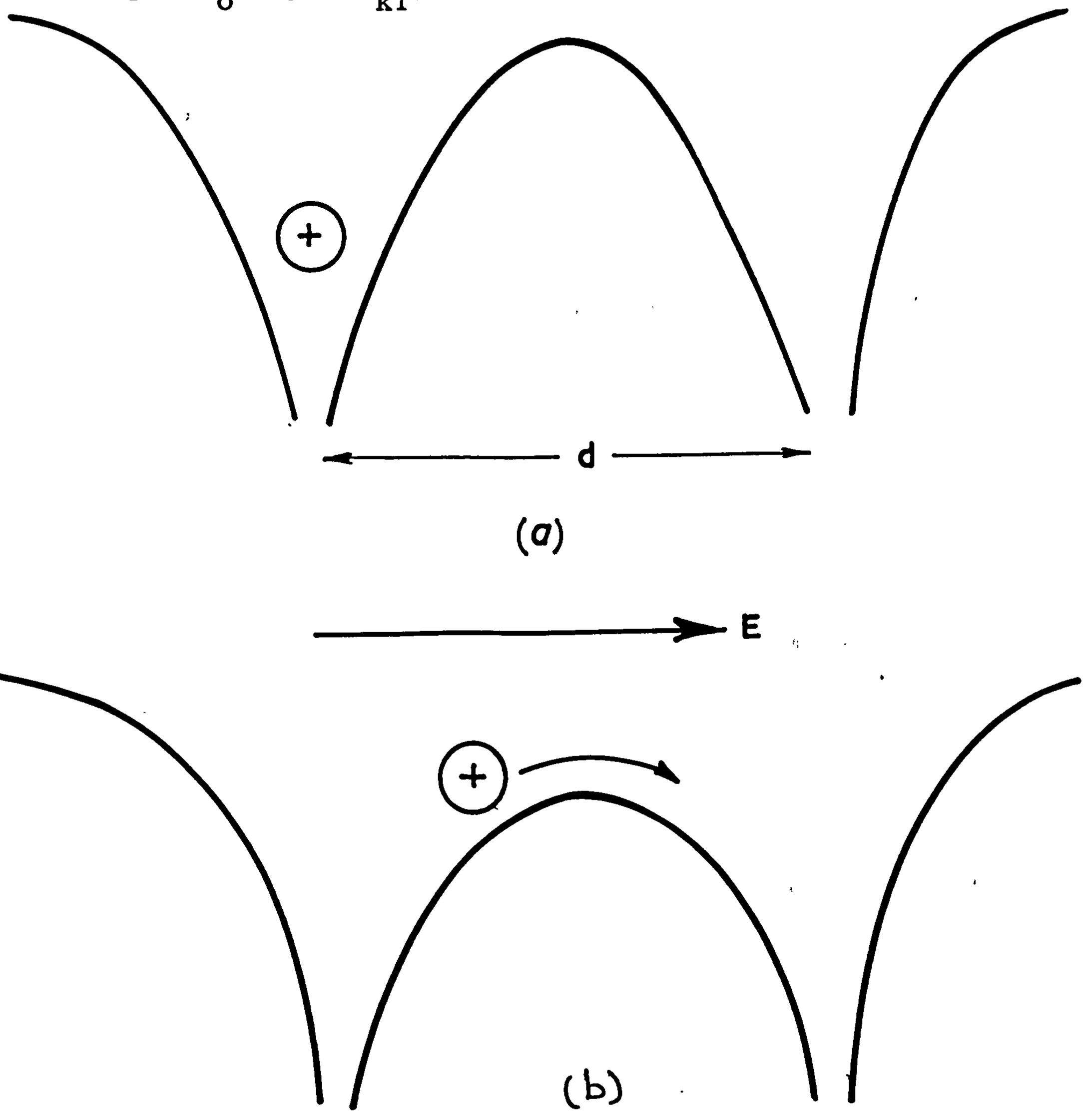

Fig. 1.1 Ionic conduction through the biological membrane

(a) The diffusion of cation is limited by a series of potential energy barriers.

(b) The rate of migration of cation increased by modification of the barrier through external electric field E.

If an electric field E or chemical (metabolic) processes are supplied, the potential barrier will be modified as shown in Figure 1.1b. A jump in the direction of metabolic activity or the applied field now takes place with an increased probability given by

$$p = f_o \exp \frac{-(\Delta W - \frac{qEd}{2})}{kT} \quad (1.2)$$

The above equations indicating that cations migration increased in the field direction.

If on the other hand the potential wells are close enough (Fig. 1.2) to interact,

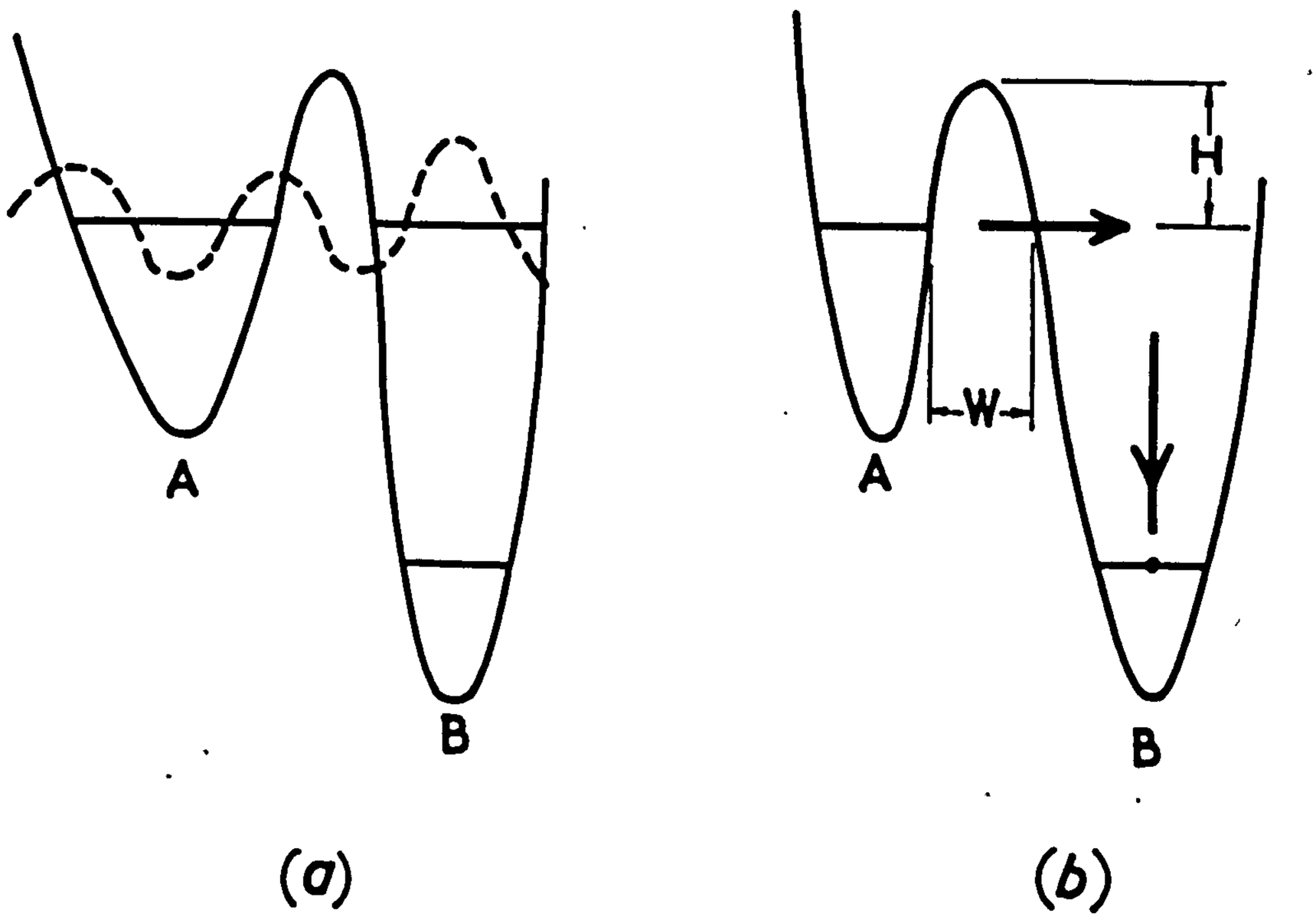

Fig. 1.2 Tunneling of ions through a membrane

(a) The two wells are close enough to interact with each other. (b) If both potential wells are coupled to an energy sink and source.

but they are isolated from any surrounding medium which can couple them into an energy sink or energy source by means of lattice vibrations (Phonons) or light interaction (Photons), cation can appear in well B. This is due to the limitation on the energy loss of the cation to get to ground state of well B. The cation will therefore be continually oscillating between A and B with the average amount of time spent in each well depending on the relative amplitudes of the corresponding wave functions. However if the wells are coupled to an energy sink and source, the cation that have appeared in B can now fall to the ground state by emitting photons or spending its energy as a lattice vibration. The rate at which the electron can tunnel from well A to B is controlled by the width W and height H of the potential barrier. If its temperature is high enough the cation could cross the barrier without having to undergo a tunnelling process.

However, a charge carrier hopping back and forth between two potential wells in response to an externally applied alternating electric field will give a dielectric response indistinguishable from that exhibited by a conventional dipole having a permanent dipolemoment. A set of dipoles with distributed relaxation times will exist if the charge carriers move between various potential wells, or if there is a distribution of barrier heights between wells.

Since all biological structures contain electric dipoles they can, in principle, be affected by an external

electromagnetic field. More significantly, the orientation of molecules, important in biochemical reactions, may be altered and biological molecules can be polarized by permanent dipole aligned or induced dipole moment. These properties are important for the function of a biological system and so make the system vulnerable to external perturbation. Because of the extremely small interaction energy of magnetic dipole moments, as compared with that of electric interaction, it is difficult to explain any observed response in a biological system as originating from the weak magnetic energy interaction of a system supposedly in equilibrium.

Sheppard and Eisenbud (1977) suggested that small amounts of orientational energy may cause steric changes in molecules located at the cell surface and that any cellular response to a field would imply communication across the cell membrane.

Control of chemical activity is, of course in many cases well understood in terms of relevant enzymes, which through their catalytic action regulate most biological chemical processes. Enzymes are proteins their electronic configuration can be perturbed by the electromagnetic field energy.

Fröhlich (1977) proposed that in biological systems through which much energy flows, coherent electrical oscillations would be created at frequencies of the order of 10^{11} Hz, and that these oscillations could cause sharp resonances in biological structures if the energy input exceeded a threshold value. He also suggested that superconducting

regions could be created by biological water, specifically the structural water located at the outer surface of biological molecules and cell membrane. The resulting structure would be a sandwich which could give rise to an a.c. Josephson effect (Bloch, 1968) coupled to the polarization waves thought to occur in biomolecular structure (Fröhlich 1975).

For several biological systems involving growth or nerve processes, the square of the activation energy is a linear function of temperature over a moderate range of physiological temperatures. This led Cope (1971) to suggest that superconductivity was closely associated with the growth of cells having superconductive micro-regions in the DNA and RNA structure, and which electrons tunnelling along the polypeptide chain, and Shaya et al (1976) suggested that superconducting Josephson junctions in living systems were sufficiently sensitive to detect variations in the ambient magnetic field.

On the assumption that the biological systems possess superconductive properties, Marton (1973) has tried to associate the local geomagnetic fields with cancer mortality data over a large part of the world. His suggestion was that there might be a (zero voltage) Josephson tunnelling current between the membranes of normal cells in contact. This current might assist the communication between the cells therefore lead to the normal growth of the cells. This current could be strongly dependent on the external magnetic field and he concluded that this might in turn result in

abnormal growth of the cells with the development of cancerous tissue preferentially in certain geographical locations.

The experimental evidence produced by some workers, for example Ahmed (1975), Shaya (1976), Aarholt (1982) and Jafary-Asl et al (1981-1983) seems to support these suggestions.

The test systems chosen for most of the work reported in this thesis was an aqueous suspension of yeast cells. The desire to use an organism with a simple shape, restricted the choice of materials to microorganisms. This in turn restricted the size and thus led to the decision of using a suspension of cells rather than a single cell. The suspension would also tend to give more reproducible "average" results when they were all growing at the same rate, that is in the logarithmic phase.

Besides being of simple shape, it was also desired the organism should be easy to grow, relatively simple to work with, non-hazardous, non-motile, and as large as possible. Saccharomyces Cerevisiae (normal diploid strain) seemed to satisfy all of these requirements and was chosen as the test organism.

CHAPTER 2 YEAST MORPHOLOGY AND GROWTH

2.1 The Yeasts

Yeasts are classified as higher protists in the group of fungi. They are plants which have a well-defined nuclear membrane and chromosomes. They exhibit mitotic cell division but lack chlorophyll so that they cannot synthesize their own food. They obtain their energy either by aerobic oxidative processes or by anaerobic fermentation depending on their circumstances. Yeasts generally occur as unicellular organisms and in a variety of shapes; they don't form colonies.

In general, yeasts are larger than bacteria. Saccharomyces Cerevisiae (normal diploid strain) cells used in this work are spherical and have an average diameter of 5 μm as observed under phase contrast microscope (Fig. 2.1). They have no organs of locomotion and thereby are non-motile. The yeast cells is surrounded by a rigid cell wall and a cell membrane. The thickness of the cell membrane is 8 nm and is believed to consist of two protein layers separated by a bi-layer of lipid (Lindegren, 1952).

Yeasts can reproduce vegetatively by budding and fission, or sexually by sporulation. Yeasts such as the Saccharomyces used in this work multiply by budding (Fig. 2.2). According to Williams (1976) the nucleus does not undergo the usual mitotic mechanisms observed in other fungi. Instead the nuclear membrane remains intact and chromosomes and spindle appear inside it. The membrane

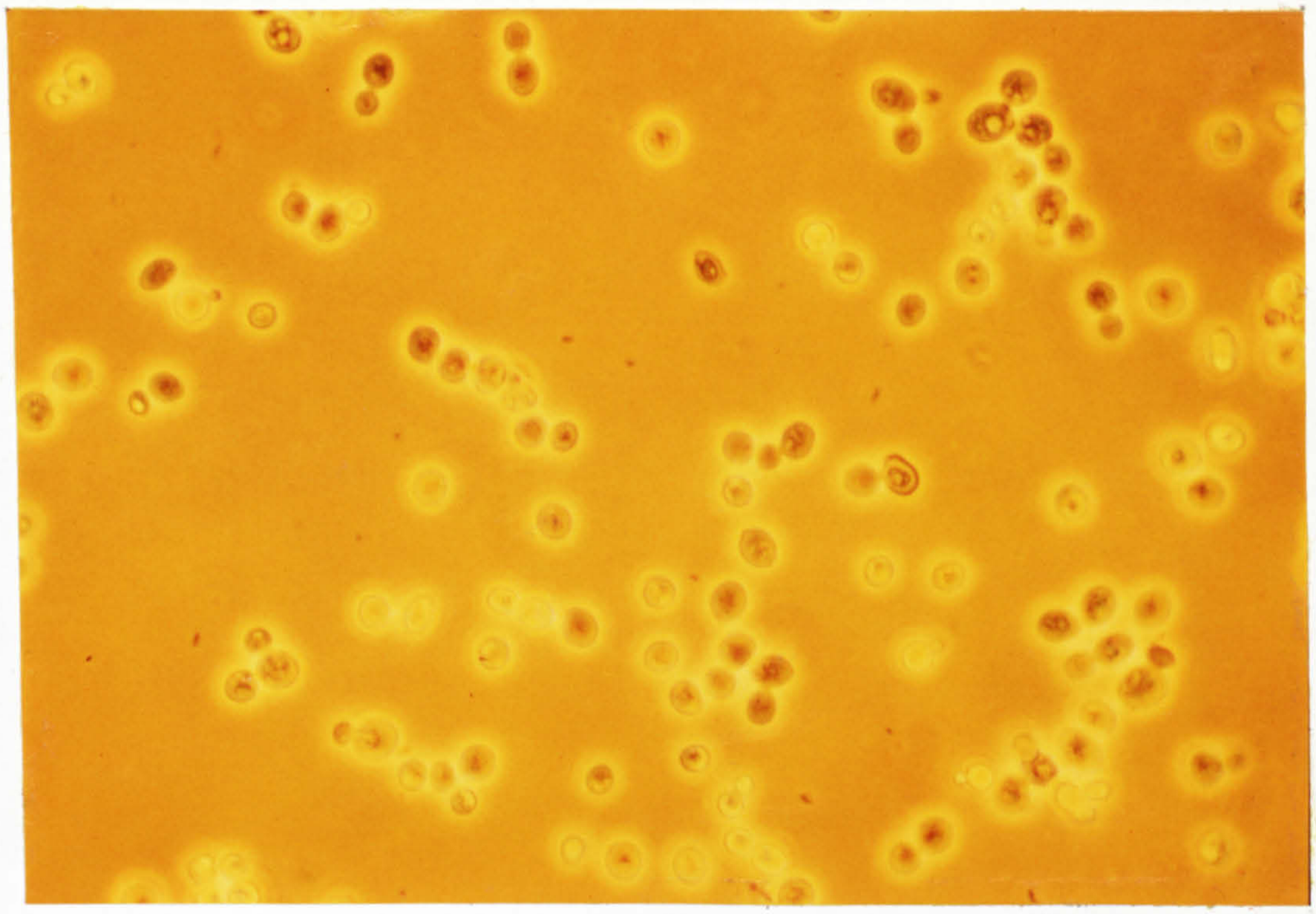

Fig. 2.1 S. Cerevisiae (normal diploid) cells growing in culture.

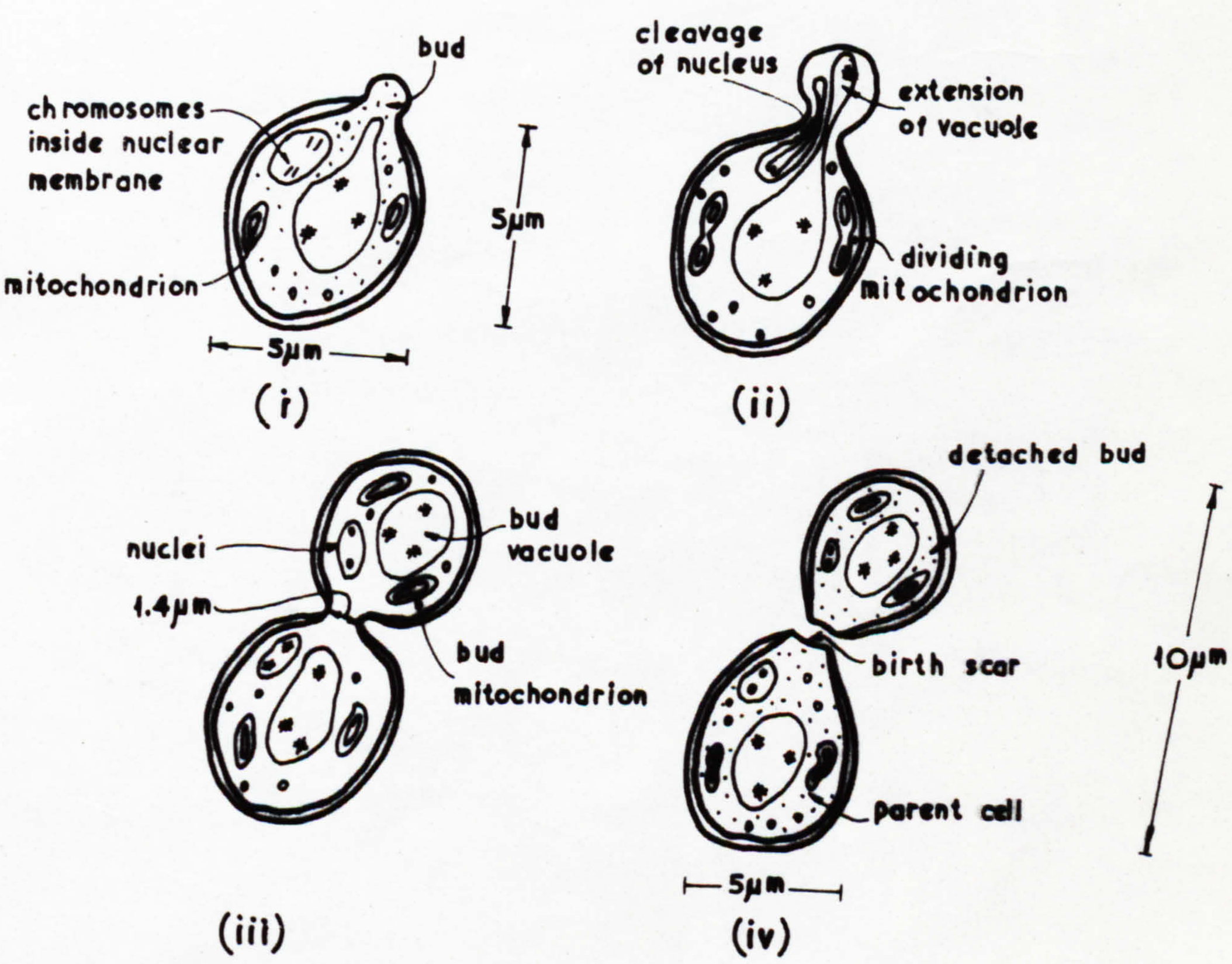

Fig 2.2
Budding in Saccharomyces Cerevisiae
(Normal dimension shown)

then undergoes constrictions and the nucleus is eventually pinched into two equal parts. One of the nuclei together with the other organelles such as mitochrndria, then enters a bulge which develops at a point adjacent to the site of nuclear division. Cytoplasmic connection between the bud and parent cell is then broken and followed by the laying down of new wall material.

Although yeasts will grow over a wide temperature range, the optimum temperature for most yeasts is 30°C. Their nutrient requirements are minimal but they will usually grow most abundantly on complex media. Any medium devised for the cultivation and isolation of yeasts can be used in liquid form or solidified by the addition of agar.

2.1.1 The cell structure

Lindegren (1952) and his collaborators carefully investigated the structure of the yeast cell and the budding process (Fig. 2.3) and compared their findings with those of earlier investigators. They reported that each yeast cell contains one or more vacuoles, or transparent droplets in the cytoplasm, which can be seen with the light microscope when appropriately stained and which can be differentiated from the surrounding cytoplasm by electron microscopy.

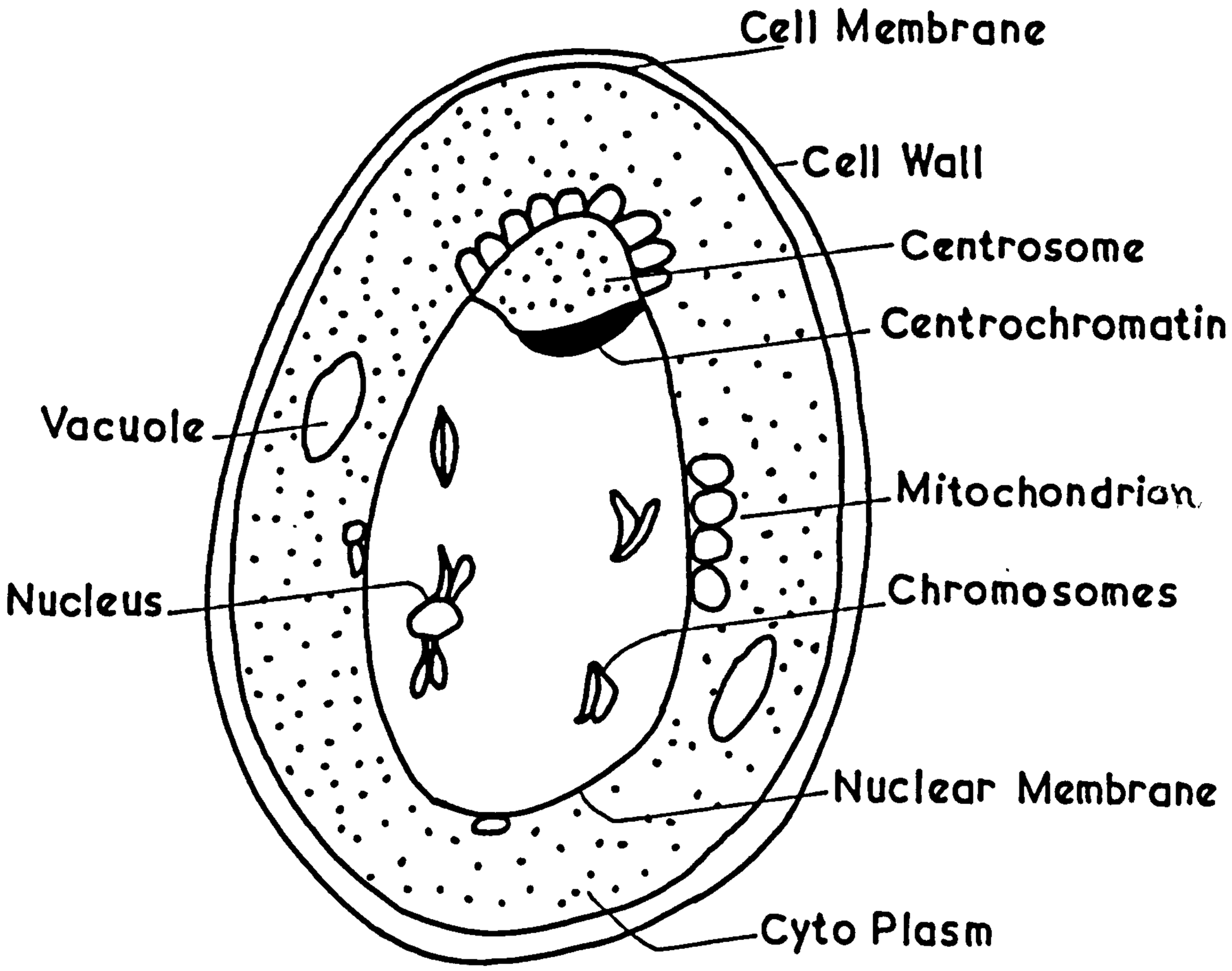

Fig. 2.3 The structure of the yeast cell according to Lindegren (1952).

Mitochondria occur as membrane-bound organelles which on microscopic examination give the appearance of a folded thread. They consist largely of lipoprotein and a small amount of RNA. The mitochondria contain the respiratory enzymes, and have beeen termed the power houses of the cell.

Although studies of the nuclear sub-structures are handicapped by their electron transparency, several facts have been established; (1) spindle formation is not seen during

the budding process; (2) the nuclear membrane remains intact during cell division; and (3) in budding, the nucleus constricts, one part going to the daughter cell and one remaining with the parent. Certain structures of more intense electron density have been observed, one of which is thought to be a nucleus.

A typical yeast cell contains what is termed cytoplasm this is a semifluid containing finely granular materials, ribosomes abundent in ribonucleic acid (RNA) and membrane-bound organelles. The cell membrane with a thickness of approximately 8 nm, it consists of two electron dense layers of lipid protein, and ribonucleic acid and is believed to be a lipoprotein structure, the inner layer being lipid and the outer protein.

The cell wall of yeast is quite thin in young cells but thickens with age. A typical cell wall of yeast is about 70 nm thick. The major constituents are two polysaccharides, glucan (30 to 35 percent) and mannan (30 per cent); there is a 6% to 8% protein content some of which is very likely to be enzymatic, invertase has been identified in cell wall material. The lipid concentration range is 8.5% to 13.5% . The cell - wall protein is linked to both the glucan and the mannan and binds the cell wall.

The presence of both "bud scars" and "birth scars" on the yeast cell had been demonstrated . A newly detached cell possesses a birth scar at the point at which it was joined to its mother cell. When this cell itself produces bud, which gradually become detached, each of the daughter cells leaves a bud scar upon the cell. The first bud

produced is situated diametrically opposite to the birth scar. One cell was studied by Lindegren which produced 23 successive buds, all of which gave rise to macroscopically identical cultures. The electron microscope was employed in the study of these bud scars by Bartholomew and Mittwer (1953) who found that the reproductive age of a cell is limited, but that a cell is potentially capable of producing about 100 daughter cells, since a bud is always formed at a new point on the cell. They were, however, unable to find any cells with more than 20 actual bud scars.

2.2 Growth rate of yeast

The prevailing means of yeast reproduction is by budding and fission, one cell divides, producing two cells. Starting with a single yeast cell, the increase in population is by geometric progression in a binary sequence. The time interval required for the cell to divide or for the population to double is known as the generation time. It has been found to be more convenient to replace the generation time by the mean generation time (MGT). This is because not all the cells will produce only one daughter cell, it is commonly observed that some cells produce two or more buds at the same time. The mean generation time is strongly dependent upon the nutrients in the medium and on prevailing physical conditions (temperature, pH etc.).

Under optimum conditions, one can easily determine the mean generation time by the simple mathematical expression of equation (2.5).

The mean generation time for yeast cells are determined by inoculating the medium with a known number of cells, allowing the yeast to grow under optimum conditions, and then determining the final cell population.

The experimental data required to calculate the MGT includes (1) the number of yeast cells present at the beginning, (2) the number of yeast cells present at the end of a given time interval, and (3) the time interval . Additional measurements would check the validity of the equation.

The relationship of cell numbers and mean generation time can be expressed by the following equations where B is the number of yeast cells inoculated into medium or cell count at zero time. b is the number of cells at end of the given time period t. G is the mean generation time (MGT) and n number of generations each of time equal to MGT.

Starting with a single cell, the total population b at the end of a given time period would be expressed by

$$b = 1 \times 2^n \qquad 2.1$$

where 2^n is the cells population after the nth generation. However, under practical conditions, the number of cells B introduced into the medium at time zero is not 1 but more likely several thousand, so the formula now becomes

$$b = B \times 2^n \qquad 2.2$$

Solving Equation (2.2) for n,

$$\log_{10} b = \log_{10} B + n \log_{10} 2$$

$$n = \frac{\log_{10} b - \log_{10} B}{\log_{10} 2} \qquad 2.3$$

If we now substitute the value for the $\log_{10} 2$, which is 0.301, in the above equation, we have

$$n = 3.3 \log_{10} \frac{b}{B} \qquad 2.4$$

Thus, by use of equation (2.4) we can calculate the number of mean generations that have taken place, providing we know the initial population B and the population b after time t and the growth is only a single exponential.

The mean generation time G is equal to t (the time which elapsed between b and B) divided by the number of generations n, or

$$G = \frac{t}{n} = \frac{t}{3.3 \log_{10}(b/B)} \qquad 2.5$$

Equation (2.5) is usually stated in hours per division.

2.3 Growth curve of yeast cells population

When a fresh medium is inoculated with a given number of cells, and the yeast cells population determined intermittently during an incubation period of 48 hours (after this period the number of cells that die exceeds the number of new cells produced), and the logarithms of the number of cells versus time is plotted, the following phases of growth can be recognized: lag phase, exponential growth phase, period of negative acceleration, stationary phase and death phase. Those are shown in figure 2.4.

2.3.1 The lag phase

The addition of inoculum to a new medium is not followed by a doubling of the population according to the generation time. Instead, the population remains temporarily unchanged, as illustrated in the yeast growth curve. But this does not mean that the cells are quiescent or dormant; on the contrary, during this stage the individual cells increase in size beyond their normal dimensions. Physiologically they are very active and are synthesizing new protoplasm. The cells in this new environment may be deficient in enzyme or coenzymes which must first be synthesized in amounts required for optimal operation of the chemical machinery of the cell. Time for adjustments in the physical environment around each cell may be required. The organisms are metabolizing but there is a lag in cell division. At the end of the lag phase, each organism divides. From Fig. 2.4, it can be

seen that it takes 4 hours before cells start dividing.

2.3.2 The exponential phase

During this period the cells divide steadily at a constant rate. As it can be seen in Fig. 2.4, the log of the number of cells plotted against time results in almost a straight line. Under appropriate conditions the growth rate is maximal during this phase, and population is then most nearly uniform in terms of chemical composition of cells, metabolic activity etc. Cells in this phase are commonly used for studies of metabolism.

2.3.3 The negative acceleration phase

This is due to the decrease in the nutrients of the medium due to an enormous increase in cell numbers. Consequently damage to the cells may occur as a result of the accumulation of metabolic end products.

2.3.4 The stationary phase

In this phase the slowing of the growth rate continues, after 40 hours it is due more to exhaustion of the nutritional factors of the medium and the accumulation of waste products. The population then remains constant for a while, perhaps as a result of complete cessation of division or the balancing of reproduction rate with an equal death rate.

Fig 2.1
Growth curve for a pupulation of yeast cells (S. Cerevisiae)

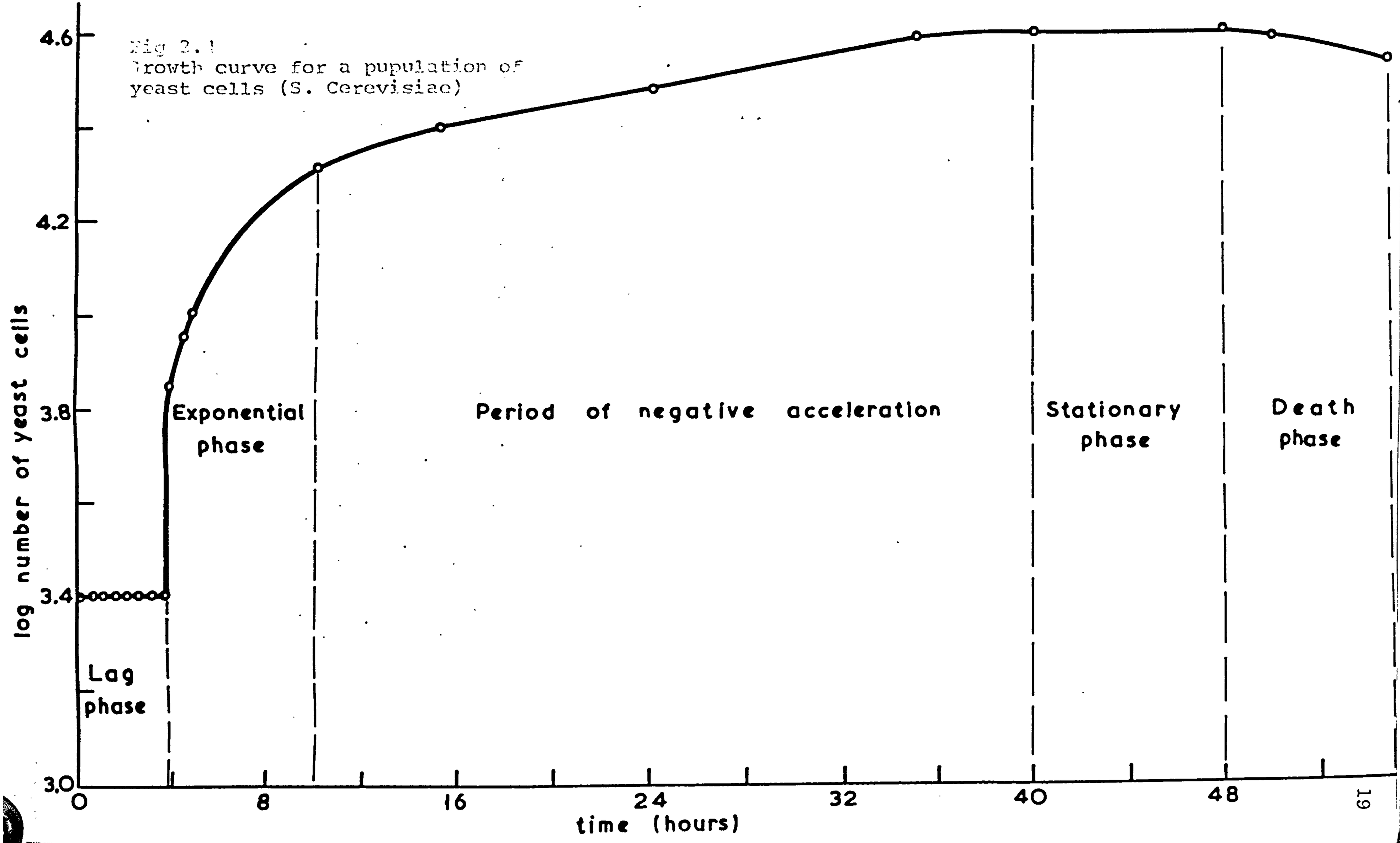

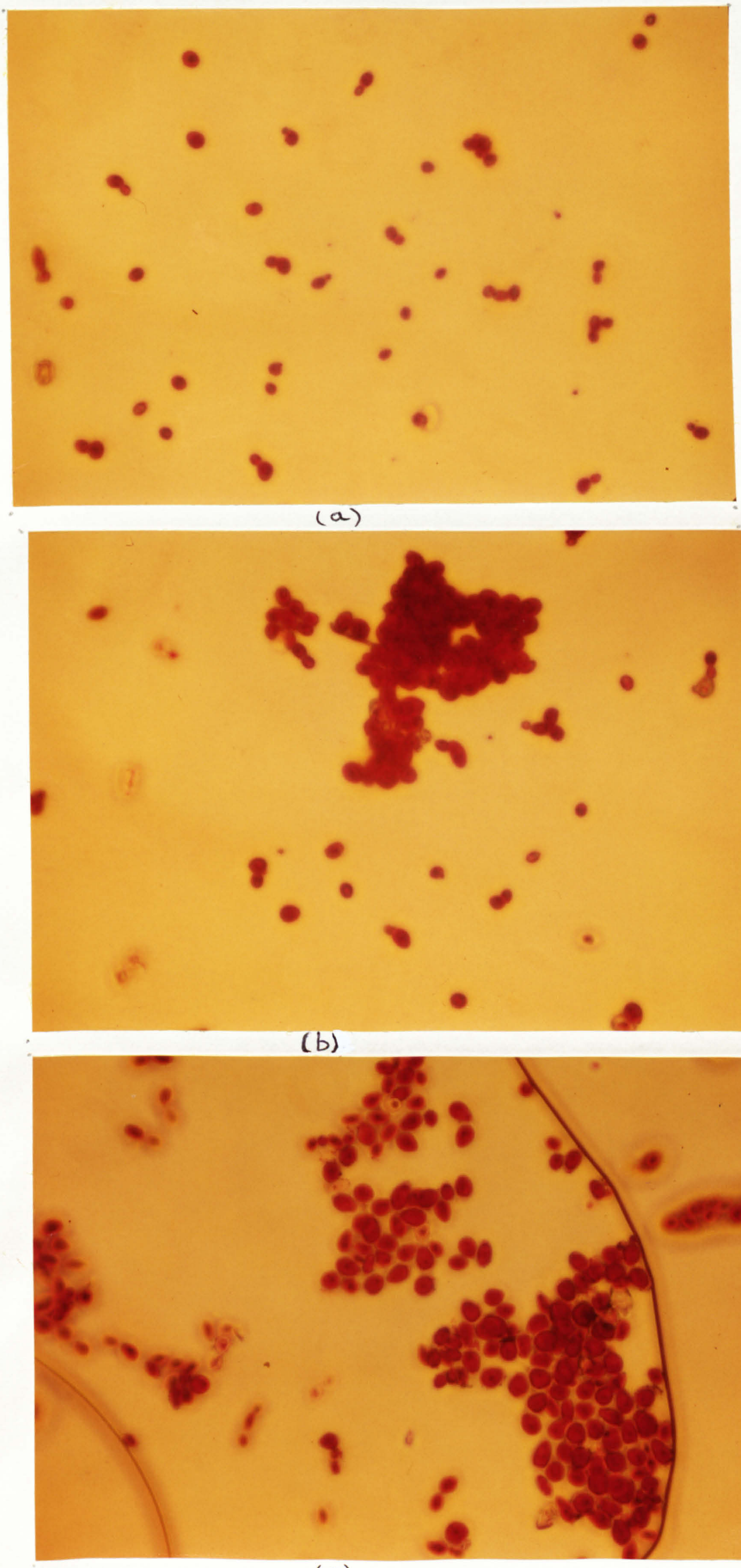

(a)

(b)

(c)

Fig. 2.5 The staining procedure (a) Live cells(b) Live and dead (c) Dead cells

2.3.5 The death phase

Following the stationary period, the cells may begin to die off faster than new cells are produced, if indeed any cells are still reproducing.

The most important conditions contributing to cell death are the depletion of essential nutrients and the accumulation of inhibitory products. During the death phase, the number of viable cells decreases geometrically, essentially the inverse of growth during the log phase.

An estimate of the proportion of viable yeast cells in the cultures can be made bythe methylene blue staining method (Baker 1962). The basis of the technique is that certain changes occur in dead cells which result in response to stains different from that of living cells (Fig. 2.5) . The staining procedure is carried out in the following way: a cell smear is made and heat fixed. It is stained with Loeffler's methylene blue solution for ten minutes , rinsed thoroughly using tap water until the smear appears a pale blue colour. Carbol fuchsin is run down the slide for as short a time as possible. The slide is then washed immediately and blotted dry. Phase contrast microscope observation shows living yeast cells stained purple and dead cells stained red.

The number of yeast cells in each phase as a function of time are determined by using serial dilution and plating technique (see Appendix 13.1).

2.4 Synchronous growth

The number of cells in a culture usually increases smoothly because at any time at least a few cells are dividing, in other words cell division is not normally synchronized. However, a population in which all the cells are undergoing division at approximately the same time is desirable particularly for some of the work reported in this thesis. Such a synchronized culture can be obtained by special methods, but the synchronism generally lasts for only a few generations since even the daughters of a single cell soon get out of step with one another.

Synchronization is achieved by inoculating cells into a medium at a suboptimal temperature, if they are kept in this condition for some time, they will metabolize slowly but will not divide. When the temperature is gradually raised to the optimum, the cells undergo a synchronized division. When these cells are observed by phase contrast microscope, they are reasonably well synchronized with each other.

2.5 Precautions during experimental measurements

2.5.1 Experimental Culture

It must be understood during some phases of growth the cells are young and actively metabolizing (especially in the exponential phase) while during others they are dying (especially in the death phase) so that there may be enormous structural and physiological differences between populations of cells harvested at different times. The physical and chemical environments may be expected to affect the organisms differently during different phases.

2.5.2 Sedementation of the yeast cells

Yeast cells are slightly more dense than water, so as a result, over a period of time, they will settle out of suspension. This needs to be kept in mind when concentration measurements are being made or when cells of some standard concentration prepared for a study have been kept in a tube or syringe for several minutes. To keep the concentration as uniform as possible from one measurement to the next, the suspension should be thoroughly but gently mixed and shaken before each sample is removed, although this may complicate by introducing aeration.

2.5.3 Microbiological techniques for electrical and magnetic measurements

To remove variables as far as possible, it is important to use proven biological methods for handling the particular organism under study (Appendix 13.1) . The original stock of the organism should be kept refrigerated so as to be available at any time when it is required to start a new culture having nearly identical characteristics to preceding one. Otherwise over an extended period of time, mutations may cause the cells to evolve to give daughter cells with very different characteristics. The stock cultures that are used for producing working cultures must be subcultured periodically, using accepted inoculation procedures, to keep them alive and free from contamination. Sterilization procedures must be followed closely to prevent contamination by foreign organisms (see appendix 13.1 for details of biological techniques).

CHAPTER 3 THE BIOLOGICAL CELL MEMBRANE

3.1 The cell membrane

Hundreds of chemical reactions and transfer processes are occuring continuously in every active cell, and membranes play a vital role in controlling these processes, in separating incompatible substances and in transporting materials about the cell. Some of the more complex chemical sequences are accelerated because it appears that the enzymes which catalyse them are so arranged on membranes that the reactants can move readily from one reaction site to the next.

In a packaging role, intracellular membranes separate components of the cell which would be self destructive if allowed to mix freely in the cytoplasm, they conserve and maintain regions of local concentrations, regulate the passage of inorganic ions and complexes between compartments and provide the principle means for the checking ordering and regulation of the metabolic processes which constitute life.

Electron microscope observations (Danielli, 1968) showed that the cell membrane consists of a lipid bi-layer which is coated on each side by proteins (Figure 3.1).

In an early estimate of the dimensions of membranes Danielli predicted an appropriate value of λ of 8 nm on the assumption that the length of the lipid molecules projecting into the core is about 3 nm and that the thickness of each protein coat would be about 1 nm. The advent of the electron microscope proved this prediction to be remarkably accurate.

Proton magnetic resonance studies indicate that a proportion of the linkages between lipid and protein is

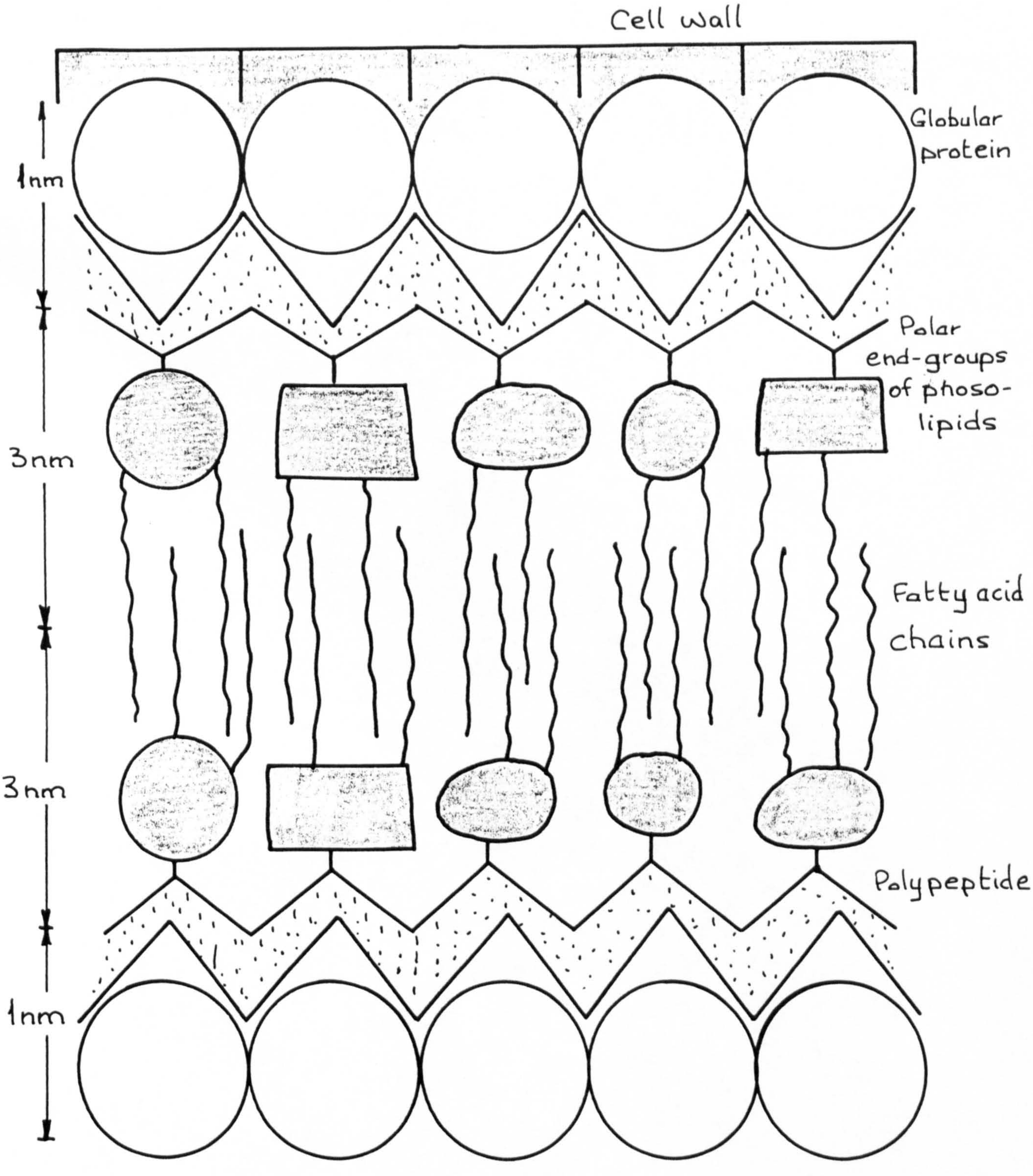

Fig. 3.1 The Davson-Danielli model for the structure of cell membranes.

by hydrophobic bonds (Wallach, 1968). This means that at least some protein is likely to occupy a core position in the membrane so that there can be linkage between hydrophobic

end-groups of the protein and the hydrogen chains of the lipid. Some enzymes such as Na-K-Mg Atpase, glucose-6-phosphatase and NADH oxidase are rendered non functional if all lipd associate with them is removed (Wallach, 1968). As a result of these and similar observations a variety of alternatives to the unit membrane type of organization has been postulated for particular membranes. The exact structure and function of the cell membrane is imperfectly understood so that any effects of electric or magnetic fields at the molecular level could lead to a more basic understanding of cell membrane function as well as higher levels of biological organization.

One of the most remarkable properties of biological membranes is their ability to restrict the passage of some substances and to permit, or even assist, the movement of others.

3.1.1 The electrical behaviour of the cell membrane

According to Webster et al. (1978) the cell membrane is a complex region which selectively transmits biochemicals to the cell interior is shown in Figure 3.2. It is highly polarized by an electric field of about 10^7 V m^{-1} originating from a static potential difference of about 100 mV across a distance of about 10 nm.

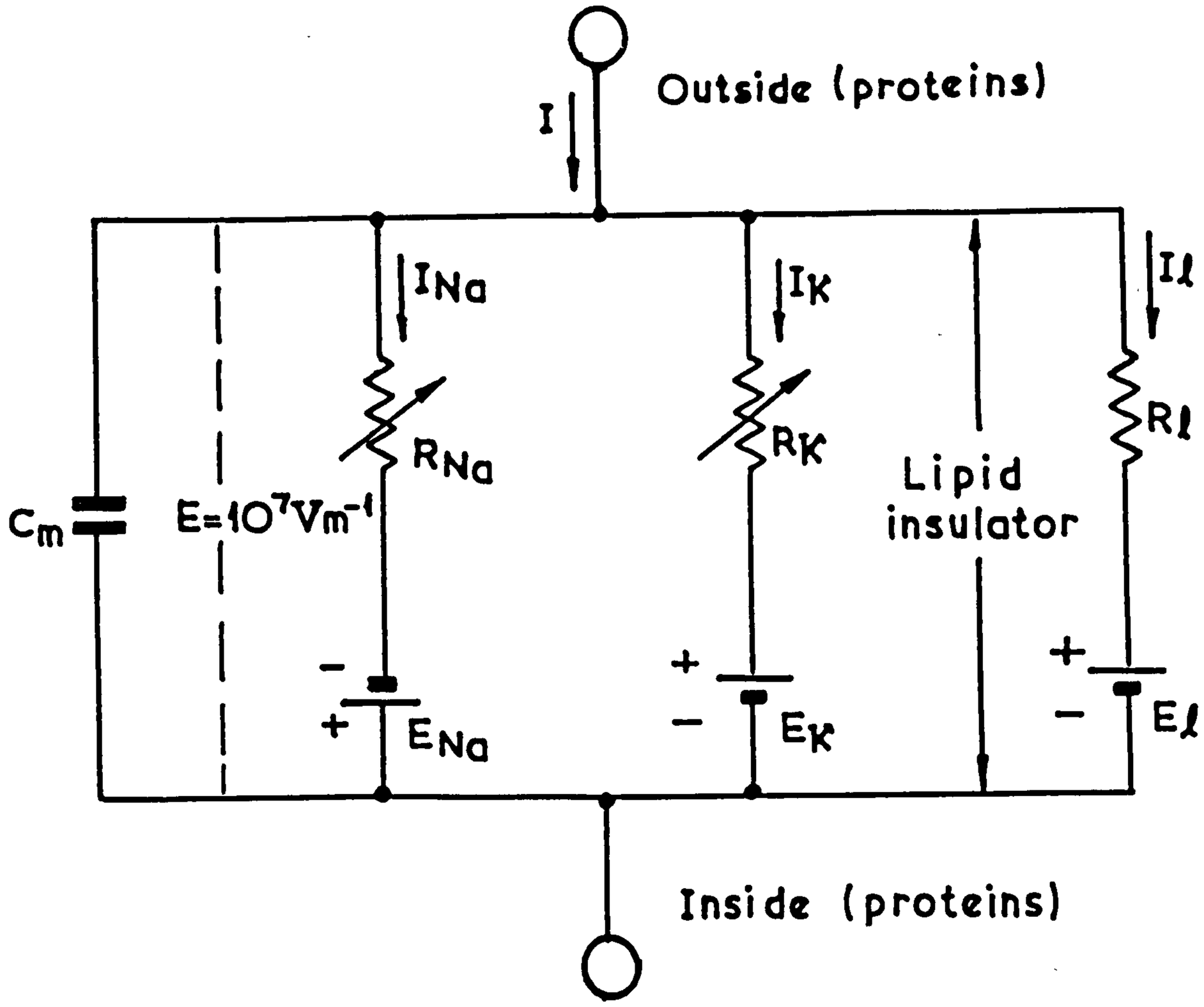

Fig. 3.2 Electrical circuit representing cell membrane (Webster et al, 1978).

Current can be carried through the membrane either by charging the membrane capacity or by movement of ions through the resistances in parallel with the capacity. The ionic current can be divided into components carried by sodium and potassium ions (I_{Na} and I_K) and a small 'leakage current' (I_ℓ) made up by chloride and other ions. Each component of the ionic current is determined by a driving force which may conveniently be measured as an electrical

potential difference and a permeability coefficient which has the dimensions of a conductance. Thus the sodium current (I_{Na}) is equal to the sodium conductance (g_{Na}) multiplied by the difference between the membrane potential (E) and the equilibrium potential for the sodium ion (E_{Na}). Similar equations apply to I_K and I_ℓ are are obtained by the relations

$$I_{Na} = g_{Na} (E - E_{Na})$$

$$I_K = g_K (E - E_K) \qquad (3.1)$$

$$I_\ell = g_\ell (E - E_\ell)$$

where E_{Na} and E_K are the equilibrium potentials for the sodium and potassium ions. E_ℓ is the potential at which the 'leakage current" due to the chloride and other ions is zero. For practical application it is convenient to write these equations in the form

$$I_{Na} = g_{Na} (V - V_{Na})$$

$$I_K = g_K (V - V_K) \qquad (3.2)$$

$$I_\ell = g_e (V - V_\ell)$$

where

$$V = E - E_r$$

$$V_{Na} = E_{Na} - E_r \qquad (3.3)$$

$$V_K = E_K - E_r$$

$$V_\ell = E_\ell - E_r$$

and E_r is the absolute value of the resting potential. V, V_{Na}, V_K and V_ℓ can then be measured directly as displacements from the resting potential.

The membrane is pictured as a leaky condenser that accumulates a resting potential of 60 to 90 mV. The leakage occurs in three separate pathways, each of which contributes to the overall potential difference across the membrane. In the case of the cations Na^+ and K^+ the potential difference opposes the diffusion potential, with Cl^-, however, the electrical potential and the diffusion potential have the same direction.

From Figure 3.2 it can be seen that the total membrane current density may be divided into a capacity current and an ionic current. Thus

$$I_{total} = C_m \frac{dV}{dt} + I_i \qquad (3.4)$$

where C_m is the membrane capacity per unit area (assumed constant), t is the time, V is the displacement of the membrane potential from its resting value; I_i is the ionic current density (that is, $I_i = I_{Na} + I_K + I_\ell$). The justification for this is that it is the simplest which can be used and that it gives values for the membrane capacitive which are independent of the magnitude or sign of V and are little affected by the time course of V (Hodgkin et al 1952). Evidence that the capacitive current and ionic current are in parallel equation (3.4) is provided

by the similarity between ionic currents measured with $\frac{dV}{dt} = 0$ and those calculated from $- C_m \times \frac{dV}{dt}$ with $I_{total} 0$ (Hodgkin et al. 1952).

The only major reservation which must be made about equation (3.4) is that it takes no account of dielectric loss in the membrane, but it is not thought to be large since the time course of the capacitive surge was reasonably close to that calculated for a perfect capacitor (Hodgkin et al. 1952).

In the course of biological dielectrics and magnetic fields measurements, an electrical model of a typical biological cell (Jafary-Asl et al and Smith 1983) is shown in Figure 3.3. It may be simultaneously regarded as a heterogeneous dielectric, a thin film spherical capacitor and a resonator, as well as an energy source.

The $\frac{\lambda}{2}$ mode for an electrical wave travelling around the circumference of a great circle of the cell corresponds to 10^{13} Hz (367 cm^{-1}) and at this frequency the half value distance is likely to be 5 μm in water and 5 mm in lipid. It is also typical of the "attempt-to-escape-frequency" for "hopping-conduction".

Because the membrane is so thin , the resting field across it and that due to the movements of single charges are comparable. With resonance, there is the possibility of periodic distortion of potential wells giving rise to stimulated hopping-conduction analogous to the "bucket-brigade-delay" . Such hopping-conduction currents would

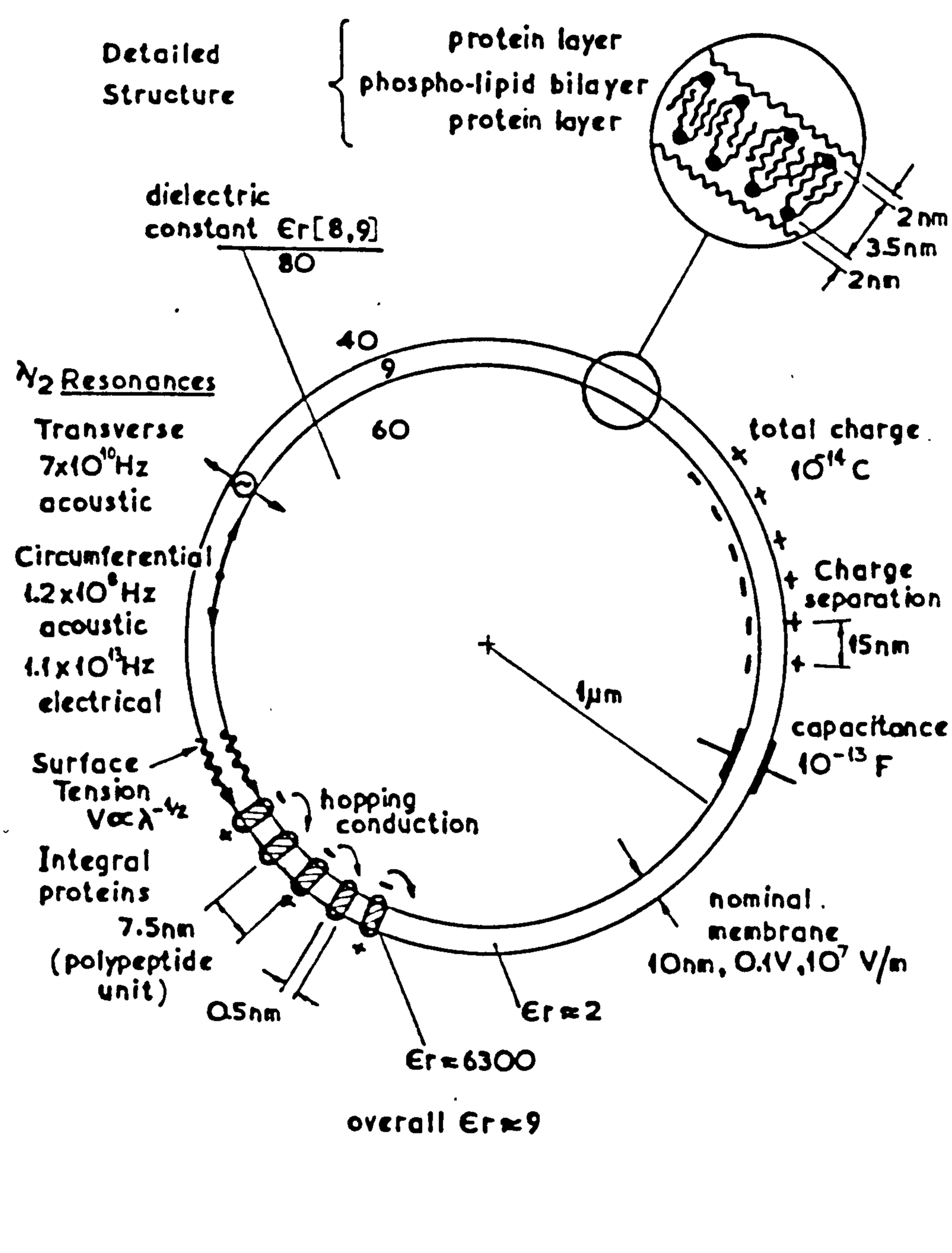

Fig. 3.3 An electrical model of a typical biological cell (Jafary-Asl et al and Smith, 1983)

continue to circulate so long as the 10^{13}Hz switching frequency persisted. Such a process would permit the

persisting circulating current loops necessary for the diamagentic properties of biological materials. As "ball-park" figures, one electron charge every 2 cycles of 10^{13} Hz is a current of 8×10^{-7} A. An integral membrane protein might have a capacitance of 2×10^{-15} F, as a switched capacitor at 10^{13} Hz this would be a lossless resistance of 50Ω and with 420 around the circumference the required emf would be 17 mv. A change in magnetic flux linkage of 2×10^{-15} Wb in 10^{-13}s would give an emf of 20 mV, enough to saturate this stimulated hopping-conduction.

A typical membrane resting resistance for sodium and potassium are 150 kΩ and 1 kΩ respectively (Strong, 1973). This gives ... electrical vibrations, with frequencies of the order of 10^{10} and 10^{12} (a typical membrane capacitance is 10^{-13} F indicating a frequency f of $f \simeq \frac{1}{CR}$) respectively. Fröhlich (1980) suggested that these electrical vibrations may be excited coherently and could cause sharp resonances in active biological membranes through chemical (metabolic) processes. Excitations of this type could have far-reaching consequences in biological systems, for they would lead to selective long-range interactions such as required to control growth. The possibility of switching on or off the collective oscillating mode through cellular metabolic processes might for example, promote changes in the configuration of large regions such as required in cell division. The supply and type of metabolic energy would have to be regulated so as to be effective at the right time. In this manner a series of temporal changes could be programmed in a cell.

The membrane differs markedly in its permeability to the passage of the ions (Na^+, K^+ and Cl^-). K^+ and Cl^- permeate most easily, Na^+ less easily, while the organic anions large proteins inside the cell are virtually unable to leave under steady-state conditions there is a diffusion potential for K^+ directed outwards and for Na^+ inwards, but since K^+ leaks out more readily than Na^+ leaks in, there is a net current of positive charges leaving the cell and making the inside of the cell negative with respect to the outside environment. Since the anions proteins of the cell cannot leak out, a limit is placed on the escape of K^+, for at a certain point the electrical potential generated by the separation of charges will balance the outwards diffusion potential of K^+.

The relationship between the potential difference across a membrane and ionic activities is expressed by the Nernst equation. In this case it is assumed that the membrane is permeable only to K^+. At equilibrium

$$E = \frac{RT}{zF} \ln \frac{[K^+_{out}]}{[K^+_{in}]} = 0.0615 \log_{10} \frac{[K^+_{out}]}{[K^+_{in}]} \qquad (3.5)$$

where

E = potential across the membrane in volts,

R = gas constant (8.312 Joules/deg./mole,

T = absolute temperature , in ^oC,

F = the Faraday (96,500 Coulombs/gram equivalent),

ℓn = the natural logarithm (2.3 x $\log_{10}$),

K^+_{out} and K^+_{in} = the concentrations of the ions on the two sides of the membrane,

z = charge per particle (here = 1).

Considerable differences in the concentrations of certain ions are maintained across membranes by the potential difference. A potential difference of approximately 90 mV with the correct sign will balance a concentration difference of 1:30 for potassium ions across a nerve fibre at 37^{o}C (Strong, 1973).

3.1.2 Active transport of solutes across cell membranes

The cell membrane of all living cells has the capacity to transport substance by means of active metabolic processes . Active transport, that is the membrane is capable of transporting a substance in the opposite direction to that in which it would diffuse if influenced only by the electrical and concentration gradients of equation (3.5). The work that has to be done in transporting materials against the electrochemical gradient and the membrane derives from the energy of the metabolic processes.

Many of the biologically important inorganic ions such as calcium, magnesium, chloride, potassium, phosphate are actively transported by specialized membranes such as those of the gut and excretory organs but only sodium appears to be universally transported by all animal cell membranes.

All cells in general have the capacity to extrude sodium, though the ability of cell membranes to do this is poorly developed. The reason for the universality of the ability of cell membranes to transport sodium is probably derived from an evolution step need to regulate cell volume in a marine environment (Robinson, 1965).

Sodium diffusing into the cell is actively transported out by the cell membrane. The extrusion of a positively charged ion in this way has to be balanced by the uptake of a similar charge and is in fact achieved by the uptake of potassium ions into the cell. However, since the main anions of the cell are proteins which cannot escape across the membrane any loss of potassium creates a separation of charge and hence a potential difference across the membrane. This potential reaches a value such that the electrochemical gradient for potassium across the membrane is zero and there is then no further net loss of potassium (Figure 3.3). On the other hand chloride ions can respond to the potential difference across the membrane. As a result of these various effects, all due ultimately to the operation of the sodium extrusion mechanism in the cell membrane, the cell is brought into osmotic balance with its bathing medium (Robinson 1965).

Interference with the operation of the sodium pump results in a disturbance of cellular water content. Skou (1965) , reported that cooling red blood cells to near freezing increased their water and sodium content and reduced the potassium. Returning the cells to blood temperature in the presence of metabolites and glucose

results in the removal of the excess sodium and recovery of the lost potassium, much of the excess water is also removed.

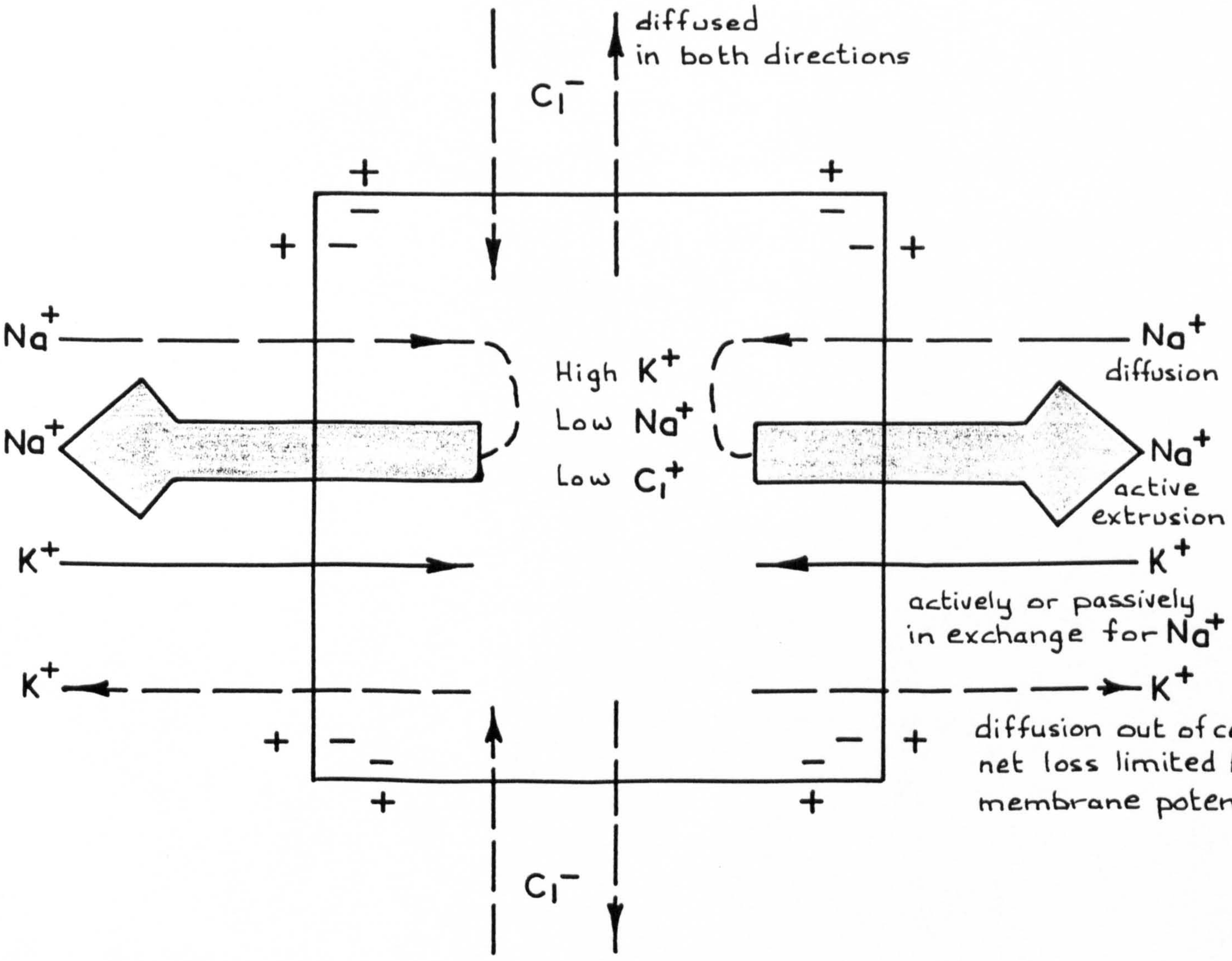

Fig. 3.4. Ion movements across the cell membrane of cells which are responsible for the production of the membrane potential and regulation of cell water content (Robinson, 1965).

3.2 Water in biological system

It is well known that water forms a necessary constituent of the cells and life cannot exist, even for a limited period, in the absence of water, so that this naturally occuring inorganic liquid is essential for the maintenance of inorganic life. Apart from acting as a proton-exchange medium, water moves through living organisms and functions as a lubricant in the form of surface films and viscous juices. Water is the solvent which promotes biological hydrolysis in which proteins and carbohydrates are broken down; lipids, although not actually modified chemically, are solubilized in the aqueous medium. Thus the energy required for biosynthesis derives partially from the energy of formation of water. Another important function of water is the thermal regulation of living organisms, its large heat capacity coupled with the high water content are responsible for maintaining isothermal conditions and the high thermal conductivity of water prevents serious local temperature fluctuations.

The physical state of water in cells is a subject of controversy. According to the "classical theory" of membranes intracellular water is in the same form as liquid water and the interior of the cell can be considered as a compartment containing a solution of ions, small molecules and macromolecules bounded by a lipoprotein membrane. This membrane is responsible for maintaining the interacellular distributions of ions by means of critical pore size and ion "pump" located within the membrane walls.

A small fraction of the water is "bound" , that is, in hydration layers of macromolecules or cellular membranes. The extent of these hydration layers is unspecified.

The "Association theory" first suggested by Ling (1962) rejects the idea that "pumps" exist and that intracellular water is in the same form as liquid water. Instead the fundamental assumption is that ions, small molecules and macromolecules exist in an "ordered" state and that ion selectively is maintained by electrostatic interactions at sites on the macromolecules which only favour certain ions. All of the water molecules are thought to exist in polarized multilayers experiencing significant "motional restriction" due to the presence of various charged sites within the cell. Muscle water vapour equilibration studies of Ling and Negenkang (1970) reported 95% of water in polarized multilayers , the remaining 5% being strongly adsorbed on macromolecules.

The electrical properties of the water molecules can be approximately represented by a resultant permanent dipole (Figure 3.4). The angle HOH was taken as 104.5^{o}, with a similar angle between the vectors from O to the negative charge concentrations (Hasted, 1973). The O-H---OH bond is called the hydrogen bond. However the electrons are attached more strongly towards the heavier oxygen molecules and this leads to the slight negative charge in this region and a slight positive charge in the region of the hydrogen nuclei. This imbalance in charge gives the molecule an electrical polarity and water

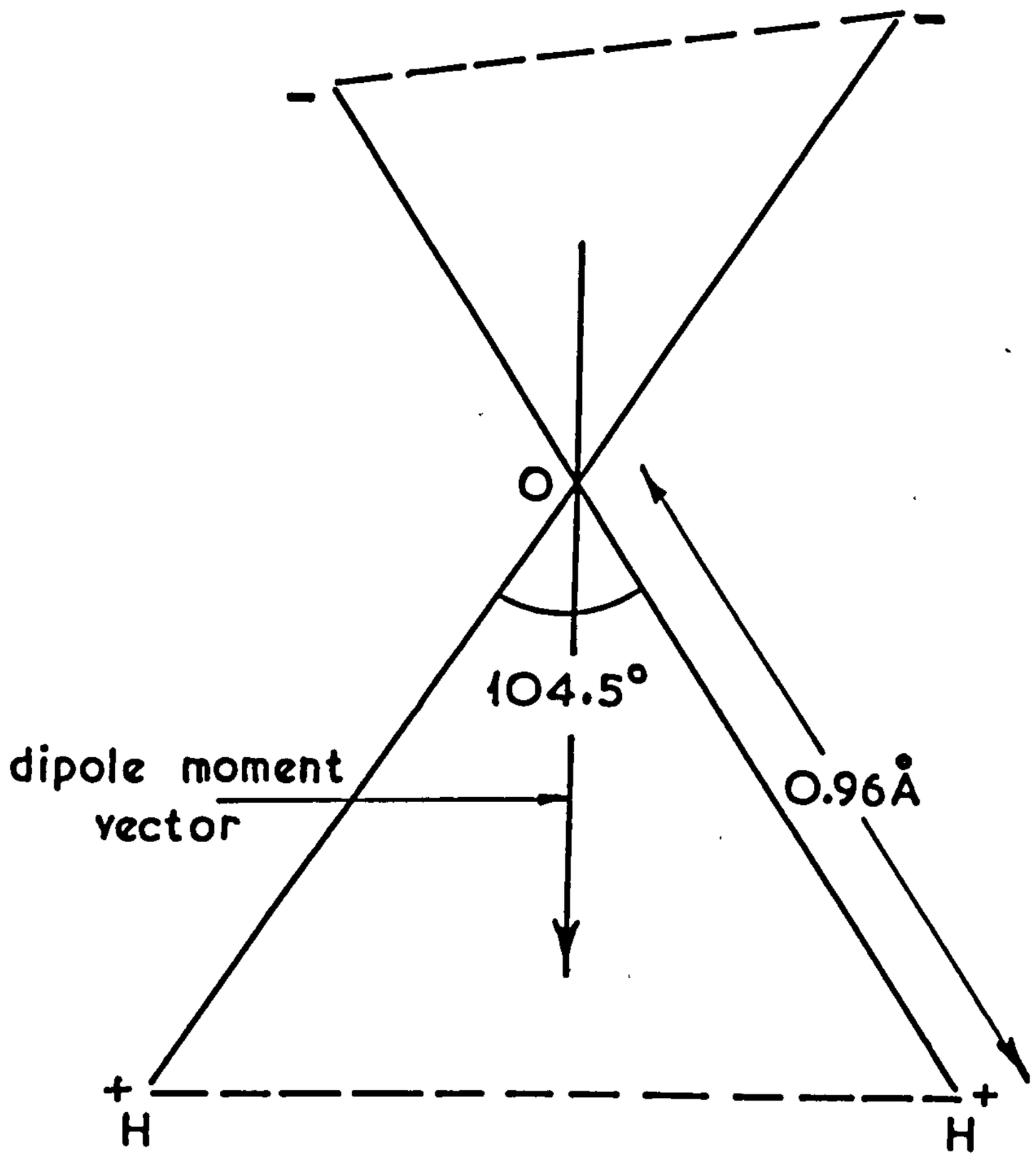

Fig. 3.5 Structure of water molecule (Hasted, 1973).

is thus a polar molecule characterized by a relaxation of about 50 picoseconds and by a single relaxation time, centred around 9.2 picoseconds at 20°C, and the dielectric constant changes from the low frequency value around 80 to 5.5 over this later dispersion region (Hasted, 1973).

The water structure does not exist for any appreciable period of time, but it might well have a meaning on a time scale of the order of picoseconds. According to Hasted (1973), the life times of any dipole ordering and the vibrational and rotational modes of any such structuring

would be very sensitive to changes in pressure, temperature and to the presence of solutes.

Water accounts for between 80% and 90% of the weight of a micro-organism. According to Rose (1976) the water requirements of micro-organisms can be expressed quantatively in the form of the water activity (a_w) of the environment or substrate, this is equal to $^{P}/P_o$, P being the vapour pressure of the solution and P_o the vapour pressure of water. Water has an a_w value of 1.00, this value decreases when solutes are dissolved in water.

Yeasts vary in the optimum a_w values required for growth, but the minimum values for these organisms (0.91 - 0.88) are lower than those of the majority of bacteria (Rose, 1976).

The general effect of lowering the a_w value of a medium below the optimum is to increase the length of the lag phase of growth and to decrease the growth rate and the size of the crop of organisms (Rose, 1976).

It can be concluded that the different ways in which water is bound up with life processes indicates clearly that water, acting as solvent and dispersing and lubricating medium, is also a versatile reactant and that morphologically and functionally, life and water are inseparable . It is therefore hardly surprising that living organisms are sensitively attuned to the properties of water.

3.3 Movement of water across cell membranes

3.3.1 Diffusion and osmosis

Even when the concentration of water on the two sides of a permeable or semi-permeable membrane is the same, water exchanges rapidly in both directions by diffusion. When no other forces are exerted the total amount of water on each side of the membrane remains constant since the diffusion between two solutions of the same water concentration is equal and opposite.

If the solutions separated by the membrane differ in concentration initially then diffusion of the water in the two directions will be unequal and there will be a net transfer of water across the membrane so that the volume of the more dilute solution will be decreased and that of the more concentrated solution will be increased. This process is termed osmosis.

In an artificial system net transfer of water will cease when the hydrostatic pressure increase resulting from the gain in volume of one solution at the expense of the other balances the difference is osmotic pressure of the two solutions.

Theoretically, the osmotic pressure of a one molal solution of any non-electrolyte will be balanced by a hydrostatic pressure difference of 22.4 atmospheres at $0^{o}C$ (approximately 750 ft. of water). At higher temperatures a larger hydrostatic pressure is necessary

to achieve balance since osmotic pressure increases with the absolute temperature according to Charles' law.

$$P_{t_1} = P_{t_2} [1 + \frac{1}{273} (t_1 - t_2)] \qquad (3.7)$$

where P_{t_1} and P_{t_2} are the osmotic pressures at the temperatures t_1 ^oC and t_2 ^oC respectively.

If the ratio of the number of water molecules to the total number of molecules in a solution (molar fraction) is known for both the media bathing the membrane and if the rate of diffusion across themembrane is also known then it is possible to calculate the net rate of water transfer by osmosis

$$H = R(M_1 - M_2)/M_1 \qquad (3.8)$$

where H is the net water transfer; R is the rate of diffusion of water in the direction 1→2; M_1 is the mole-fraction of water in solution 1; M_2 is the mole-fraction of water in solution 2.

It must be clearly recognized , however, that an exact measure of net osmotic transfer can only be obtained from such determinations when the membrane under study is truly semi-permeable that is permeable to water but not to solute particles. Movement of solute particles can modify the water fluxes (Brown, 1961).

3.3.2 Osmosis in biological systems

When yeast cells are placed in deionised water they swell and burst. It is due to osmosis. The cell membrane acts as a semi-permeable membrane, allowing the passage of water into the cell, but not the movement of salts out of the cell. The cell is with a higher osmotic pressure (hypertonic) with respect to the deionised water, and, therefore, water enters the cells, making it at first more spherical (spherocytosis). Finally, the cell membrane ruptures.

If on the other hand, yeast cells are placed in a deionised 0.25M sucrose, they do not change their shape. This is because 0.25 M is isotonic with the cells (two solutions which produce no resultant flow through a semi-permeable membrane are said to be isotonic).

For all the experiments reported in this thesis, the yeast cells were washed and suspended in a 0.25 M sucrose which also served as a nutrient.

CHAPTER 4 DIELECTRIC PROPERTIES OF BIOLOGICAL MATERIALS

4.1 Introduction

Most cells of biological interest possess an electric dipole moment which, in general, gives rise to a high dielectric constant and a well defined dispersion region (Schwan, 1957). The behaviour of a pure polar liquid is shown in Figure 4.1. where it is noticed that the dielectric constant (ε') falls from a high value ε_s to ε_∞ as the frequency increases through the dispersion region. When dispersion occurs, there is a phase lag between the motion of the dipoles and the applied field, with a conseqent loss of energy. The lower curve in Figure 4.1 shows the variation of the energy absorbtion per cycle (ε''), the frequency corresponding to maximum absorption being termed the relaxation frequency f_R. Corresponding to this parameter is a relaxation time $\tau = \frac{1}{2\pi f_R}$

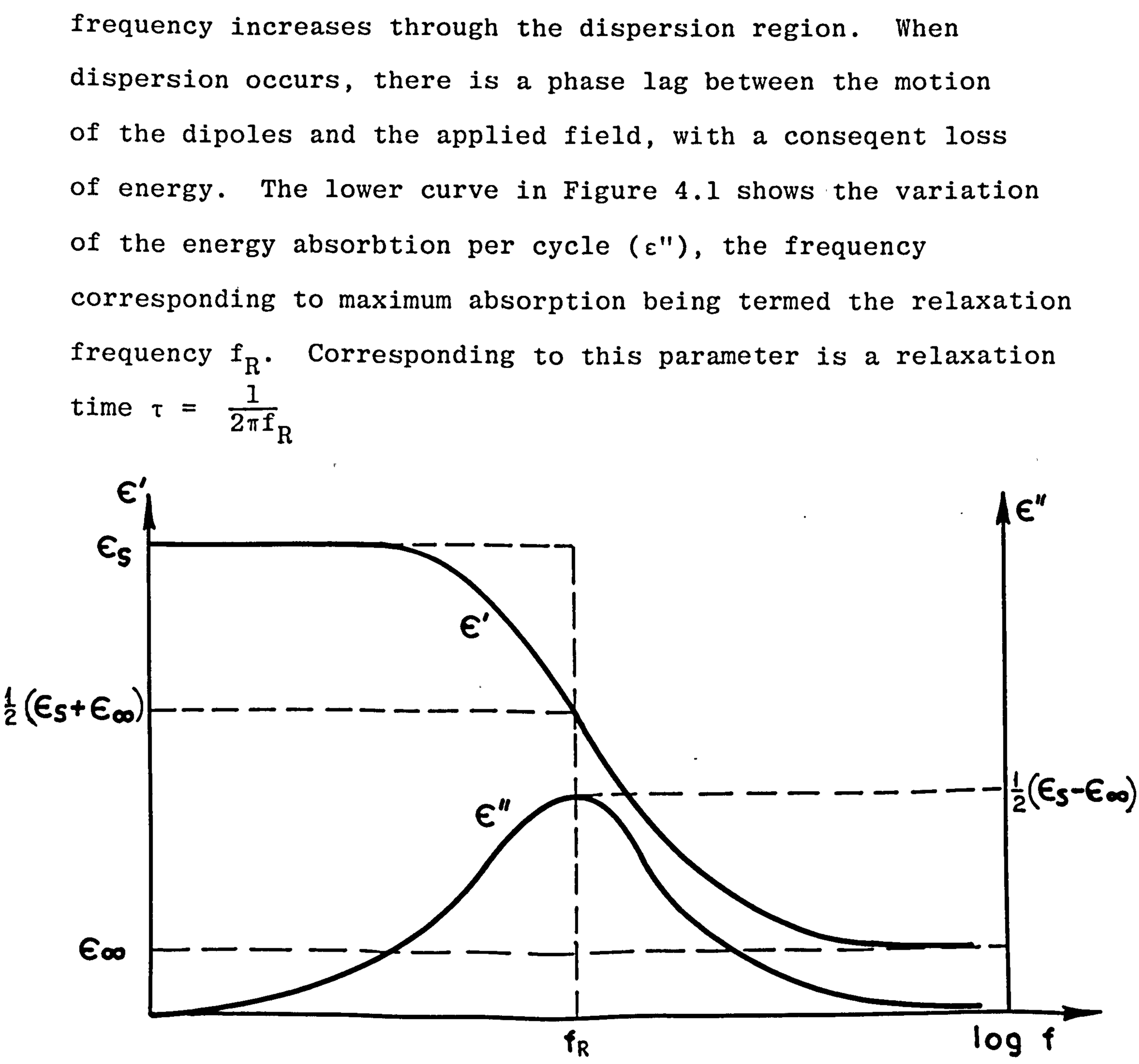

Fig. 4.1 Dispersion (ε') and absorption (ε'') curves for a pure polar liquid.

Both ε' and ε'' may be combined in the form of a complex dielectric constant (ε^*) where

$$\varepsilon^* = \varepsilon' - j\varepsilon'' \qquad (4.1)$$

This notation indicates that the real and imaginary parts of the permittivity are 90^o out of phase with each other.

4.2 Molecular polarizability and dielectric dispersion

Consider an infinite parallel plate capacitor which has been placed in vacuum. If a potential difference V is applied across the plates so that they acquire the charges +Q and -Q respectively per unit area, then the capacitance per unit area (Hasted, 1973) defined as

$$C_o = \frac{Q}{V} \qquad (4.2)$$

If the space between the plates is filled with suspension of yeast cells, then the electric field between the plates will polarize the cells with the result that the charges -P and +P per unit area appear on the surfaces of the substance, inducing a charge of corresponding magnitude but opposite polarity on the plates of the capacitor, which therefore now holds a charge of (Q+P) per unit area, and the capacitance per unit area is increased to

$$C_s = \frac{(Q + P)}{V} \tag{4.3}$$

The relative permittivity of the material between the plates is defined as

$$\varepsilon' = \frac{C_s}{C_o} \tag{4.4}$$

Defining polarizability as the induced dipole moment per unit volume it is obvious that the greater the polarizability of the molecule the higher will be the relative permittivity of the material.

The polarizability of an isolated sphere has been discussed in some detail by Scaife (1971). For a spherical particle of real permittivity ε'_2 and volume of $^4/_3\pi R^3$ (Fig. 4.2) in a continuum of real permittivity ε'_1 behaves as a point dipole (Coelho, 1979) of moment μ given by

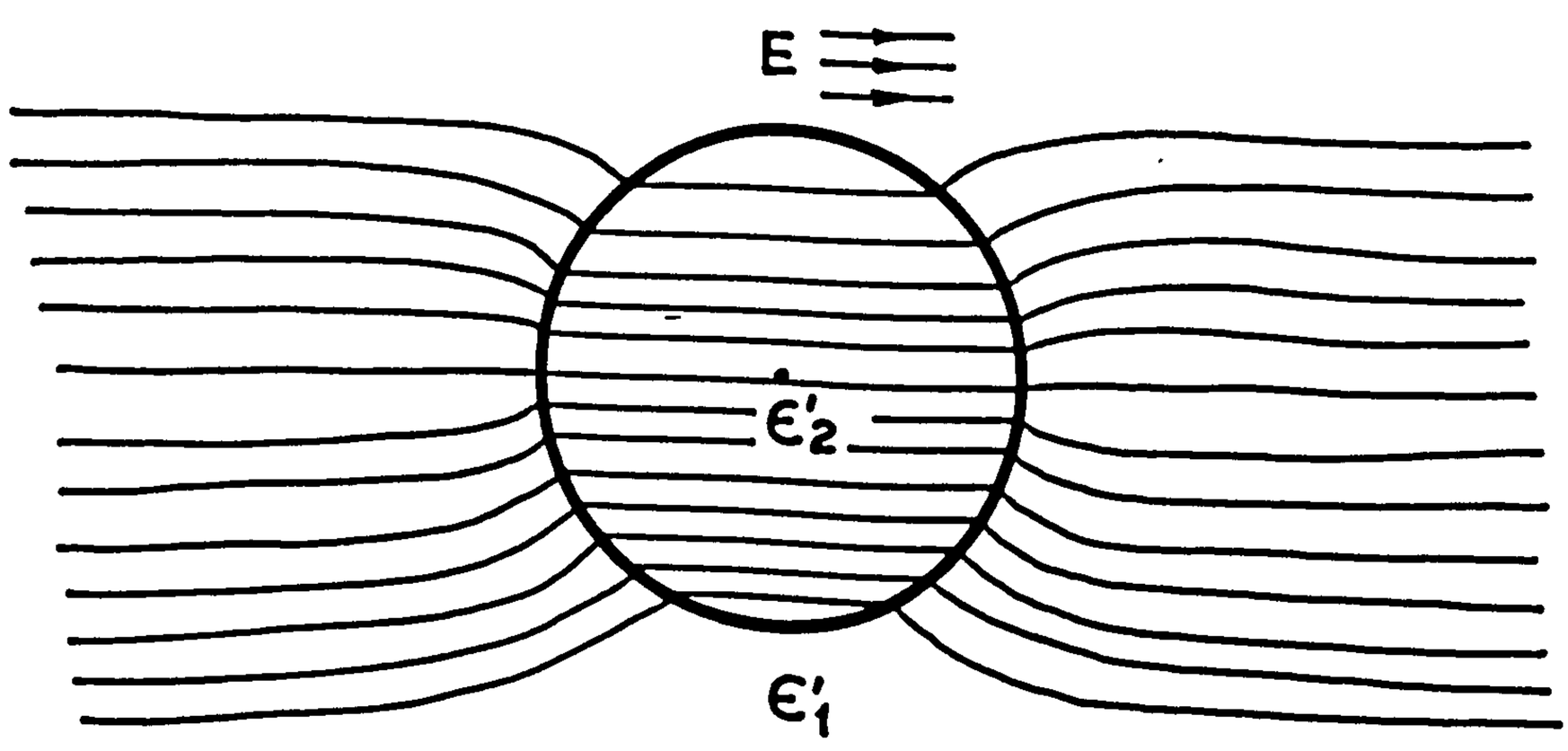

Fig. 4.2 Spherical particle of permittivity ε'_2 in a continuum of permittivity ε'_1 and uniform applied field E.

$$\mu = 4\pi R^3 \varepsilon_o \varepsilon_1' \left(\frac{\varepsilon_2' - \varepsilon_1'}{\varepsilon_2' + 2\varepsilon_1'}\right) E \qquad (4.5)$$

and its polarizability α therefore is

$$\alpha = 3\varepsilon_o \varepsilon_1' \left(\frac{\varepsilon_2' - \varepsilon'_1}{\varepsilon_2' + 2\varepsilon_1'}\right) \qquad (4.6)$$

In the case where R = 2.5 μm (radius of a spherical yeast cell), E = 20 kV m^{-1}, ε_2' = 26000 and ε_1' = 80 μ and α are only of the order of 2.8×10^{-22} C m (or 84×10^6 Debye) and 2×10^{-9} Fm^2.

In addition to the permanent dipole moments the material will also contain dipoles induced by the field. This polarizability arises for two reasons.

(a) Electronic polarization. This is due to the electric field causing a displacement of the electrons relative to the nucleus in each atom.

(b) Atomic polarization, which is due to the atomic nuclei being displaced relative to each other.

In the absence of an electric field, the permanent dipole moments of the molecules are randomly distributed and their direction fluctuates due to the thermal motion of the molecules. However, in the presence of an electric field the molecules tend to align themselves with the field. This orientation polarization in addition to the electronic and atomic polarizations causes an increase in the permittivity of the materials.

The relationship between permittivity and these three types of polarization has been discussed by Hasted (1973) and Von Hippel (1954).

The permittivity of biological material is given in terms of the polarization P by

$$\varepsilon_r = 1 + \frac{P}{\varepsilon_o E} \tag{4.7}$$

where E is the applied field and ε_o is the permittivity of free space.

P, which as introduced above is the density of the surface charge induced on the material, is also the electric moment induced per unit volume. So for N_1 molecules per unit volume, each with an average total moment m

$$P = N_1 m \tag{4.8}$$

and

$$m = \alpha_T E_{av} \tag{4.9}$$

where E_{av} is the average electric field acting on a molecule, that is the local field, and α_T is the total polarizability of the molecules.

$$\alpha_T = \alpha_e + \alpha_a + \alpha_o \tag{4.10}$$

where α_e, α_a and α_o are respectively the electronic, atomic and orientation contributions to the polarizability.

Hence

$$\varepsilon_r = 1 + \frac{N_1 \alpha_T E_{av}}{E\varepsilon_o} \qquad (4.11)$$

Each of the three types of polarizability is in general a function of the frequency of the applied field but it is only α_o which exhibits a strong frequency variation. For example when an alternating electric field is applied to a parallel plate capacitor filled with a suspension of yeast cells, then as the field reverses, the distribution of the molecules and their average orientation must change. When the frequency of the applied field is sufficiently low, then all the three types of polarization can reach the value that they would have had in a steady field equal to the instantaneous value of the alternating field, but as the frequency of the field increases this is no longer the case.

As the frequency increases, first of all the orientation polarization fails to reach its equilibrium value and so polarizability decreases from

$$\alpha_T = \alpha_e + \alpha_a + \alpha_o$$

to

$$\alpha_T = \alpha_e + \alpha_a$$

with related decrease in permittivity and the occurence of an absorption. At much higher frequencies, comparable with the natural frequencies of vibration of the atoms within the molecule, further dispersions occur, first as the atomic polarizability fails to reach its equilibrium value, and then at optical frequencies the electronic polarization behaves in the same way.

4.2.1 The Maxwell-Wagner dispersion

The dielectric relaxations due to the orientation, atomic and electronic polarizations were discussed in the previous section. There are numerous other possible mechanisms to account for dielectric dispersion and one of importance to the present work is the Maxwell-Wagner dispersion. This occurs in a dielectric specimen which is inhomogeneous, and is made up of components each having a different permittivity and conductivity. Biological materials are particularly rich in such heterogeneous systems (Muller, 1969).

In the case of spherical particles having a real permittivity ε_2' and a conductivity σ_2, sparsely distributed throughout some other dielectric whose real permittivity is ε_1' and a negligibly small conductivity, the apparent permittivity observed for the material as a whole is found to be (Buchanan, 1952 and Hasted 1973).

$$\dot{\varepsilon}' = \varepsilon_\infty \left(1 + \frac{K}{1 + \omega^2\tau^2}\right) \qquad (4.12)$$

where

$$\varepsilon_\infty = \varepsilon_1' \left(1 + 3V_2\left(\frac{\varepsilon_2' - \varepsilon_1'}{2\varepsilon_1' + \varepsilon_2'}\right)\right)$$

$$K = \frac{9V_2\varepsilon_1'}{2\varepsilon_1' + \varepsilon_2'}$$

$$\tau = \frac{2\varepsilon_1' + \varepsilon_2'}{4\pi \times 0.9 \times 10^{12}\sigma_2}$$

where V_2 is the volume fraction of the spherical particles.

For

$$\omega^2\tau^2 \ll 1$$

$$\varepsilon' = \varepsilon_\infty (1 + K) \qquad (4.13)$$

and for

$$\omega^2\tau^2 \gg 1$$

$$\varepsilon' = \varepsilon_\infty \qquad (4.14)$$

This gives a frequency dependence for the apparent dielectric constant which is identical in form with that given by Debye equations referred to in section (4.3).

4.3 The dielectric parameters investigated for the magnetic resonance measurements

In practice, the investigation of dielectric behaviour involves the measurement of ε' and ε'' as a function of frequency and temperature through measurement of capacitance and loss tangent of a sample of known dimension from which the dispersion, $\varepsilon' = \frac{cd}{A\varepsilon_o}$, and loss tangent, $\tan\delta = \frac{\varepsilon''}{\varepsilon'}$ may be deduced . These, in turn, are interpreted in terms of structure. For biological material this may be quite a complicated procedure due to the possible presence of several dispersion regions which, in some cases, may overlap (Grant, 1965 and Schwan, 1965).

The simplest case is a single dispersion region with a single relaxation time which conforms to the Debye (1929) equations

$$\varepsilon' = \varepsilon_\infty + \frac{(\varepsilon_S - \varepsilon_\infty)}{1 + \omega^2\tau^2} \qquad (4.15)$$

$$\varepsilon'' = \frac{(\varepsilon_S - \varepsilon_\infty)\omega\tau}{1 + \omega^2\tau^2} \qquad (4.16)$$

which are derived from

$$\varepsilon^* = \varepsilon' - j\varepsilon'' = \varepsilon_\infty + \frac{(\varepsilon_S - \varepsilon_\infty)}{1 + \omega^2\tau^2} \times (1 - j\omega\tau) \qquad (4.17)$$

Pure water is an approximation to the above case although a small distribution of relaxation is also possible. When a spread of relaxation times exists, several distribution functions are available leading to appropriate modification in equations (4.15) and (4.16) . Cole and Cole (1941) have deduced the following equation for the case of a distribution of relaxation times

$$\varepsilon^* = \varepsilon' - j\varepsilon'' = \varepsilon_\infty + \frac{\varepsilon_S - \varepsilon_\infty}{1 + (j\omega\tau)^{1-\alpha}} \qquad (4.18)$$

where α is the parameter $0 < \alpha \leq 1$. For a single relaxation time $\alpha = 0$ and α tends to 1 as the distribution tends to an infinite one.

A common way of representing results is to plot ε'' against ε' (a Cole-Cole plot) which will result in a semicircle with its centre on the ε' axis if the Debye equations are obeyed. If, on the other hand, the dielectric behaviour approximates more to equation (4.18) a semicircle will be obtained with its center below the axis. Another

possibility is a skewed arc (Davidson and Cole, 1950). If two overlapping dispersions are present, the shape of the Cole-Cole plot will be suitably modified. The Cole-Cole plot for a single relaxation time is shown in Figure 4.3.

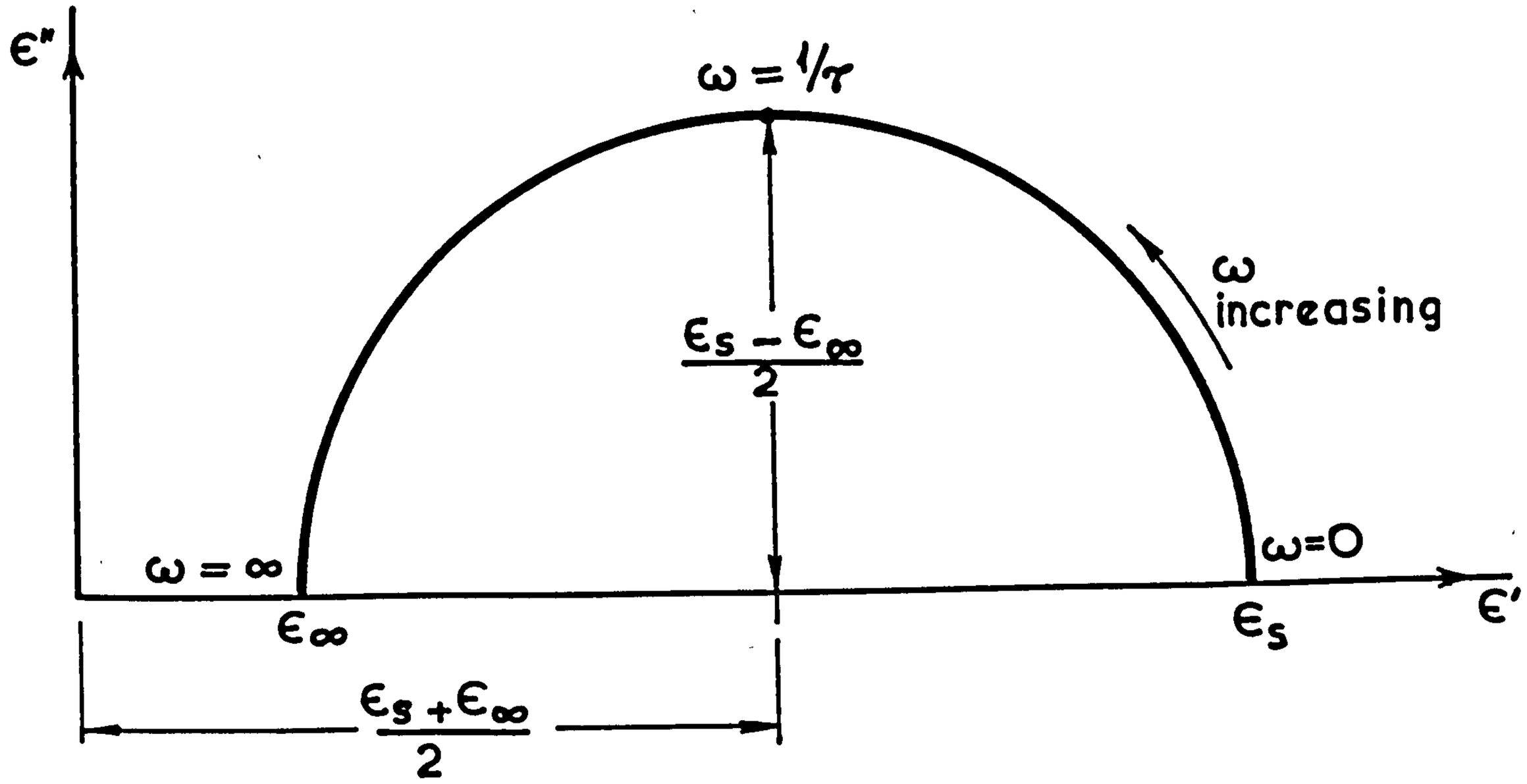

Figure 4.3 Construction of the Cole-Cole diagram.

The dielectric dispersion measurements can also be used to obtain information about the effective size of the molecule (Schwarz, 1962) in solution and the activation enthalpy of the substance (Pethig, 1979).

Debye (1947) suggested that the dielectric relaxation of a polar molecule in solution might be treated as being analogous to the motion of a sphere rotating in a continuous, viscous medium having the viscosity of the liquid in bulk, and applying Stoke's Law he derived the formula

$$\tau = \frac{4\pi\eta a^3}{kT} \qquad (4.19)$$

where τ is the relaxation time

η the viscosity of the solution, which for dilute solutions will be approximately that of water

and a is the radius of the molecule.

τ is also a measure of the time taken for the molecule rotating in a field to overcome a certain potential barrier ΔH. ΔH is defined as the activation enthalpy of the substance and the potential barrier is due to the local interactions between the molecule and the environments, and can be attributed to the breaking of chemical bonds.

The value of the activation enthalpy can be calculated using the Arrhenius relation for rate coefficients

$$\frac{1}{\tau} = \frac{kT}{h} \exp\left(\frac{-\Delta H}{RT}\right) = A \exp\left(\frac{-\Delta H}{RT}\right) \qquad (4.20)$$

where ΔH is the activation enthalpy

h Planck's constant

R the gas constant

τ can be found from dielectric loss measurements by finding the frequency f_m ($f_m = \frac{1}{2\pi\tau}$) which the loss factor ε'' reaches a maximum.

CHAPTER 5 BIOLOGICAL DIELECTROPHORESIS

5.1 Introduction

Dielectrophoresis, the motion produced by the action of nonuniform electric field upon a neutral object, has been shown (Pethig, 1979) to be a simple and useful technique for the study of cellular organisms.

Cell dielectrophoresis can be observed in aqueous media with living cells even though both the medium and the cell are quite dependent upon the frequency of the applied field a.c. fields, as well upon the complex permittivity (ε^*). In view of the complex permittivity and frequency effect, simple dielectric theory based upon only static dielectric constant, while applicable to perfect insulators, proves to be inadequate for biological systems. A more detailed analysis is needed (Pohl, 1972). Dielectrophoresis applied to suspensions of cells shows that the collection rate of these bodies at the regions of highest field strength does reflect the effective differential complex permittivities, including both the dielectric constant and the conductivity factors, differential in the sense of directly comparing the difference between the total polarization of the body and that of the medium in which it is suspended ($\varepsilon_2^* - \varepsilon_1^*$). When applied to biological cells, dielectrophoresis readily reflects those polarization mechanisms sensitive to their physiological state.

5.2 Basic theory of dielectrophoresis

Cell dielectrophoresis is based on the fact that cells with different electrical characteristics will behave differently in a non-uniform electric field. The effect of a non-uniform electric field on a dielectric particle free to move depends on the charge and dielectric constant of the particle considered.

If the particle possesses a net charge then there is an electrostatic interaction between the charge and the field, resulting in particle motion. This motion is known as electrophoresis.

If the material contains permanent dipoles, they will tend to align with the field and will then experience a force in the direction of field gradient toward the strongest field if $\varepsilon_p > \varepsilon_m$ and away if $\varepsilon_p < \varepsilon_m$. The material will also contain dipoles induced by the field and these too will be forced in the direction of increasing field strength. The translational motion of a particle due to the interaction of a non-uniform electric field with all of its dipoles either permanent or induced and expressed through the dielectric constant has been termed dielectrophoresis (Pohl, 1972). The force associated with this motion is termed the dielectrophoretic force.

The force on a small dielectric sphere in a nonuniform field suspended in a fluid medium based on that given by Pethig (1979) can be derived in the following way:

First consider a small sphere of an ideal dielectric (zero conductance) of relative dielectric constant ε_2 in an ideal dielectric fluid of relative dielectric constant ε_1, and of infinite extent in which an electric field is present. If the field in the fluid medium is uniform before the insertion of the sphere, then the field is distorted by the sphere to give a field interior to the sphere boundary, E_{in}, associated with an external field E is given by

$$E_{in} = \left(\frac{3\varepsilon_1}{\varepsilon_2+2\varepsilon_1}\right) E \qquad (5.1)$$

In a static field at equilibrium, the net translational force on a small neutral body at equilibrium is given by

$$F = (\mu.\nabla)E \qquad (5.2)$$

where μ is the dipole moment vector, ∇ is the del vector, and E is the external electric field. For the case where the neutral dielectric is homogeneously, linearly and isotropically polarizable the dipole moment is given by

$$\mu = \alpha V E \qquad (5.3)$$

where α is the polarizability , V is the volume of the body, then it can be seen that

$$F = \alpha V\ (E.\nabla)E$$

$$= \tfrac{1}{2}\alpha V \nabla |E|^2 \qquad (5.4)$$

The induced polarization per unit volume is

$$H = \varepsilon_o (\varepsilon_2 - \varepsilon_1) E_{in} \qquad (5.5)$$

The induced moment μ, of a polarizable sphere

$$\mu = VH = \alpha VE$$

From equation (5.1) and (5.5) the polarizability α per unit volume is given by

$$\alpha = \frac{H}{E} = \varepsilon_o(\varepsilon_2 - \varepsilon_1) \frac{E_{in}}{E}$$

$$= 3\varepsilon_o\varepsilon_1\left(\frac{\varepsilon_2 - \varepsilon_1}{\varepsilon_2 + 2\varepsilon_1}\right)$$

Hence total dielectrophoretic force F equation (5.4) acting on the small sphere of volume $V = \frac{4}{3}\pi a^3$ is given by

$$F = 2\pi a^3 \varepsilon_o \varepsilon_1 \left(\frac{\varepsilon_2 - \varepsilon_1}{\varepsilon_2 + 2\varepsilon_1}\right) \nabla |E|^2 \qquad (5.6)$$

From equation (5.6) it is useful to note that the dielectrophoretic force effect has built - in restrictions as regards the role of the dielectric constants. The force does not, as might at first glance be inferred, increase without limit as small body becomes very polar. The force (net force on the body) is of course zero if the two dielectric constants are equal. But if the sphere is given a larger and larger dielectric constant, the force increases only to a limited amount determined by the dielectric

constant of the surrounding medium (from equation (5.6) for $\varepsilon_2 = \infty$ and $\varepsilon_1 = 1$ the net force F is 1).

Equation (5.6) , however, contains no provision for conduction or frequency effects. In order to account for the observed variations of dielectrophoresis with frequency and conductivity, a particular simple investigation scheme should be considered. This is achieved by replacing the simple (absolute) dielectric constant, ε, equation (5.6) by the complex (absolute) dielectric constant, or permittivity.

$$\varepsilon^* = \varepsilon' - j\varepsilon'' = \varepsilon' - j\frac{\sigma}{\omega}$$

in the expression

$$F \propto \varepsilon_1\left(\frac{\varepsilon_2 - \varepsilon_1}{\varepsilon_2 + 2\varepsilon_1}\right) \rightarrow R_e \tilde{\varepsilon}_1^*\left(\frac{\varepsilon_2^* - \varepsilon_1^*}{\varepsilon_2^* + 2\varepsilon_1^*}\right) \qquad (5.7)$$

where the terms ε_2 and ε_1 are now complex quantities, ε_2^* and ε_1^*, and $\tilde{\varepsilon}_1^*$ is the complex conjugate of ε_1^*. From equation (5.7) it can be seen that, the difference term $(\varepsilon_2^* - \varepsilon_1^*)$ is now focussed upon and its absolute value is pulled out.

Equation (5.6), can now be written as

$$F = 2\pi a^3 \varepsilon_o \tilde{\varepsilon}_1^* \left(\frac{\varepsilon_2^* - \varepsilon_1^*}{\varepsilon_2^* + 2\varepsilon_1^*}\right) \nabla |E|^2 \qquad (5.8)$$

where F is the total force upon the spherical particle of volume $\frac{4}{3}\pi a^3$ in an external electric field which has a value E at a great distance from the particle.

5.2.1 Comparison of dielectrophoresis and electrophoresis

An illustration of the contrast between electrophoresis and dielectrophoresis is given in figure 5.1. Here positive , negative and neutral particles are in a non-uniform field produced by two concentric spheres.

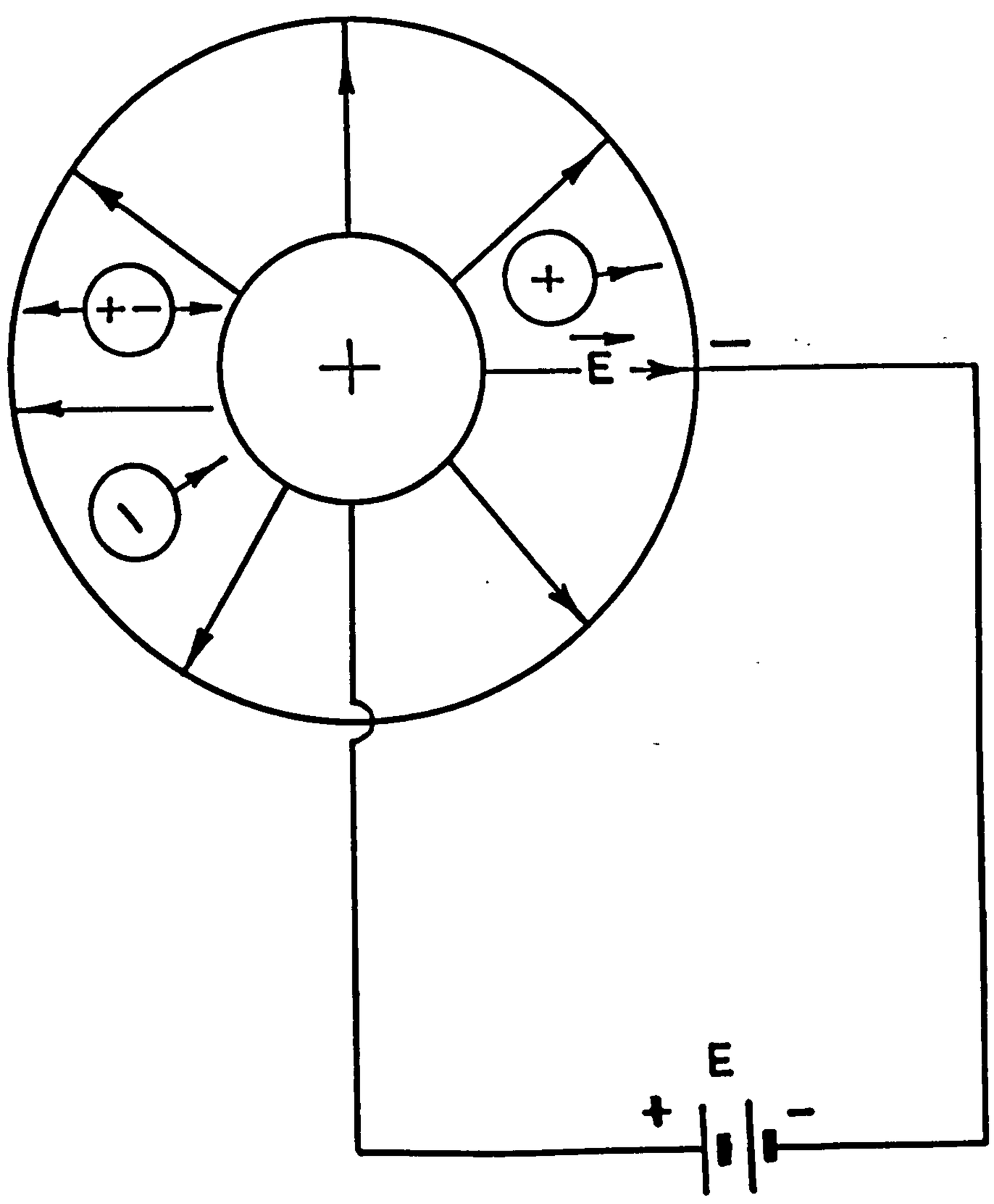

Figure 5.1 Electrophoresis and dielectrophoresis

The charged particles obey the laws of electrostatics and move to the oppositely charged electrodes, the positive charge toward the outer wall and the negative charge toward the central sphere. The neutral particle is polarised by the field and its individual charges lie in a stronger

field than the positive charges, they experience a stronger force. The result is a net force on the particle in the direction of the central electrode. A change in polarity of the electrodes causes the charge particles to reverse their directions of motion. The neutral particle, however, continues to be pulled inward. An alternating electric field will cause the electrophoresis forces to average to zero, leaving only the dielectrophoresis effects. In dielectrophoretic studies it is therefore important to use alternating fields.

Dielectrophoresis deposits volume of particles proportional to the applied voltage during equal time of deposition provided a substantial difference exist in the relative permittivities of the particle and the surrounding medium [that is $(\varepsilon_2^* - \varepsilon_1^*) \geq 1$]. Electrophoresis can be appreciable even when the free charge per unit volume of the particle is quite small, it is unlike dielectrophoresis in that it does not depend upon the particle volume (and hence upon the total polarization available), but rather upon the free charge on the particle.

5.2.2 Pearl-chain formation (the yield)

The pearl-chain or bunching effect is the stringing, clumping or bunching of groups of neutral particles by the action of an applied field. It is particularly evident when particles of high dielectric constant suspended in a medium of lower dielectric constant are subjected to an

external a.c. field and undergo dielectrophoresis.

Particles undergoing dielectrophoresis often exhibit a mutual attraction. The pearl-chain formation arises in the following way. The particles which have a polarizability larger than that of the surrounding medium, distort the field. Each particle then experiences a nonuniform field near the other. As each is already polarized by the external field, the particles are then attracted to the regions of higher field intensity near each other. The average length of the chains of cells collected after a specified time interval is reported as the 'yield' or 'dielectrophoretic' collection rate (DCR).

If the spherical particle has a dielectric constant higher than that of the surrounding fluid medium, that is $\varepsilon_2 > \varepsilon_1$, then the field lines external to it tends to focus or concentrate at the surface of the sphere (Fig. 5.2). This inhomogenity of the field about the particle causes two or more particles to be mutually attracted.

5.2.2.1 Theory of Pearl-chain growth from a cell suspension

In equation (5.8) the force upon a suspended spherical particle exerted by nonuniform electrical field was given as

$$F = {}^{3}/_{2}\ V\ \mathrm{Re}\ \{\tilde{\varepsilon}_1^* \frac{(\varepsilon_2^*-\varepsilon_1^*)}{(\varepsilon_2^*+2\varepsilon_1^*)}\}\nabla|E_o|^2 \qquad (5.9)$$

the dielectric constants factor may be replaced by P given by

$$P = \mathrm{Re}\ \{\ \varepsilon_1^* \frac{(\varepsilon_2^*-\varepsilon_1^*)}{(\varepsilon_2^*+2\varepsilon_1^*)}\ \} \qquad (5.10)$$

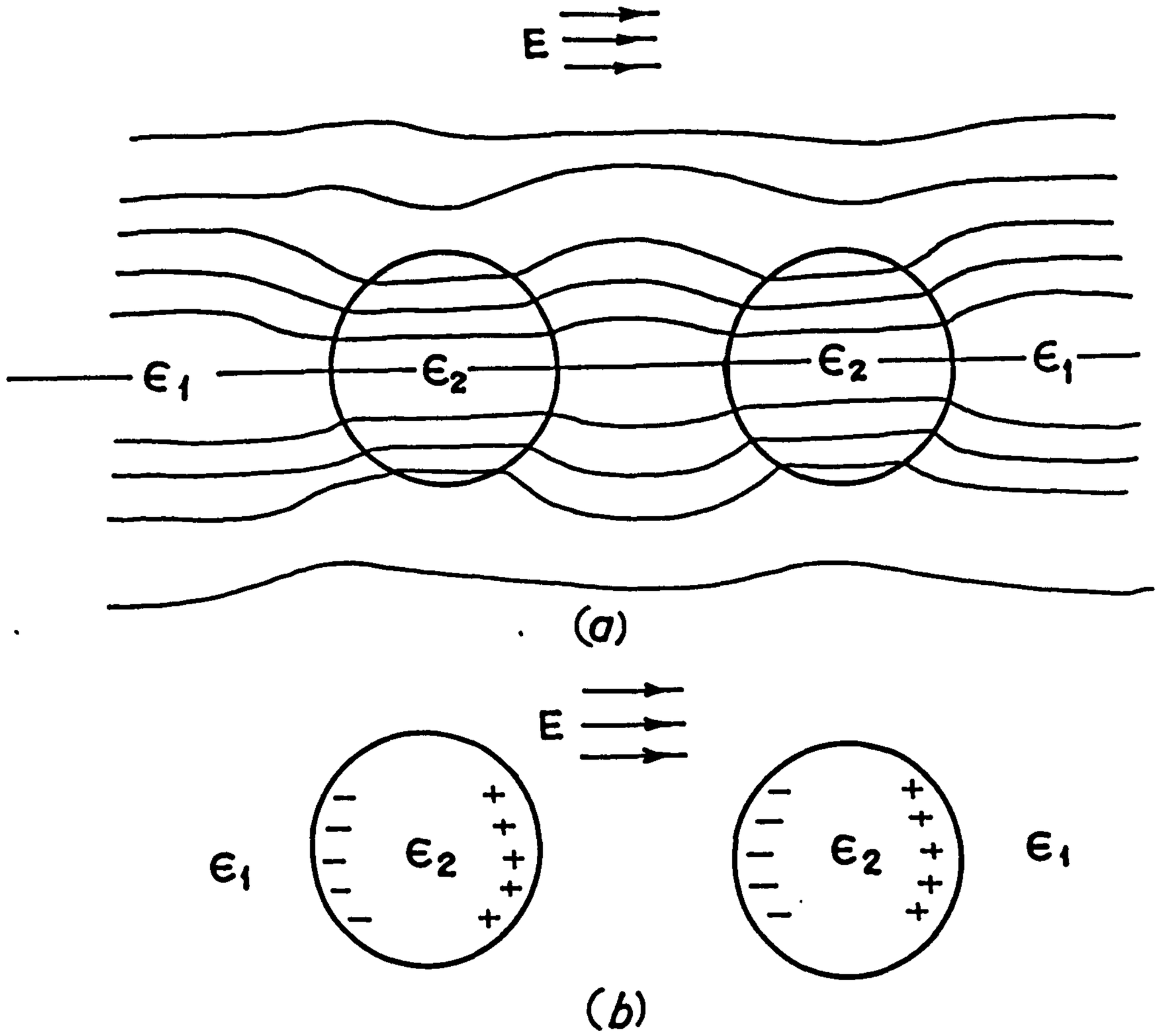

Fig. 5.2 (a) Two particles close to each other in a medium with dielectric constants $\varepsilon_2 > \varepsilon_1$ and their effect on the field. (b) Polarization produced by the two particles when $\varepsilon_2 > \varepsilon_1$. (c) Dipoles are attracted rather than repulsed when the two particles are subjected to an external field.

This bunching effect due to the enhancement of field nonuniformity by the particles themselves, frequently causes the formation of pearl-chain of cells.

Hence equation (5.9) can be rewritten as

$$F = {}^{3}/_{2}\ V\ P\ \nabla\ |E_o|^2 = 2\pi a^3 P \nabla |E_o|^2 \qquad (5.11)$$

By specifying the electrode geometry, the resulting field and the corresponding force could be determined. The rate of the collection of a suspension of similar bodies can be found from the knowledge of the force on the body which results in the prediction of its motion. The force in a radial field can be derived following Pohl (1972).

Mirrored symmetry exists between two rounded pin tips and the electric field is essentially that between a round pin tip and a flat plate electrode. The field is approximately the same as that produced by concentric spherical electrodes near one of the spherical pin tips. This type of geometry is like those which are used for the work described in this thesis and will be considered here.

At some radius r the potential between two concentric spheres of radii r_1 and r_2 such that $r_1 << r_2$ is

$$V_o = \frac{v_1 r_1 (r_2 - r_1)}{(r_2 - r_1)_r} \qquad (5.12)$$

where v_1 is the r.m.s.a.c. potential of the inner spherical electrode, and $v_2 = 0$. Since

$$E_o = - \nabla V_o = \frac{v_1 r_1}{r^2} \left(\frac{r_2}{r_2 - r_1} \right) r_o \qquad (5.13)$$

$$(E_o)^2 = \frac{v_1^2 \, r_1^2 \, r_2^2}{r^4 (r_2 - r_1)^2} \qquad (5.14)$$

and

$$\nabla |E_o|^2 = - 4 \left[\frac{v_1 r_1 r_2}{r_2 - r_1} \right]^2 \frac{r_o}{r^5} \qquad (5.15)$$

where r_o is the unit r-vector, from (5.11) the force on a spherical particle in this field is given by

$$F = - \frac{8\pi v_1^2 \, r_1^2 \, r_2^2 \, P \, a^3}{r^5 (r_2 - r_1)^2} r_o \qquad (5.16)$$

When P is positive the negative sign indicates that the force is directed inwards towards the region of strongest field.

A spherical particle will experience a viscous drag force (Stokes law) opposing its motion when it moves under the action of the dielectrophoretic force (5.16).

$$F_d = -6\pi a \eta v \qquad (5.17)$$

where η and v are the viscosity of the suspending fluid and particle velocity through the medium respectively. Under dynamic equilibrium

$$F + F_d = 0 \tag{5.18}$$

By substituting (5.18) into (5.16) an equation for the velocity can be obtained

$$V = -\frac{4}{3}\frac{v_1^2 r_1^2 r_2^2 P a^2}{\eta r^5 (r_2-r_1)^2} \quad r_o = \frac{dr}{dt} r_o \tag{5.19}$$

For a particle to travel from a radial distance r_o to the central electrode the required time is given by

$$t = \int_o^t dt = r_o \int_{r_o}^{r_1} \frac{dr}{v} \tag{5.20}$$

From (5.19) into (5.20) and integratedgives

$$t = \frac{\eta(r_2-r_1)^2(r_o^6-r_1^6)}{8a^2 v_1^2 r_1^2 r_2^2 P} \tag{5.21}$$

By taking $r_o > 2r_1$ for most cases of interest, and then as $r_o^6 > 64r_1^6$ equation (5.21) may be reduced to

$$t \simeq \frac{\eta(r_2-r_1)^2 r_o^6}{8a^2 v_1^2 r_1^2 r_2^2 P} \tag{5.22}$$

The particles collected, normally projecting outward from the inner electrode in the form of a pearl-chain formation and is approximately cylindrical in shape with an approximate volume v_c given as

$$v_c = y d\sigma \quad = y\ r_1^2\ d\Omega \tag{5.23}$$

where y is the length of the chain (that is the yield) and $d\sigma$ is the cross sectional area at which the point of attachment to the central electrode subtends a solid angle $d\Omega$ generated at the center of the electrode. If $r_o >> a$, then the volume of suspension swept out to form the pearl chain during time t is just the volume of the cone of solid angle $d\Omega$ extending out to a distance of r_o, as sketched in Fig. 5.3. This volume v_s swept out in time t is

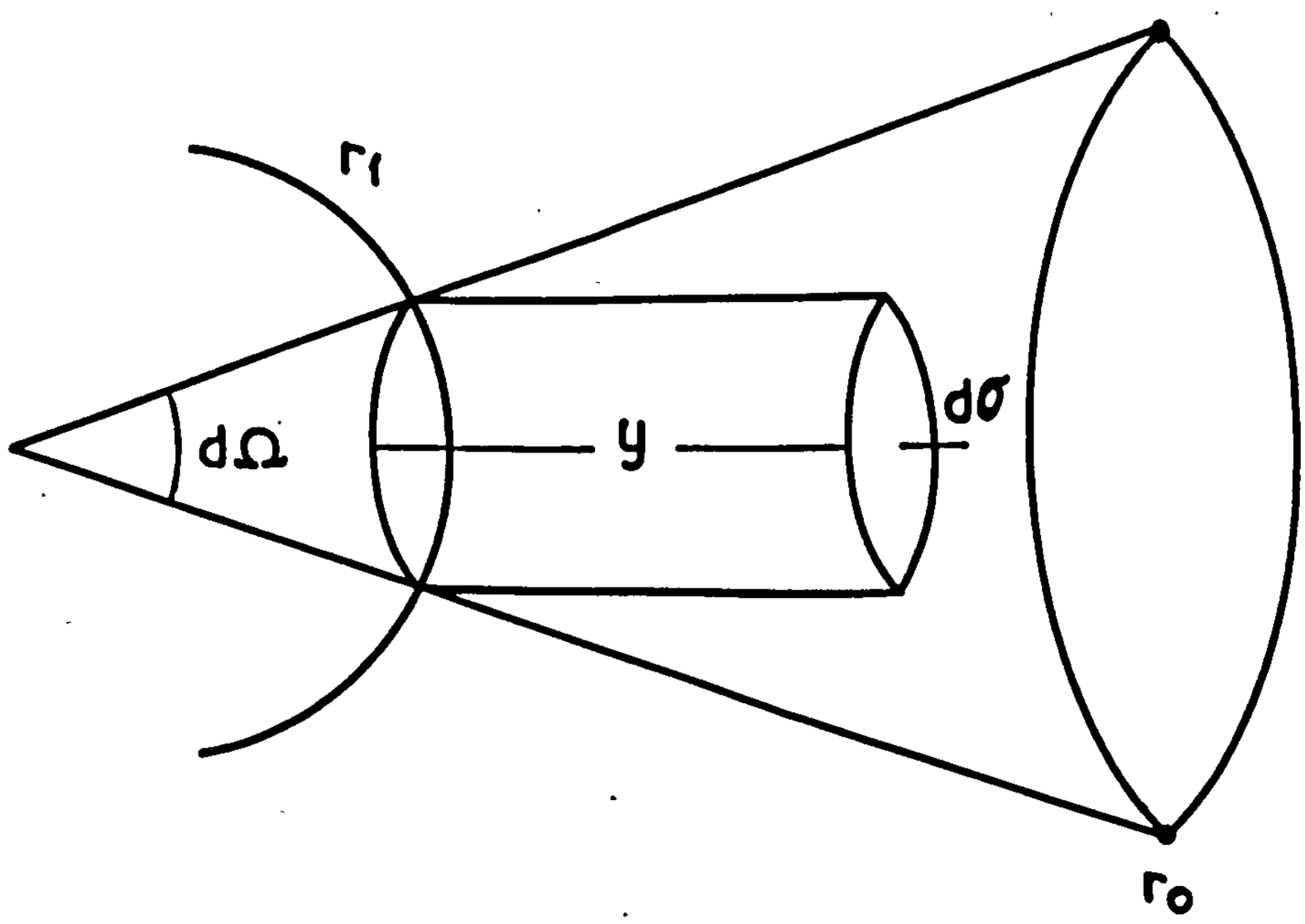

Fig. 5.3. Relation of the volume of suspension swept out in time t to the volume of a pearl-chain of particles.

$$v_s = \frac{(r_o^3 - r_1^3)}{3} d\Omega \simeq \frac{r_o^3}{3} d\Omega \tag{5.24}$$

The volume of particles contained in this cone is given by

$$v_c = \frac{4\pi a^3}{3} c\, v_s \tag{5.25}$$

where c is the concentration of particles. By using equations (5.23), (5.24) and (5.25) an equation for the yield can be obtained as

$$y = \frac{4\pi a^3 c\, r_o^3}{9\, r_1^2} \tag{5.26}$$

r_o^3 can be obtained by solving (5.22) and then substituting in (5.26) gives

$$y = \frac{8\pi c v_1 r_2 a^4}{9 r_1 (r_2 - r_1)} \left[\frac{2tP}{\eta}\right]^{\frac{1}{2}} \tag{5.27}$$

By substituting (5.10) in (5.27) one obtains

$$y = \frac{8\pi c v_1 r_2 a^4}{9\, r_1 (r_2 - r_1)} \left[\frac{2t\, \tilde{\varepsilon}_1^* (\varepsilon_2^* - \varepsilon_1^*)}{\eta(\varepsilon_2^* + 2\varepsilon_1^*)}\right]^{\frac{1}{2}} \tag{5.28}$$

Application of equation (5.28) to real systems (that is, to real, not "perfect" dielectric) shows good agreement with experiment in some respects. Linear response of the yield with voltage over much of the range and the amount of cells collected would vary directly with the square root of the time, $y \propto t^{\frac{1}{2}}$.

5.3 The mechanisms involved in the response of the living cells to a nonuniform electric field over the suspending medium

The cells will be polarised by the application of an electric field. The polarised dipole will be unequally pulled upon in a nonuniform field and a net force would results.

For the cells to move to the region of highest field intensity, they must therefore exhibit higher polarizability equation (5.8) than the suspending medium, which is in fact a highly polar material and it will itself be strongly pulled towards the region of the highest field intensity by the nonuniform field.

The cells, however, attain the higher polarizability in a number of ways. Firstly, the cell itself is largely water. Secondly, there are dissolved in the intra cellular regions numerous polar molecules (Proteins, DNA, RNA, etc.). all of which can contribute to the polarization . Thirdly, there are structured regions which can act as capacitive regions (e.g. lipid membranes across which the electrolytes can act to produce charge distribution). Fourthly, there are structured areas in the surface where ionic double layers can produce enormous values of polarization.

However when the live cells are killed their response to a nonuniform field is somewhat different. Cells - - - had been killed by exposing the freezedried powder to a

TUV lamp (254 nm) overnight which inflicts damage to the membrane and the nucleus. The nucleus appeared granular as it observed under phase contrast microscope, and resulted in the cells being unable to reproduce. For these cells the dielectrophoresis did not reflect those polarization mechanisms sensitive to their physiological state as for the live ones.

CHAPTER 6 MAGNETIC PROPERTIES OF BIOLOGICAL MATERIALS

6.1 Introduction

Atoms or molecules having no unpaired electrons are diamagnetic (e.g. water, glass, mercury, bismuth, oxygen ions O^{--}), that is they have negative values of magnetic susceptibility (Selwood, 1956) which are independent of the magnetic field and temperature. Atoms or molecules with unpaired electrons (e.g. atomic hydrogen, free sodium atoms, molecular oxygen) are paramagnetic with a positive, field independent magnetic susceptibility and positive temperature dependence. Although most of the biological materials are diamagnetic, some are paramagnetic (e.g. oxyhemoglobin and other blood-colouring derivatives of hemoglobin are diamagnetic, whereas the hematin and heme are paramagnetic). In general biological materials may be diamagnetic, paramagnetic or rarely ferromagnetic.

The ferromagnetic properties of the biological materials had been investigated by Baker (1980). He had found that a wide range of animals were able to orient toward home when subjected to displacement-release experiments. When comparable experiments were performed on blindfolded humans, a similar ability emerged. In his experimental series included ten separate journeys to eight different release sites. Altogether, the series produced 86 individual estimates of home direction. He had also found that the orientation in humans were influenced by placing at the backs of their heads bar

magnets. The estimates made by the control subjects wearing brass bars were significantly clustered about the home direction. At neither site, however, was this true for the experimental subjects wearing magnets.

Gould (1980) had suggested that the ability of humans and animals to detect a magnetic field may be associated with deposits of magnetite which have been found in a variety of organisms. In vertebrates, magnetic remanence had been found most often in the head region (in the anterior part of the head in an area associated roughly with the olfactory region but not directly with brain tissue).

6.2 Basic magnetism

The magnetic induction or magnetic flux density B is given by

$$B = \frac{\Phi}{A} \qquad (6.1)$$

where ϕ is the total flux passing through an area $A(m^2)$ and is measured in Webers, the unit of flux density is the Weber per square metre (W/m^2) or tesla. One Weber per square metre (1T) = 10,000 gauss. The relationship between the flux density B and field intensity H is given by

$$\mu = \frac{B}{H} \qquad (6.2)$$

where $\mu = \mu_r \mu_o$ is the permeability of the material, μ_r and μ_o are the relative and free space permeabilities and H is the magnetic field strength or intensity, and is measured in the ampere-turn per metre (A_t/m).

The relationship between intensity of magnetization and magnetic field can be expressed by

$$M = \chi_m H \qquad (6.3)$$

where χ_m is the magnetic susceptibility and M is the magnetic moment per unit volume of a magnetic substance. The magnetic induction or magnetic flux density B is related to M by the expression:

$$B = \mu_o (M + H) \qquad (6.4)$$

Magnetic materials can be classified according to their χ_m value and the way in which this varies with magnetic field intensity and temperature (Rudden, 1971) The categories into which magnetic substances can be divided are ferromagnetic, paramagnetic and diamagnetic. Biological materials may be diamagnetic, paramagnetic or ferromagnetic.

6.2.1 Diamagnetic substances

In principle, the diamagnetic effect takes place in all materials, but is normally swamped by the much greater paramagnetic effect. The basic principle of diamagnetic behaviour is that of Lenz's Law, an induced current is always in such a direction as to oppose the motion or change causing it.

Considering a current loop with its associated magnetic field any attempt to change the magnetic flux linking the loop by applying an external field, B, a current is induced in such direction that the magneticfield resulting from the induced current counteracts the field B. Suppose now that the electrical resistance of the loop is zero; the induced current will then persist as long as the external field is present. Such a situation is realised in the loop current represented by the motion of an electron in an atomic orbit producing a contribution to the diamagnetic susceptibility.

With reference to Figure 6.1 in which an arbitrary direction for the angular momentum vector P_a relative to the magnetic field B is assumed,

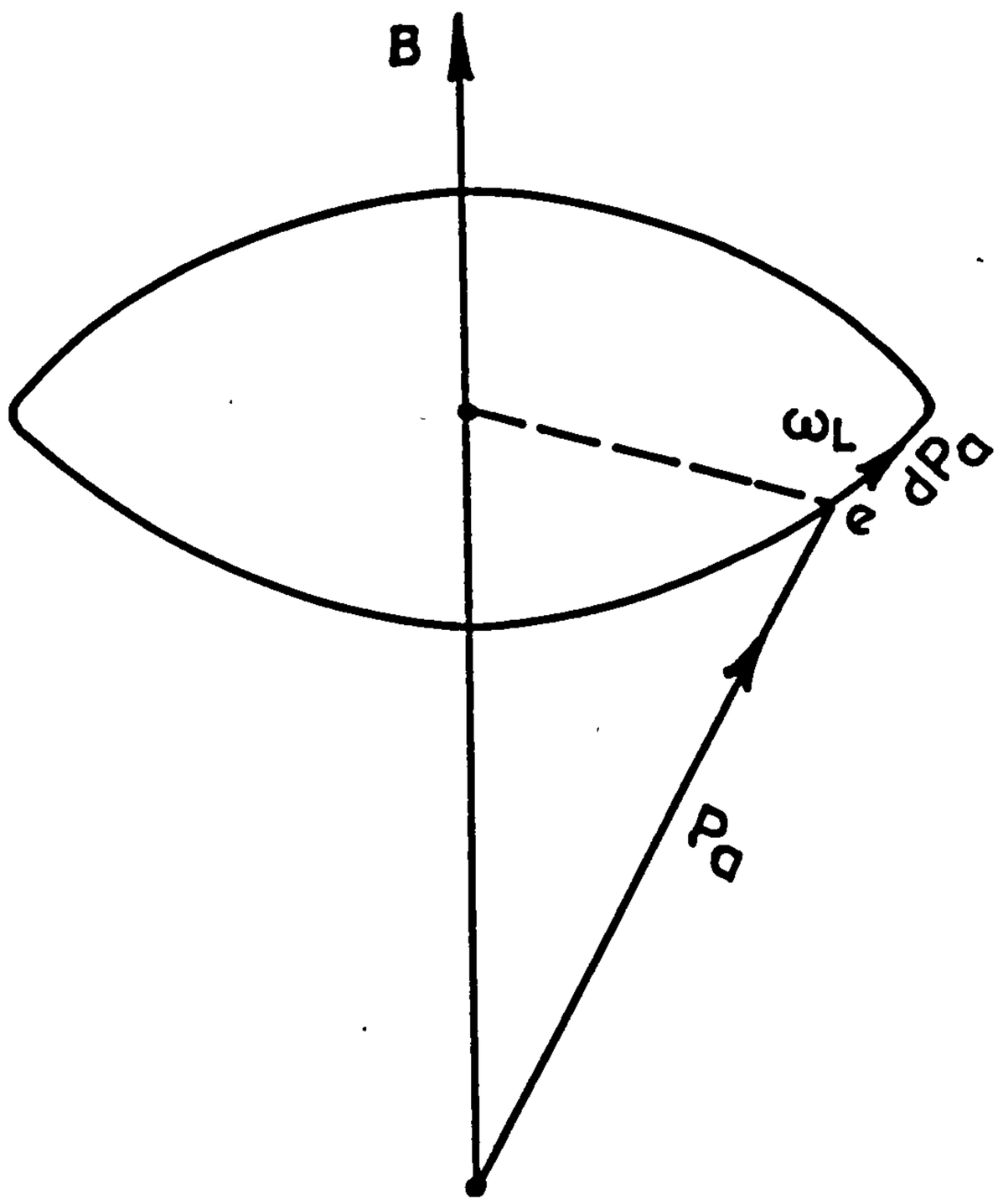

Figure 6.1 The angular moment vector P_a precesses about B with the Larmor frequency ω_L.

The electron orbit corresponds to a ring current and consequently produces an orbital magnetic dipole moment, which for a rotation frequency ν in an orbit of radius r, equals

$$\mu_m = - e\nu\pi r^2 \qquad (6.5)$$

The electron has simultaneously an angular momentum

$$P_a = mvr = mv2r\pi r \tag{6.6}$$

which can be represented by a vector P_a oriented antiparallel to μ_m. Hence, the magnetic and mechanical moments of circling electrons are interrelated by

$$\mu_m = - \left(\frac{e}{2m} \right) P_a \tag{6.7}$$

where e and m refer to the charge and mass of the electron respectively.

The applied magnetic field B produces a torque $\mu m \times B$ on the dipole, so that, according to Newtonian mechanics, we may write

$$(^d/dt)P_a = \mu_m \times B = - (\frac{e}{2m})P_a \times B \tag{6.8}$$

This is the equation of motion of a vector P_a precessing about the direction of B with angular frequency

$$\omega_L = \frac{eB}{2m} \tag{6.9}$$

where ω_L is called the Larmor frequency and the quantity $^e/2m$ is called the gyromagnetic ratio expressed by

$$\gamma = \frac{e}{2m} \tag{6.10}$$

that this can be seen from (Fig. 6.1), from which it follows that for a precession of the type (6.9)

$$dP_a = \omega_L \times P_a \, dt = (^e/2m)B \times P_a$$

From what has been said above, it follows that under the influence of an external field, the plane of the orbit is not stationary, but precesses about B. As a result of the charge of the electron, the precession produces an induced magnetic moment with a component opposite to that of B equal to

$$(\mu_{m_{ind}})_B = - (^e/2m)m \, \omega_L \bar{\rho}^2 = - (\frac{e^2}{4m})B\bar{\rho}^2 \qquad (6.11)$$

where $\bar{\rho}^2 = \bar{x}^2 + \bar{y}^2$ is the mean square of the perpendicular distance of the electron from the field axis through the nucleus. The mean square distance of the electrons from the nucleus is $\bar{r}_l^{\,2} = \bar{x}_i^{\,2} + \bar{y}_i^{\,2} + \bar{z}_i^{\,2}$. For a spherically symmetrical distribution of charge we have $\bar{x}_i^{\,2} = \bar{y}_i^{\,2} = \bar{z}_i^{\,2}$, so that $\bar{\rho}^2 = {}^2/3 \, \bar{r}_i^{\,2}$. When this treatment is extended to a solid containing N atoms per cm^3, each containing z electrons, one obtains for the diamagnetic susceptibility defined as the induced moment per cm^3 per gauss.

$$\chi_{dia} = - Nz \, (\frac{e^2}{6m}) \, \bar{r}_i^{\,2} \qquad (6.12)$$

where $\bar{r}_i^{\,2}$ is the sum of the mean square radii of the orbit of the ith electron projected perpendicular to the direction of the applied field. Diamagnetism thus depends only on the effective radius of the electronic orbit, the electrons in the outermost orbits contribute

most to the atom susceptibility. Langevin's equation (6.12) also shows diamagnetism to be independent of temperature and applied field. The negative sign of diamagnetism is a consequence of Larmor precession and all atoms possess this universal property of diamagnetism.

The susceptibilities of diamagnetic materials are negative, mostly about -10^{-5} emu/cm^3, numerically much less than typical paramagnetic susceptibilities. The permeabilities of diamagnetic materials are very slightly less than $\mu_o = 4\pi \times 10^{-7}$ H m^{-1}. Wood is an example of this kind of material with a permeability $0.999999 \times \mu_o$ (Kittle, 1976).

6.2.2 Paramagnetic substances

The essential feature of a paramagnetic material is that it has a positive but small magnetic susceptibility ($\chi_m << 1$) mostly between $+10^{-3}$ and $+10^{-4}$ emu/cm^3 at 0^oC. (273K). It results from the presence of permanent magnetic dipoles that are free to be oriented under the influence of an external field. These dipoles exert very small interaction forces on each other; therefore; at ordinary temperatures, thermal vibrations of the solid ensure random orientation giving an average magnetization of zero.

According to the classical theory of Langevin, the molar paramagnetic susceptibility

$$\chi_m = N \mu^2/3kT \qquad (6.13)$$

where μ is the permanent moment, T is the absolute temperature, N is the number of atoms per cubic-centimeter, and k is Boltzmann's constant.

Previously Curie had established experimentally to Langevin's work that the paramagnetic susceptibility χ_m is inversely proportional to the absolute temperature T, and the expression

$$\chi_m = \frac{C}{T} \qquad (6.14)$$

is known as Curie's law; C is called the Curie constant. Equations (6.13) and (6.14) show paramagnetism to be dependent of applied field and temperature.

Paramagnetic substances are unlike diamagnetic substances in that they possess less reluctance than a vacuum to the passage of lines of force. The greater the applied magnetic field, the more nearly the dipoles tend to be aligned and the greater is the net magnetic moment per unit volume or magnetization M. The permeability of paramagnetic material is slightly greater than that of free space (Lee, 1963).

6.2.3 Ferromagnetic substances

The orbital electrons within an atom not only revolve around the nucleus, each one also spins about its own axis. In the atoms of magnetic materials, more electrons spin in one direction than in the other. These uncompensated or unblanced spins give rise to additional

magnetic moments. Ferromagnetic materials (i.e., iron, steel) are peculiar in that they contain groups of atoms in which the unbalanced electron spins are all in the same direction. These relatively large groups of atoms are called domains. The thousands of parallel spins in a single domain result in intense local 'pockets' of magnetism. When a specimen of iron or other ferromagnetic material is placed in a magnetic field the domains align. If the magnetizing field is strong enough the gradual process of alignment goes on until all the domains are parallel and specimen is said to be saturated. Permeabilities of these materials extend over a range from several hundred to tens of thousands of times greater than the permeability of free space (KiP, 1963).

Because of these three properties discussed above, the biological effect of magnetic field could not be dismissed.

6.3 Biological effects of the geomagnetic field (GMF)

Since dia, para and ferromagnetic materials all occur in biological materials, it is reasonable to assume that living creatures become not only accustomed to the GMF as part of their natural evolutionary habitat. Biological processes may have evolved which could be influenced by fields of the order of the GMF (0.5 gauss or 50 μT).

Experiments to clarify the biological effect of the geomagnetic field usually involve shielding the control specimens from the GMF by placing them in a closed mu-metal box which has a very high permeability at low field strengths.

Some results make it obvious that removal of the GMF does greatly disturb the functional state of organisms have been already established (Dubrov, 1978). Numerous investigations by various methods and techniques indicate that the GMF plays an important role in the activity of living organisms and the course of physiochemical reactions on earth. Emphasising the existence of a close link between the GMF and the biosphere.

Piccardi (1971) has postulated that "the main substance responsible for the universality of the action of the GMF on living organisms is the water contained in the structure of biological systems and the processes occurring in the water molecule." Buchachenko (1974) has confirmed Piccardi's postulation by investigating the action of the magnetic and electric field on the water molecules.

Dubrov's(1969) experimental work on geomagnetobiology has revealed an important mechanism of perception of the GMF by living organisms through the change in the permeability of biological membranes.

Biological membranes, which are structural elements of any cell, are mainly responsible for maintaining the function and for the fine regulation of all organs of the living organism. The coordinated work of the membrane permeability mechanism is responsible for the precise homeostasis of the living organism and the self-regulating ability of all its parts, whose basis is the membrane mechanism of an asymmetry of sodium and potassium ions (Kogan, 1969).

By altering the permeability of biological membranes, the GMF can affect the whole organism, causing the entire range of changes in the biological organism (Pilla, 1974).

However, in addition to the important and unique role of biological membranes in securing a relation between the GMF and the living organism, there is another very important property that can account for this connection, that is the presence of a biomagnetic field in living organisms.

Krylou (1961) has reported an effect of the GMF on the asymmetry of the electromagnetic fields of living objects. Brauner (1968) has confirmed that these factors are implicated in the induction of bioelectric activity and in the alteration of the value of the biopotentials (Travkin, 1971).

6.4 The interaction of electromagnetic fields with biological tissues

Biological processes are mainly complex chemical reactions. Chemical properties in general results from the arrangement and motion of electrons and nuclei in molecules, as determined by the interactions of the magnetic and electric fields of the atomic particles making up the molecules. Consequently, electrical and magnetic fields would seem to be the natural experimental devices to be used to obtain information regarding the basic phenomenon themselves. The medium in which the chemical reactions of biological processing occur is a weakly conducting electrolyte which is essentially non-magnetizable. An applied magnetic field, therefore, is unaffected by the continuum encountered in biological systems, and thus seems to be ideally suited to be used as a probe.

It has been suggested that most biological materials are functionally affected in some way by the presence of a magnetic field (Barnothy, 1964). The effect has been termed "Biomagnetism". It has certain common features; there seems to be a threshold field strength below which the field does not produce any effects; magnetic field effects persist for long periods of time (hours, days) after the termination of exposure to the field.

Bacteria which orientate and swim in preferred (northwards) direction in geomagnetic fields were observed in marine sediments environments by Blakemore (1975).

These magnetotactic bacteria orientate in uniform magnetic fields as weak as 0.5 gauss, reversal of the magnetic field caused the bacteria to swim in the opposite direction. Later electron microscopic examination of the cells revealed the presence of structured particles rich in iron, within intracytoplasmic membrane vesicles. This suggests that the bacteria, which favour downward and northward motion, orientate through ferromagnetism using the earth geomagnetic field to find their way (Blakemore 1975).

Semm (1980) reported that activity in pineal cells was depressed by an induced magnetic field of 0.5 gauss and restorted when the magnetic field was removed. Dixey (1982) reported that weak magnetic fields of only 1.6 gauss to 8.5 gauss greately affected ^{3}H-noradrenaline released in nerve cells and that the effect could not be explained by ion diffusion.

Moore (1979) reported that 6 different microorganisms were affected by magnetic fields of 50 gauss to 900 gauss and frequencies of DC to 0.3 Hz using square, triangular or sine waveform. Cell growth was stimulated or inhibited depending upon the field strength and frequency.

Ahmed et al (1976) found that the enzyme lysozyme at room temperature shows an unexpectedly large dependence of the dielectric constant on the magnetic field. At the same time magnetic susceptibility measurements show an unexpectedly large diamagnetic value at certain strengths of magnetic field.

In 1962 Gerencser reported inhibition of bacterial growth by magnetic fields. He used a mean field gradient of 5200 gauss/cm which slowed down growth to a probability level better than $P < 10^{-6}$. He suggested that the magnetic field does not affect fission rate, but that it has an unpleasant effect on some of the cells.

Suspension of yeast cells placed in a constant magnetic field (CMF) of 750 gauss, at room temperature for two to eight or more hours, and in studying the effects of short exposure, for one hour in an incubator at temperature of 22 to 29 ^{o}C, the inhibition action of the CMF on the increase of yeast culture was established. The inhibiting effect of magnetic fields on the multiplication of the yeast also showed itself at various temperatures. The increment of cells in the yeast suspension exposed to a magnetic field for one hour was one third of the increment of the control, and after two hours exposure of the culture to same field, it was approximately 50% less. When the exposure time was lengthened (over 8 hr) the intensity of the inhibition of cell division did not increase. The inhibition of the yeast multiplication took place only during the period of the action of the magnetic field. After the termination of the action, the rate of increase in the amount of cells in the experiment and the control was the same (Kholodv, 1974).

The author (Jafary-Asl et al and Aldrige , departmental report Barts, 1980), designed and constructed an air-cored

electromagnetic bone growth stimulator. The magnetic field waveform chosen was based on that used for in-vitro studies and is the one most commonly used in clinical practice. The performance of this clinical stimulator has subsequently reported satisfactory in bone healing.

6.4.1 The magnetic energy density (U) associated with a magnetic field

According to Barnothy (1964) continuous exposure to static fields ranging from 150 μT to 1.8 T has been shown to produce changes in growth metabolism and life span of various living tissues. These changes have usually only become apparent over a period of days. Similar effects have been observed in field gradients. In excised tissue samples there will be much reduced metabolism, and it is to be expected that the effects on the tissue will only be due to interaction of the field with, for instance, the mobile electrons of macromolecules and various magnetic moments within the tissue. The magnetic energy density, U, associated with a magnetic field, B is given (Bleaney, 1959), by

$$U = \frac{BH}{2} \tag{6.16}$$

Since $B = \mu_o H$. For magnetic material of susceptibility χ_m, placed in a field B, the energy density within the material

$$U = \mu_o(1 + \chi_m)\,{}^{HH}/_{2}$$

$$= B^2(1 + \chi_m)/_{2\mu_o}$$

The interaction energy, U, is

$$U = \chi_m B^2/_{2\mu_o} \qquad (6.17)$$

For biological materials $\chi_m \sim -4\pi \times 10^{-10}$ (Mulay, 1964) and if placed in a field of 1 tesla then

$$U = \tfrac{1}{2} \times 4\pi \times 10^{-10} / 4\pi \times 10^{-7}$$

$$= 5 \times 10^{-4} \text{ J/mole} = 8 \times 10^{-23} \text{ eV/mole}$$

Thermal energy at 25^oC is 2.5×10^3 J/mole = 4×10^{-16} eV/mole therefore, the effects on the thermodynamic properties will be negligible. The energy of the H-bond is $\sim$ 12 kJ/mole $\sim$ 19×10^{-16} eV/mole which suggests that the nature of any chemical bonds in the material is unlikely to be affected. The activation energies of molecular effects in biological systems (Cleary, 1973) are given in Table 1.

Effect	Activation energy		Radiation parameters	
	k cal/mole	eV	Frequency (GHz)	Wavelength(μm)
Thermal or Brownian motion (at 30°C)	0.60	0.026	6.3×10^3	47.6
Ionization	230	10	2.4×10^6	0.12
Covalent bond disruption	115	5	1.21×10^6	0.25
London-Van der Waals interactions	23	1	2.4×10^5	1.25
Hydrogen bond disruption	1.8 - 4.6	0.08 - 0.2	1.9×10^4 - 4.8×10^4	15.8 - 6.25
Proton tunneling	16.1	0.7	1.71×10^5	1.76
Disruption of bound water	12.9	0.56	1.4×10^5	2.14
Rotation of polar protein molecules	0.92 - 9.2	0.04 - 0.4	9.7×10^3 - 9.7×10^4	30.9 - 3.1
Reversible conformational changes in protein molecules	9.2	0.4	9.7×10^4	3.1
Charge transfer interaction	138 - 69	6.3	1.45×10^6 - 7.25×10^5	0.2 - 0.4
Semi-conduction	23 - 69	1 - 3	2.4×10^5 - 7.25×10^5	1.2 - 0.41
Microwave radiation	0.03	1.2×10^{-3}	0.03 - 300	10^7 - 10^3

TABLE 1

According to Cleary (1973) the effects summarized in Table 1 include phenomena that are known or expected to occur in biological systems. The effects are considered in terms of the energy required to produce the alteration in the molecule; that is, the activation energy (when known), and the possibility is considered that the effect could result from a frequency specific interaction with an impressed electromagnetic field.

CHAPTER 7 ASPECTS OF MAGNETIC RESONANCE THEORY RELEVANT TO BIOLOGICAL MATERIALS

7.1 Introduction

This chapter describes the nuclear magnetic resonance (NMR) and electron spin resonance (ESR) and discusses their applications to biological materials (Berliner, 1978, 1980, 1981). The approach has been made from a classical stand point since this is particularly useful in describing the relaxation behaviour of the systems which have been studied.

The NMR technique relies on the fact that atomic nuclei with an odd number of nucleons (Protons and neutrons) have an intrinsic magnetic moment that makes each such nucleus as a magnetic dipole. On the other hand the ESR technique relies on the magnetic moment associated with the unpaired electrons spin.

7.2 Basic NMR resonance theory

When magnetic nuclei with an odd number of nucleons placed in a magnetic field, they behave as if they were spinning charged particles. Nuclei possessing this property have angular momentum P (Tulloch, 1971). Defining I as the spin quantum number, the maximum observable component of P is I. The angular momentum thus has 2I + 1 states (+I, I-1,.....-I) along which the component of P may have values.

The spinning nucleus generates a magnetic dipole moment μ_N which is parallel to and proportional to P. This relationship is given by

$$\mu_N = \gamma P \qquad (7.1)$$

where γ is termed the gyromagnetic ratio and has different values for different nuclei. The magnetic moment is also quantized. The maximum observable component of μ_N has values of $m\mu_N/I$, where m is the magnetic quantum number and may have the values

$$m = I\ ,\ I-1,\ \ldots\ldots\ -I \qquad (7.2)$$

The only requirement for a nucleus to give an NMR absorption is that the nucleus should possess a resultant magnetic moment. All experiments to date indicate that the magnetic moment is zero if I = O. Thus nuclei with $I \neq O$ give rise to NMR absorption. The magnetic moment takes up the allowed orientations when a nucleus of spin $I \neq O$ is placed in a magnetic field B_o. For a spin $\frac{1}{2}$ nucleus (^1H), the possible orientations in terms of the magnetic quantum number are $m = +\frac{1}{2}$ and $-\frac{1}{2}$ as shown in Figure 7.1. The interaction between μ_N and the applied field B_o results in a torque acting on μ_N which tends to tip it towards B_o. However, since the nucleus is spinning, instead of tipping μ_N towards B_o, the torque cause μ_N to precess about the magnetic field B_o. The precessional frequency of μ_N about B_o is given by the Larmor equation

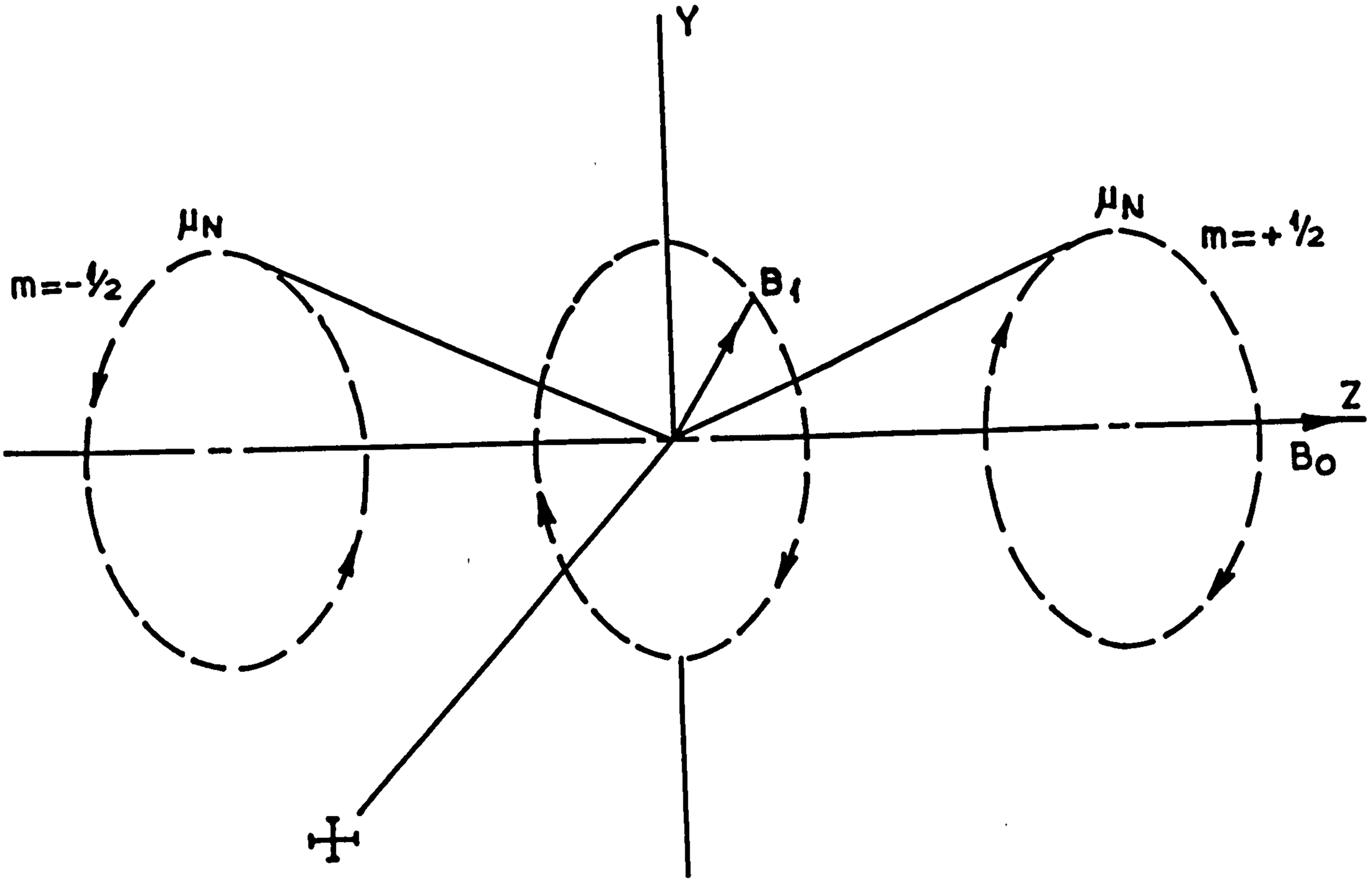

Fig. 7.1 The two orientations of the magnetic moments of a spin I = ½ nucleus.

$$f_o = \frac{\gamma}{2\pi} B_o \qquad (7.3)$$

or

$$\omega = \gamma B_o$$

where f_o is the precessional frequency in Hz and ω is the angular frequency. As can be seen from equation 7.3, the precessional frequency is dependent on both B_o and γ and thus is different for each type of nucleus.

If a second, smaller magnetic field B_1 is in the x-y plane, and rotating in the same direction as μ_N, interactions between B_1 and μ_N occur. So long as B_1 is rotating at some frequency f other than the Larmor frequency f_o,

the effect of B_1 on μ_N results in slight oscillations of the angle between μ_N and B_o. When B_1 is rotating at a frequency $f = f_o$, μ_N will experience the effects of both B_1 and B_o and will exhibit large oscillations in the angle between μ_N and B_o such that the direction of μ_N with respect to B_o changes. Energy is absorbed by the nucleus and the magnetic moments of the nuclei became oriented in direction related to the magnetic field according to the allowed energy levels. The absorption of energy when $f = f_o$ what is detected in NMR.

The nuclear spin energy levels are split by the magnetic field B_o. For a system of identical $I = \frac{1}{2}$ nuclei, there will be two allowed energy levels corresponding to the orientation of μ_N either aligned with or opposed to B_o as shown in Figure 7.2.

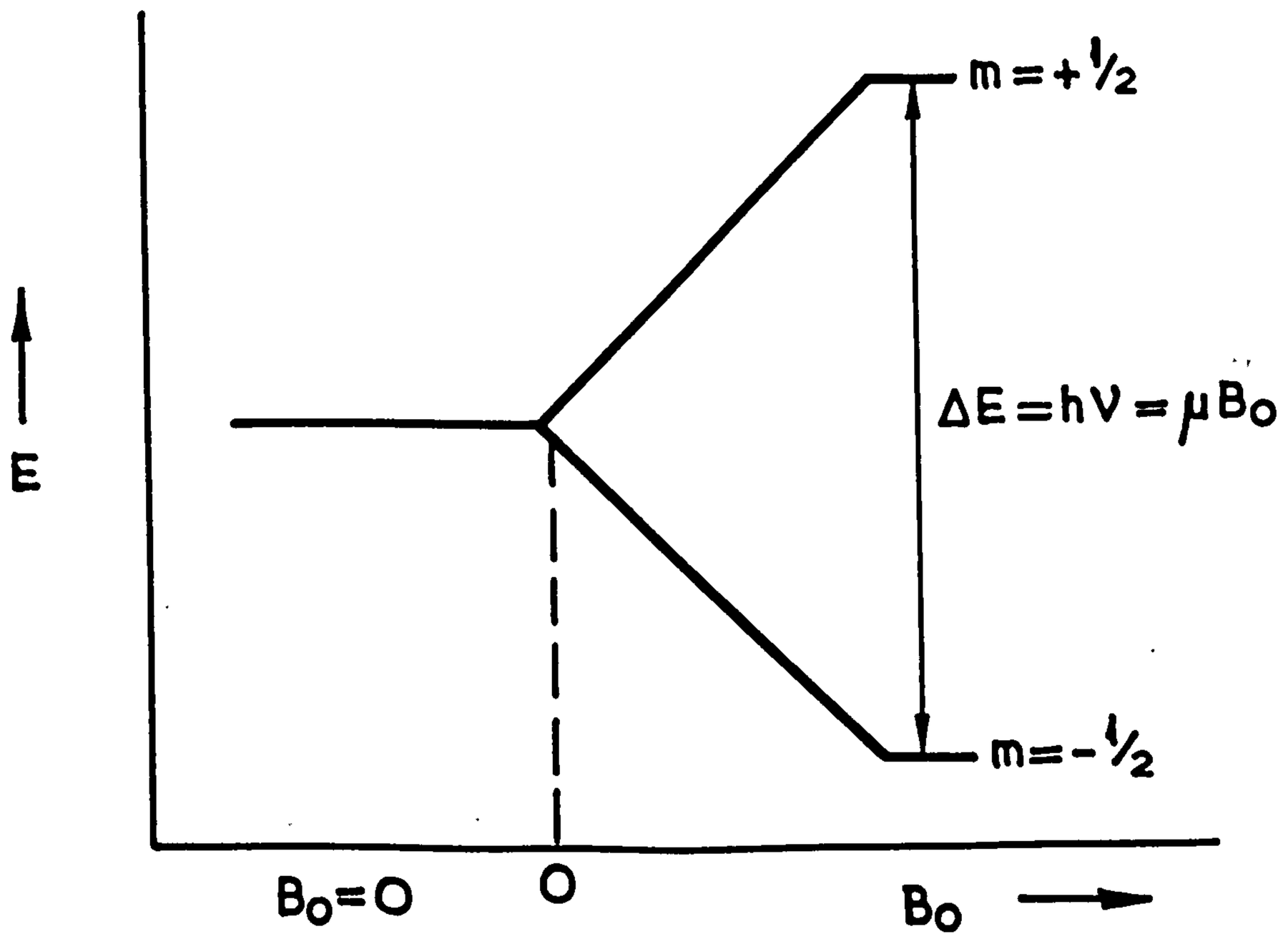

Figure 7.2. The splitting of the energy levels for a spin $I = \frac{1}{2}$ nucleus when placed into the magnetic field B_o.

The tendency for the nuclei to populate the lower energy level is opposed by thermal motion, which tends to equalize the populations of the two levels. The equilibrium population of the two energy levels at some temperature T is given by the Boltzmann equation

$$n_{2/n_1} = \exp\left(\frac{-\Delta E}{kT}\right) \qquad (7.4)$$

where n_2 and n_1 are the number of nuclei per unit volume in the upper and lower energy levels respectively, k is the Boltzmann constant, T is the absolute temperature, and ΔE is the energy separation between the two energy levels Substituting for ΔE, equation 7.4 becomes

$$n_{2/n_1} = \exp\left(\frac{-2\mu B_o}{kT}\right) \qquad (7.5)$$

Transition between the two energy levels can be excited by the absorption of electromagnetic radiation of quantum energy $\gamma\hbar B_o$ resulting in a resonance in the sample. If ν is the frequency of this radiation then

$$h\nu = \gamma\hbar B_o$$

$$\omega = \gamma B_o \qquad (7.6)$$

Comparing equation 7.6 with equation 7.3 it is seem that the angular frequency ω of the radiation is identical with the Larmor precessional frequency.

The nuclei are subject to thermal motion and are not in general aligned with B_o, consequently they will precess about B_o. In order that the electromagnetic field can interact with the nuclei it must contain a component circularly polarized perpendicular to B_o and rotating in the same sense as the precessing nuclei. The electromagnetic field is generally denoted by B_1 and is most commonly a radiofrequency (r.f.) field. In practice B_1 is generated by applying a linearly polarized field $2B_1 \cos\omega_o t$ to the sample which may be resolved into two circularly polarized fields of amplitude B_1 and angular frequency $\pm\omega_o$, only the component $+\omega_o$ will produce a resonance, the other component $-\omega_o$ will have a negligible effect providing $B_1 << B_o$ (Abragam, 1961).

Of the three types of transition, absorption, stimulated emission and spontaneous emission; the third has a probability of occurrence 10^{-25}sec^{-1} (Purcell, 1946) which is negligible compared with the other two. The transition probabilities (10^{-10}sec^{-1}) of the other two are equal (Einstein, 1917) and since there is a population excess in the lower state, net absorption from the r.f. field takes place tending to equalize the populations in the two levels. When the two population densities are equal no further absorption takes place and the spin system is said to be saturated.

When the B_1 field is removed the spin populations revert to their equilibrium values, not instantaneously but exponentially with a characteristic time constant known as the spin-lattice relaxation time T_1. This recovery or relaxation process occurs because the spins are not mutually isolated from each other or from their environment. The spin system interact with the immediate surroundings of the precessing nucleus, which is often a lattice of other atoms and molecules. The magnetic energy of the spin system is converted into thermal energy and dissipated through the whole molecular system in which they are contained.

This interaction arises because each spin not only experiences the applied field B_o but also a much smaller field B_{local} produced by the thermal motion of the neighbouring spins. B_{local} varies both in direction and magnitude throughout the sample and consequently the net field

$$B_{Tol} = B_o + B_{local} \qquad (7.7)$$

experienced by each nucleus will be different and the two previously sharply defined energy levels will each be homogeneously broadened by an amount $\gamma\hbar B_{local}$.

7.2.1 Nuclear magnetic resonance relaxation times

In the magnetic resonance phenomenon it is to be expected that the resonant absorbtion line will have a finite width of minimum value equal to the inverse of the life time that a nucleus remains in a given energy level, this minimum width is given by

$$f_{\frac{1}{2}} = \frac{1}{2\pi T_1} \tag{7.8}$$

where $f_{\frac{1}{2}}$ is the full width at half maximum of the absorption line. Since the energy levels have already been broadened by $\gamma\hbar B_{local}$ then this has the effect of giving the resonance line a natural line width of

$$f_{\frac{1}{2}} = \frac{\gamma B_{local}}{2\pi} + \frac{1}{2\pi T_1} \tag{7.9}$$

There is another relaxation time that is characteristic of the spin system known as the spin-spin relaxation time T_2. At equilibrium the precessing spins bear no special phase relationship to each other but when the B_1 field is on they can achieve phase coherence and consequently M_{xy}, the net magnetic moment in the xy plane, is no longer zero. When B_1 is removed the spins lose this phase coherence by mutual exchange of energy via interactions induced by B_{local} and M_{xy} approaches zero in an exponential manner with T_2 as the characteristic time constant.

Until now the B_o has been considered as perfectly homogeneous but in practice this is not the case. B_o will have an associated inhomogeneity ΔB_o which causes a further broadening of the energy levels by an amount $\gamma \Delta B_o / 2\pi$ in turn resulting in another or alternative contribution to the line width

$$f_{\frac{1}{2}} = \frac{1}{2\pi T_2} + \frac{\gamma \Delta B_o}{2\pi} \qquad (7.10)$$

the relative magnitudes of $f_{\frac{1}{2}}$ in equations 7.9 and 7.10 will determine what is observed in practice.

In viscous liquids and in solids spin-spin (T_2) relaxation time dominates the relaxation process, this is due to the neighbouring magnetic moments remaining fixed in position for relatively long periods of time, so they can alter the local field in the sample through dipolar interactions while shorten the life time of the excited state by allowing an energy exchange to take place within the spin system . In nonviscous liquids spin-lattice (T_1) relaxation time becomes predominant.

7.3 Choice of frequency and magnetic field strength

Consider for example the magnetic resonance of protons in a sample of water. From equation 7.3 we have

$$\gamma = \frac{2\pi f_o}{B_o} \qquad (7.11)$$

For the precession of protons of charge e and mass m_p, $\gamma = \frac{e}{2m_p}$, is 42.6 MHz per tesla or 4.26 kHz per gauss*. The Larmor frequency is 2.13kHz for a typical geomagnetic field of 0.5 gauss. Some characteristics resonance phenomenon may be expected when the driving frequency is equal to their Larmor frequency.

7.4 Biological NMR studies

Protons give the best signal with NMR because they are very plentiful in most biological tissues and intrinsically protons emit a strong NMR signal (De Certaines, 1982). The largest proton resonances arise from water and mobile molecules containing hydrogen.

The strength of the signal obtained from protons depends on the number of protons in the sample, thus proton density maps of the material can be constructed. These are especially useful in the case of biological tissue or human tissue which typically contains about 75% of water.

*1 Tesla = 10^4 Gauss

Relaxation times T_1 and T_2 their relative magnitudes depends on many factors, especially the immediate molecular environment of the precessing nuclei. Hence the protons or water molecules situated in the different tissues, their T_1 can depend on the type of tissue and, most interestingly on whether the tissue is malignant or not (Alfidi, 1982).

Further information can be obtained by observing the NMR spectra of other magnetic nuclei in the tissues. In its applications to the biological materials, studies have in fact already done with phosphorous ^{31}P and sodium ^{23}Na (Ross, 1981).

By far the greatest amount of the published data deals with ^{23}Na, the most abundant isotope of sodium in nature. Very few papers have presented studies of ^{39}K, the common isotope of potassium. Despite its relatively high concentration, intracellular K^+ presents with a signal which is at least an order of magnitude smaller than that provided by intracellular Na^+ (Lauterbur, 1973). Shporer (1977) reported that the NMR properties of ^{39}K are very similar to those obtained from ^{23}Na.

Salhaney et al (1975) studied the high resolution ^{31}P NMR of intact yeast cells. The yeast preparations used were aqueous suspensions containing about 50% cells by volume. These workers were able to resolve and assign several peaks to various intracellular metabolites known to be present in the yeast cell.

With reference to imaging, NMR is now beginning to contribute to the solution of problems not approachable by other methods. This field is now at a stage where the

mere demonstration of NMR spectra on living systems is no longer noteworthy and workers in this field are now in the process of attempting to realize the obvious promise of this technique as applied to various basic scientific as well as clinical, problems.

7.5 Possible dangers associated with NMR studies on biological materials

Various groups have investigated the possible dangers of NMR to live biological materials. The absorption of the RF waves that are transmitted through the live cells releases energy and so can heat the tissues. The static magnetic field in which the biological sample is situated may produce unwanted effects.

There are recognized standards for maximal permitted heating of human tissues by RF waves and no NMR technique currently in use or planned approaches these thermal levels (Buddinger, 1979).

The constant magnetic field is claimed to have serious adverse effects if it is too large. Biological cell membranes including human cell membranes contain large proteins that control their permeability to many ions and compounds and also enzymes, that can be perturbed by sufficiently intense magnetic field; such effects have been observed in practice in animal experiments (Budinger, 1979).

Therefore, from the above observations it can be seen that , some recognized exposure limit on the combination of steady magnetic field strength and frequency of RF radiation

which are biologically significant should be considered.

7.6 Electron spin resonance (ESR)

The above theory is equally applicable to electron spin resonance as well as NMR.

Electron spin resonance (also called, electron paramagnetic resonance (EPR) or electron magnetic resonance (EMR)) is similar to NMR except that the orientation of the magnetic moment of an unpaired electron rather than a nucleus is observed in a magnetic field. Electron spin resonance is applicable only to unpaired electrons, since the magnetic moments of paired electrons cancel.

The magnetic moment μ_e of an electron is about $1836\mu_B$, compared with μ_N for a proton 2.8. This large magnetic moment causes a large energy separation between the spin states in a given magnetic field, as may be seen from

$$\Delta E = h\nu = \frac{\mu_e B_o}{I} \qquad (7.12)$$

where μ_e is the magnetic moment , h Plancks constant and I the spin quantum number.

From sec. 7.2 in NMR spectroscopy (equation 7.4) the ratio of protons in the upper nuclear spin energy state

and the lower spin energy state is typically only $\sim 10^{-6}$. Under typical ESR operating conditions, the ratio of electrons in the upper spin state to the lower spin state is about 10^{-4} at room temperature (Purcell, 1946). It is this much greater population difference that gives ESR its superior sensitivity as a spectroscopic technique.

7.6.1 Choice of frequency and magnetic field strength

The effect of the magnetic moment of the electron on the choice of applied frequency and magnetic field strength can be seen from equation (7.12).

$$\Delta E = h\nu = \frac{\mu_e B_o}{I}$$

The spin of an electron is $I = \pm \frac{1}{2}$ hence

$$\Delta E = h\nu = 2\mu_e B_o \qquad (7.13)$$

Since μ_e = 1836 nuclear magneton units for a free electron and each nuclear magneton unit $\mu_B = (eh/4\pi m_e)$ has a value of 5.051×10^{-24} erg/gauss (5.051×10^{-27} J/Tesla)

$$\nu/B_o = \frac{2\mu_e}{h} = \frac{(2)(1836)(5.051 \times 10^{-27} \text{ J/Tesla})}{6.62 \times 10^{-34} \text{ J - s}}$$

or

$$\nu/B_o = (2.8 \times 10^6) \text{ (Hz per gauss)} \qquad (7.14)$$

Hence in a geomagnetic field of 0.5 gauss, the required frequency for ESR is

$$\nu = (2.8 \times 10^6) \times 0.5 = 1.4 \times 10^6 \text{ Hz}$$

7.6.2 Biological ESR studies

Electron spin resonance spectrometers respond only to systems containing unpaired electrons, such as atoms and molecules having an odd number of electrons, e.g., atomic hydrogen or nitrogen.

Within its sphere of application ESR is an extremely useful tool for obtaining electron density information and performing structural analysis (Ingram, 1958).

Only a few years after the discovery of ESR was this tool applied to biological problems. For the past quarter century, there has been the idea that many of the electron transport processes in biological systems may go by one electron steps (Ingram, 1967).

Michaelis (1946) to make his famous proposal that, 'it will now be shown that all oxidations of organic molecules, although they are bivalent, proceed into two successive univalent steps, the intermediate being a free radical.'

Because ESR is applicable directly to the detection and identification of free radicals, this tool made a tremendous contribution to the state of knowledge in biochemical reactions (Ehrenberg 1967)

Barnothy (1969) noted that considerable interest had been generated in the possible clinical uses of ESR spectrometry. The fact that free radical reactions have been shown to occur in biological systems raises the question of whether deleterious changes in body chemistry might not demonstrate their presence by altered free radical concentrations. The study of radiation damage and carcinogenesis are two cases in point.

A large variety of biological membrane preparations were investigated by Hubbell and McConnell (1968, 1969). They included nerve fibres, mitochondrial membranes and human erythrocytes an ESR spectra detected from these membranes.

Samoilova (1961) studied the changes in the magnetic properties of yeast during growth and cell division using ESR techniques. He reported that resting yeast cells possess only very weakly marked magnetic properties the intensity of the ESR signal did not exceed 3×10^{19} unpaired electrons per gram. Inoculation of the cells into a nutrient medium in conditions in which processes of cell division and growth were virtually absent did not lead to an increase in the magnetic properties. The start of the process of cell division and growth of the culture was always accompanied by a sharp rise in the intensity of the ESR signal (at least by 50 - 100 times and possibly much more). The cessation at the end of the experiment of the processes of growth and division was always accompanied

by a sharp drop in the intensity of the ESR signals to the point of the original, practically zero level.

Commoner, et al. (1956) had noted that a relationship between the concentration of free radicals in a tissue and its rate of metabolic activity. The experiments of Truby and Goldzieher (1958) showed that the relationship is not a simple one, since neither stimulation of guinea-pig adrenals by adrenocorticotrophin hormone nor suppression by hydrocortisone phosphate had much influence on the intensity of the ESR spectrum of the adrenal tissue.

Several investigations had noted significant differences between ESR spectra from cancer tissues and from the corresponding normal tissues.

Commoner and Ternberg (1963), reported that neoplastic tissues had relatively low, or wholly undetectable, free radical contents. This finding was confirmed by Mallard and Kent (1966), also using the surviving-tissue technique, who found that the free radical signal was absent from cancer tissue.

Their findings, suggested that ESR spectroscopy may have three important applications: (a) to investigate differences of metabolism between cancer tissues and normal tissues, (b) to provide information on the mechanism of the induction of tumours, (c) to provide an early warning system for the detection of cancer in suspicious but not clearly malignant tissues.

CHAPTER 8 BIOLOGICAL EFFECTS OF NMR ON THE SODIUM AND POTASSIUM CONTENT OF BOVINE EYE LENSES THROUGH MICROWAVE MODULATION

8.1 Introduction

During the experimental work on the yeast cells the opportunity presented itself for some irradiation measurements on bovine eye lenses. The results presented in section (10.5) on both control and irradiated eye lenses suggested that by modulating microwaves with an NMR frequency appropriate to the ambient magnetic field would give abnormal effect on the sodium and potassium content of the eye lenses. Dielectric measurements were made on both actively metabolising lenses and lenses whose metabolism had been disrupted by Ouabain in an ambient magnetic field of 0.5 gauss.

An introduction to the physiology and biochemistry of the eye lens, together with an account of known effects of microwave irradiation on eye lenses are discussed.

8.2 The mammalian eye lens

According to Duke-Elder (1972) the eye lens is a transparent biconvex body, the apeces of its anterior and posterior surfaces are called the anterior and posterior poles respectively Figure 8.1. Lines on the surface of the lens passing from pole to pole are called meridians,

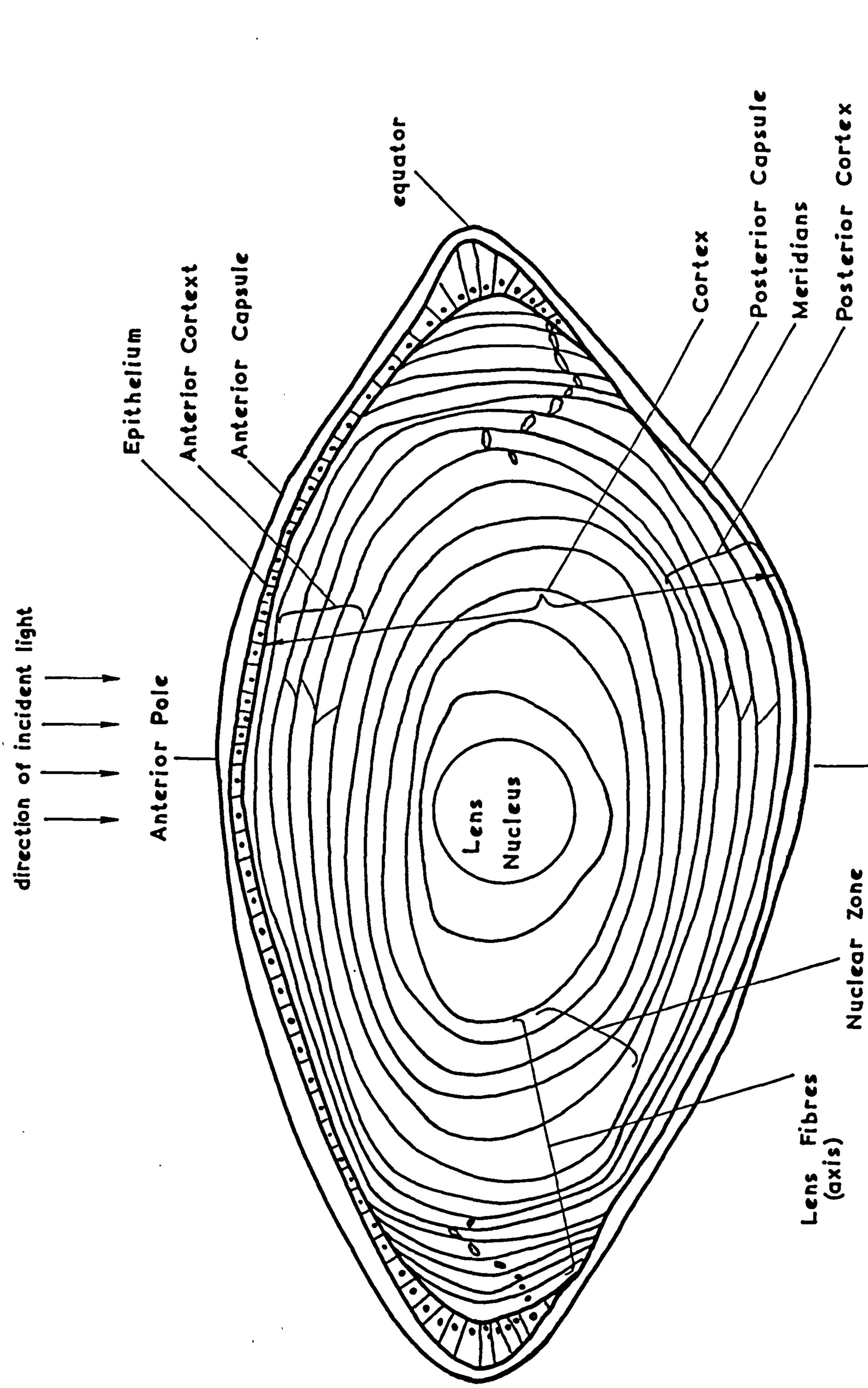

Fig. 8.1 The mammalian eye lens

whilst the line running through the lens and joining the poles is the axis. The equator is a circle on the surface at right-angles to the axis.

The lens vesicle is a sphere whose wall consists of a single layer of epithelium. The outer aspect of these epithelial cells secrete a structureless hyaline membrane, the capsule. The cells of the posterior wall and the equatorial region undergo marked differentiation and it is from these that the adult lens is formed. The cells of the posterior wall differentiate first, becoming primitive fibres by a process of elongation. Their nuclei ultimately disappear and each becomes an optically clear embryonic nucleus in the centre of the mature lens. The equatorial cells elongate to become fibres, the anterior end of each passing forward towards the anterior pole, the posterior end passing back towards the posterior pole. As this process continues and each new fibre passes immediately under the epithelium, it forces the earlier forward fibres deeper and deeper. Successive layers thus encircle the central nucleus of the primitive fibres. This process occurs because the epithelial cells at the equator tend to become arranged in meridional rows and assume a pyramidal shape. Finally, their inner parts elongate and turn to run under the epithelium of the anterior capsule. The upper cell is now a young fibre and its inner end, which must now be referred to as its anterior and grows forwarded whilst its outer (posterior) end is pushed back by a similarly developing cell immediately in front. As the cells grow into the lens substance,

the nuclei gradually recede with them, becoming arranged in a wide bend which curves round anteriorly as the process of elongation proceeds, forming a wide bow known as the nuclear zone.

A recently formed lens fibre thus has its centre approximately at the equator, whilst the two limbs pass forward and backward towards the anterior and posterior poles respectively to meet the limbs of another cell developing from an "opposite" position. The superficial lens fibres are long, prismatic, ribbon-like cells some 8-10 mm long, 8-12 μm broad, and 2 μm thick.

Since the oldest fibres become more sclerosed and less transparent than the more recently formed ones. The lens is not optically homogeneous, it is differentiated into a central nucleus and a softer cortex (Figure 8.1).

The lens grows throughout life in man, its weight increases from an average 130 mg at 0 - 9 years to 255 mg at 80-89 years. The bovine lenses used in this investigation are considerably larger, and weighing 2.0131 gram.

8.2.1 The chemical composition of the lens

The essential of the chemical composition of the lens are given in Table 2 (Davson, 1972). Water is

Chemical	Young	Old
Water (%)	69.0	64.0
Protein (%)	30.0	35.0
Sodium (^{meq}/Kg H_2O)	17.0	21.0
Potassium (meq/Kg H_2O	120.0	121.0
Chloride (meq/Kg H_2O)	27.0	30.0
Ascorbic acid (mg/100g)	35.0	36.0
Glutathione (mg/100g)	2.2	1.5

Table 2

the main constituent of the lens. The average water content of a calf lens containing a high percentage of young fibres, was found to be 2.1 g of H_2O per gram of dry weight, compared with 1.89 for the Ox lens. Amor et al. (1959) found the water content of the innermost zone of the lens to be less than half that of the outermost zone.

8.2.2 Sodium and potassium content of the eye lens

Since the lens is a cellular body, one would except a high concentration of potassium and a low concentration of sodium. Work by Amoore et al (1959) confirms this figures of sodium concentration of approximately 20 mM and potassium concentration of approximately 120 mM. These figures apply to the whole lens, there being no significant differences throughout its many layers.

Similar to many other tissues where there is a mass of cells with high internal potassium and high external sodium, the lens contains a pump which, by an active transport process, maintains concentration gradients. The Na^+ pump is linked to the transport of the K^+ ion, thus extrusion of Na^+ from the cell is accompanied by uptake of K^+, and a steady state is attained with the passive leaks of Na^+ (in) and K^+ (out) being compensated for by active extrusion of K^+.

Amoor et al. (1959) showed that it is not only at the lens capsule that Na^+ is transported outwards, but also that each successive layer of fibres has some power to transport Na^+ from the nucleus to the centre.

8.3 The biological effects of microwaves

According to Clearly (1973) the biological effects of electromagnetic radiation are classified into two broad categories depending upon the macroscopic and microscopic characteristics of biological systems.

The macroscopic electric and magnetic behaviour of a dielectric material in sinusoidal fields is determined by the complex permittivity (ε^*), complex permeability (μ^*) and the dielectric conductivity (σ). The values of these parameters as well as the size and shape of the medium will determine the extent to which an electromagnetic wave will be reflected, refracted, scattered or absorbed.

Discontinuities in the dielectric parameters, such as would be encountered at the interface between two dissimilar media result in significant perturbation of the field leading to alterations in the mode of propagation such as for example the production of standing waves.

The reflection of high frequency electromagnetic radiation at a boundary separating two media of different dielectric characteristics, in the case of normal incidence of plane waves with no internal reflections, can be described in terms of the rate of the reflected to the incident amplitude of the electric field. At the boundary the reflection coefficient R_E is given by

$$R_E = \frac{E_R}{E_I} = \frac{z_2 - z_1}{z_2 + z_1} \qquad (8.1)$$

where E_R is the amplitude of reflected electric field strength, E_I amplitude of incident field strength and z_1 and z_2 are the intrinsic impedances of the dielectric on each side of the boundary. The intrinsic impedance of the dielectric (von Hipple, 1954) can be written as

$$Z_I = \left(\mu_I^* / \varepsilon_I^*\right)^{\frac{1}{2}} \qquad (8.2)$$

From equations (8.1 and 8.2) it can be seen that the amplitude of the electric field strength is a function of the boundary conditions as well as the dielectric properties of the medium.

In the case of non-normal incidence on non planar boundaries , the electric field is also a function of the size and shape of the absorbers. Since the power adsorbed per unit volume is related to the amplitude of the electric field strength by the expression

$$P = \tfrac{1}{2}\ \sigma\ |E|^2 \qquad (8.3)$$

so that variations in boundary conditions and dielectric properties will affect the rate of absorption of microwave radiation. Typical values of R_E (Johnson and Guy, 1972) for air-muscle interface, muscle-fat interface and air fatty tissue interface are 0.8, 0.5 and 0.4 respectively. These significant differences in the reflection and absorption of incident radiations encountered in various tissues are due to the variations in their dielectric properties.

Schwan (1957) has found that high water content tissues, such as lens and muscle, exhibit high dielectric constants and conductivities relative to low water content tissues such as fat and bone and greater relative absorption occurs in high water content tissues.

The effect on high water content fibres could be explained in terms of ε' and σ which are both frequency dependent variables rather than true constants. The interaction of an alternating electromagnetic fields with molecules (H_2O) having dipole moments will result in a transfer of energy in the dielectric. Any change in the

polarization of the dielectric leads to a displacement current and Joule heating per unit volume. Propagation in dielectrics thus results in attenuation of the incident radiation. This is described by expressing the dielectric constant as a complex number; that is $\varepsilon^* = \varepsilon' - j\varepsilon''$; where ε' is the relative dielectric constant and ε'' is the dielectric loss. ε'' is related to σ by the expression.

$$\sigma = \omega\varepsilon'' \qquad (8.4)$$

where ω is the angular frequency of the applied field.

In contrast to high field intensity , thermal effects which involve an overall increase in the average molecular kinetic energy. "Nonthermal" effects, would be defined as being due to the interaction of the impressed field with specific species or specific assemblages of "receptor" molecules. The end result of such interactions energy would reside in the "receptor" for a sufficient time to result in a functional alteration of some type. The specificity of such interactions would be a function of the radiation frequency since molecules or atoms with specific relaxation times would couple more efficiently than others with a field at a given frequency. This type of interaction has some similarities with the NMR measurements on the sodium (Na^+) and potassium (K^+) content of the bovine eye lenses reported by Jafary-Asl (1982).

A survey of these references leads to the same general conclusion reached by early investigators in this field. That is the absorption of electromagnetic radiation in biological media result in thermal damage.

8.3.1 Cataracts

The term 'cataract' means the occurence of an optical discontinuity in the lens, of such magnitude as to cause a noticeable dispersion of light. In a more restricted sense it is an accumulation of irreversibly coagulated lenticular protein. The accumulation of other partly opaque substances, such as crystals of calcium salts, may be regarded as lens opacities, but technically not cataracts.

Cataracts may occur as a senile change as a result of trauma, metabolic or nutritional defects, or as a consequence of radiation damage. They may be sub-divided into those occuring in the nucleus, and those occuring in the cortex of the lens. Nuclear cataract, in which the nucleus of the lens becomes yellow or brown, is probably an exaggeration of normally occuring senile changes. On the other hand, the cortical cataracts represent opacities in the newly-formed lenticular fibres, thus representing the response to some abnormality in metabolism.

One type of nuclear-cortical cataract has been shown by Rubin and Mattis (1966) by using does of the order of 5g/Kg of Dimethyl Sulphoxide (DMSO) administrated orally, by dermal application, and by direct application to the eye of dog five times a week; lens changes were observed after some months.

The lens appeared to be divided into two zones, both a clear central zone, simulating the nucleus, becoming more and more distinct and spherical as time goes on, and the cortical zone which seems to lose its normal property and become optically clear (Fig. 8.2).

Many cortical cataracts are of the osmotic type, the end feature in all of them being a dramatic hydration of the lens fibre (Kinoshita et al, 1974). This hydration is due to an influx of Na^+ and Cl^- ions , and an eflux of K^+ ions, resulting in an increase in osmotic pressure within the lens . Membrane disruption follows, accelerating the cataract growth (Williams, 1975).

8.3.2 Microwave induced cataractogenesis

When microwaves are absorbed by living tissue, heat is dissipated which may, in turn, produce an observable biological effect. The majority of such effects that have been reported are reversible, but one important exception is the production of cataract. Microwave-induced cataract is a

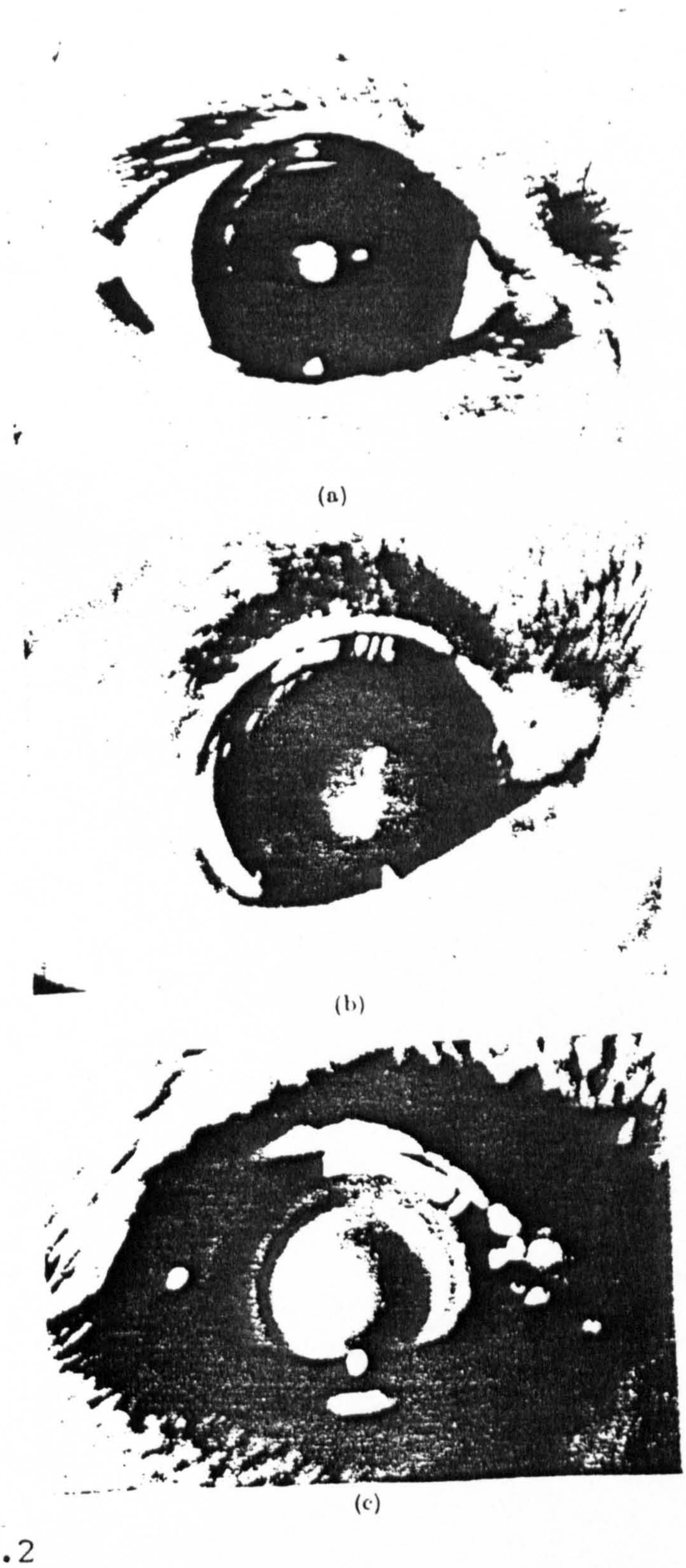

(a)

(b)

(c)

Fig 8.2
(a) Control dog; the appearance of the lens is one of uniform density. (b) DMSO-treated dog. The lens is divided into a central (nuclear) and peripheral zone. The central zone appears opalescent in direct light. (c) DMSO-treated dog. Appearance of lens viewed in light reflected from tapetum. (Rubin and Barnett, 1967.)

well documented phenomenon in experimental animals subjected to sufficiently high exposure power densities (Kramer et al 1975, 1978). The evidence for its observed occurence in man is controversial (Zaret, 1974) and is still incomplete. In order to quantify this phenomenon it is necessary to understand the mechanism of microwave absorption in lens material.

Microwave radiation is electromagnetic radiation with wavelengths ranging from 10m to 1mm, and frequencies ranging from 30 MHz to 300 GHz. According to McAfee (1961) biological systems irradiated with microwave radiation leads to an interaction with electronic charges and an absorption of energy. This occurs principally between the electric field and the polar molecules in tissue. Clearly then, tissues with a high water content, such as the lens, will absorb more energy than tissues such as fat or bone, which have a lower water content. When the rate of energy absorption exceeds the rate of energy dissipation, there is an elevation in the temperature. Whether this temperature elevation is diffused or confined to a specific anatomical site depends on two factors:

(a) The electromagnetic field characteristics, and field distribution within the body, localised field considerations.

(b) The passive and active thermoregulatory mechanism radiation, conduction, connection and evaporative cooling available to the particular biological system.

Due to its avascularity and consequent inability to transfer heat as efficiently as well vascularised tissues, the lens is very susceptible to thermal damage from microwave radiation.

A direct relationship exists between the wavelength of microwave radiation and its penetration. A 12 cm microwave will penetrate approximately 1 cm in to the eye, compared with 1 mm penetration by a 3 cm wave. Therefore, the thermal effects of longer wavelength radiation occur at deeper positions within the eye (Guy, 1975).

Experiments by Richardson et al (1948) showed that when the eye is exposed to 12 cm microwaves, the maximum heating effect occurs in the posterior cortex of lens, whilst with 8.5 cm wavelength radiation, maximum heating occurs in the anterior lens cortex. With short wavelength (3 cm), the highest temperature gradient is located in the conrnea Figure 8.3.

Weiter (1975) has shown that microwave radiation induces damage in ocular tissues, the site of damage depending upon the wavelength of the radiation and mode of exposure. The extent of damage is dependent upon the radiation intensity of power density, and the duration of exposure.

Acute high-intensity microwave exposure of rabbits cause immediate production of tear and pupiliary constriction, the extent of which is dependent upon the field intensity and exposure duration (Guy et al, 1975).

Electron microscopic (Williams et al, 1975) analysis of lenses exposed to cataractogenic doses of 10 cm microwave radiation showed cellular deformation in the subcapsular region of the lens. The cells were swollen and vacuolated, many containing coarsely granular and clumped cytoplasm. Cataractogenic microwave exposure results in extensive damage to membranes in lens fibres.

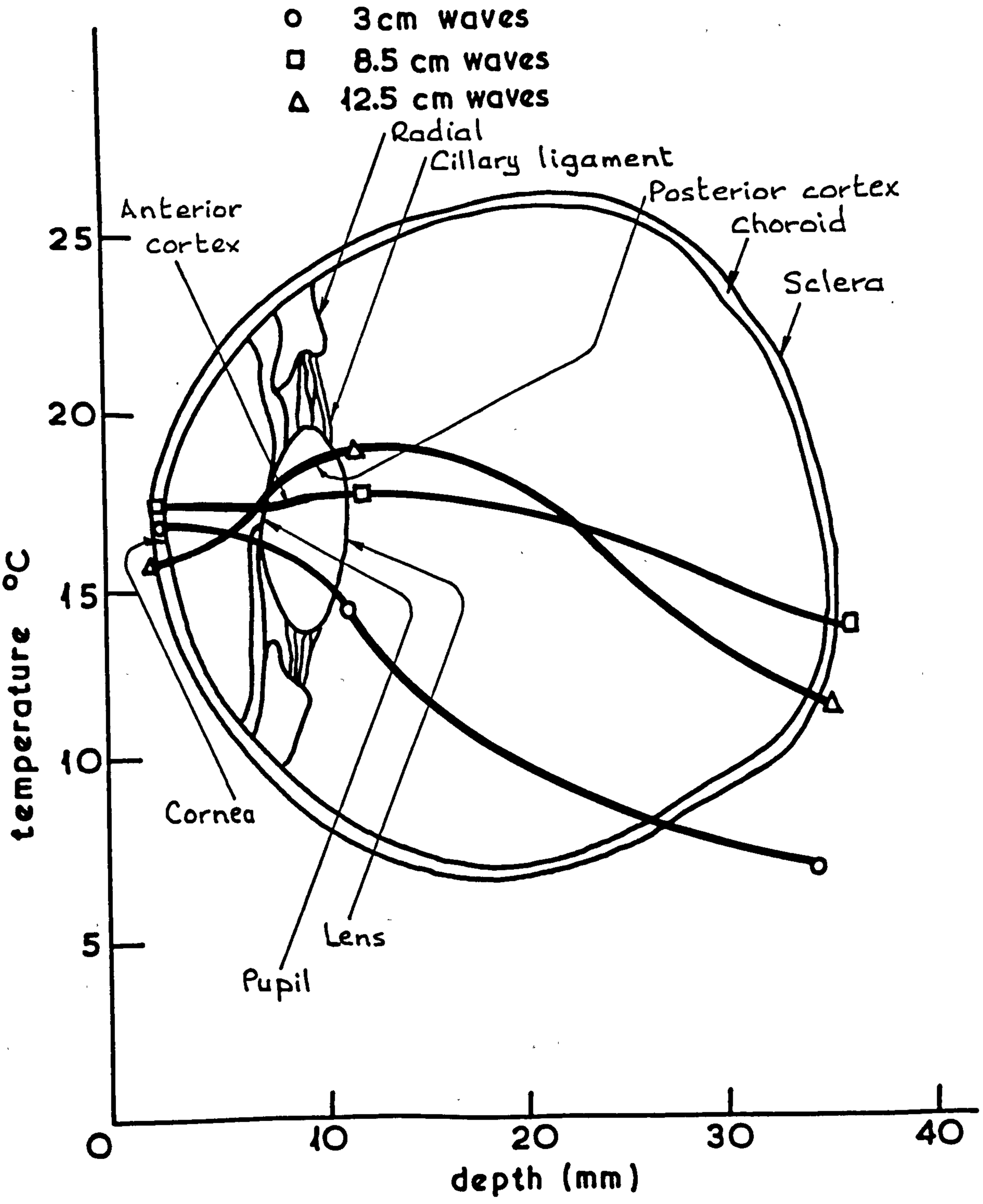

Fig. 8.3 Temperature effect of depth of various wavelength in the eye exposed to microwaves.

CHAPTER 9 EXPERIMENTAL TECHNIQUES, DESIGN AND PROCEDURES

9.0 INTRODUCTION

The complete range of measurements reported in this thesis was obtained using a wide range of equipment most of which was borrowed for short periods. The details of this and of the apparatus specifically designed and constructed for this work are discussed in detail under the following sub-sections.

9.1 Dielectrophoresis measurements.

9.2 Dielectric measurements.

9.3 Measurements of the steps in the voltage-current characteristics.

9.4 Measurements of radio frequency emission from dividing yeast cells.

9.5 Measurements of effects on bovine eye lenses.

9.1 Apparatus used for measurements of the dielectrophoresis

9.1.1 The cell electrodes

A nonuniform field will be produced by any electrode design other than parallel plates. The small dielectrophoresis cell used for the dielectrophoretic experiments had been kindly loaned by Dr. R. Pethig (University College North Wales, Bangor) (1979). It was constructed on a standard microscope slide and consisted of a pair of spherical platinum electrodes

(diameter 0.8 mm) sealed into a shallow well that contained the suspension of cells. The schematic electrode arrangement is shown in Fig. 9.1.

9.1.2 The power supply

The power supply was an Advance audio frequency signal generator (Adv. type J1). It was capable of giving the open circuit voltage of 40 V_{rms} across the electrodes. The output frequency and voltage were read on a digital counter type TSA 5536 and a broadband voltmeter type TM6A. This signal generator was found to be stable to 1 part in 10^5 for short periods.

9.1.3 The conductivity

The conductivity was measured by a conductivity bridge (Switch Gear-London Type MC3). The conductivity was adjusted using dilute KCl solution when necessary. Changes in the conductivity of the suspensions have a great effect on dielectrophoretic response. A conductivity of not greater than 10^{-4} mho m^{-1} was found to be satisfactory.

9.1.4 Observations

The suspension of yeast cells was viewed through a Wild M11 microscope with 200X magnification, which gave sufficient resolution to count the individual yeast cells but sufficient depth to focus to view the tip of one of the electrodes. The average length of the pearl chains

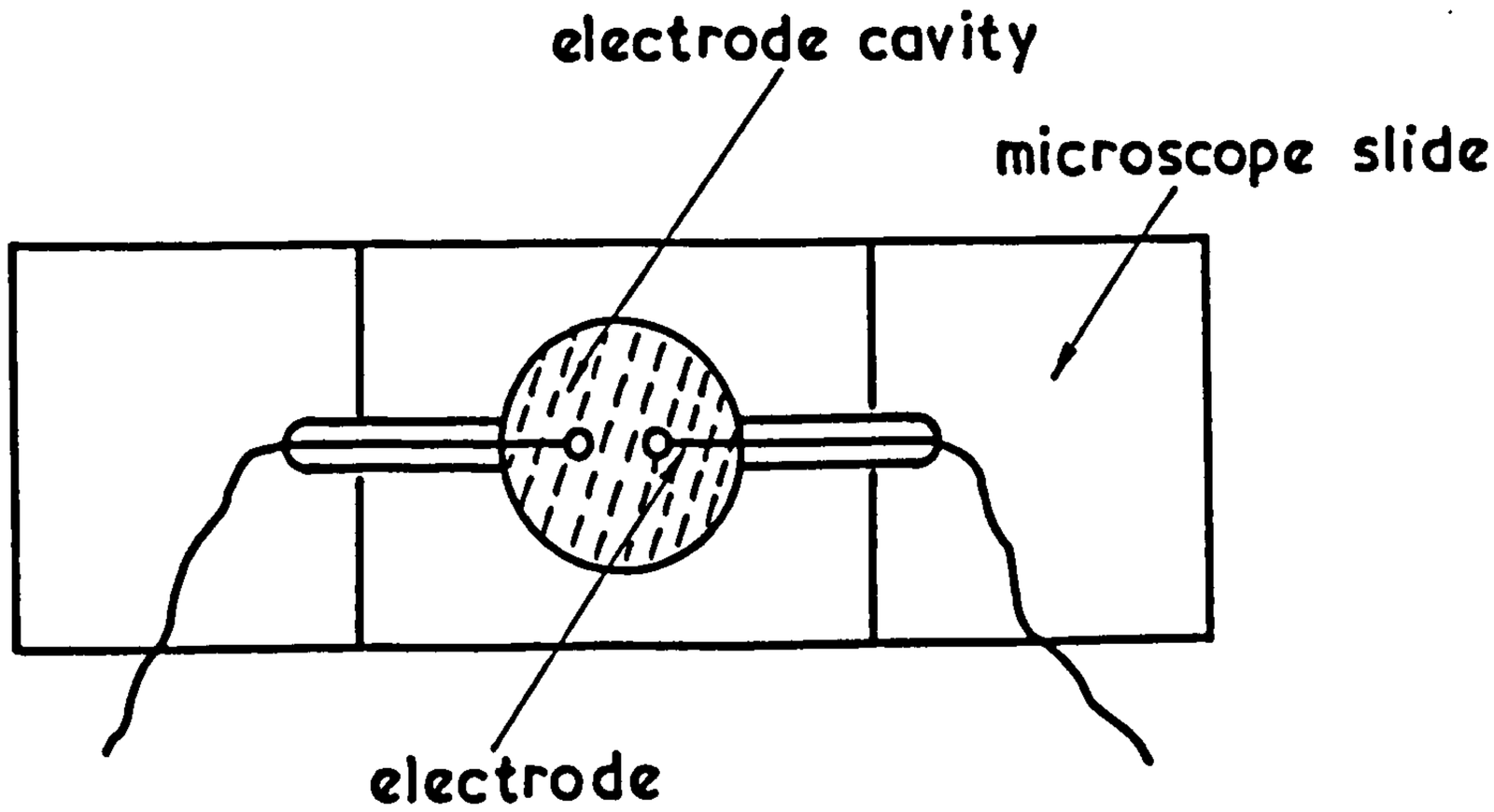

Fig 9.1
Dielectrophoresis test cell (Kindly loaned by Dr. R. Pethig).

of cells collected after a specified time interval, in the range of 2 to 3 minutes, is termed the yield or dielectrophoretic collection rate (DCR). In the present work the yields are arbitrarely expressed in divisions of the reticule of the microscope eyepiece; one division corresponds to 2.5 μm, about half a yeast cell diameter. The experimental arrangement is shown in Fig. 9.2.

9.1.5. Electrode cleaning

To begin with, the electrodes should be as smooth as possible. They must certainly be clean. After each yield measurement there is the problem of removing the collected cells from the electrodes. Merely turning off the applied field will not dislodge all of them. The best simple method is to remove the electrode cell from the microscope stage and rinse it with a hard stream of deionised water (from a plastic squeeze bottle). This usually removes all of the old cells. The cell can be dried in a current of air as to avoid error in the sample concentration.

9.1.6 Source of error

One of the most likely sources of error to the unwary is the accidental change in the conductivity of the suspension, especially when working with low conductivities. This can occur when the suspension comes in contact with any surface where ions are present. Fingers are especially troublesome. Ions can be easily transfered from them to

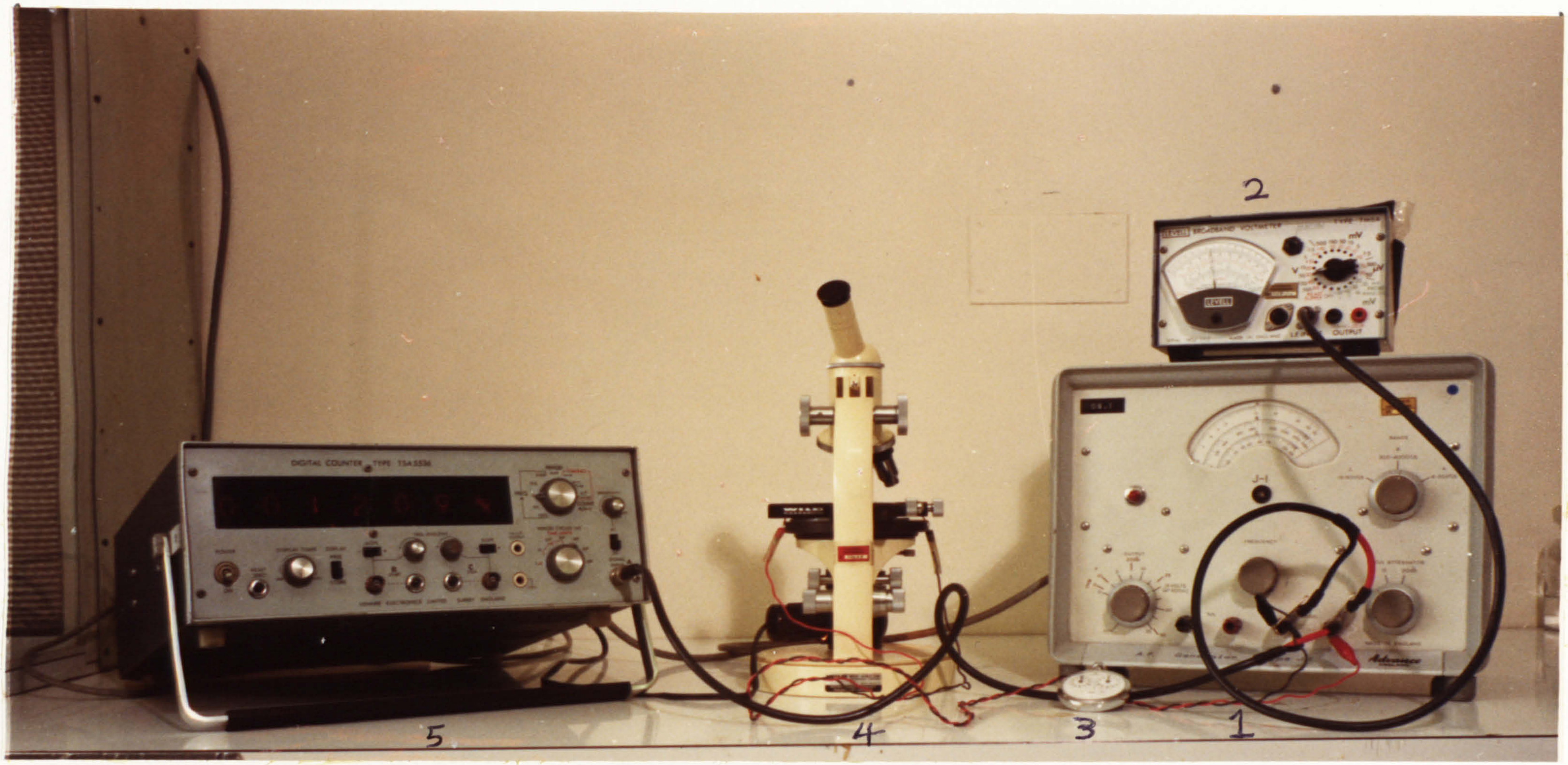

Fig. 9.2 Experimental apparatus for dielectrophoresis measurements.

1 - Advance audio frequency signal generator (Ad. type J1)

2 - Broadband Voltmeter (TM6A)

3 - Stop Watch

4 - Microscope (Wild M11)

5 - Digital counter (TSA 5536)

a utensil and then to the suspension. It is good practice for the experimenter to wear sterilised plastic gloves during the experimental procedure.

Other sources of ion contamination are the atmosphere CO_2 absorbtion and the cells themselves. The cells when placed in a low conductivity medium, will immediately begin to lose ions from their interior into the medium. For these reasons it is recommended that whenever possible, conductivity measurements should be made both before and after an experiment.

9.1.7 Preparation of the samples for synchronous growth and subsidiary measurements

The yeast used in this experiment obtained from Griffin and George Ltd. (No. ZEB-120-E) Saccaromyces cerevisiae (normal diploid strain) although a baker's yeast and a burgundy wine yeast, both commercial preparations, were also tried. Cells were grown at $30^{o}C$ to pure colonies in sterilised medium containing 10g potassium acetate, 6.7 g Difco yeast nitrogen base, 1g Difco yeast extract and 40 mg adenine per litre of 50 mM potassium hydrogen phthalate. The cells were harvested in late log phase by cooling to ambient temperature and then stored at $4^{o}C$ for some time. At this temperature cell division is inhibited, although the cells metabolize slowly to a point just short of division. As a result of this low-temperature storage, therefore, cell division commences synchronously in all the cultures of a batch, since inoculation is for

practical purposes simultaneous.

To perform an experiment the suspension of the required cells whose concentration had to be determined and adjusted using serial dilution and plating techniques (see appendix 13.1) , was raised (from 4°C) to the ambient temperature (~ 22°C). The suspension was centrifuged, and the supernatent liquid decanted. The cells were then resuspended in 0.25 M deionised sucrose and isolated by resuspension and centrifuging three times. An experimental sample prepared in this way provides cells all in the same growth phase which has special importance in biological studies.

9.1.8 Experimental procedure

The clean and dry electrode chamber (0.5 ml) was filled using a syringe graduated in 0.1 ml steps. After filling, the chamber was mounted on the microscope stage and the electrodes connected to the power supply.

When the selected frequency and voltage were applied it was usually observed that the cells migrated to the spherical electrode. They attached themselves in chain-like formations, commonly referred to as pearl chains, which aligned parallel to the field lines. The formations of pearl chains were clearly evident within a few seconds after switching on the field. The average length of these chains was measured after a given time using the reticule in the microscope and is designated the 'yield' or, more exactly, the dielectrophoretic collection rate. The elapsed time was measured with a stop watch.

9.2 Apparatus used for measurements of the dielectric properties

9.2.1 Three terminal test cell

Low frequency measurements of capacitance and dielectric loss were made using a three terminal test cell constructed as shown in Fig. 9.3.

This cell consists of a high electrode of 17 mm diameter and 0.7 mm in thickness, the common "low" electrode of 13 mm in diameter and 0.7 mm in thickness and a guard ring separated by a small gap of width 2 mm. The relative permittivities were calculated by dividing the capacitance of the cell containing a sample by that of air only $\varepsilon' = \frac{C_s}{C_o}$ whereas the dielectric losses ε'' were measured by multiplying ε' with D, the dissipation factor D measured by the capacitance bridge. The three terminal cell was made from brass coated with a thick layer of Ag-Ag Cl (see Appendix 13.2) as to minimize the electrode polarization.

9.2.2 Capacitance bridge

Measurements were made between 90 Hz and 100 kHz using a (GR 1656) capacitance bridge. An external oscillator (GR 1310 B) together with an external null detector (GR 1232A) were connected to the bridge to provide for operation at frequencies other than 1 kHz. A precision GR 1621 capacitance measurement system was also tried.

Fig. 9.3
Dielectric test cell
1 - Three terminal test cell
2 - 10ml beaker

9.2.3 Difficulties in bridge measurements

For the measurement of a dielectric dispersion curve the equivalent cell circuit can be complicated mainly by three factors:

1. Lead impedances
2. Stray capacitances around the test cell
3. Electrode polarization.

Long leads represent an appreciable inductance, which reduces the effective capacitance of the system. This effect is frequency dependent. To overcome this the test cell was designed to clamp onto the terminal of the bridge by three rigid copper wires each 6 cm long, thereby reducing the lead inductance to negligible proportions. The test cell would be firmly screwed to the bridge terminals thus preventing movement during measurement or during the filling or draining of the test cell.

To minimise the stray capacitance, efforts must be made to ensure that the electric field is mostly contained within the specimen, and that it is of a known geometrical form. For this reason a parallel plate with guard ring test cell was designed because it produces a uniform field through thespecimen. The guard ring of the test cell is connected to the earth terminal of the bridge for elimination of the stray capacitances around the test cell.

Electrode polarization is due to the migration of ions in a solution to the test cell electrodes where they form an ion layer which results in a contribution to the total capacitance of the system. This is eliminated by coating the electrodes with a thick layer of Ag-AgCl.

9.2.4 The temperature control system

The sample is placed inside a copper coil and the ends of this coil are connected to a rubber tubing carrying the circulating liquid from a water bath heating/cooling unit to the copper coil. The coil is placed inside a glass beaker. The spacing between the calorimeter and the glass is filled with teflon ensuring good insulation. Some water is placed inside the calorimeter, and the copper coil and the sample is placed in this water. Care should be taken not to allow water to enter the test cell. This routine provides very good temperature conduction and temperature equilibrium inside the sample is quickly reached. A mercury thermometer is placed near the copper coil. The top of the calorimeter is covered with a piece of cork with three small holes for the sample leads, thermometer and the ends of the copper coil. The thermometer is not placed inside the sample to avoid contamination.

Stabilization of the temperature in the cell usually takes 1½ to 2 hours to achieve and hence it is found to be more convenient to take measurements at several frequencies at one temperature rather than changing the temperature

at one frequency.

Since the bridge takes a three terminal measurement, the heating coils needed to be earthed and hence needed to be well insulated from the electrodes. The complete experimental arrangement is shown in Fig. 9.4.

9.2.5 Cell assembly

An arrangement was found such that the cell could be dismantled and reassembled with a change of only ± 0.25% in the cell constant. When assembled the cell was cleaned by rinsing several times first with deionised water and then with ASAB (a disinfectant/detergent) before finally being dried by a current of air.

9.2.6 Sample preparation

The sample was prepared in the same way as described for the dielectrophoresis measurements (9.1.7).

9.2.7 Sample concentration

If the solution is too dilute, the difference between the complex permittivity of the solution and that of pure water (the solvent) is small and consequently harder to measure accurately. A cell concentration of 1.9×10^6 ml^{-1} was found to be optimum for the work presented in this thesis.

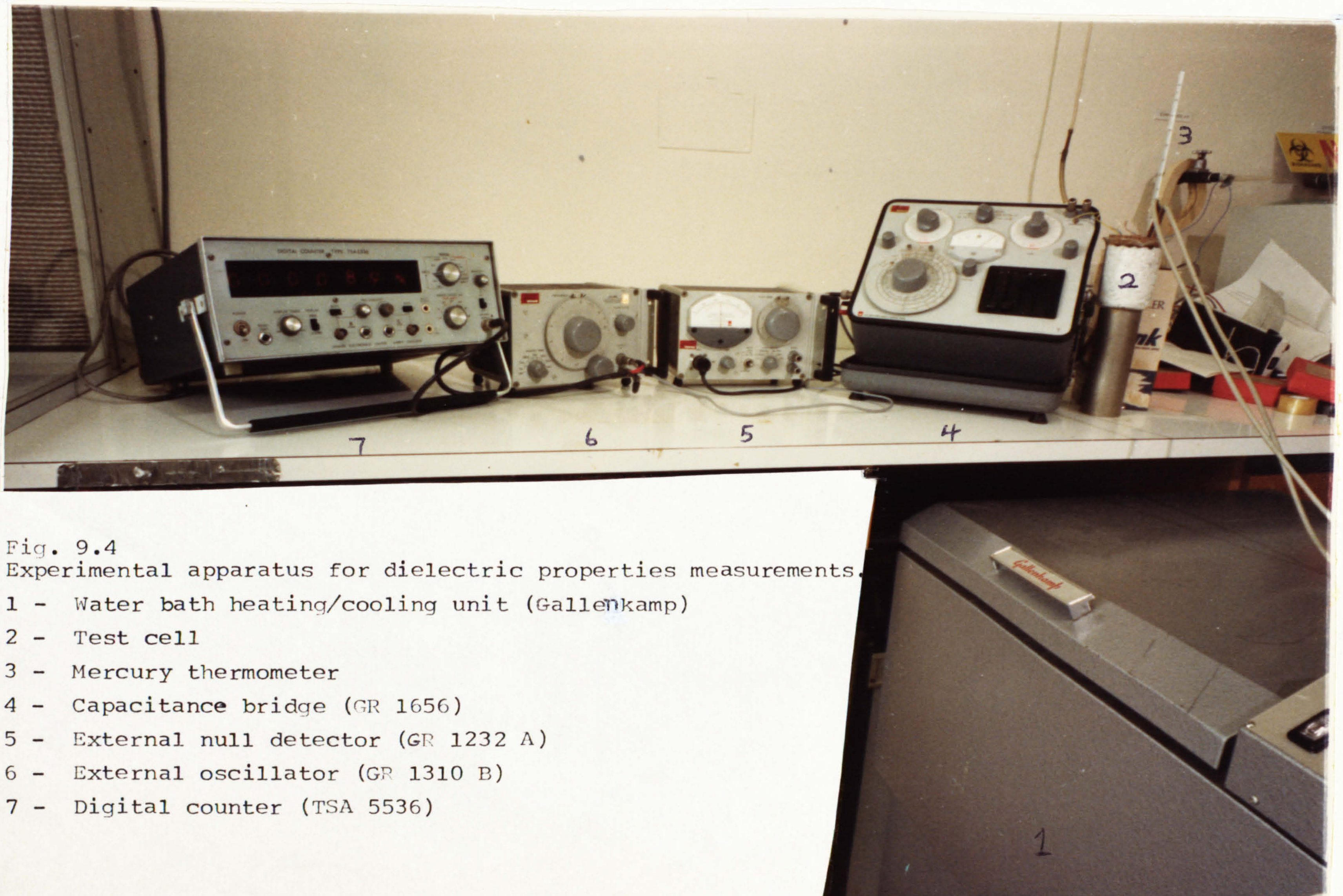

Fig. 9.4
Experimental apparatus for dielectric properties measurements.

1 - Water bath heating/cooling unit (Gallenkamp)
2 - Test cell
3 - Mercury thermometer
4 - Capacitance bridge (GR 1656)
5 - External null detector (GR 1232 A)
6 - External oscillator (GR 1310 B)
7 - Digital counter (TSA 5536)

9.2.8 Details of the experimental procedure

For the measurement of a dielectric dispersion curve.

1. Set the heating unit to the desired temperature.
2. While temperature equilibrium is being established, remove the cell from the TUV cabinet and place inside the 10 ml cavity.
3. Fill the cell with test solution ensuring that no bubbles form by viewing through the electrode gap.
4. Screw the cell onto the bridge terminals and measure the temperature in the heat control block. The heater unit thermostat may require slight adjustment to ensure exact temperature setting.
5. Measure the temperature in the vicinity of the sample.
6. Balance the bridge at the frequency to be investigated and look for any drifting of the reading. Wait until the reading is stable.
7. Record the C and D reading and adjust the oscillator to the next frequency to be investigated, balance the bridge . Continue throughout all frequencies (90 to 100 KHz).
8. When the last reading has been taken return and check the first reading for any drift.
9. All bridge readings were recorded on specially prepared sheets.

10. Remove the solution from the cell, rinse several times with water and ASAB and finally rinse several times with deionised water, dry and place inside the TUV cabinet for the next measurement.

Some notes on the procedure:-

(i) If the heating unit was at the correct temperature, it generally took only 10-15 minutes for a solution to reach equilibrium after being introduced into the cell.

(ii) The temperature unit itself could take an hour or more to reach temperatures below ambient.

(iii) In balancing the bridge, sufficient signal must be received by the detector to make an accurate measurement. This is achieved by increasing the sensitivity of the bridge when needed or out put of the oscillator.

9.3 Apparatus used for measurements of the steps in voltage-current characteristics observed using live yeast cells

The dielectrophoretic techniques used for the observation of steps in the current-voltage characteristic.

For these experiments the electrodes (Fig. 9.5) are set very close to each other. The spacing between them is adjusted under a Wild M11 microscope spacings down to 1 μm have been used. To keep the spacing between the electrodes at 1 μm during sealing with Araldite epoxy resin, a 1 μm piece of mica is kept between the electrodes gap.

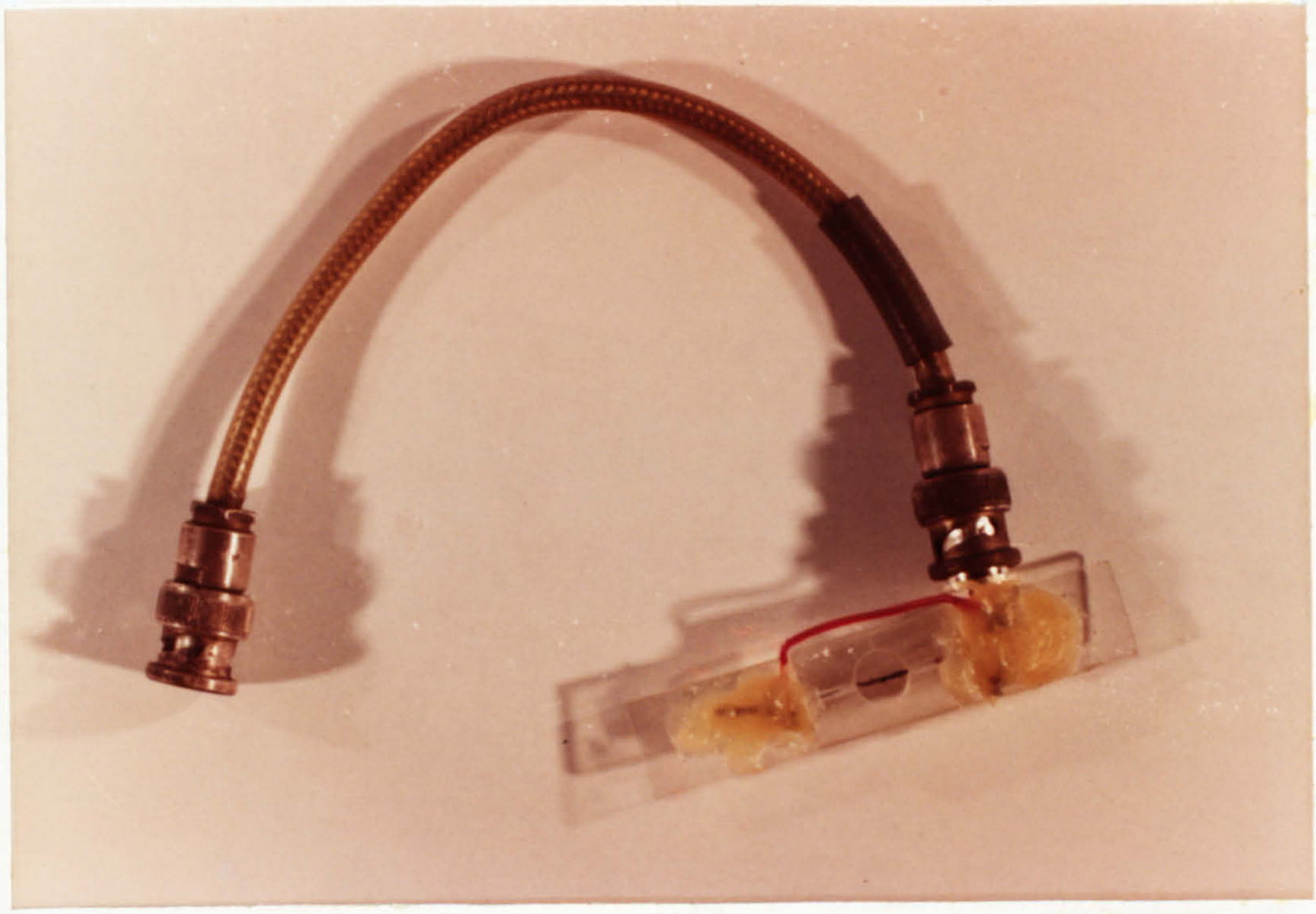

Fig. 9.5

Test cell used for measurements of the steps in Voltage-current characteristics of a Pearl-chain of live yeast cells.

The cavity around the electrodes is filled with the yeast cell suspension and an RMS voltage of the order of 30-40 volts, 1 KHz - 50 KHz is applied to the electrodes until the space between the electrode is bridged by a single cell in the case of 1 μm gap or else filled by a pearl chain of yeast cells within three to five minutes. The electrode chamber is then removed from the microscope stage and placed in an electrical or magnetic shield or else electromagnet without disturbing the pearl-chain . A slowly varying current is applied to the junction by a saw-tooth generator in series with a high value resistor at a frequency of no greater than 0.01 Hz. The voltage across the cells and the current are measured by microvoltmeter (Keithely 150 B) and a microammeter respectively. Their outputs are connected to an X-Y plotter which is calibrated in μv and nA per mm respectively. The complete experimental arrangement is shown in Fig. 9.6.

9.3.1 Sample preparation

A 5 ml aliquot of growing yeast cells S. Cerevisiae (normal diploid strain) are inocculated into the nutrient medium (9.1.7) in a 25 ml sterile bottle. The sample is then incubated for 48 hours at 30°C. As soon as this period of time is elapsed, the cells are harvested from growth by cooling to ambient temperature and then placed inside the refrigerator at 4°C for 5 days to achieve cell synchronization. After this period of time the cells are brought to the room temperature,

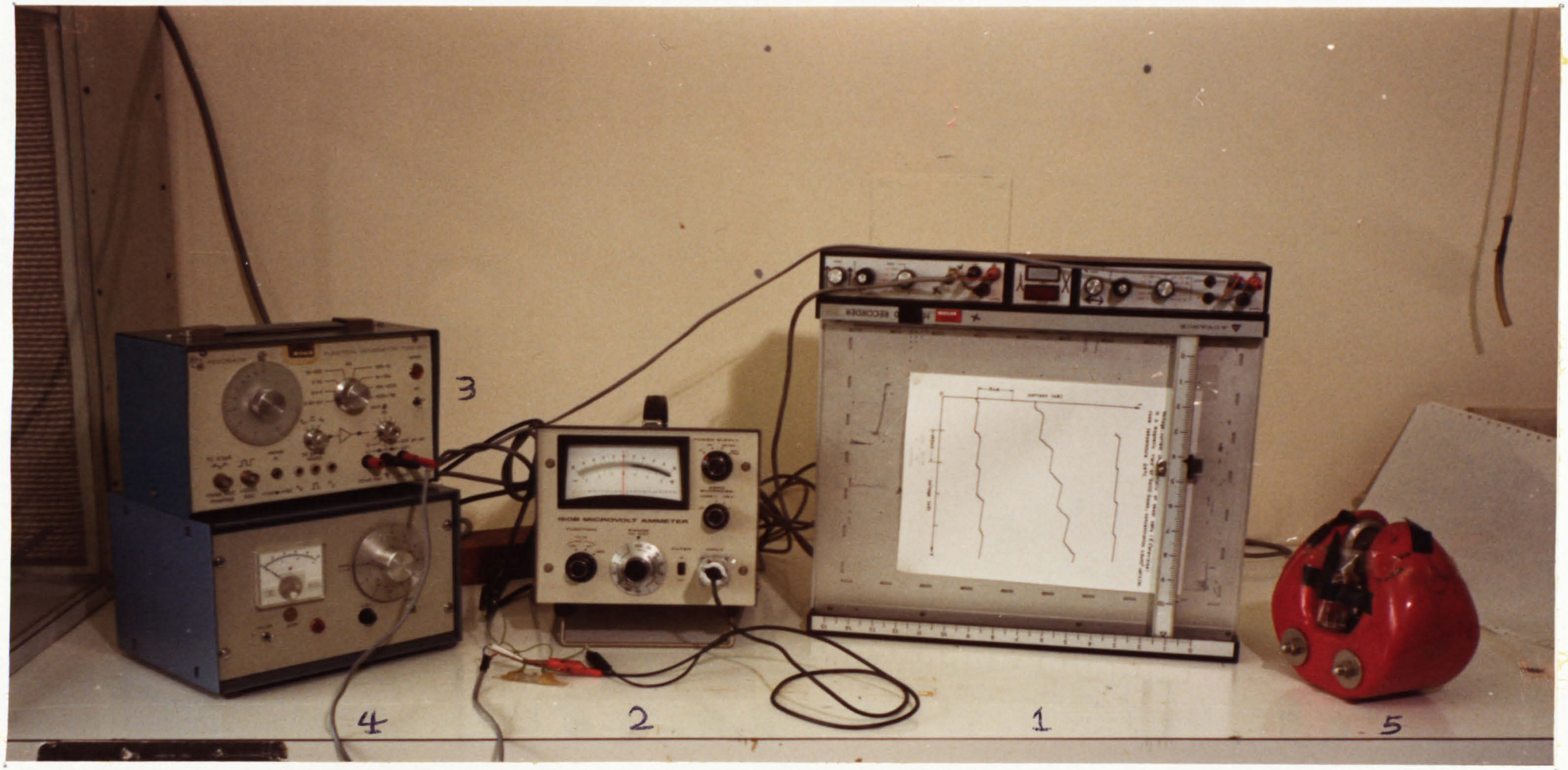

Fig. 9.6. Experimental apparatus for measurements of the steps in voltage-current characteristics observed using live yeast cells.

1 - X - Y Plotter
2 - Microvoltmeter (Keithely 150B)
3 - Saw-tooth generator
4 - Microammeter
5 - Permanent Magnet

distributed into four 5 ml sterilised bottles to balance the centrifuge. They are then centrifuged and the supernatant liquid is decanted. The cells are then washed three times, with deionised 0.25 M sucrose, then combined into a single 5 ml bottle, suspended in 5 ml of deionised 0.25 M sucrose solution and incubated for 3 hours at 30°C . An experiment should definitely be started within the period 3 to 5 hours from commencing inocculation. The mean generation time is 4 hours . After filling the electode cavity the remaining of the 5 ml bottle should be immediately returned to incubation at 30°C in case further samples are required within the next couple of hours.

9.3.2 Types of electrodes configuration used

The electrodes were 78 RPM steel gramophone needles. Besides a two electrode configuration , a four electrode geometry (Fig. 9.7) was also tried.

9.3.3 Water

The deionised water was recirculated for 7 hours through the deioniser (Lang, type Ka) using a PTFE diaphragm pump. It was found that a single pass water was less effective on the cells collected dielectrophoretically due to the high conductivity of the water.

Where necessary the water was sterilised after deionising.

Fig. 9.7

Types of electrode configuration used.

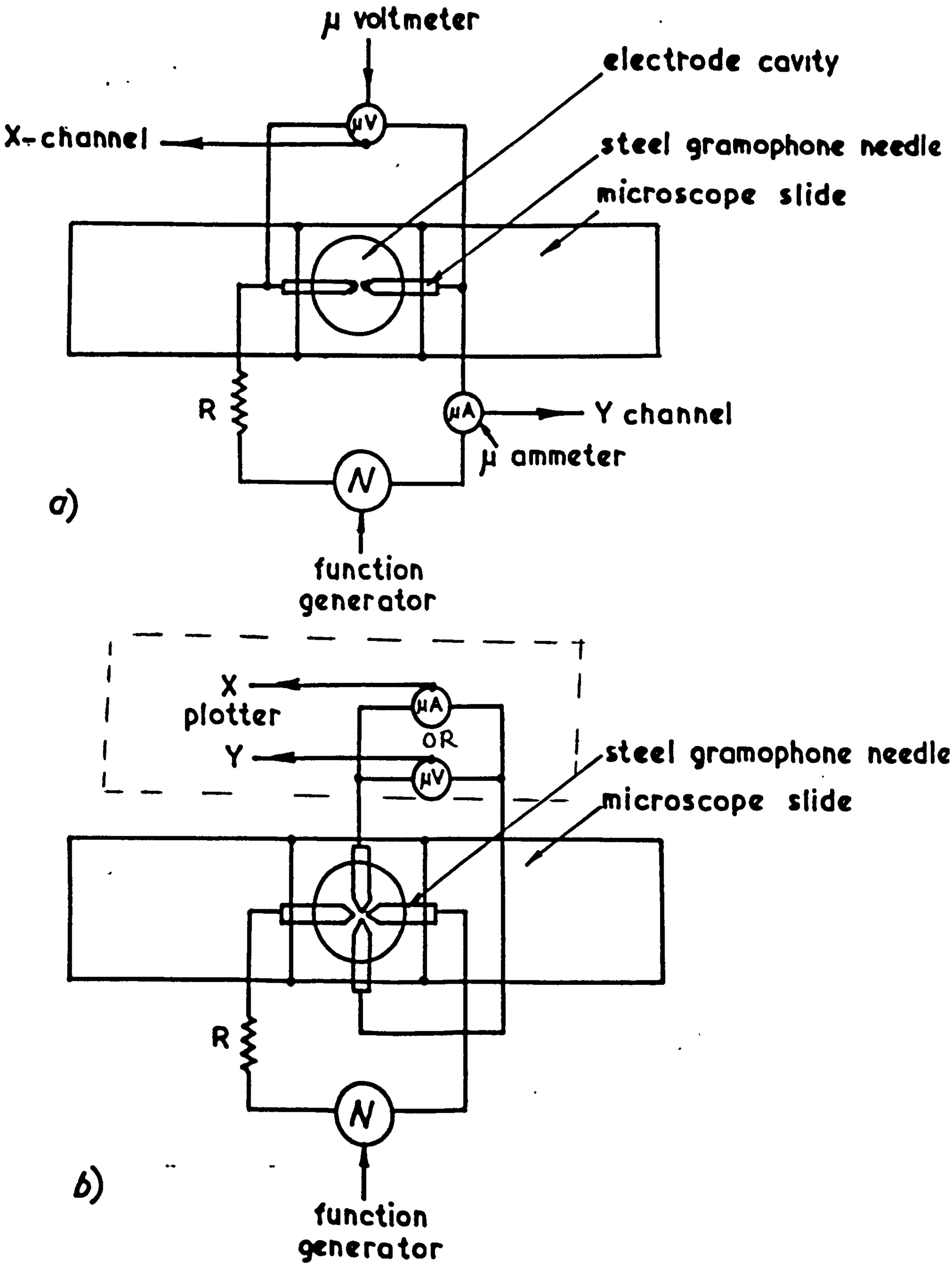

9.4 Apparatus used for measurements of the oscillations emitted from dividing yeast cells

The apparatus used for this experiment was a Hewlett Packard Spectrum Analyser (H.P. 8553B). The Tracking Analyser (H.P. 8443B) was used to measure and set the centre frequency of the scan on the display.

The experiment was used in an electrically screened laboratory with filtered power supplies. Even so at maximum sensitivity of the apparatus it was just possible to detect TV transmissions above 50 MHz, and the campus paging network transmission on 13 MHz.

Although various electrodes were tried, the sample preparation remained the same as that described in section 9.3.1 Electrodes responses were found as follows:

(a) The steel needle electrodes with a gap of 1 μm gave the best results. (b) Ag/AgCl with the 1 μm gap gave an emission at one occasion only (c) Anodised aluminium electrodes gave no emission at all accompanied by a reduction in the noise level.

It was also found that pouring the solution in the electrode cavity directly from the solution bottle without using a pipette and dielectrophoresis technique gave better results.

During the experimental work as soon as the oscillation emerge from the noise the following steps were followed:

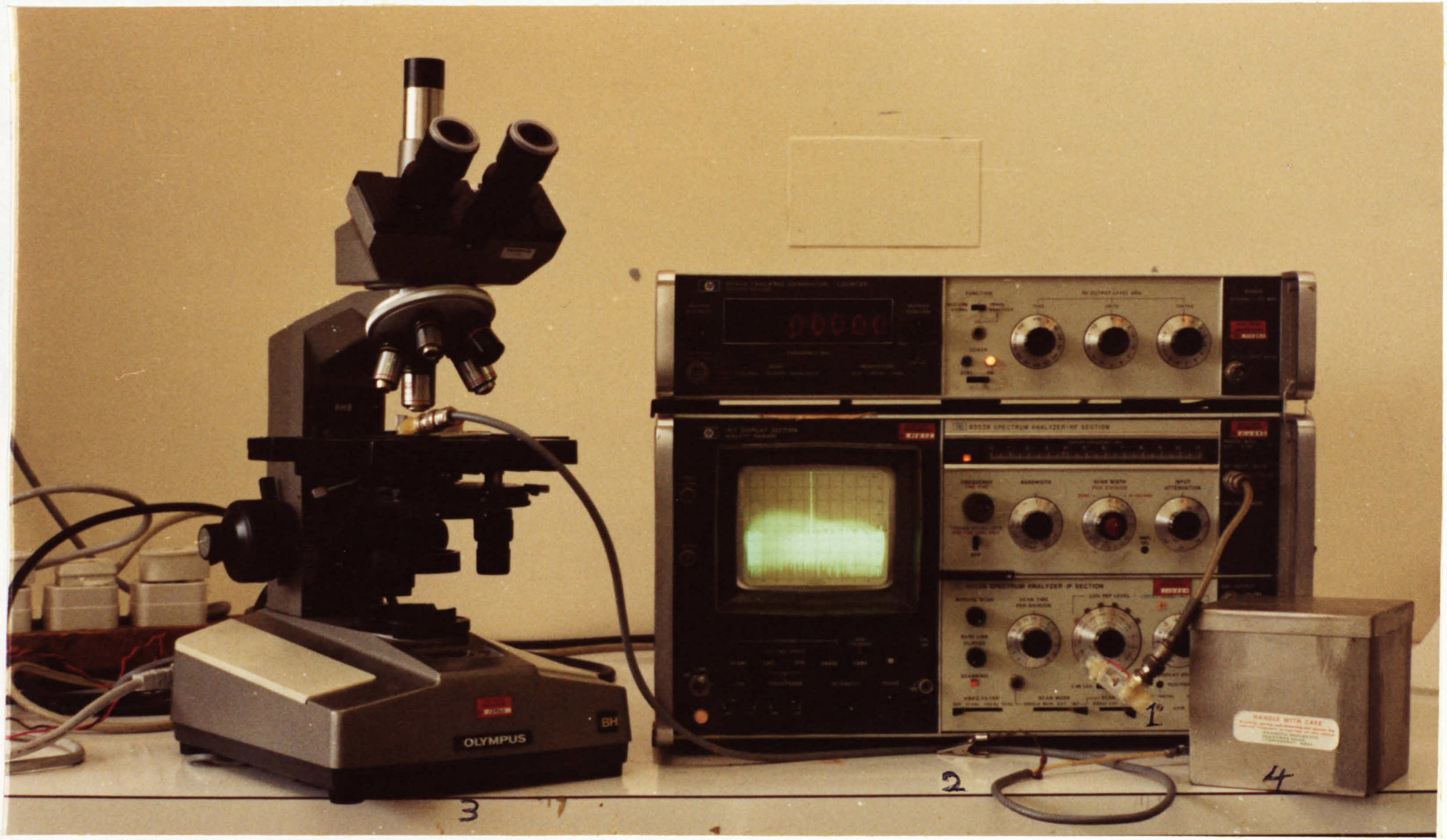

Fig. 9.8 Experimental apparatus for radio frequency detection from dividing yeast cells.

1 - Test cell
2 - Spectrum analyser
3 - Phase contrast microscope
4 - Mumetal container - Extra Shield

(a) The emission was stored. (b) Photographed within a period of 1 minute. (c) The rest of the time which was of the order of another couple of minutes were spent on the confirmation of the oscillation and not to be an artefact or a foreign transmissions. The complete experimental arrangement is shown in Fig. 9.8.

9.5 Apparatus used for measurements of magnetic resonance effects on the potassium and sodium content of bovine eye lenses through microwave modulation

The apparatus shown in Figure 9.9. was used for the irradiation with microwaves and microwaves modulated under NMR conditions of bovine eye lenses.

An advance audio frequency signal generator type J_1 was used to provide the NMR frequency. Its output frequency and voltage were read on a digital frequency counter type TSA5536 and a broadband voltameter type TM6A respectively. After reading the right frequency and voltage, the output was fed to the modulation input of the microwave frequency generator (GRC 1209-C) which was used to set the microwave frequency and its output was placed in black box and was well sealed off during the period of exposure so that no radiation could escape to the surrounding environment. The whole experimental materials of these measurements were provided and analysed by the biochemistry Laboratory, are described in appendix 13.3.

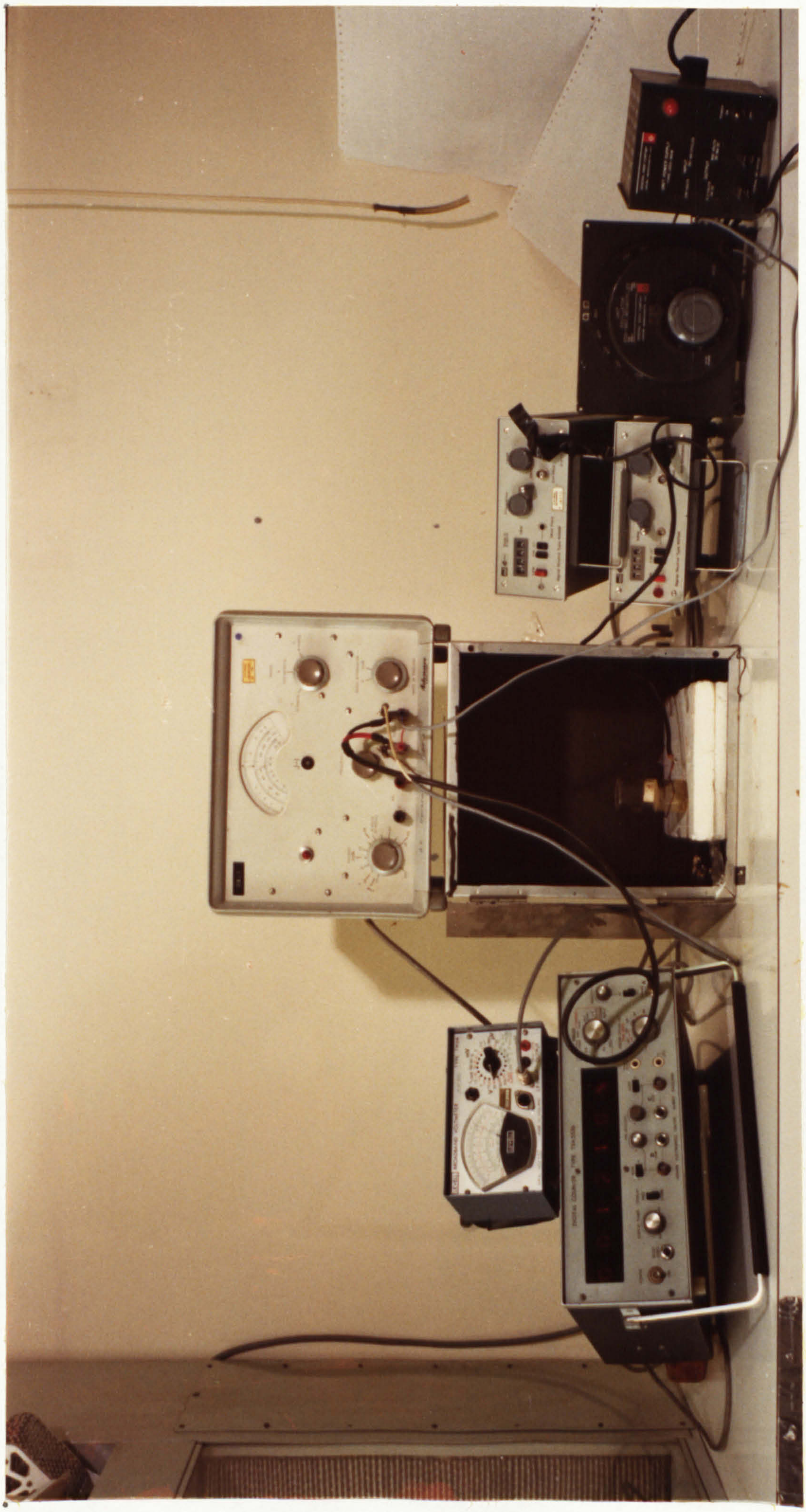

Fig. 9.9
Experimental apparatus for irradiation with microwaves and microwaves modululation satisfying the appropriate magnetic resonance conditions.

CHAPTER 10 EXPERIMENTAL RESULTS

The results are divided into five parts. In the first part are the results of a suspected anomaly in the region of 2kHz noted in published dielectrophoretic yield curves on a suspension of live yeast cells are given. The possibility that it could be due to magnetic resonance phenomenon, associated with the interaction of the geomagnetic field was checked first. The second part is concerned with dielectric measurements as a function of frequency and temperature for different magnetic isotopes on a suspension of live yeast cells. The third part is concerned with the steps in the voltage-current characteristics of a pearl-chain of live yeast cells with point electrodes. The fourth part is concerned with oscillations from dividing yeast cells . The fifth part is concerned with the effect on the sodium and potassium content of the Bovine eye lenses through microwave modulation that satisfied the appropriate magnetic resonance conditions.

10.1 Dielectrophoresis measurements

Several published dielectrophoretic yield curves for biological cells showed unexplained deviations in the region of 2kHz. Figure 10.1 shows the dielectrophoretic yield as a function of frequency for both live and killed yeast cells. The live cells had been killed by exposing the freeze-dried powder to a TUV lamp (254 nm) overnight which inflicts damage

Fig 10.1

Dielectrophoretic yield spectra of live and dead yeast cells as a function of frequency of the electric field. Ambient magnetic field 0.5 gauss.

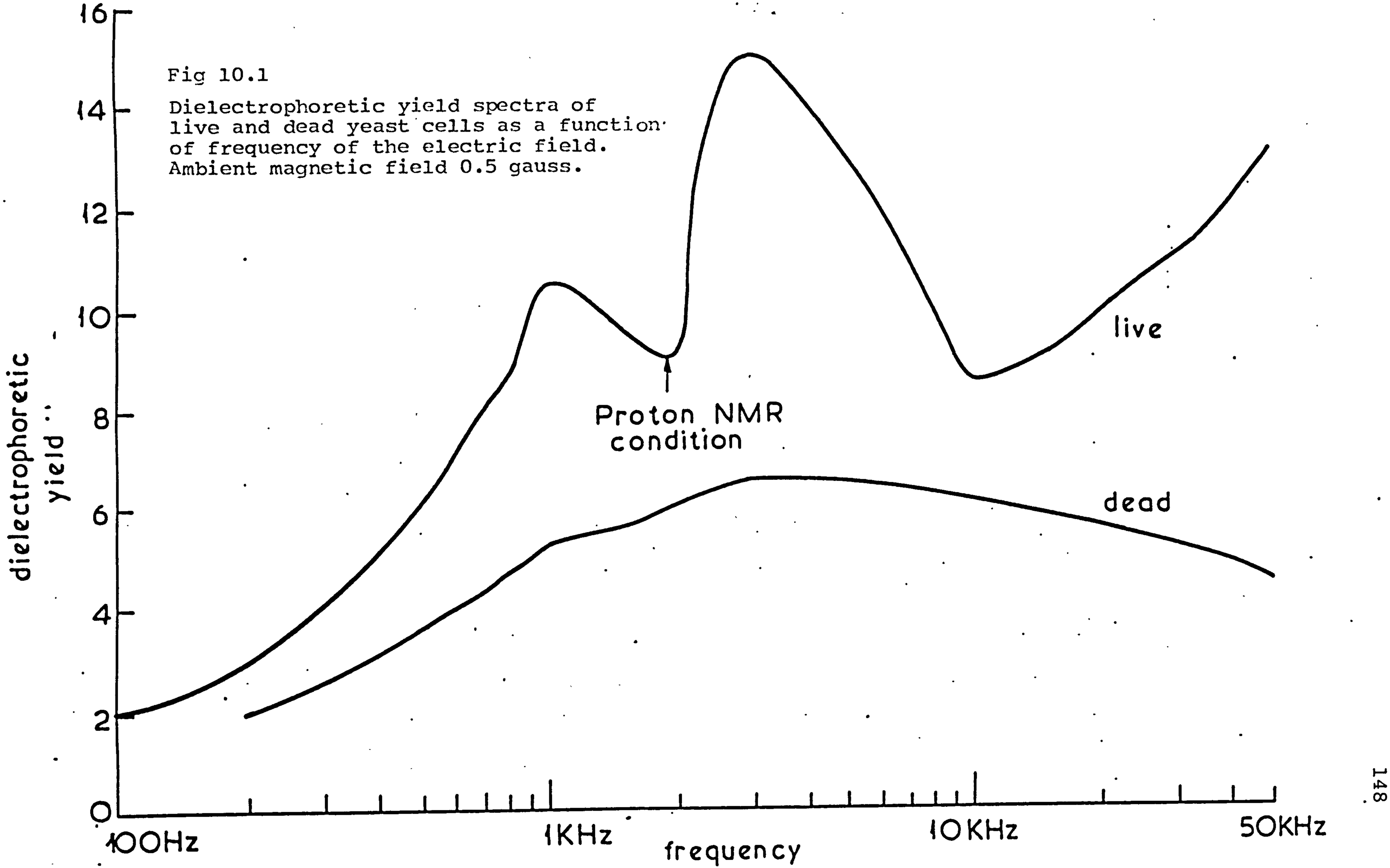

to the membrane and the nucleus on subsequent plating on malt-extract agar, no growth was observed. The anomaly in the region of 2kHz is clearly seen in the curve for the live cells. Figures 10.2 and 10.3 show that the dielectrophoretic yields as a whole are proportional to the applied voltage over much of the range as is predicted from the theory, although the anomaly in Fig. 10.2 remains at the same frequency. Figure 10.4 shows that the yield of both live and dead cells is proportional to the square root of the collection time (i.e. $Y \propto t^{\frac{1}{2}}$) which confirms that the experiment was carried out under conditions relevant to the theoretical considerations mentioned.

In Figure 10.5, the anomaly is seen to move in frequency in proportion to the field from a bar magnet placed near the microscope stage. The field strength was measured with a Bell-610 gaussmeter. Some features of the curves are clearly independent of the magnetic field, but there are others at lower frequencies which are magnetic field dependent and were found to correlate with other resonances, Figure 10.6 shows the results of measurements on live cells from 0.5 to 5G (50μT to 500μT) normalised by plotting as the abscissa kHz/G. The anomaly then shows up clearly as a sharp resonance at exactly the proton magnetic resonance condition of 4.26 kHz/G.

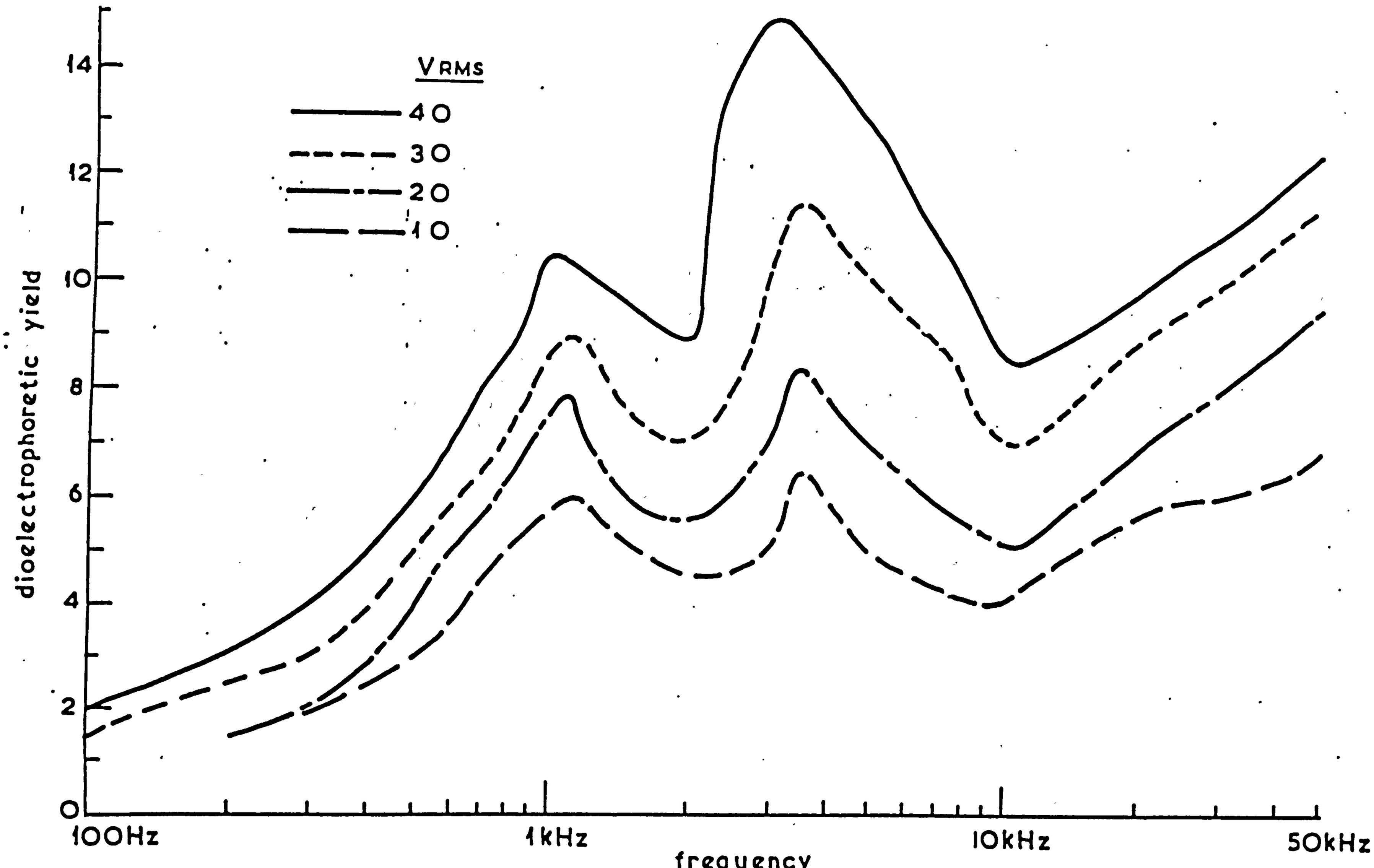

Fig10.2 DIELECTROPHORETIC YIELD SPECTRA OF LIVE YEAST CELLS AS A FUNCTION OF THE FREQUENCY OF THE ELECTRIC FIELD.

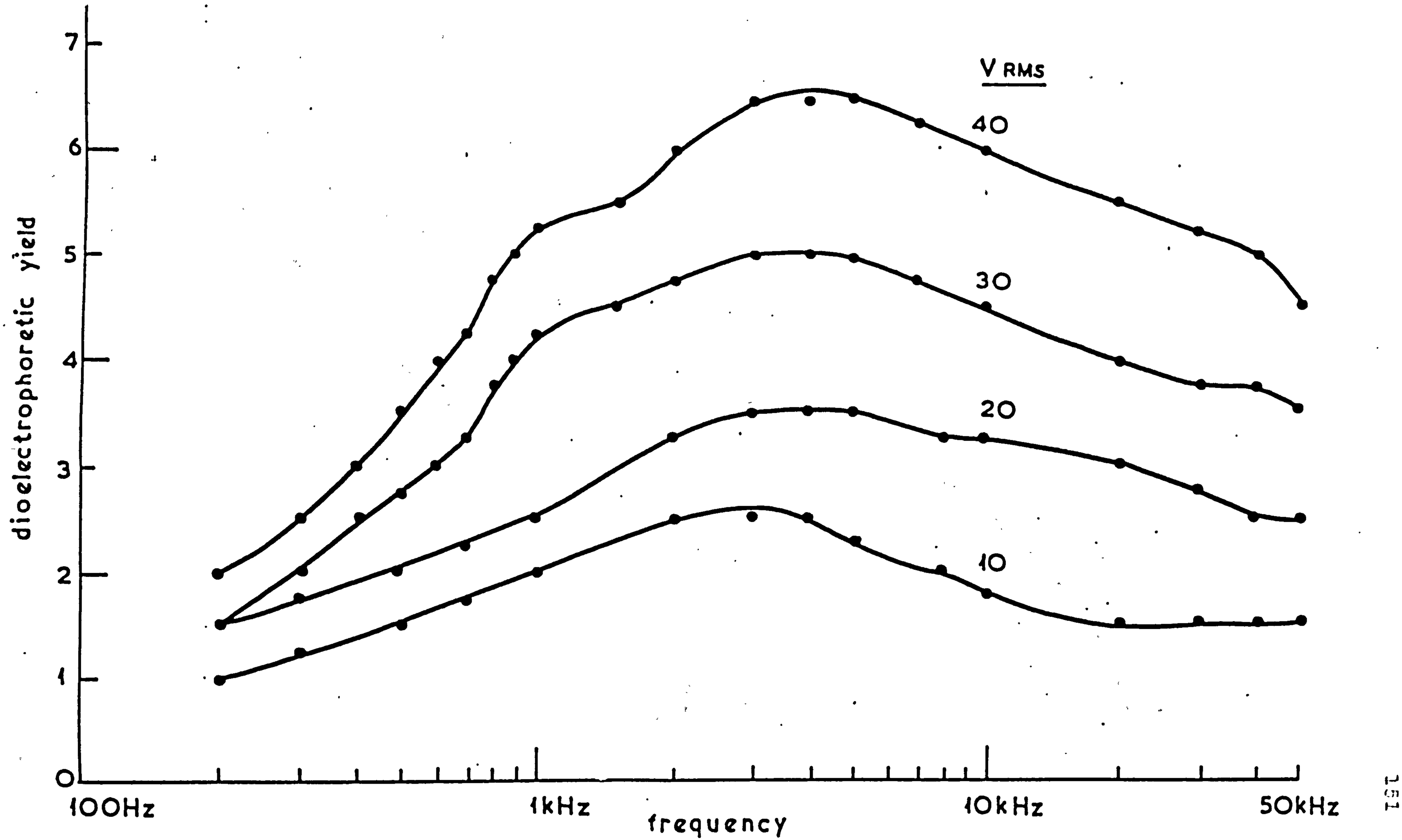

Fig 10.3DIELECTROPHORETIC YIELD SPECTRA OF DEAD YEAST CELLS AS A FUNCTION OF THE FREQUENCY OF THE ELECTRIC FIELD. YEAST CELLS IRRADIATED WITH UV LIGHT (254 nm).

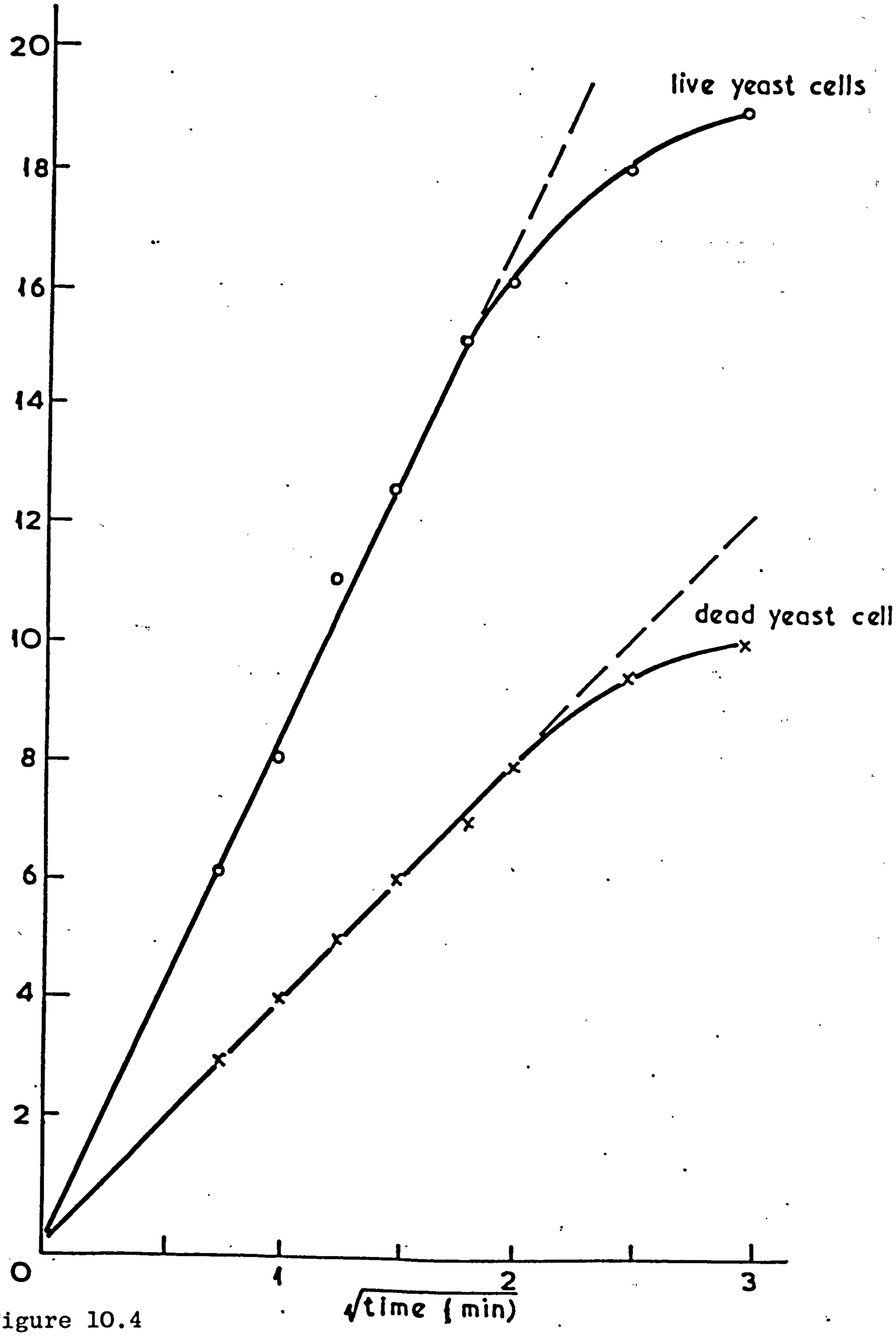

Figure 10.4

VARIATION OF DIELECTROPHORETIC YIELD WITH THE SQUARE ROOT OF THE LENGTH OF TIME THE FIELD IS APPLIED V = 40 Vr.m.s., FREQUENCY = 3 kHz.

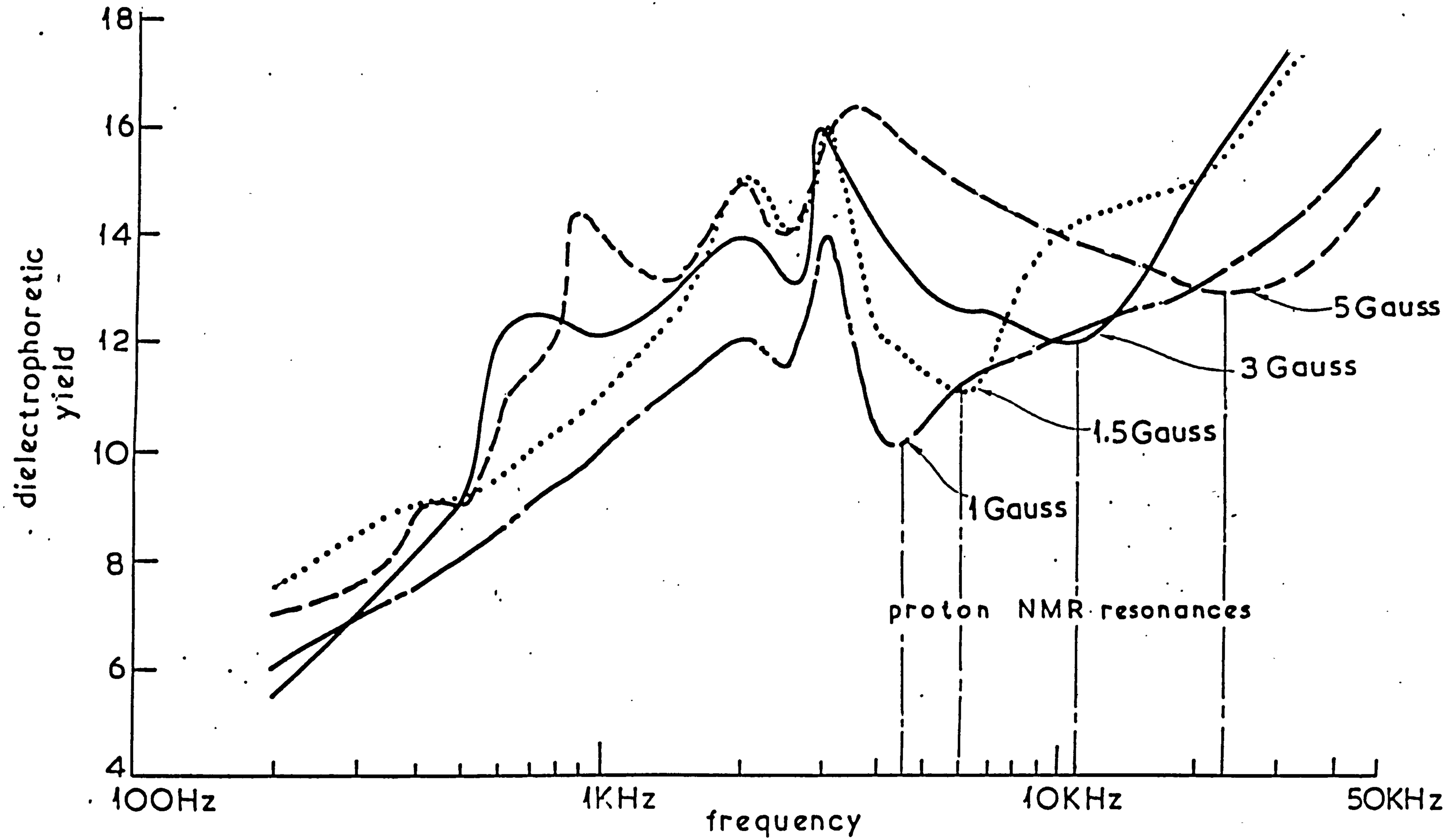

Fig 10.5 Electromagnetophoretic yield spectra of live yeast cells as a function of the electric field freauency.

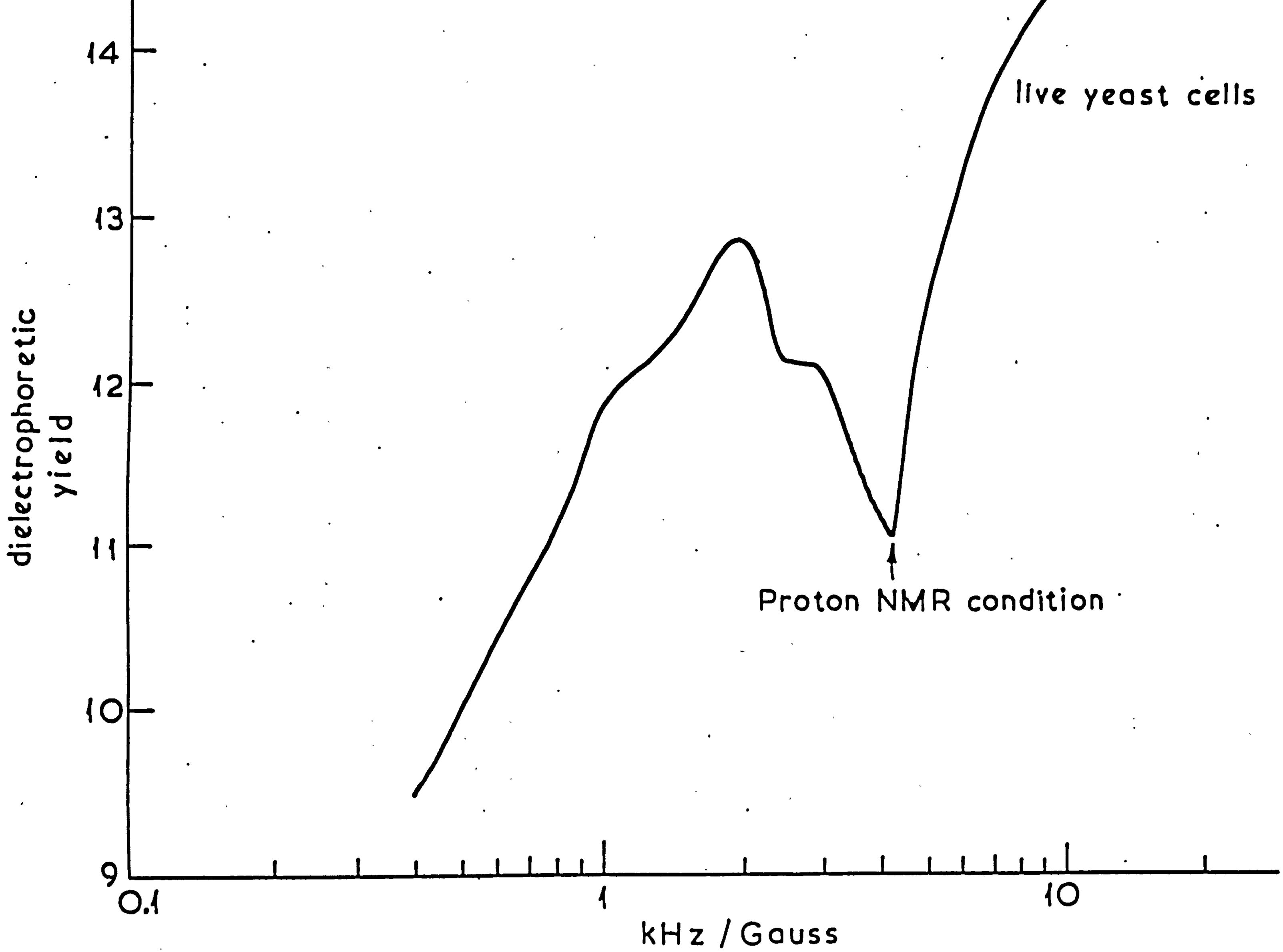

Fig 10.6 Average values frequency ÷ magnetic field (0.5G to 5G)

10.2 Dielectric measurements

The permittivity and loss for live yeast cells were measured for a suspension containing 1.9 x 10^6 cells/ml at room temperature and in magnetic fields from the laboratory ambient of 0.5G to 5G. Figure 10.7 shows the very sharp resonances, about 1Hz bandwidth, which were observed in the dielectric loss. It was necessary to use a digital frequency meter (Venner type TSA 5536) to be able to set the frequency of the oscillator to an accuracy of 0.01% and to monitor its stability. Figure 10.8 shows values of the frequency and magnetic field for both the dielectric loss peaks and the anomalous field-dependent features in the dielectrophoretic yield curves, the line represents the proton magnetic resonance condition. Figure 10.9 shows the simultaneous frequency and magnetic field for proton NMR conditions. Figure 10.10 shows measurements within of 2Hz intervals this is as close as it was possible to take readings corresponding to the magnetic isotopes ^{34}K, ^{35}Cl, ^{23}Na and ^{31}P, are shown as anomalies in the dielectric loss and the dielectric constant in addition to those corresponding to protons (^{1}H).

The Larmor frequency in a magnetic field strength of 100 μT (1 gauss) for the magnetic isotopes shown in Figure 10.10 are as follows:-

Magnetic Isotopes	Spin	NMR Frequency B=100 μT (1G)
^{39}K	$^{3}/_{2}$	198.69 Hz
^{35}Cl	$^{3}/_{2}$	417.2 Hz
^{23}Na	$^{3}/_{2}$	1126 Hz
^{31}P	$^{1}/_{2}$	1723.5 Hz
^{1}H	$^{1}/_{2}$	4260 Hz

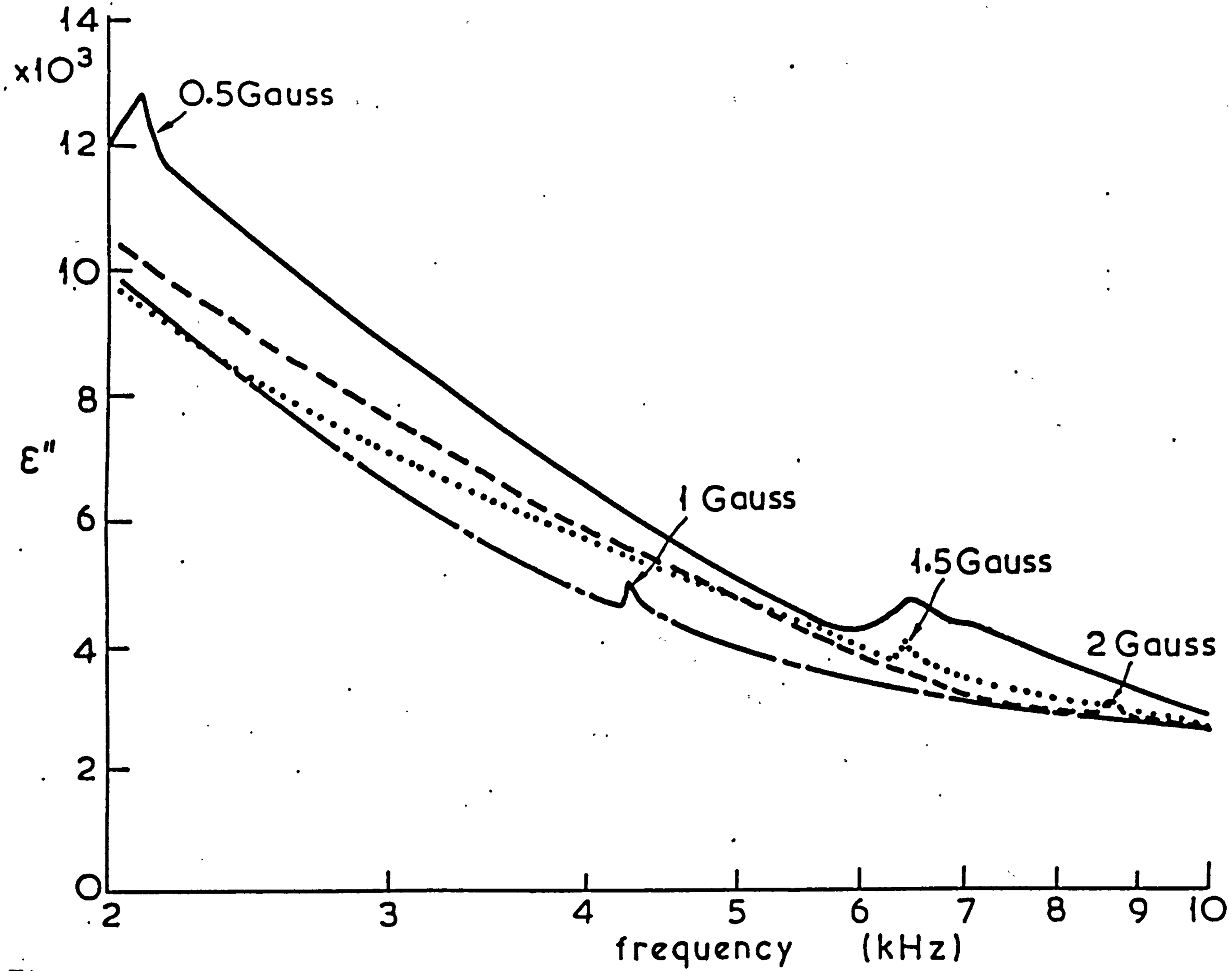

Fig. 10.7
Dielectric loss peaks at NMR field conditions of a 1% by weight bakers yeast in deionised water at 24°C.

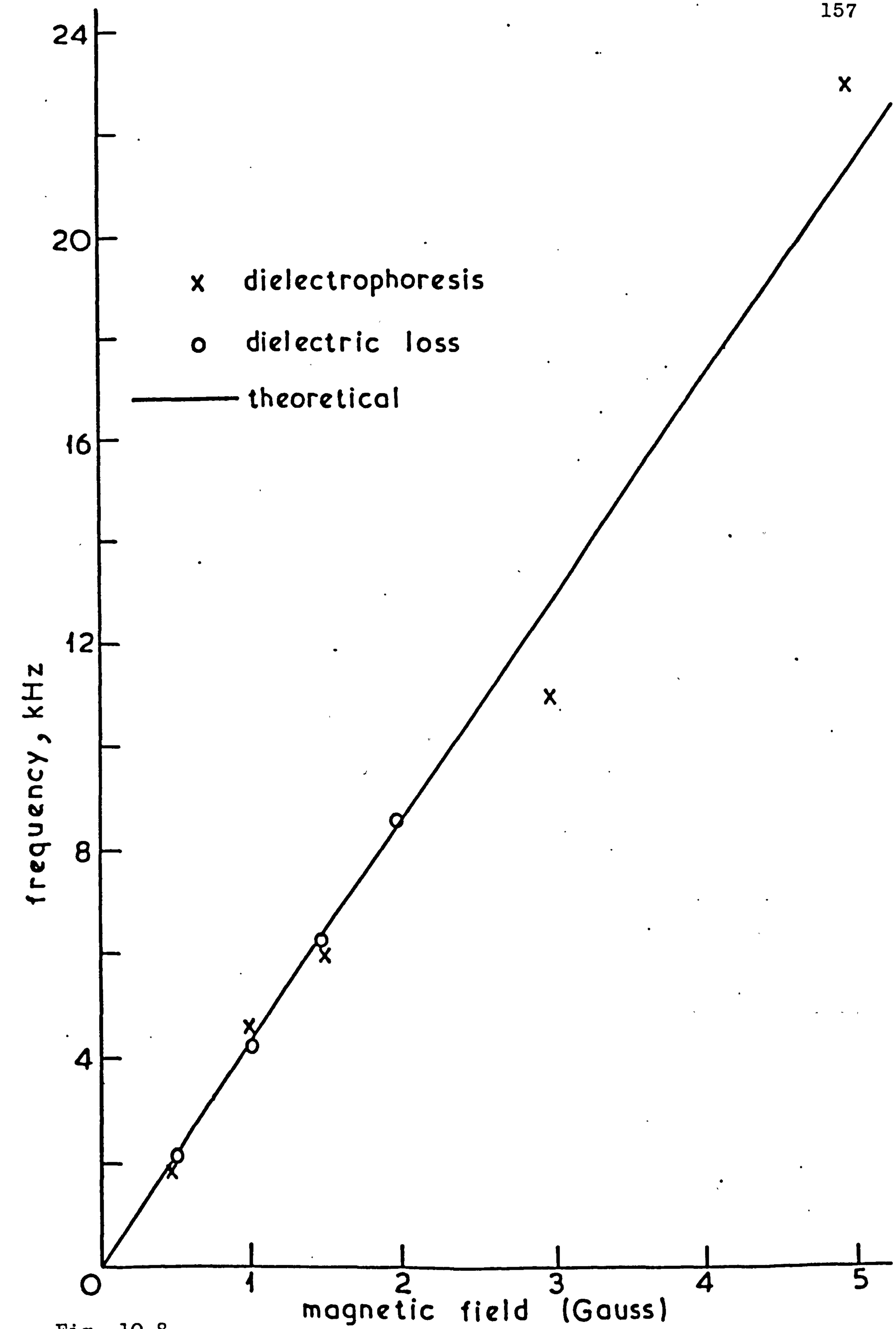

Fig. 10.8
Variation of Proton NMR peaks in frequency with applied magnetic field.

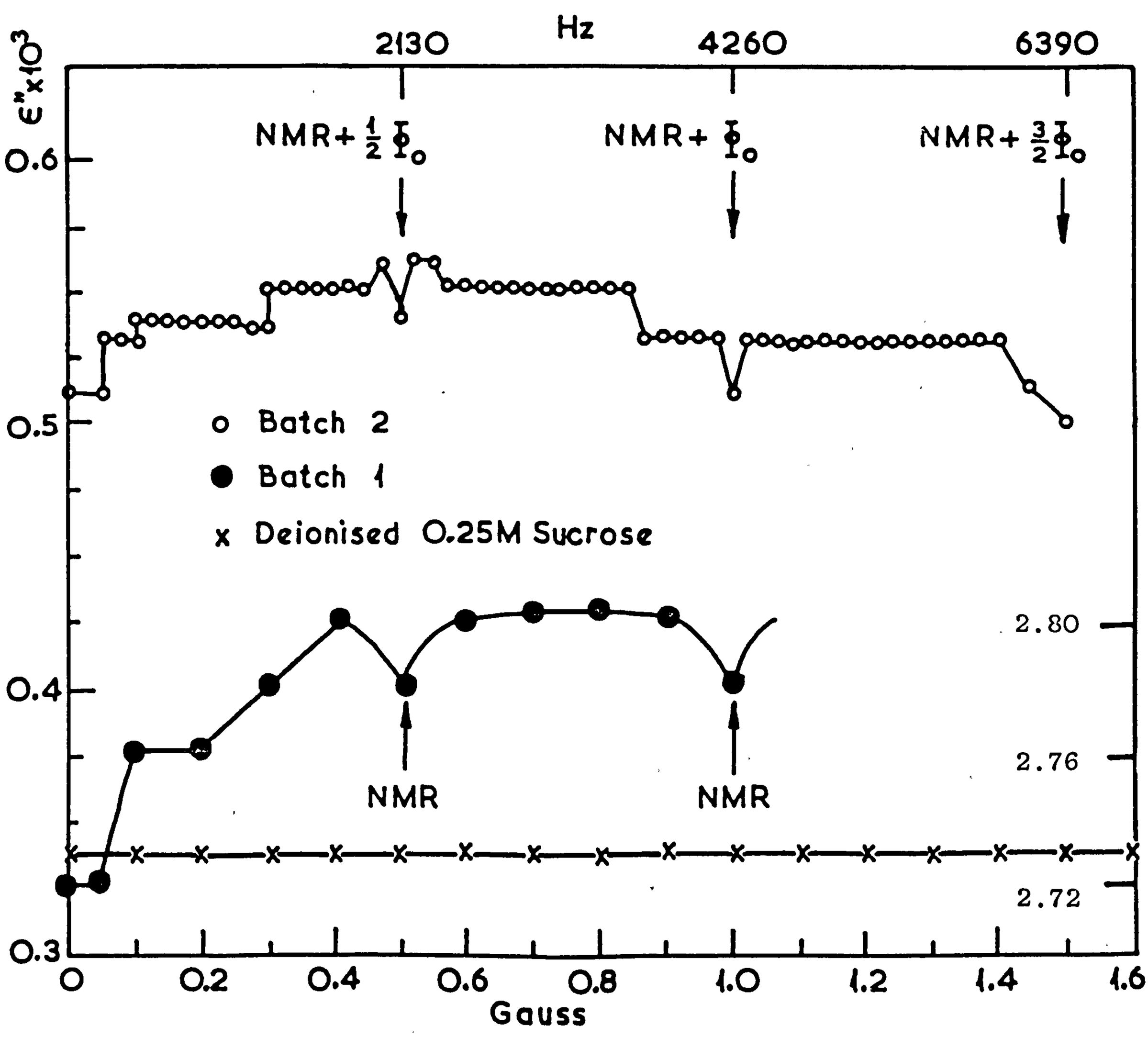

Fig. 10.9 Simultaneous frequency and magnetic field for proton NMR conditions.

Text cut off in original

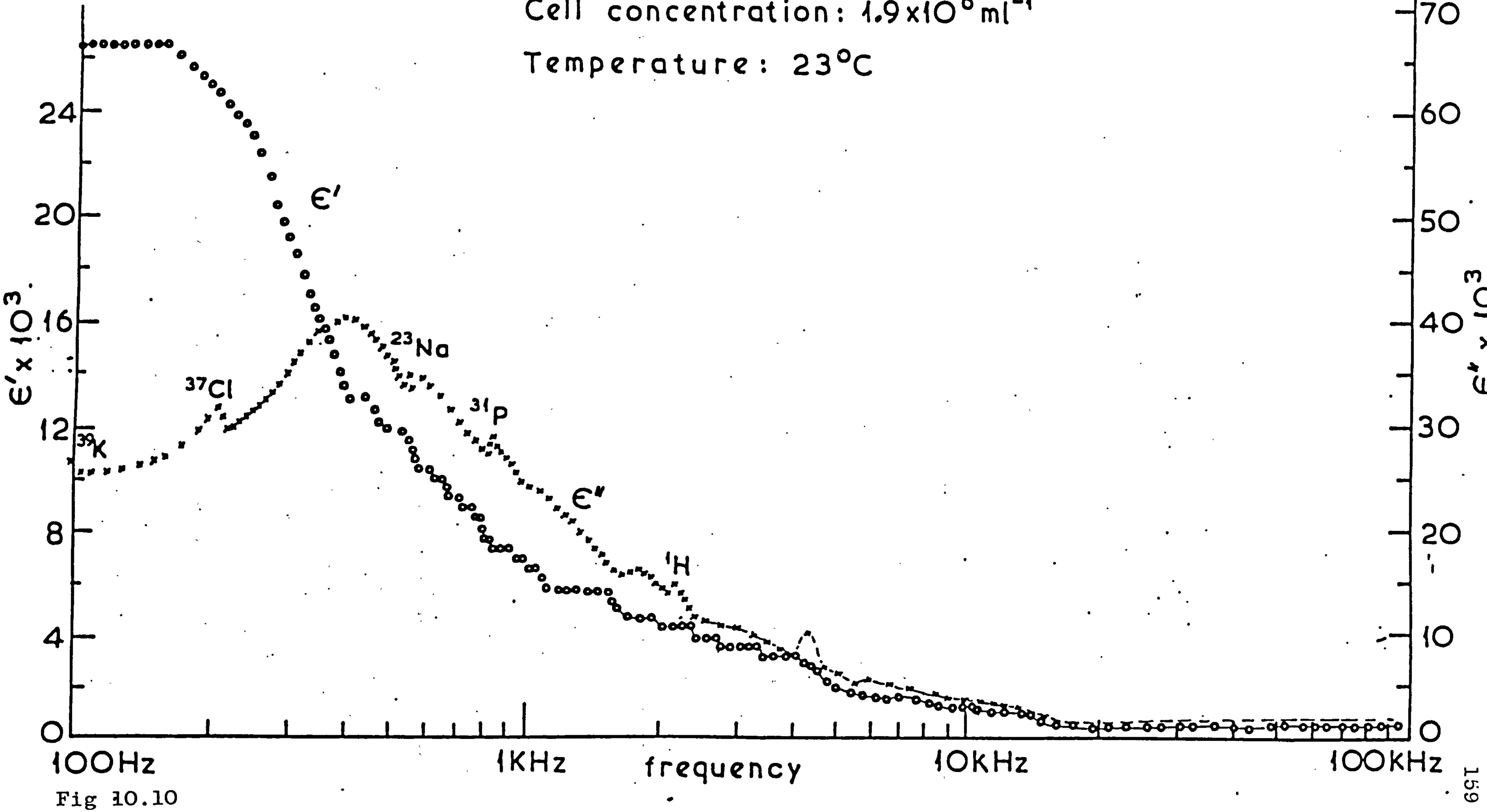

Fig 10.10

The real and imaginary parts of the complex permittivity of the live yeast (s. cerevisiae as a function of frequency. Laboratory ambient magnetic field: 0.5 Gauss.

Repeating the measurement by using exactly the same technique but first killing the cells by heat (by autoclaving them under high pressure steam at 121^{o}C in a pressure cooker) and condition as for live cells Figure 10.11 shows these peaks to be absent.

Sterilising the enzyme lysozyme in the same way, Ahmed et al (1982) had lost the anomaly observed in the course of magnetic susceptibility measurements.

Effect of temperature on the resonances observed in the permittivity and dielectric loss was investigated. They seem to be related to the cells status during the most active part of the life cycle when the cells are in the process of division (cytokinesis).

The magnitudes of these resonances are temperature dependent, as shown in Figures 10.12, 10.13 and 10.14, where the points were taken at 1 Hz intervals and represent the limit of accuracy of the present apparatus rather than the shapes of the resonances.

Figure 10.15 shows the mean generation times (a) in the ambient (earth's) magnetic field and (b) under proton (^{1}H) NMR conditions. When the cells are grown under proton NMR conditions the mean generation times show slight shift from that for cells grown in the earth's magnetic field. Comparison of this with the dielectric constant and loss increments at the corresponding temperatures (Fig. 10.16) shows that when the MGT is least, the cells are dividing most rapidly, and the dielectric increments are greatest.

A further resonance effect was observed in the live yeast cells when the conditions for electron spin resonance

(ESR) were satisified, i.e., at 2.8 MHz/G, as seen in Fig. 10.17. These measurements were taken between 0.5G and 1.5G with a Q-meter.

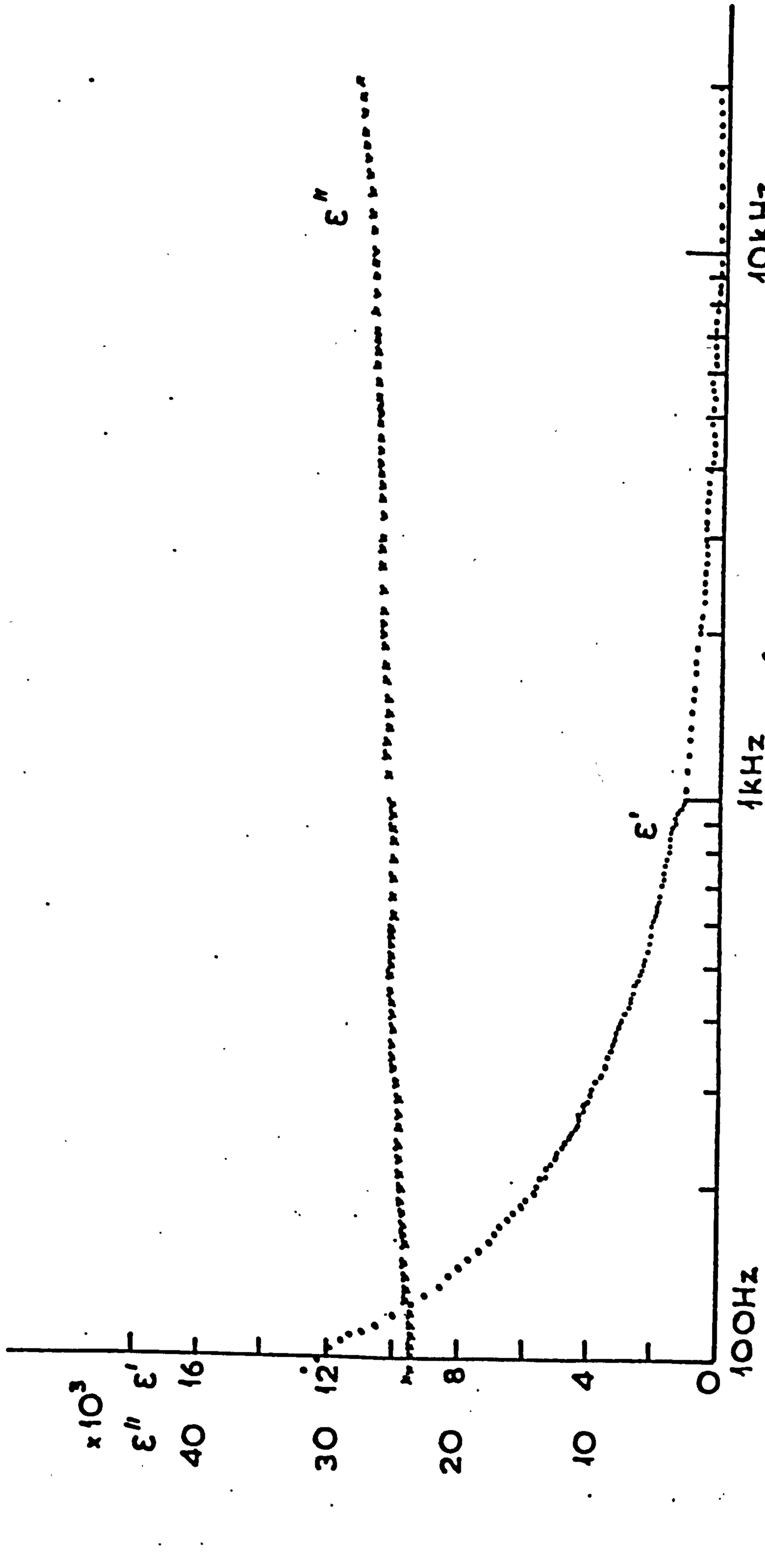

Fig. 10. 11
DEAD YEAST CELLS. STERILIZED AT 121 °C (15 lb/sq. in) for 15 MIN. GR 1621 CAPACITANCE MEASUREMENT SYSTEM.
AMBIENT FIELD 0.5G (50μT).

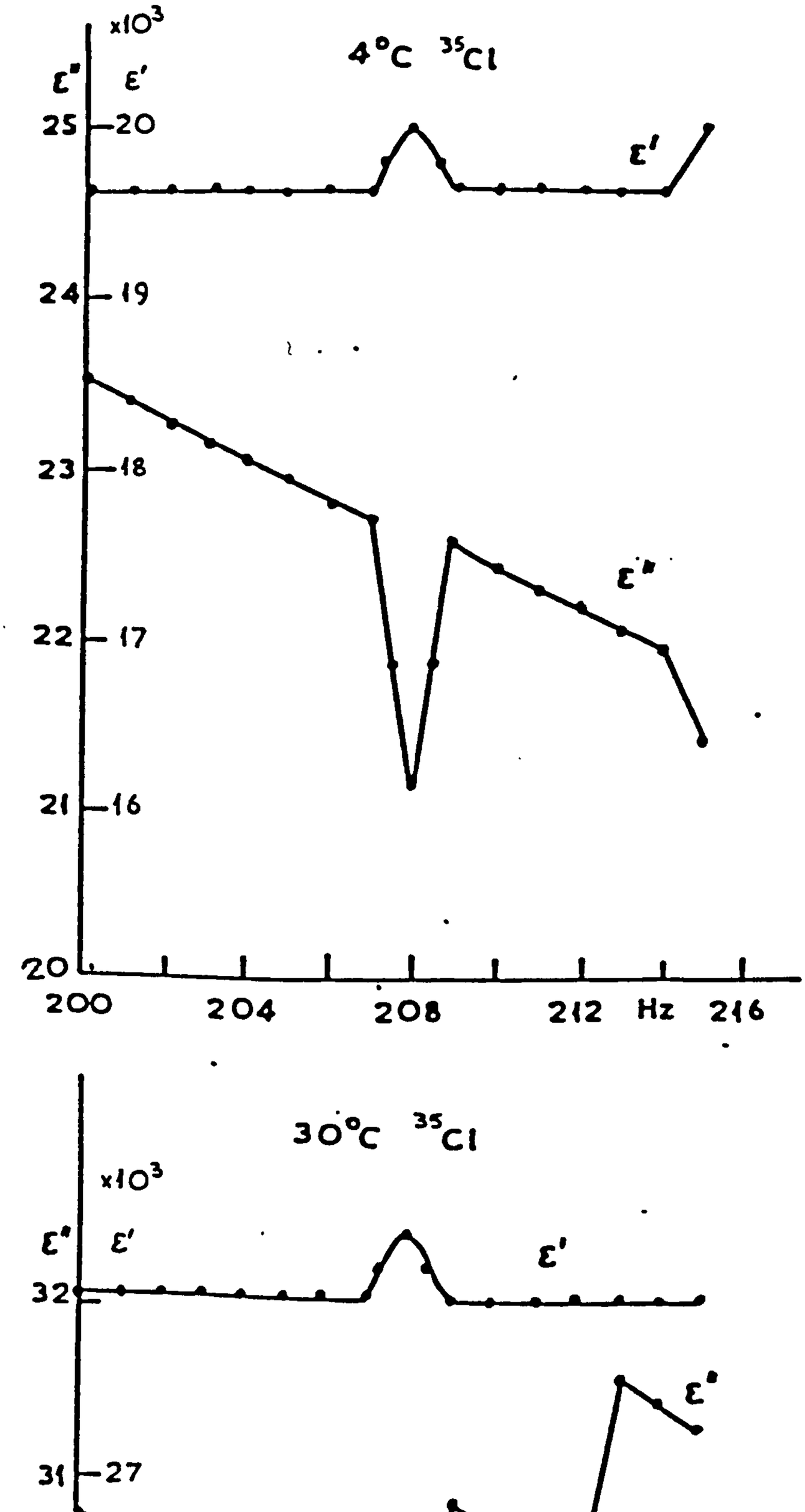

CHLORINE NMR IN A LABORATORY AMBIENT FIELD OF 0.5G (50μT), SUSPENSION CONCENTRATION OF 1.9 x 10^6 CELLS/ML. TEMPERATURES 4 °C and 30 °C, ELECTRIC FIELD STRENGTH OF THE ORDER OF 20 KV/m.

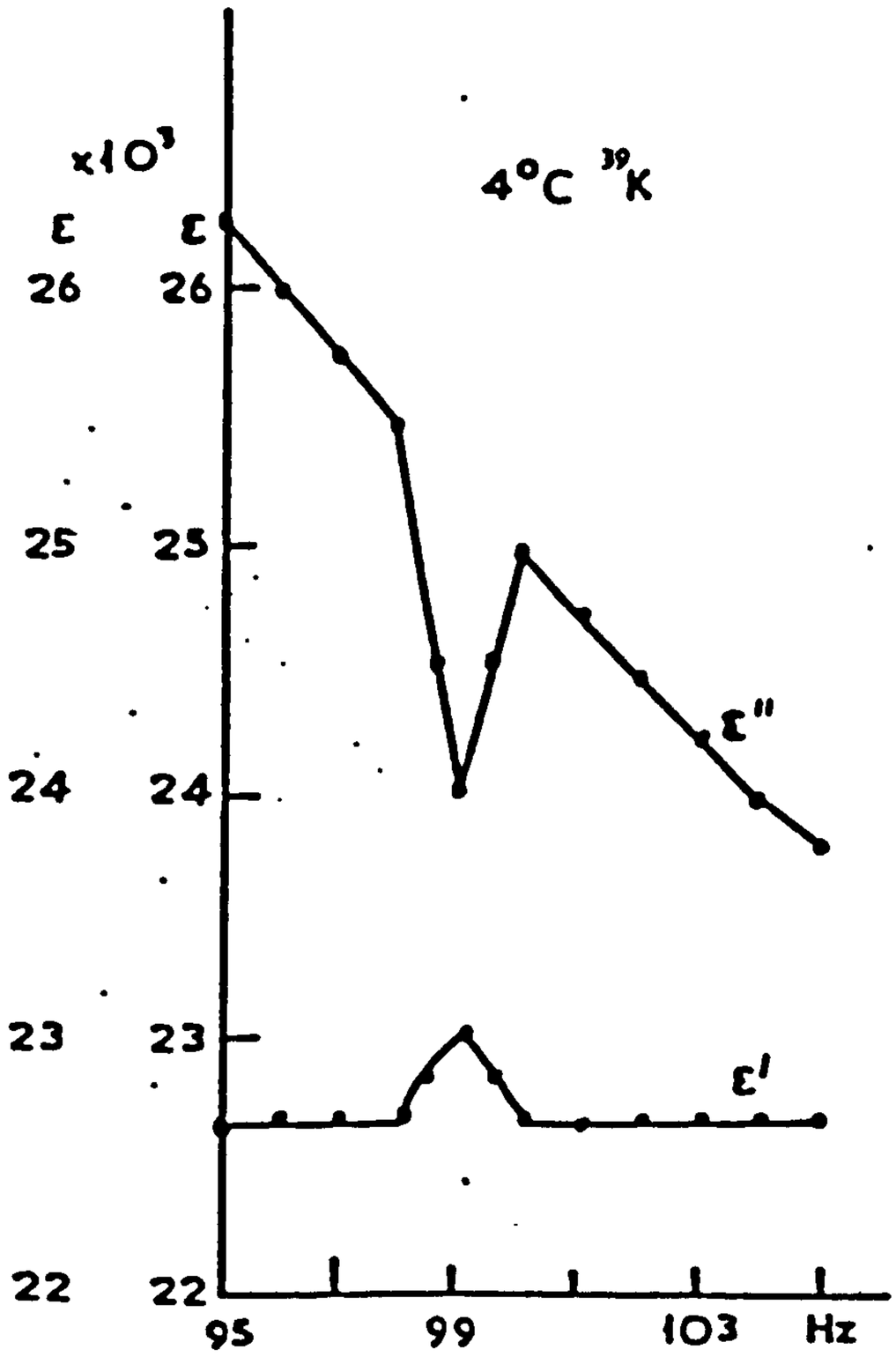

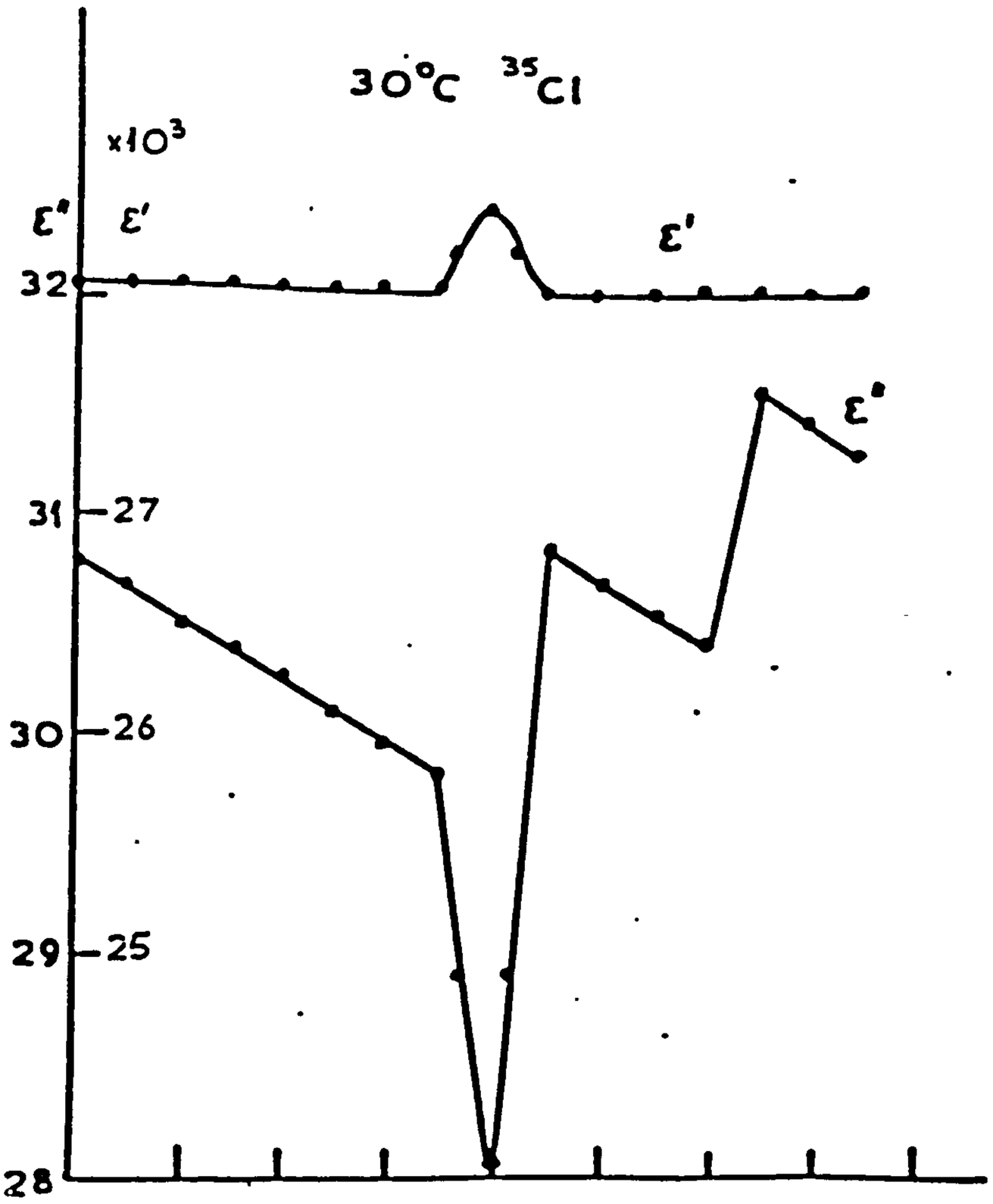

Fig. 10.12 frequency

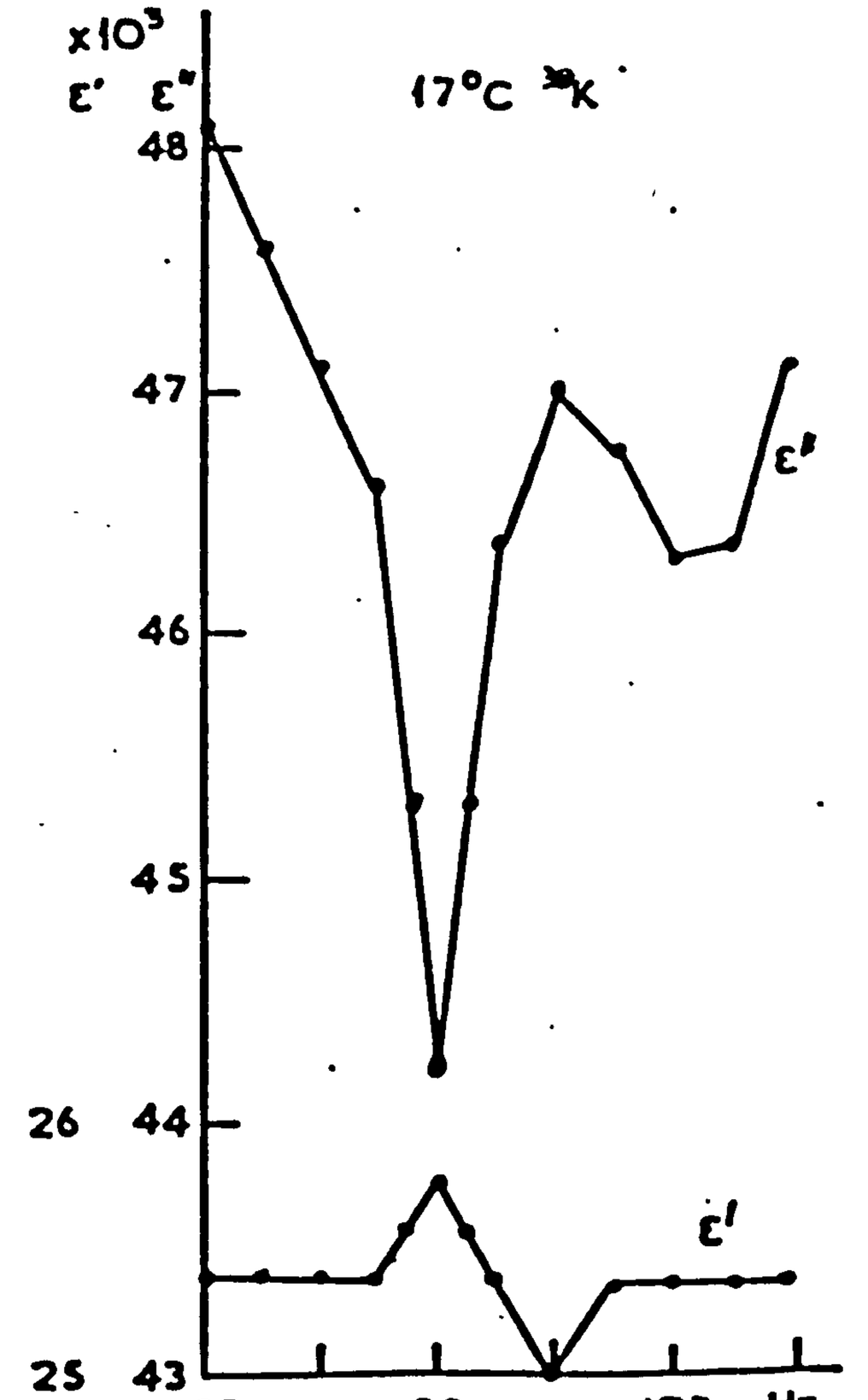

frequency

POTASSIUM NMR IN A LABORATORY AMBIENT FIELD OF 0.5G(50μT), SUSPENSION CONCENTRATION OF 1.9 x 10^6 CELLS/ML. TEMPERATURES 4° AND 17 °C, ELECTRIC FIELD STRENGTH OF THE ORDER OF 20 KV/m.

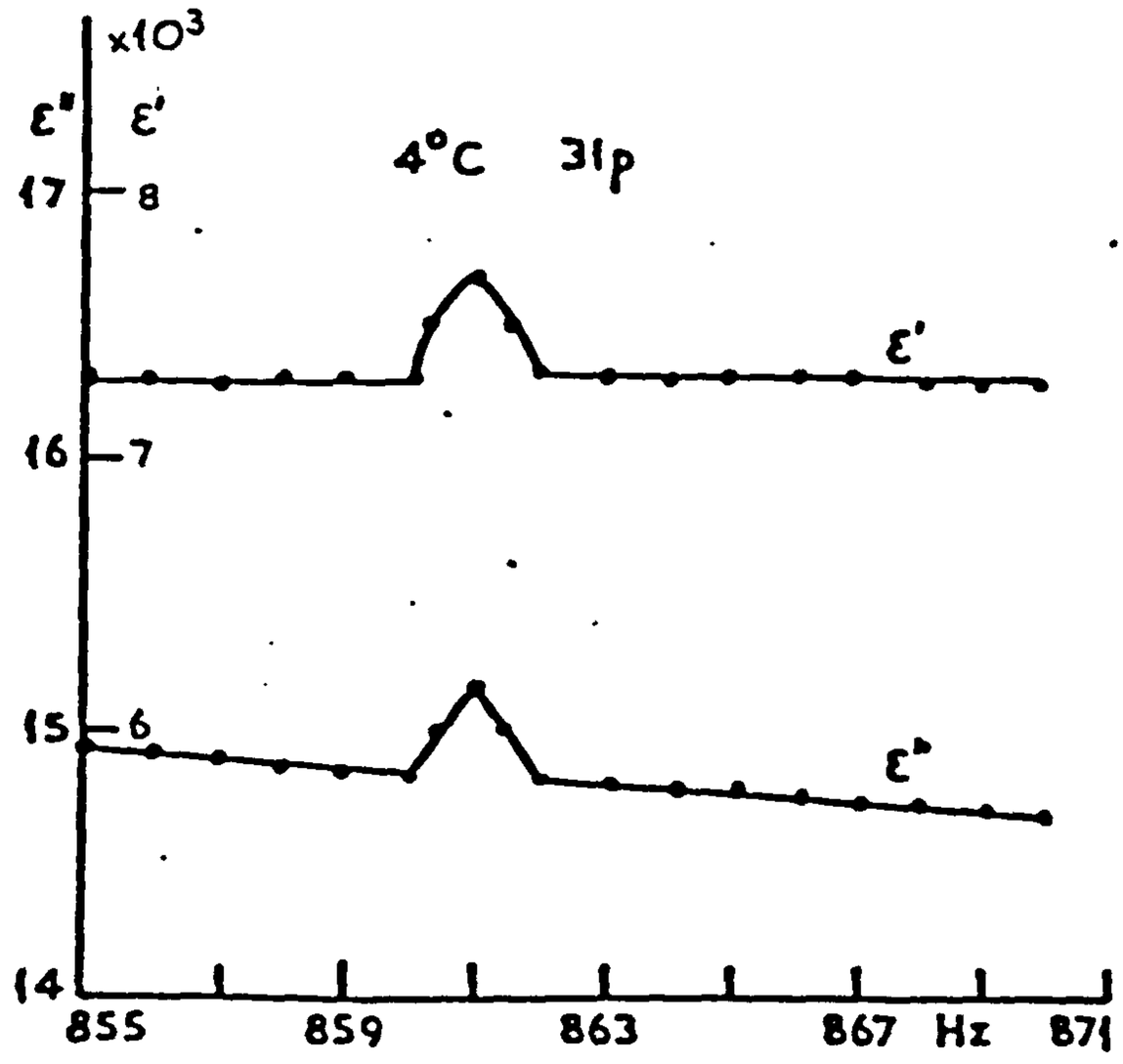

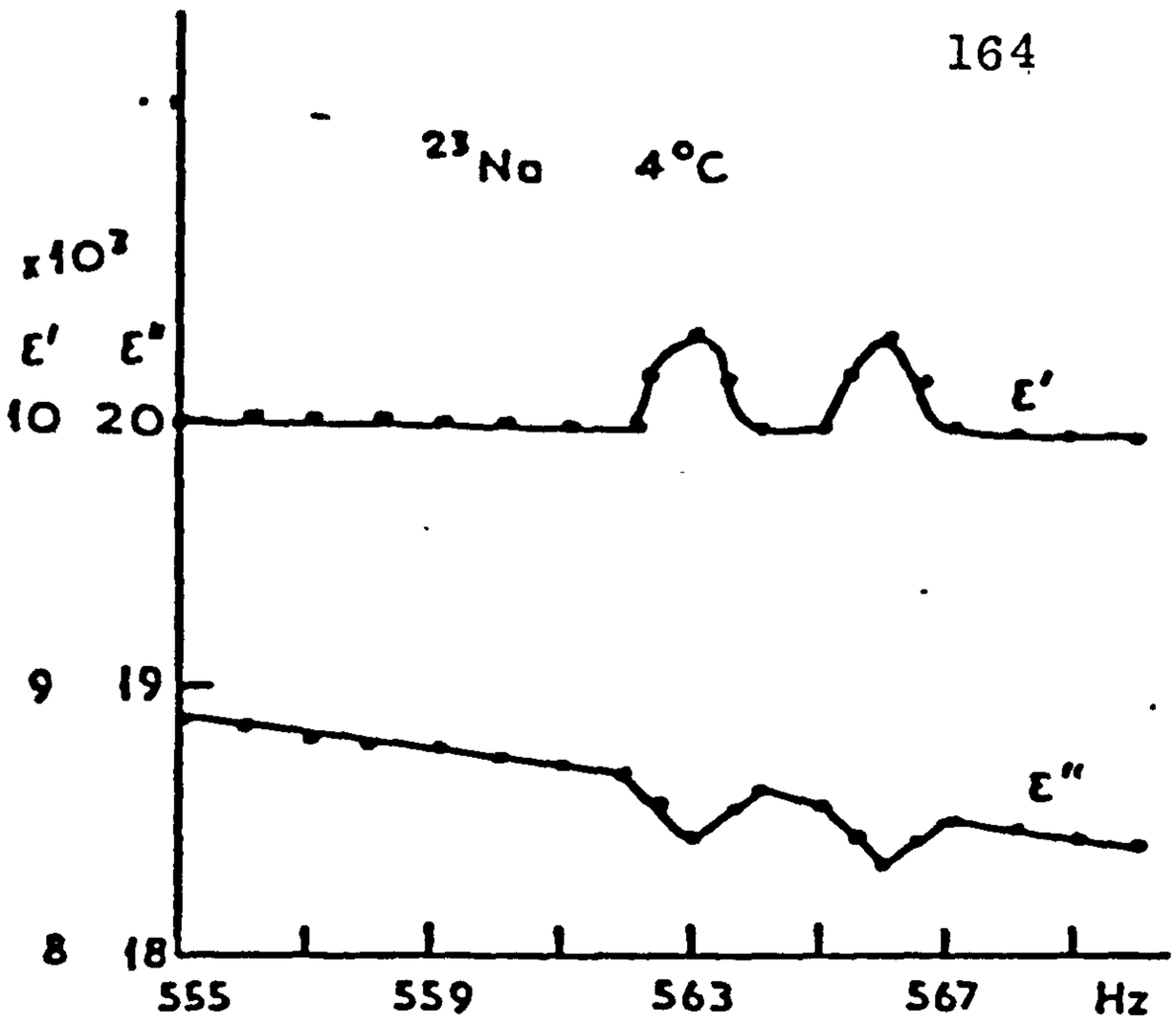

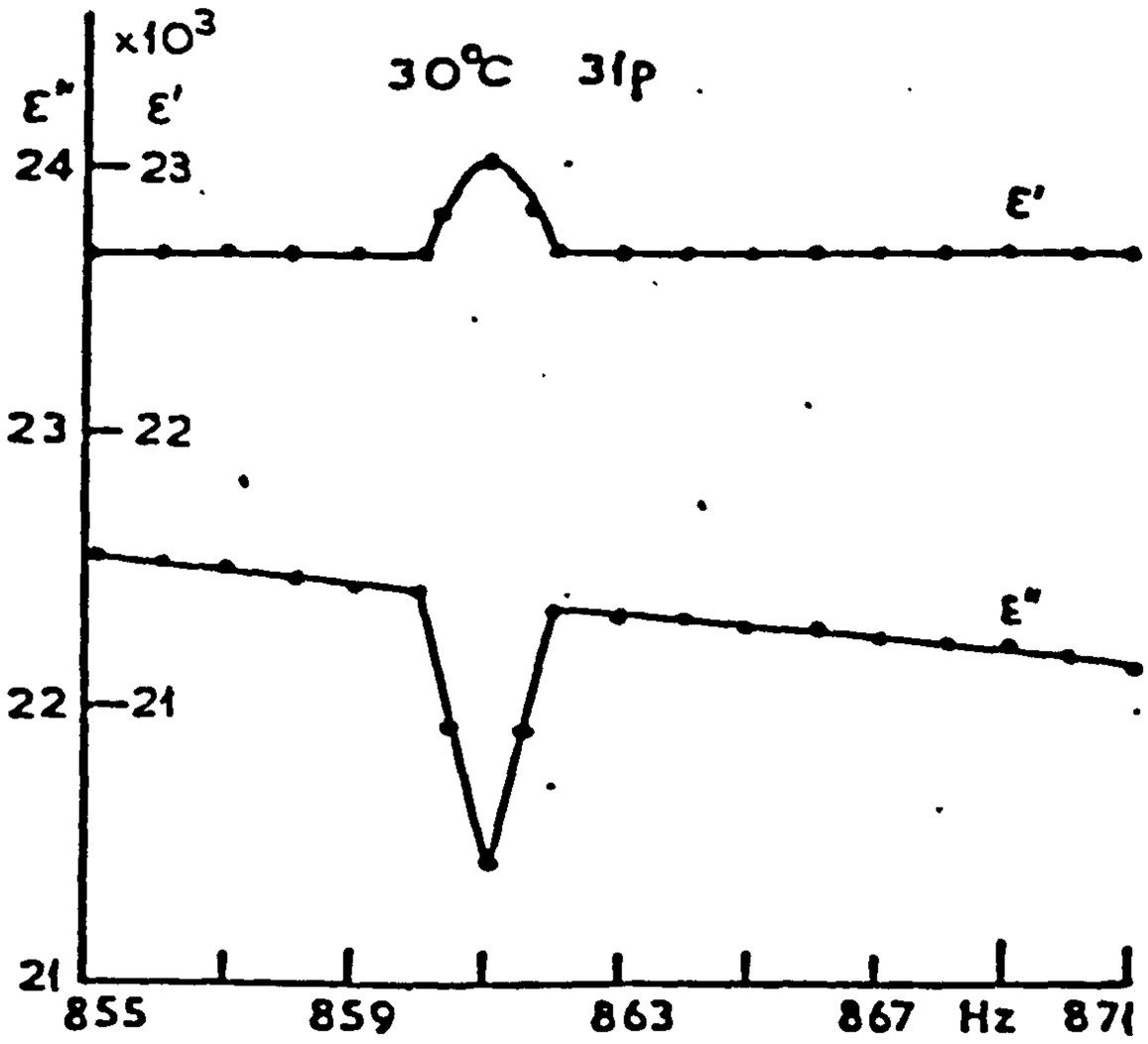

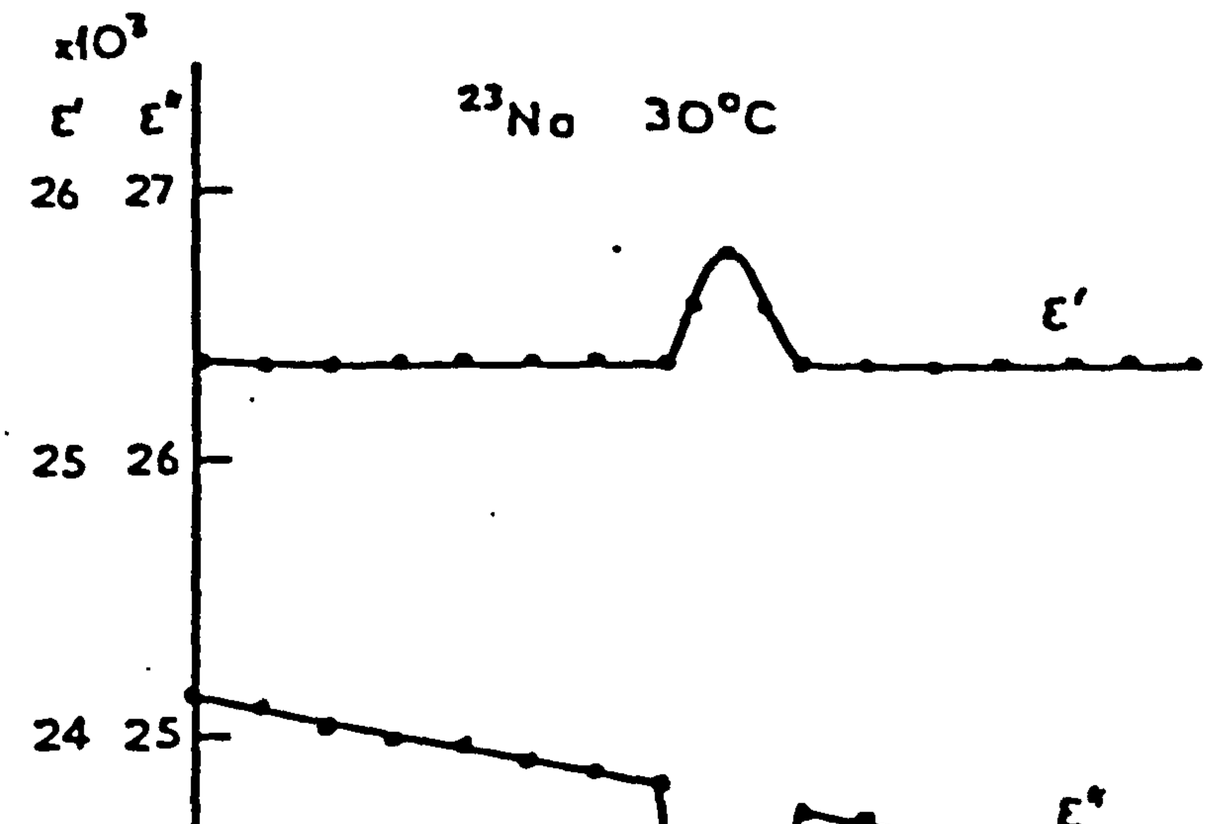

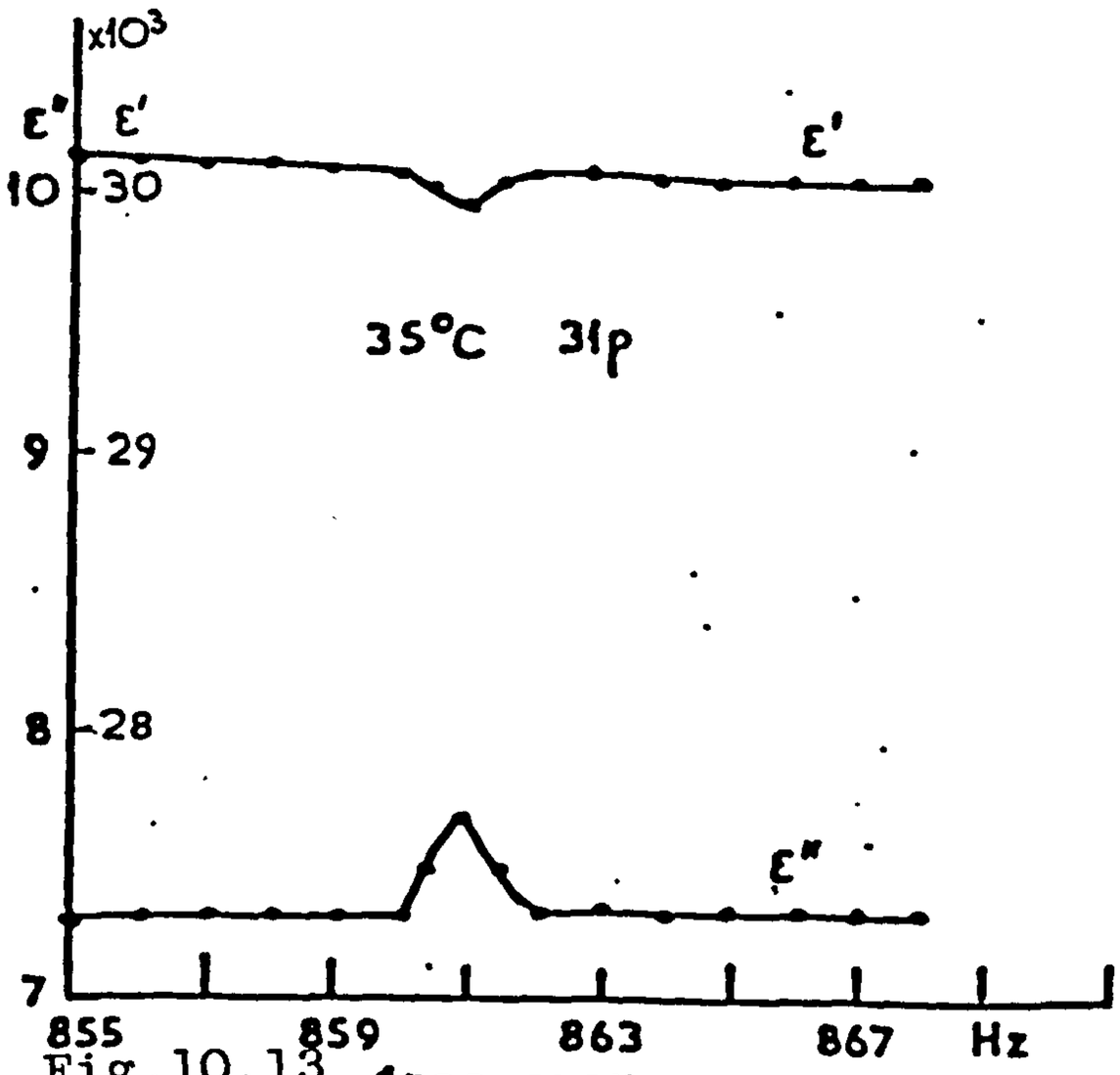

Fig.10.13 PHOSPHORUS NMR IN A LABORATORY AMBIENT FIELD OF 0.5G (50 μT), SUSPENSION CONCENTRATION 1.9×10^6 CELLS/ML, TEMPERATURES 4 °C, 30 °C, and 35 °C, ELECTRIC FIELD STRENGTH OF THE ORDER OF 20 KV/m.

SODIUM NMR IN A LABORATORY AMBIENT FIELD OF 0.5G (50μT), SUSPENSION CONCENTRATION 1.9×10^6 CELLS/ML, TEMPERATURES 4 °C, and 30 °C, ELECTRIC FIELD STRENGTH OF THE ORDER OF 20 KV/m.

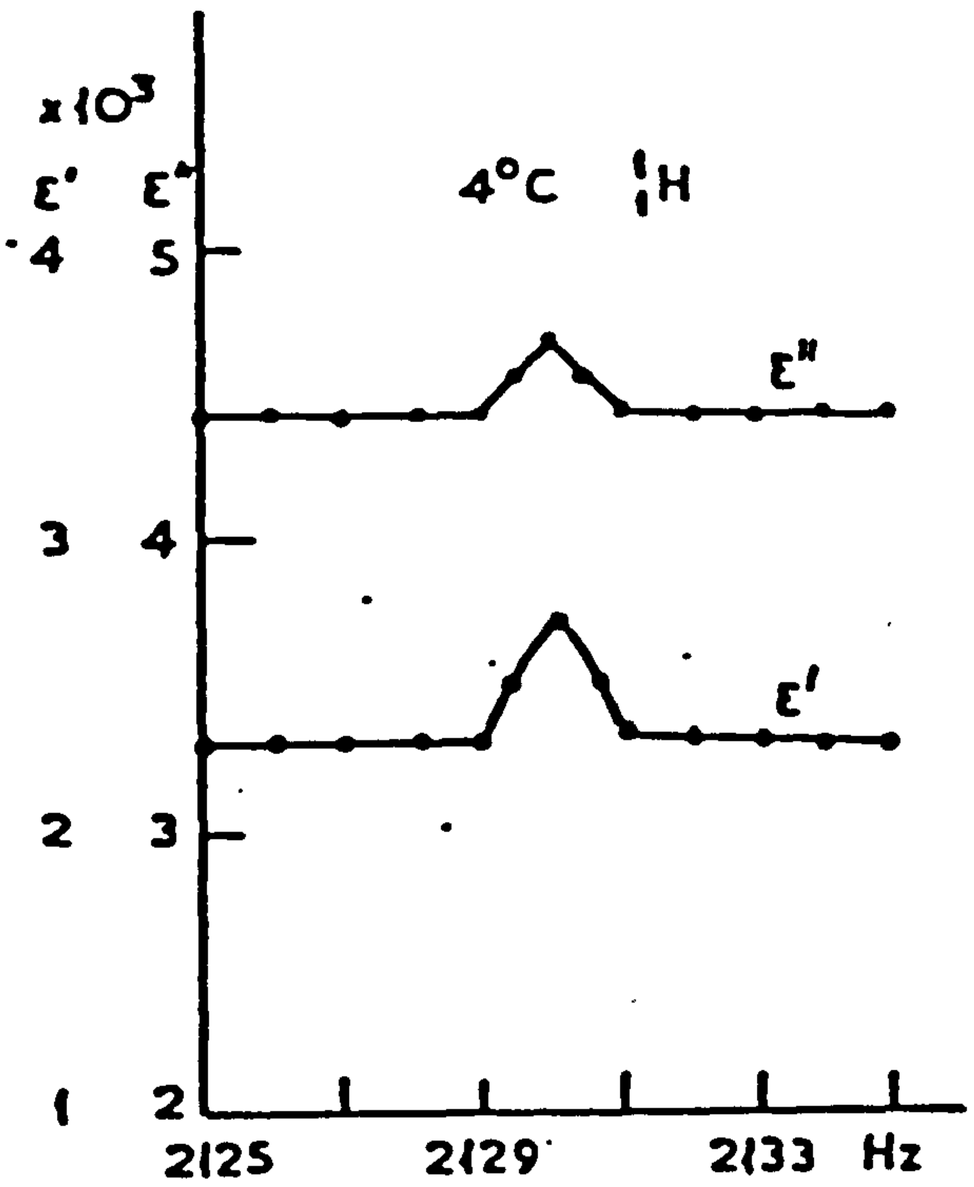

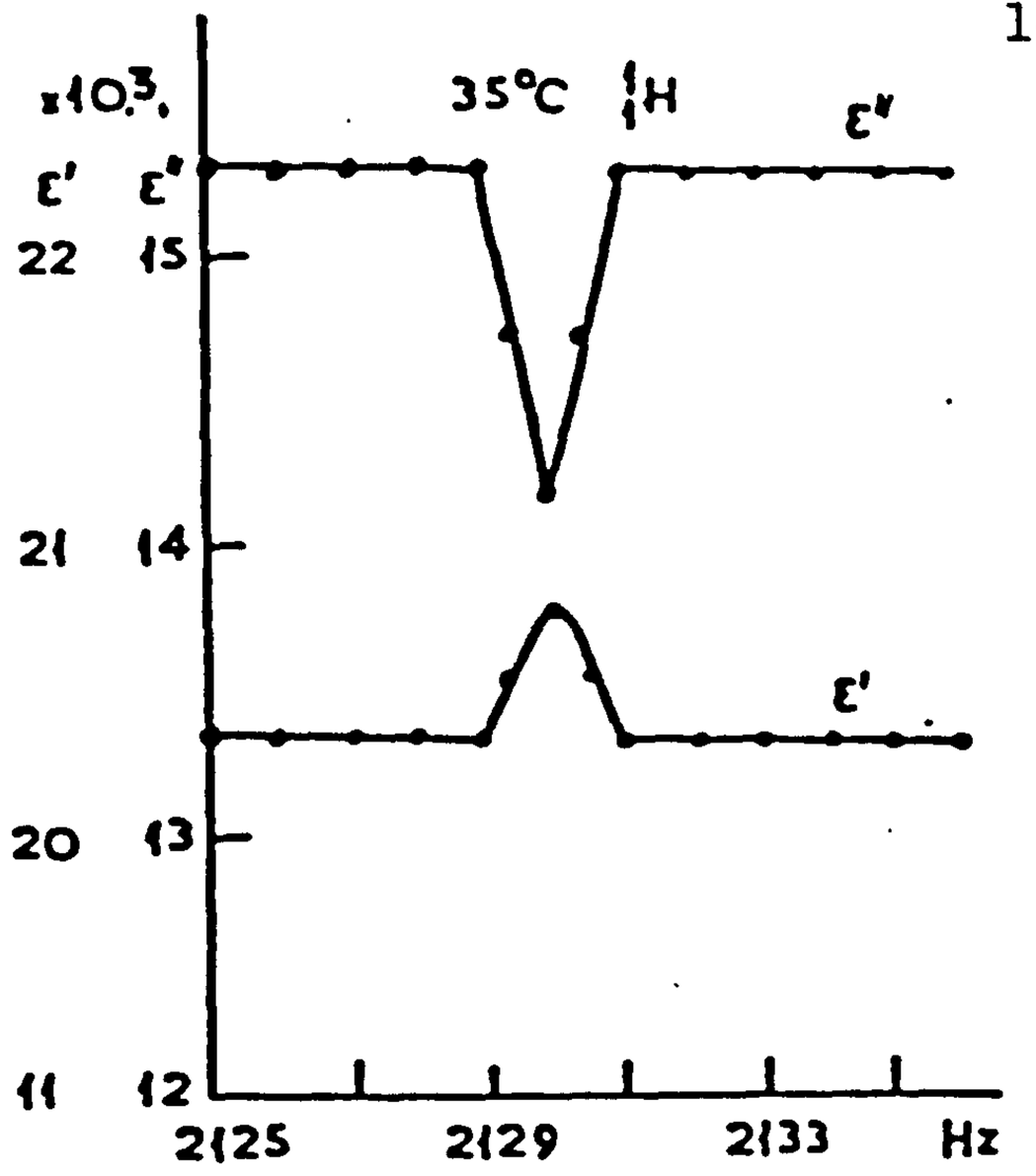

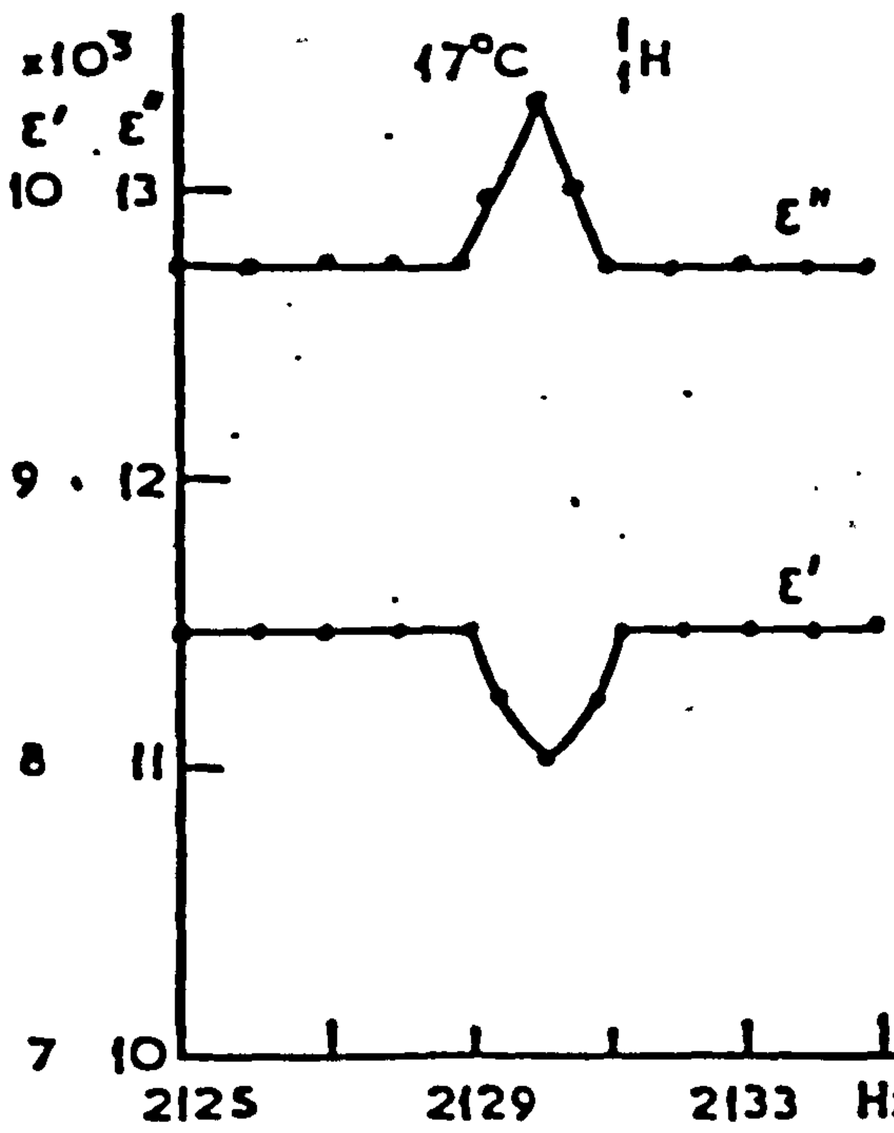

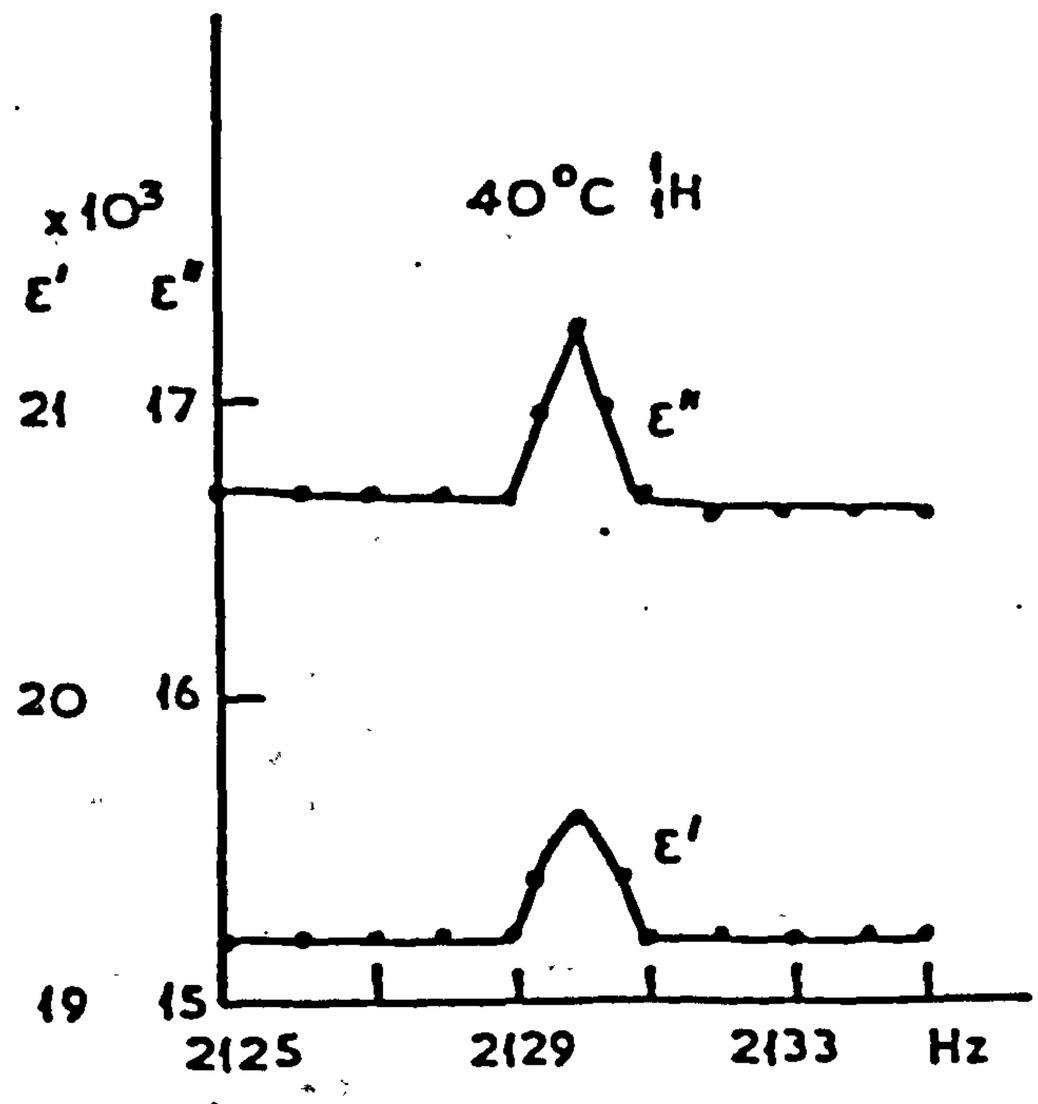

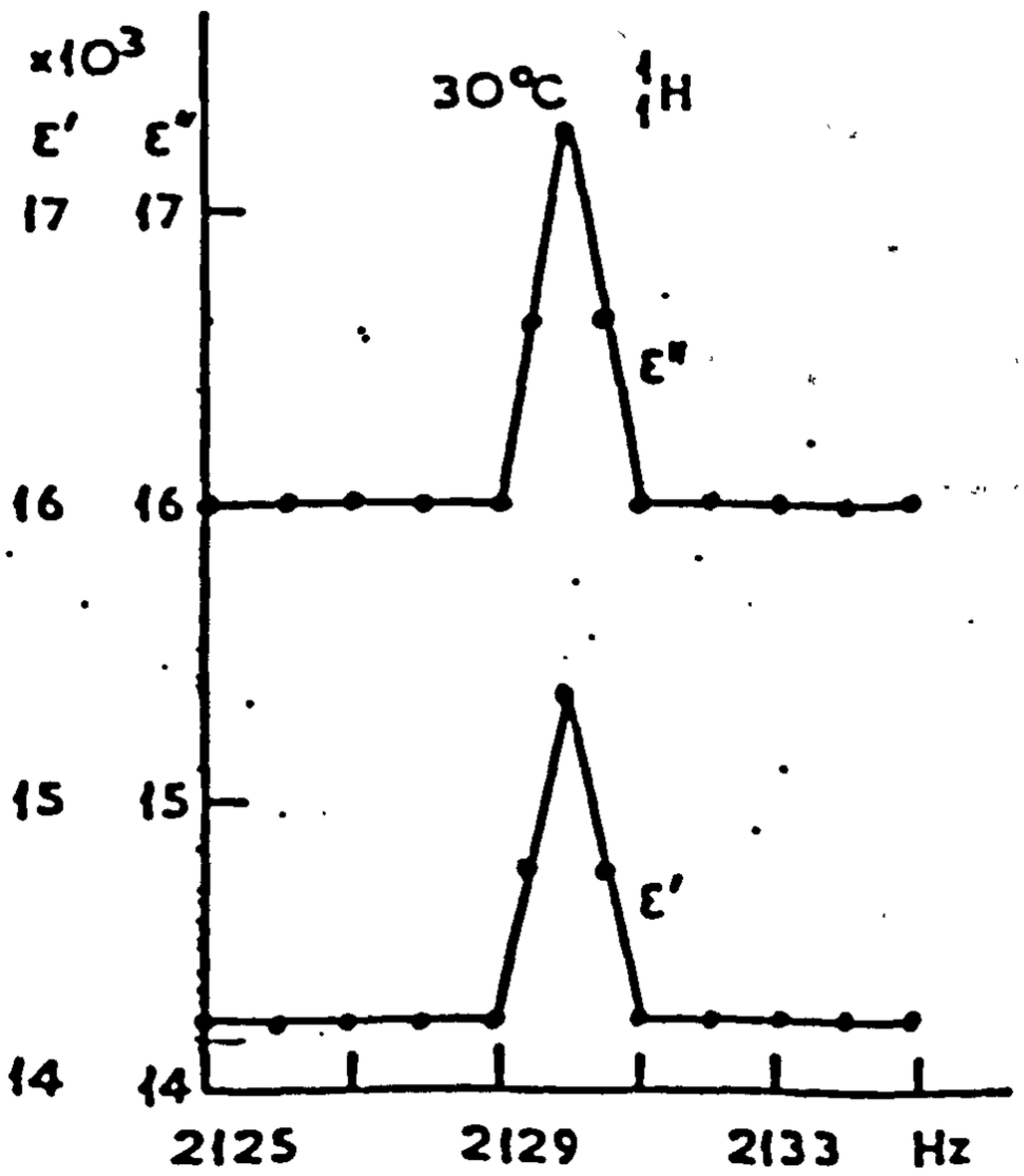

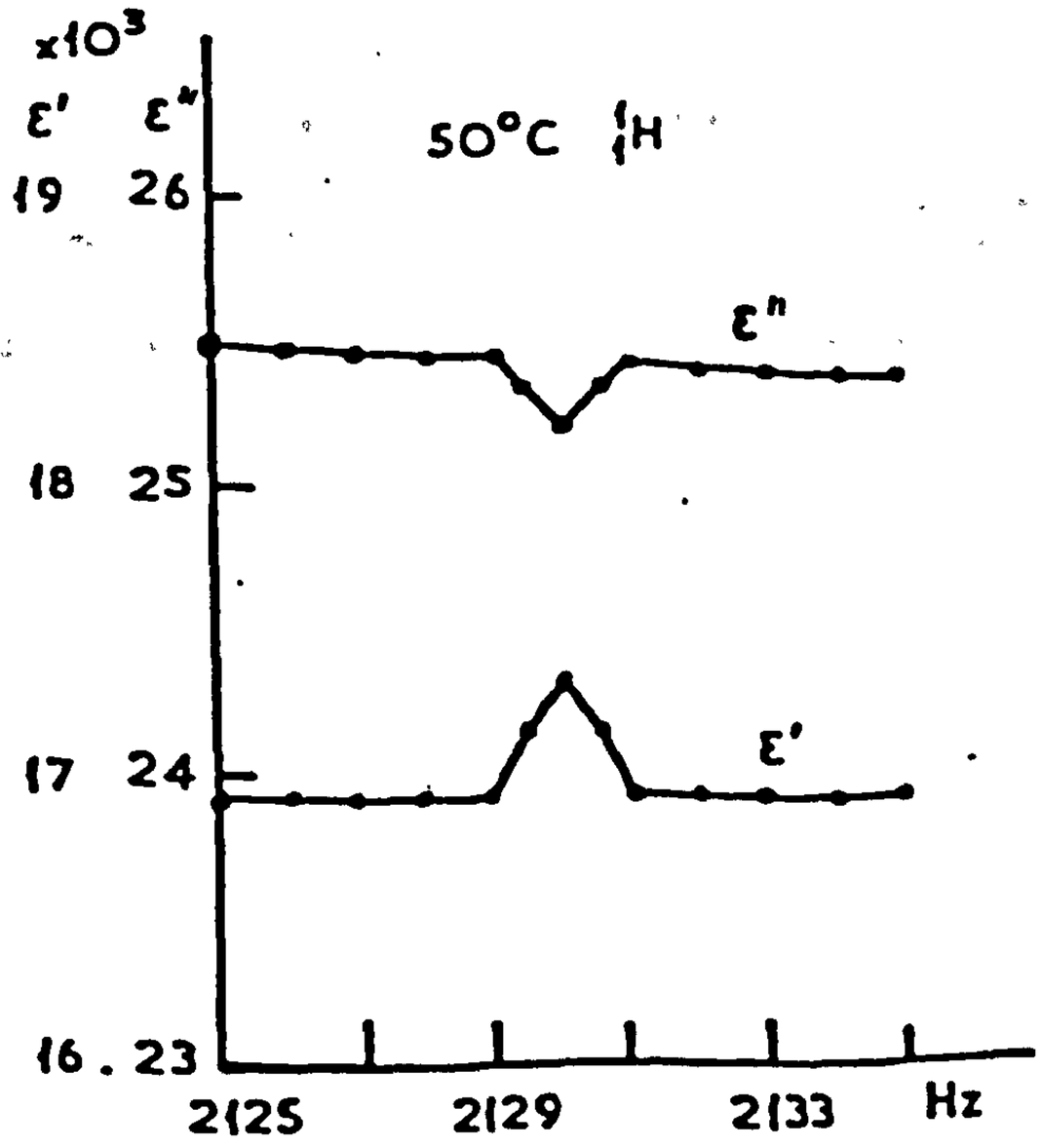

Fig. 10.14 frequency

PROTON NMR IN A LABORATORY AMBIENT FIELD OF 0.5G (50μT), SUSPENSION CONCENTRATIO
OF 1.9 x 10^6 CELLS /ml, TEMPERATURE 4 °C, 17 °C, 35 °C. 40 °C and 50 °C,
ELECTRIC FIELD STRENGTHOF THE ORDER OF 20 KV/m.

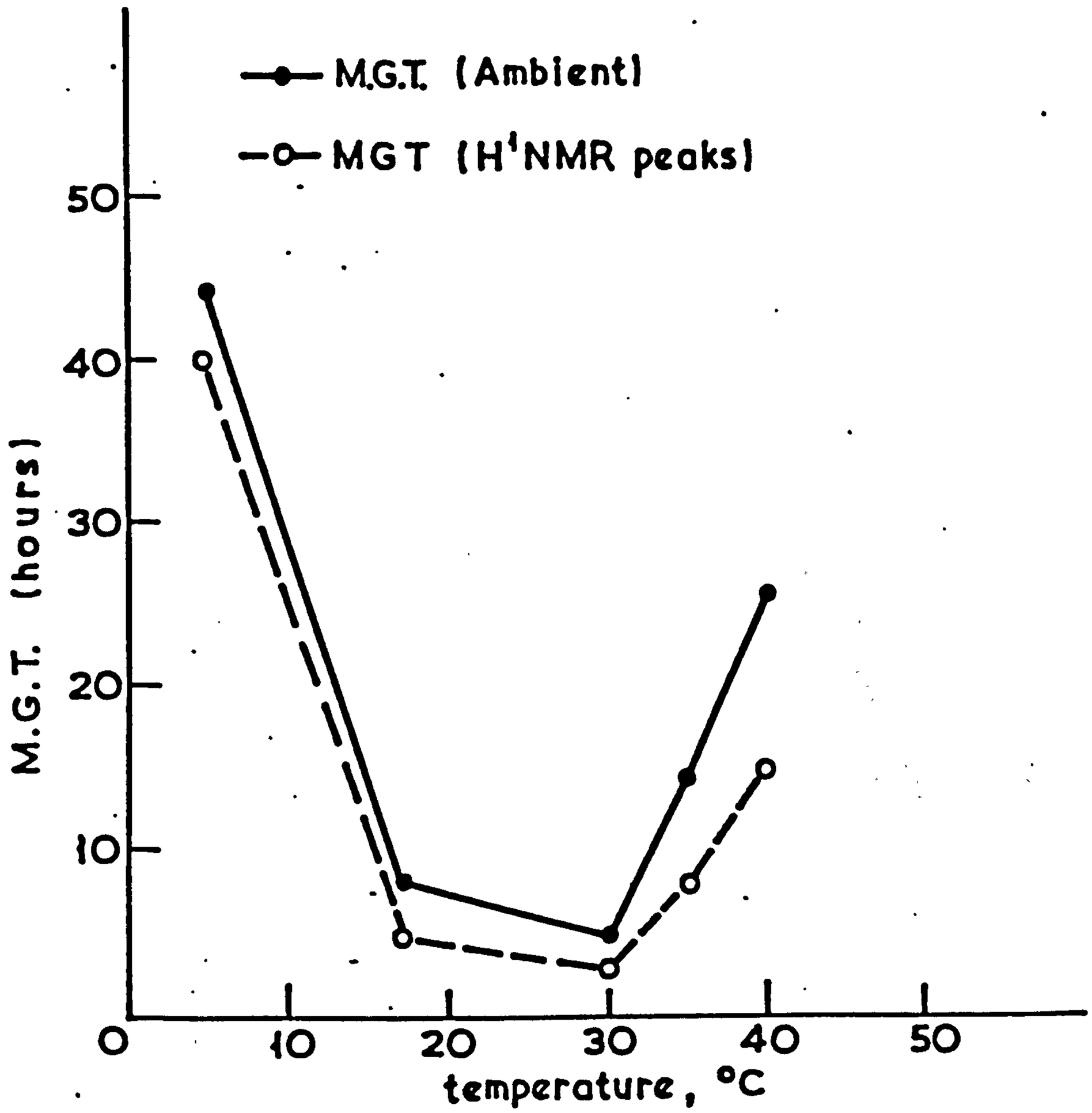

Fig. 10.15

Mean generation time of yeast cells (S.Cerevisiae) in a magnetic field of 50μT and at proton NMR peaks as a function of temperature.

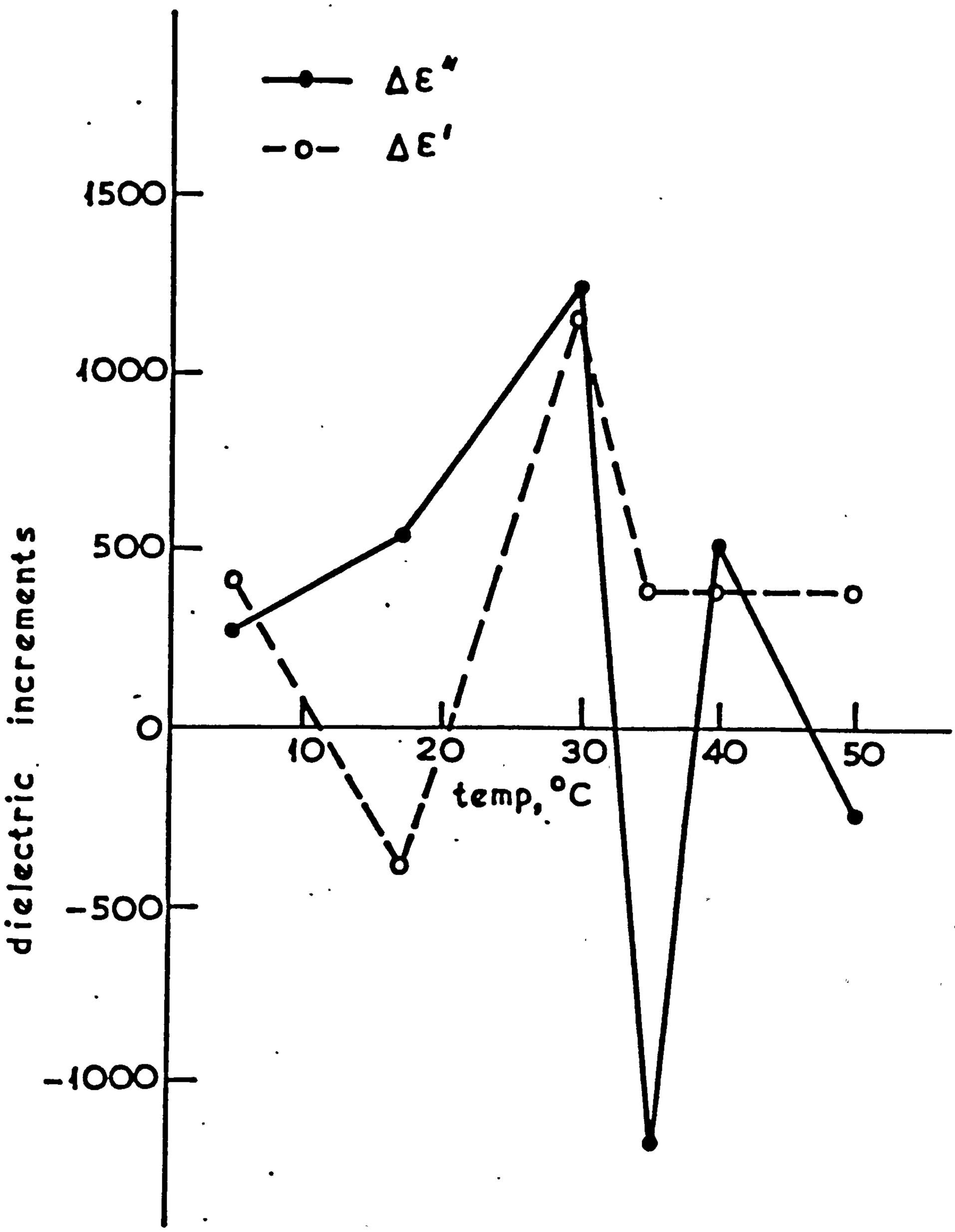

Fig. 10.16

Dielectric increments ratio to mean proton (H^1) NMR resonance of live yeast (S. Cerevisiae) in a magnetic field of 50μT, concentration 1.9×10^6 cells ml^{-1} in 0.25M deionised sucrose as a function of temperature.

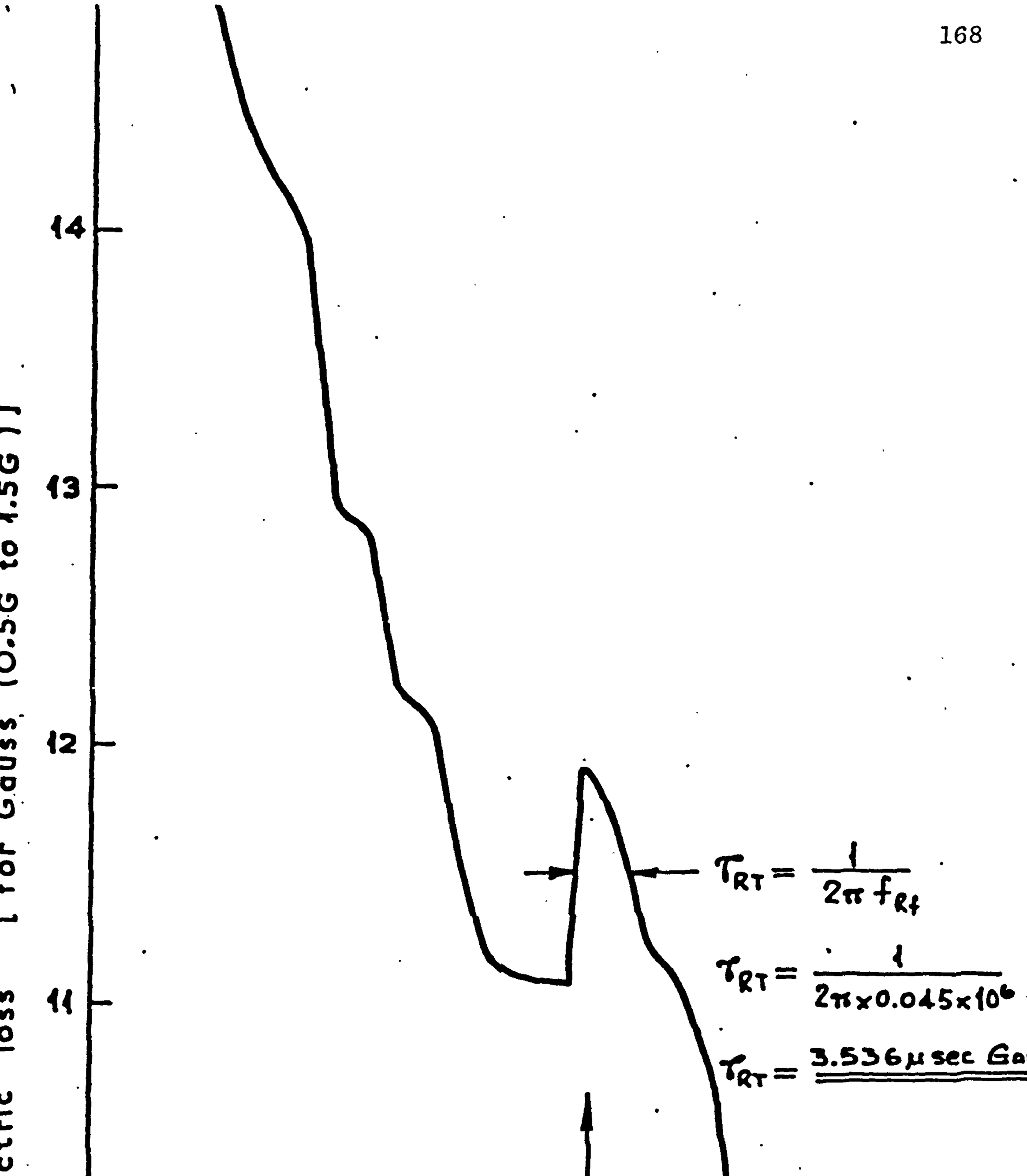

Fig. 10.17

Electron spin resonance (e.s.r.) spectrum of dielectric loss of live yeast (s. cerevisiae) concentration 1.9×10^6 ml^{-1} temperature 23°C from 0.5G to 1.5G In 0.25M deionised sucrose.

10.3 Steps in the voltage-current characteristics observed using a pearl-chain of live yeast cells

After trying as many as 1000 samples or more and running the experiments every 5 minutes , steps were detected just when the cells are around the time of cytokinesis just before dividing. At this stage all the cells are synchronised with a distinct nucleus. The recorded steps in the voltage-current characteristic are shown in figures 10.18, 10.19, 10.20, 10.21 and 10.22. The whole results of the experimental observations are summarised in Figures 10.23 and 10.24. The steps appear only for a fairly short time of the order of 2 to 3 minutes.

The experiment was repeated with deionised 0.25M sucrose killed yeast cells (autoclaved) and placing a resistor across the junction all of these showed a straight line only Figure 10.25. This indicates that the effect is due to the activity of the live cells around the time of cytokinesis and is not an artefact noise generated by the system.

Fig. 10.18

Voltage-current characteristic of yeast cells (S.Cerevisiae) in a magnetic field of 3600 Gauss, concentration 1.9×10^6 cells/ml. room temperature 24°C.

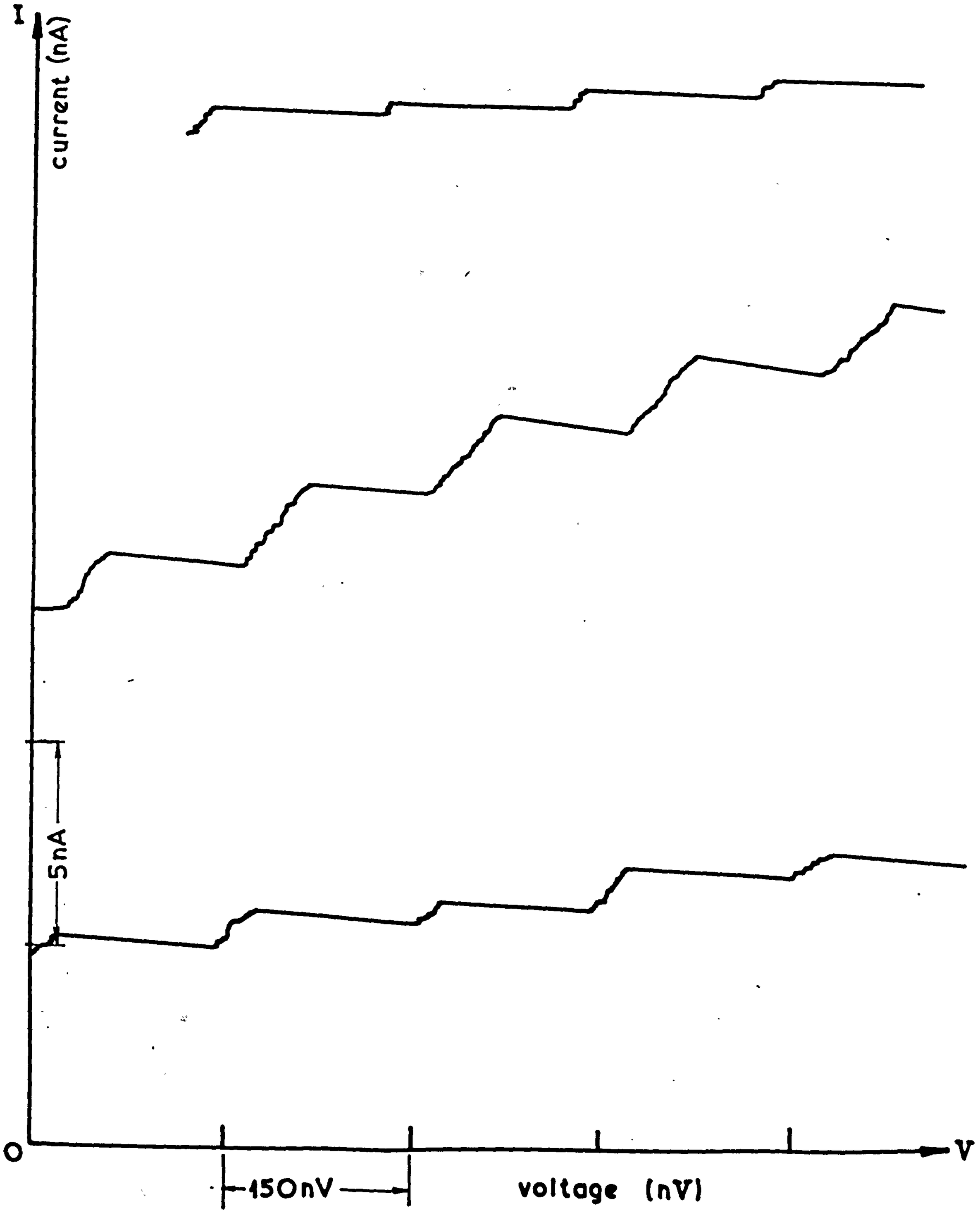

Fig. 10.19
Appearance and disappearance of steps in current-voltage characteristic of yeast cells (S. Cerevisiae), room temperature 23°C.

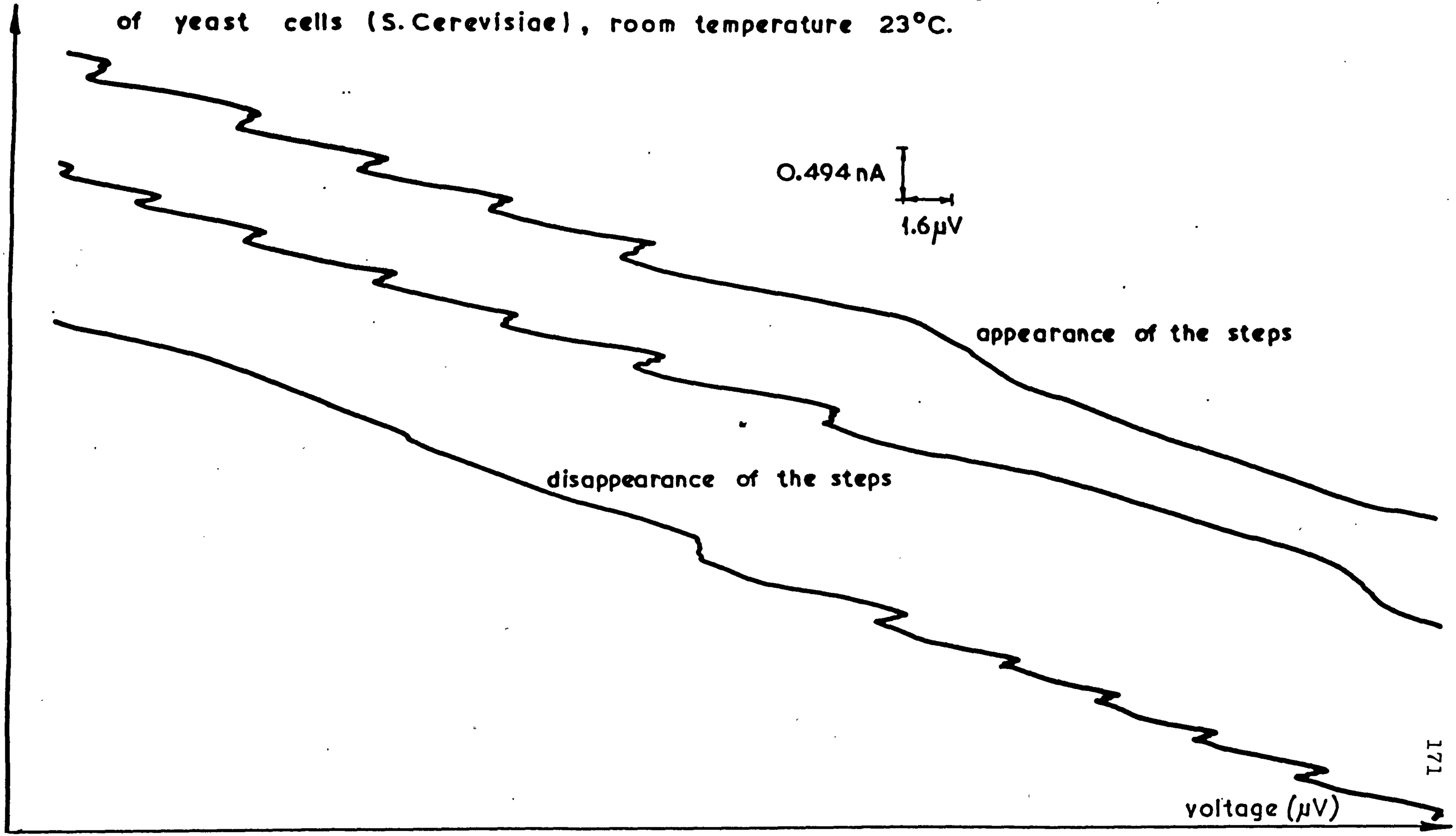

Fig. 10.20

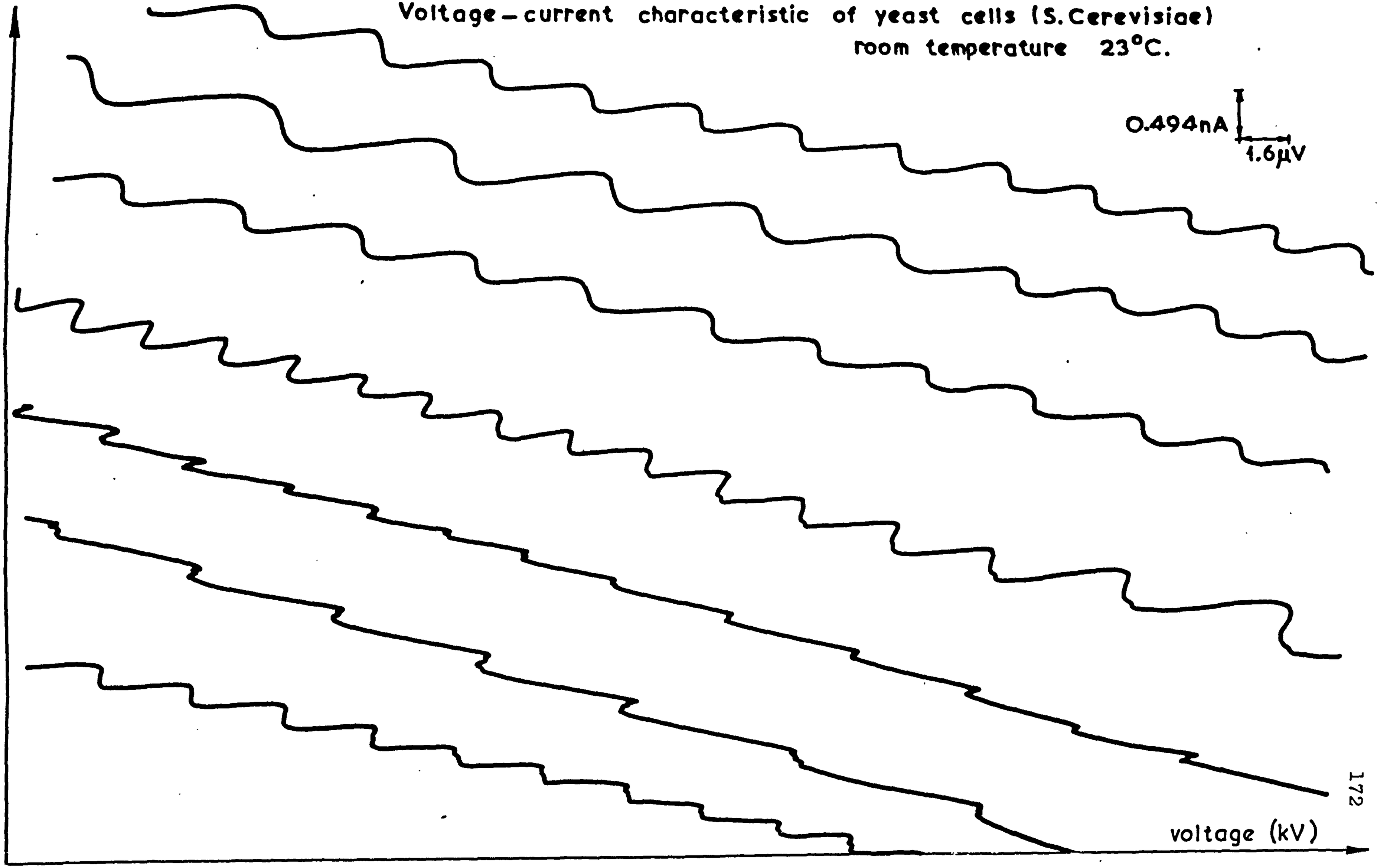
Voltage – current characteristic of yeast cells (S.Cerevisiae)
room temperature 23°C.
0.494nA
1.6μV
current (nA)
voltage (kV)

Fig. 10.21

Voltage-current characteristic of yeast cells (S.Cerevisiae) in a magnetic field of 4700 Gauss, concentration 1.9×10^6 cells/ml. room temperature 24°C.

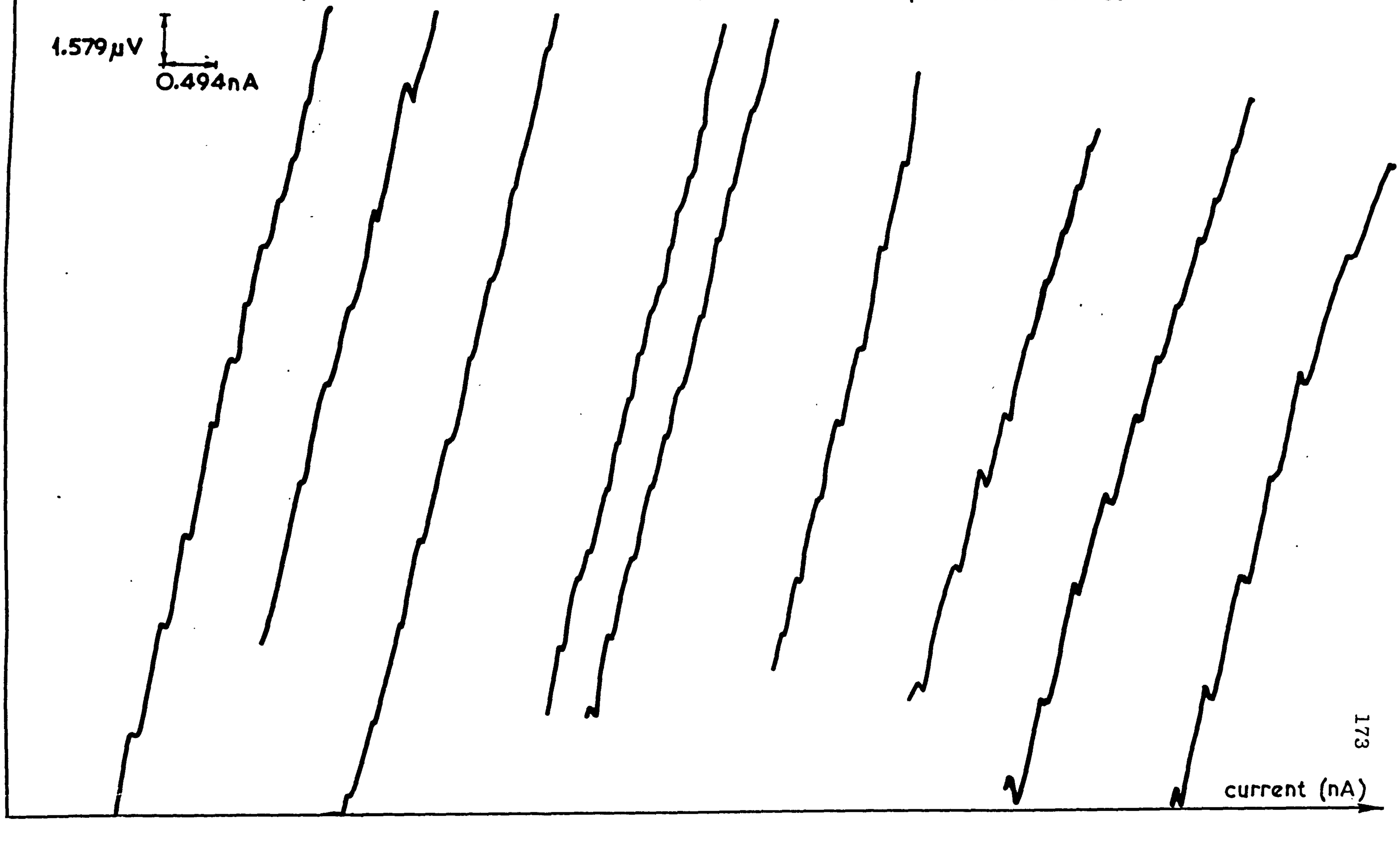

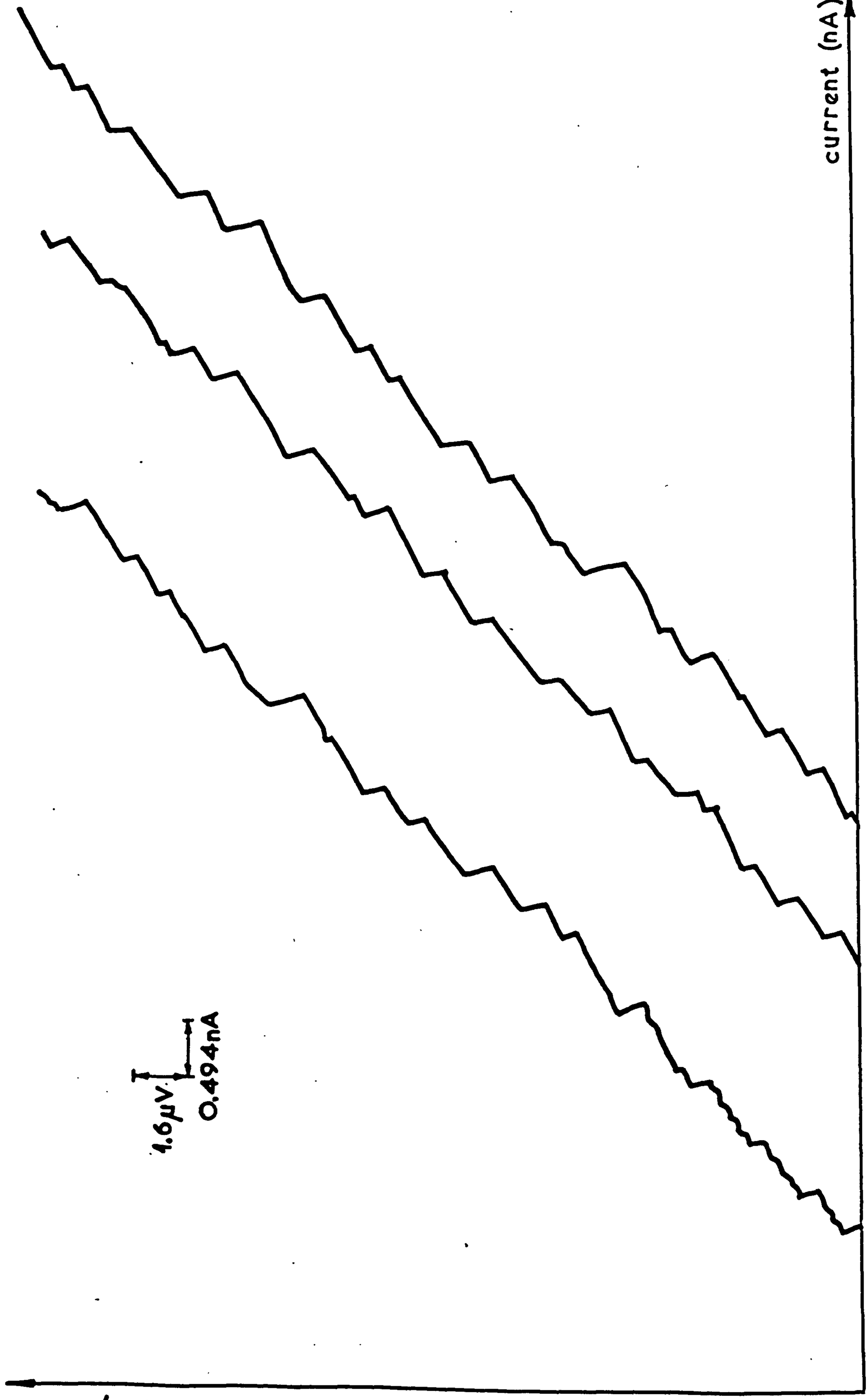

Fig. 10.22 Voltage - current characteristic of yeast cells (S. Cerevisiae I, room temperature 22°C.

Fig 10.23

Voltage steps in V-I characteristic for single S.Cerevisiae cell between electrodes measured during time of appearance. Laboratory ambient magnetic field 0.5 Gauss. Room temp. 22°C.

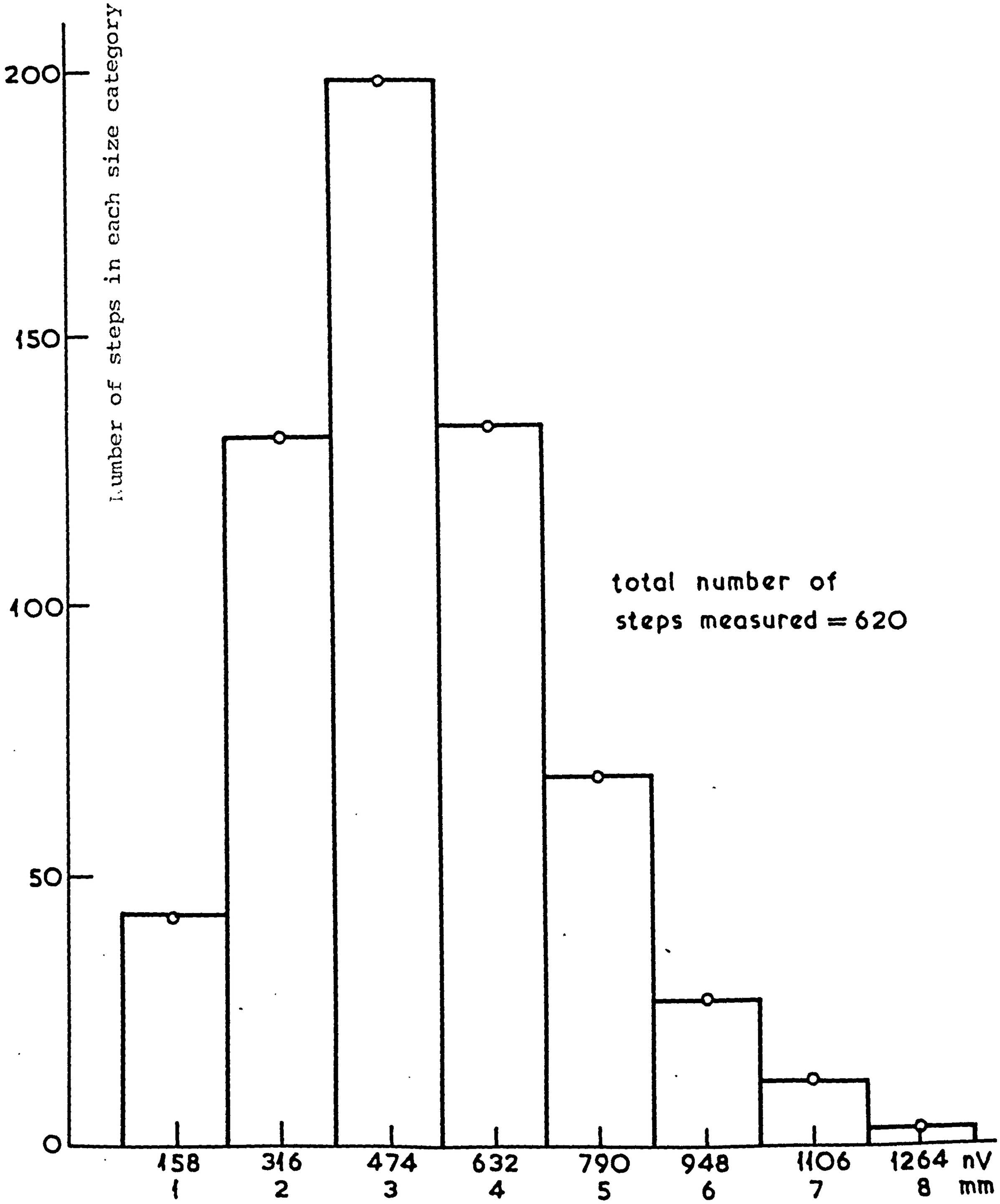

Fig 10.24

Voltage steps in V-I characteristic for single S. Cerevisia cell between two point electrodes measured during time of appearance in a magnetic field of 4kG.

Room temp. 22°C

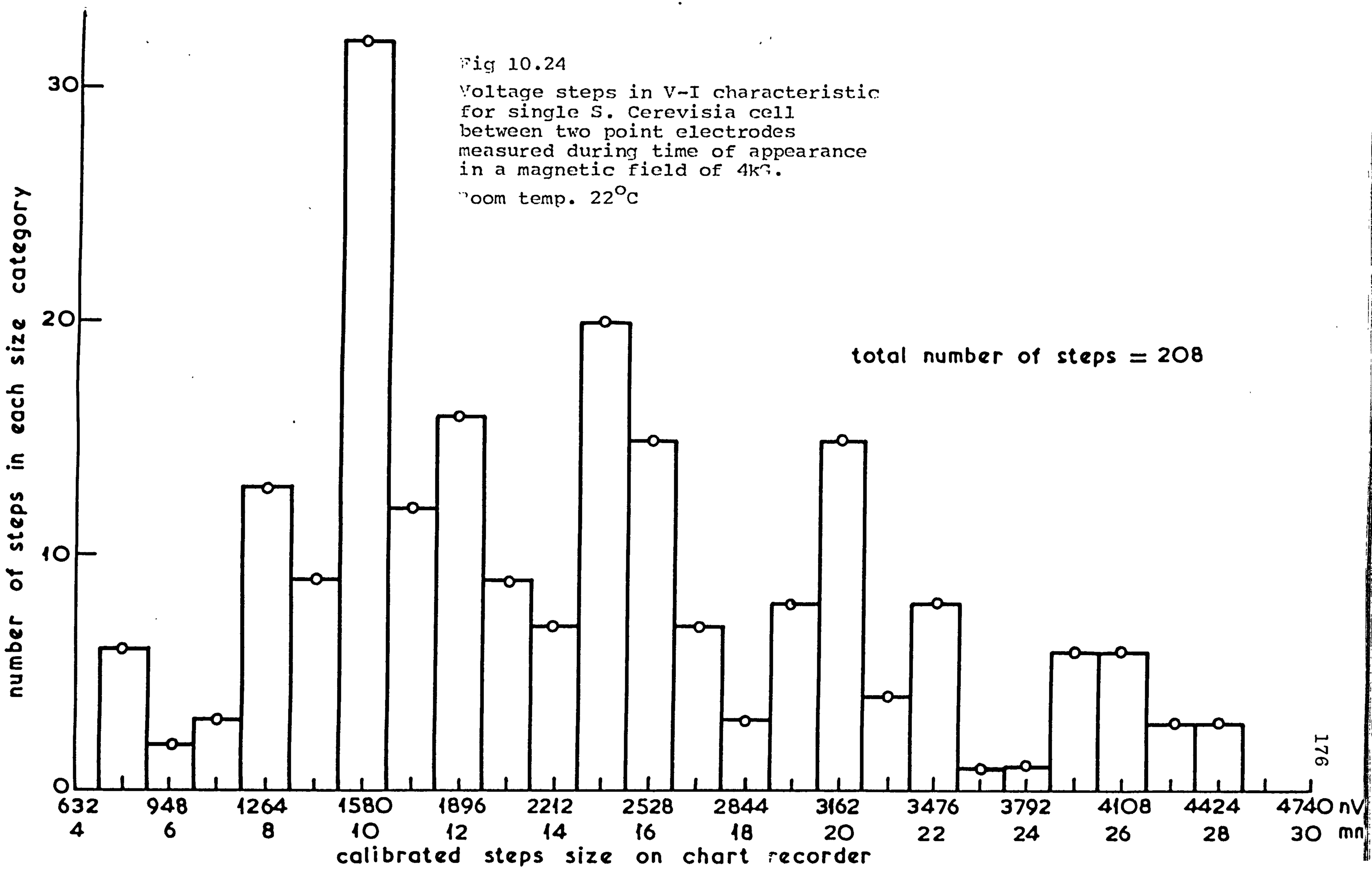

Fig. 10.25
Voltage-current characteristics showing noise level for sterilised yeast cells, deionised 0.25M sucrose, 4kG magnetic field and a 100kΩ resistor across the junction, temperature 23°C.

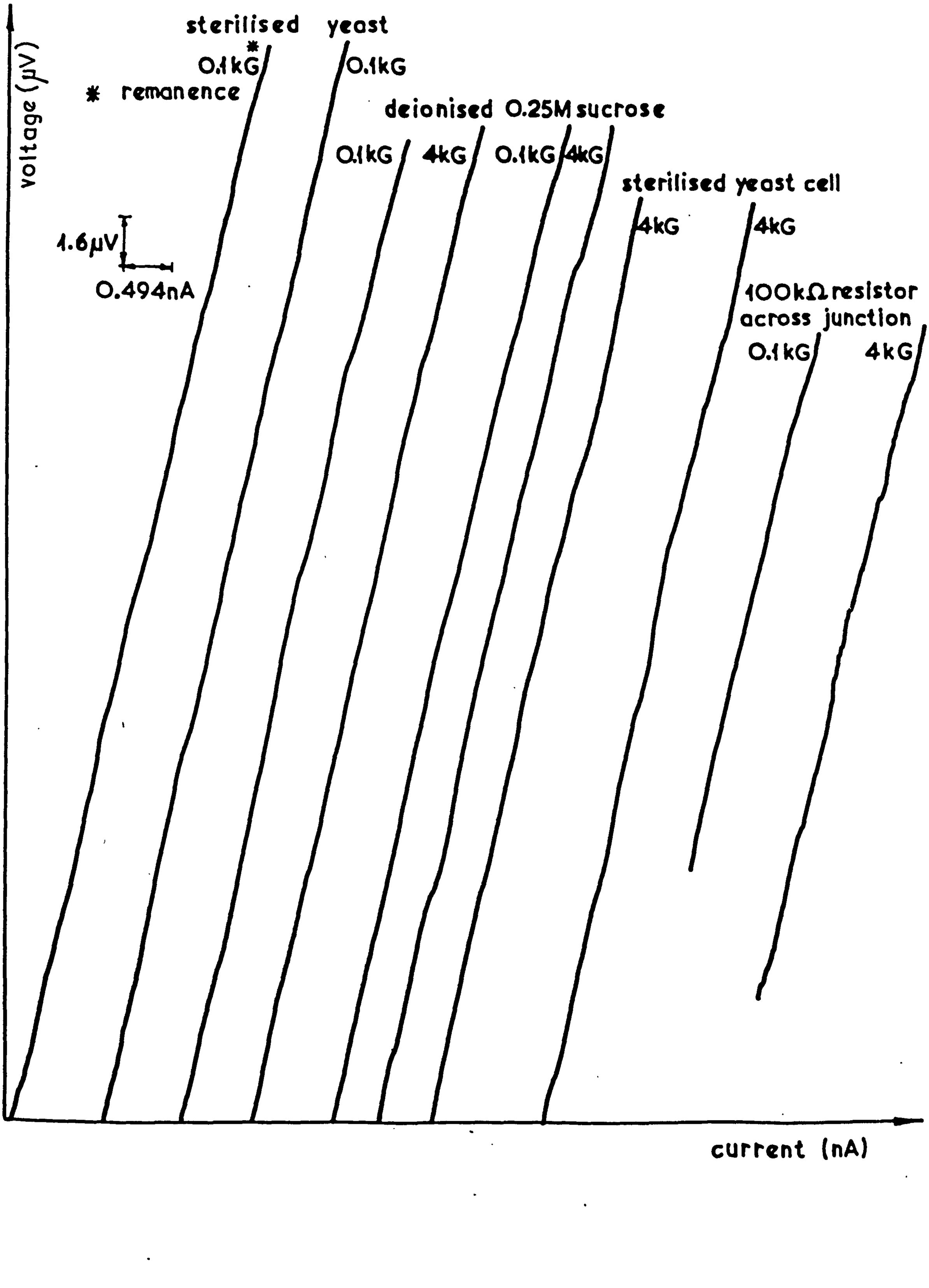

10.4 Oscillations from dividing yeast cells

An emission of a radio frequency signal from yeast cells in the region of 7 MHz and in the range of 50 MHz - 80 MHz were found to occur about one mean generation time after starting the incubation of the cells for synchronous growth. The cells at this state seem to act like small signal generators and emit radiation at a level of a fraction of a μV which is just detectable with a spectrum analyser. The emission was found to last twice as long in the range of 50 MHz - 80 MHz.

In order to confirm the emission was from the cells and not from radio transmissions or other sources of interference. Firstly an aerial of 2m long was connected to the input of the spectrum analyser in place of the experimental sample to see if the emission coincident with any radio transmission detected. No such coincidence was obtained.

The emission was confirmed in the second way by connecting a variable resistor and capacitor boxes one at a time across the electrodes. A resistor of the order of 10 MΩ or a capacitor of 100PF removed the radiofrequency emission whilst the radio transmissions was not removed by their presence.

Third way of confirmation was achieved by the removal of the yeast cells between the electrodes, as soon as the gap between the electrodes was cleared off the radiofrequency emission disappeared at the same time.

The whole results are shown in Figures 10.26, 10.27, 10.28, 10.29, 10.30, 10.31, 10.32, 10.33. Shaya and Smith (1977) had observed effects at similar frequencies by measuring

the change in reaction rate resulting from subjecting partially inhibited lysozyme solution for 2h to the range of frequencies from 10kHz to 1GHz (Fig. 10.34).

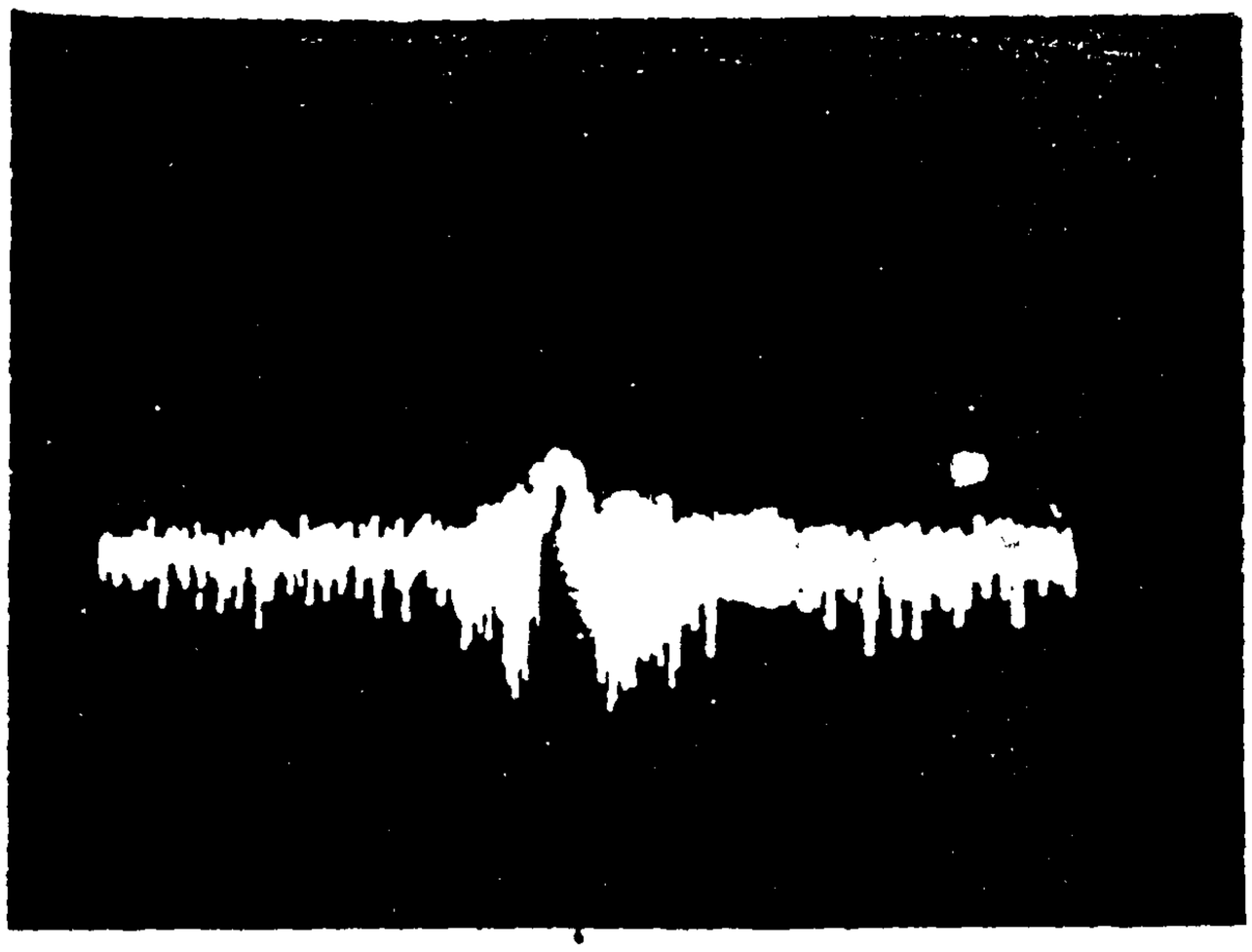

7 MHZ

CENTRE FREQUENCY

7.0002 MHz.

SCAN WIDTH 0.5 kHz/div.

BANDWIDTH 0.3 kHz

H.P. 855313 SPECTRUM ANALYSER

H.P. 8443A TRACKING ANALYSER

LOG DISPLAY 1μ V/div.

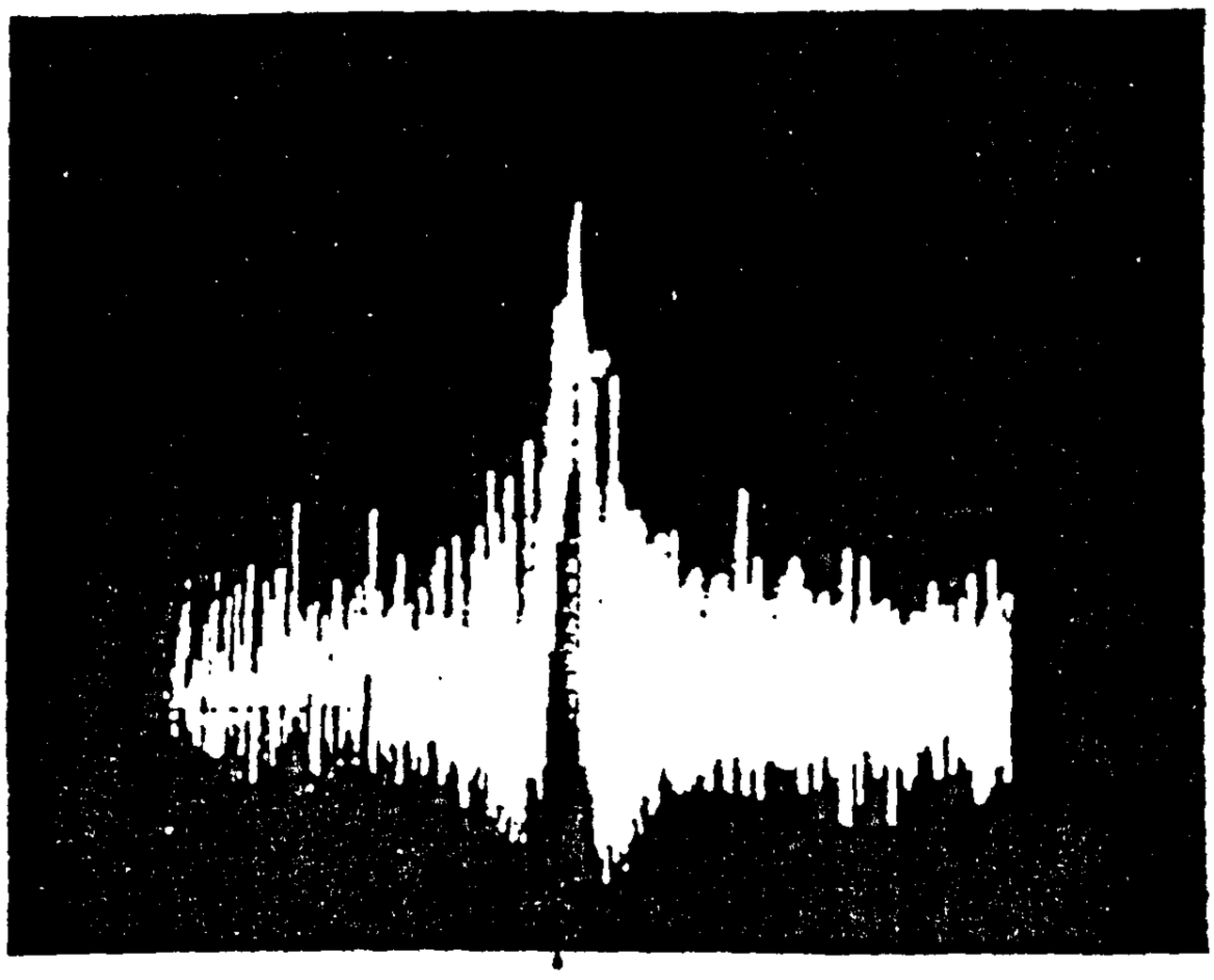

7 MHZ

LINEAR DISPLAY 0.1μ V/div.
(APPROX.)

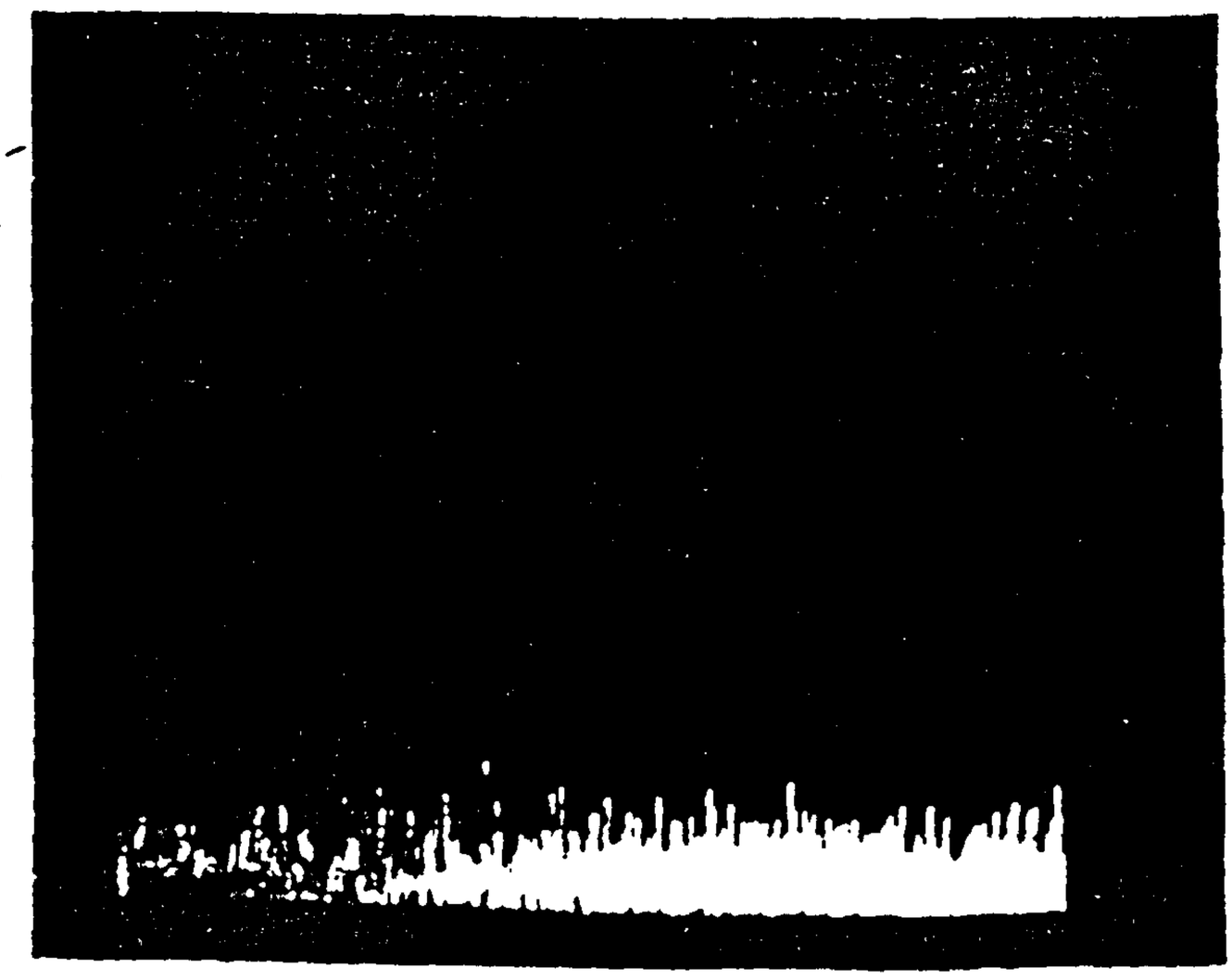

SPECTRUM ANALYSER

NOISE (CELL DISCONNECTED)

Fig 10.26 S.CEREVISIAE 4 HOURS AFTER STARTING INCUBATION. 2 POINT ELECTRODES.
6 APRIL 1983.

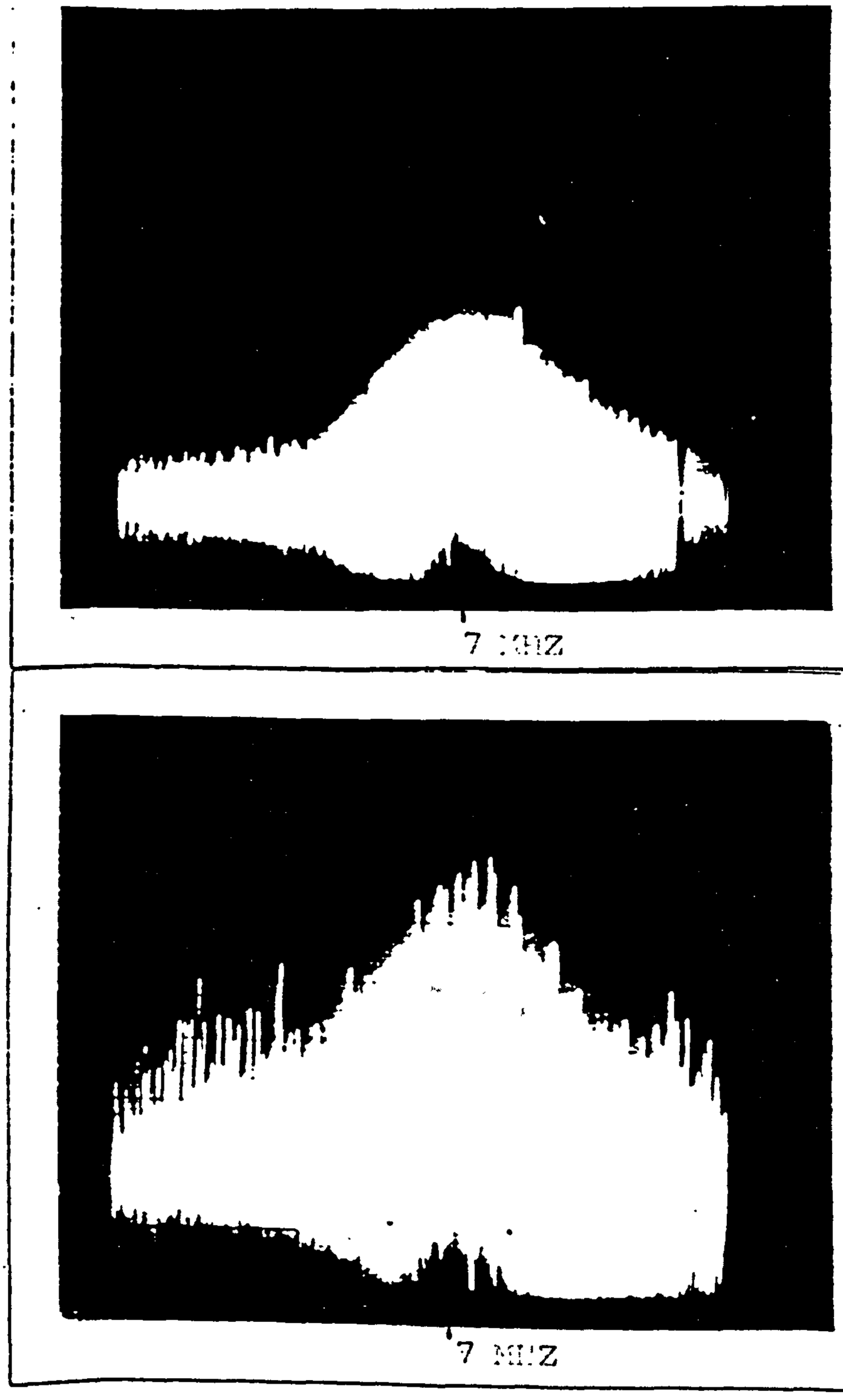

Fig 10.27

S.CEREVISIAE. 3½ HOURS AFTER STARTING INCUBATION

2 POINT ELECTRODES. H.P. SPECTRUM ANALYSER 8553B

CENTRE FREQUENCY 7.0 MHz. BANDWIDTH 0.3 KHz.

SCAN 0.2 kHz/DIV. GAIN 0.1μV/DIV (LINEAR).

SPECTRA AT 2 MIN. INTERVAL.

5 APRIL 1983.

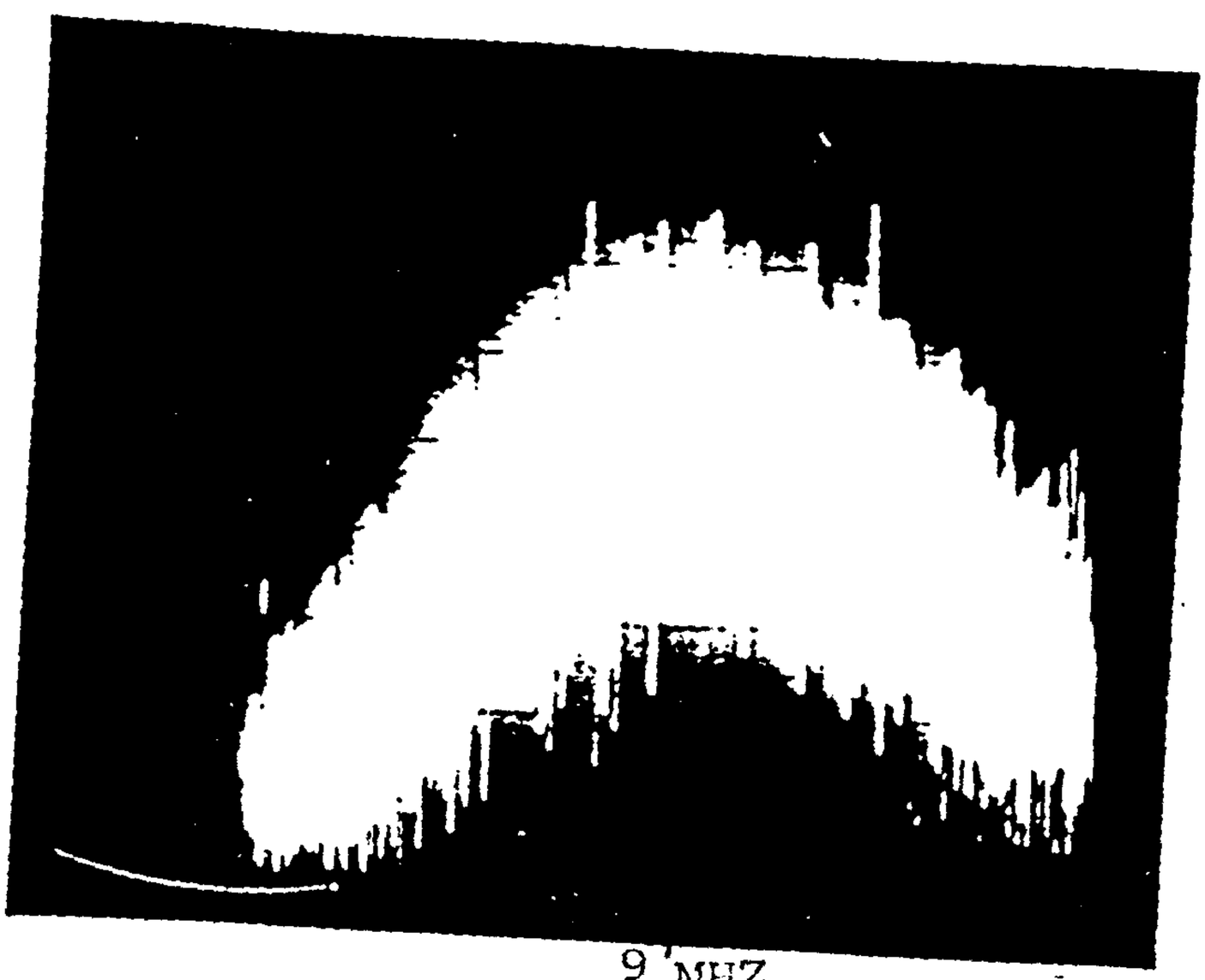

SCAN 1 kHz/DIV.

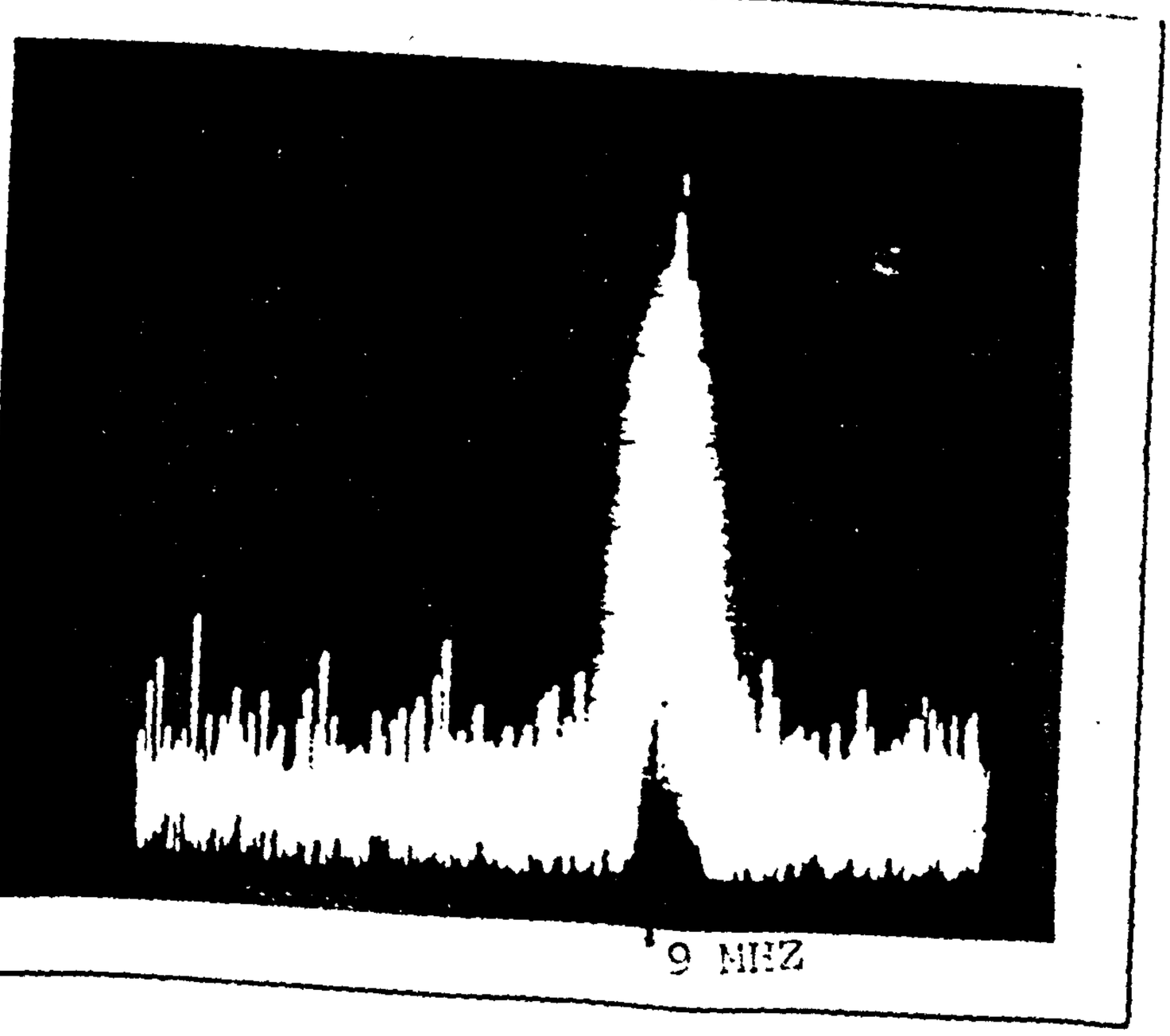

SCAN 0.1 kHz/DIV

2 MIN.LATER

Fig 10.28
S.CEREVISIAE, 4 HOURS AFTER STARTING INCUBATION

2 POINT ELECTRODES. H.P. SPECTRUM ANALYSER 8553B

CENTRE FREQUENCY 8.5 MHz, BANDWIDTH 0.3 kHz

GAIN 0.1μV/DIV (LINEAR)

14 APRIL 1983

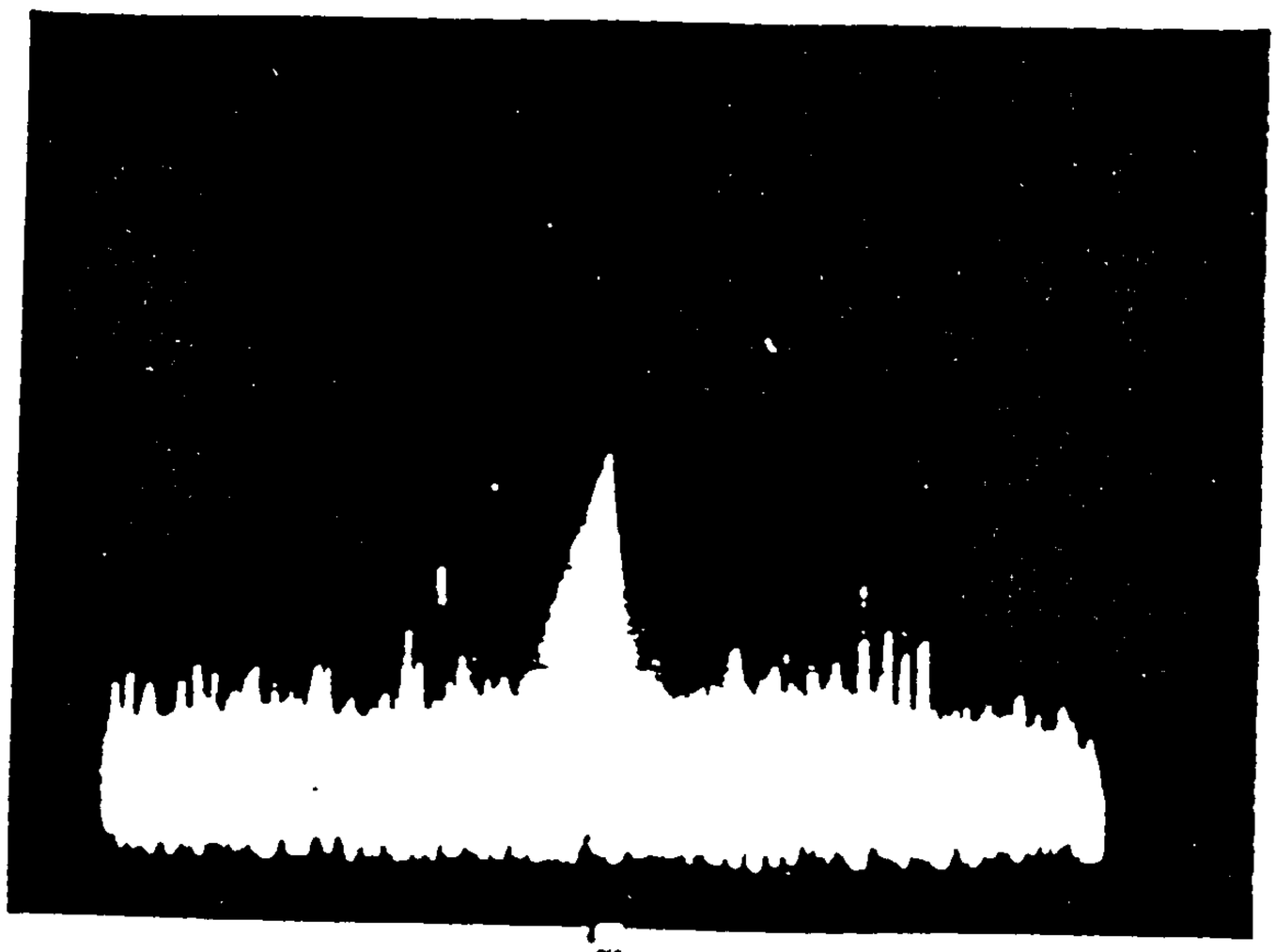

7 MHZ

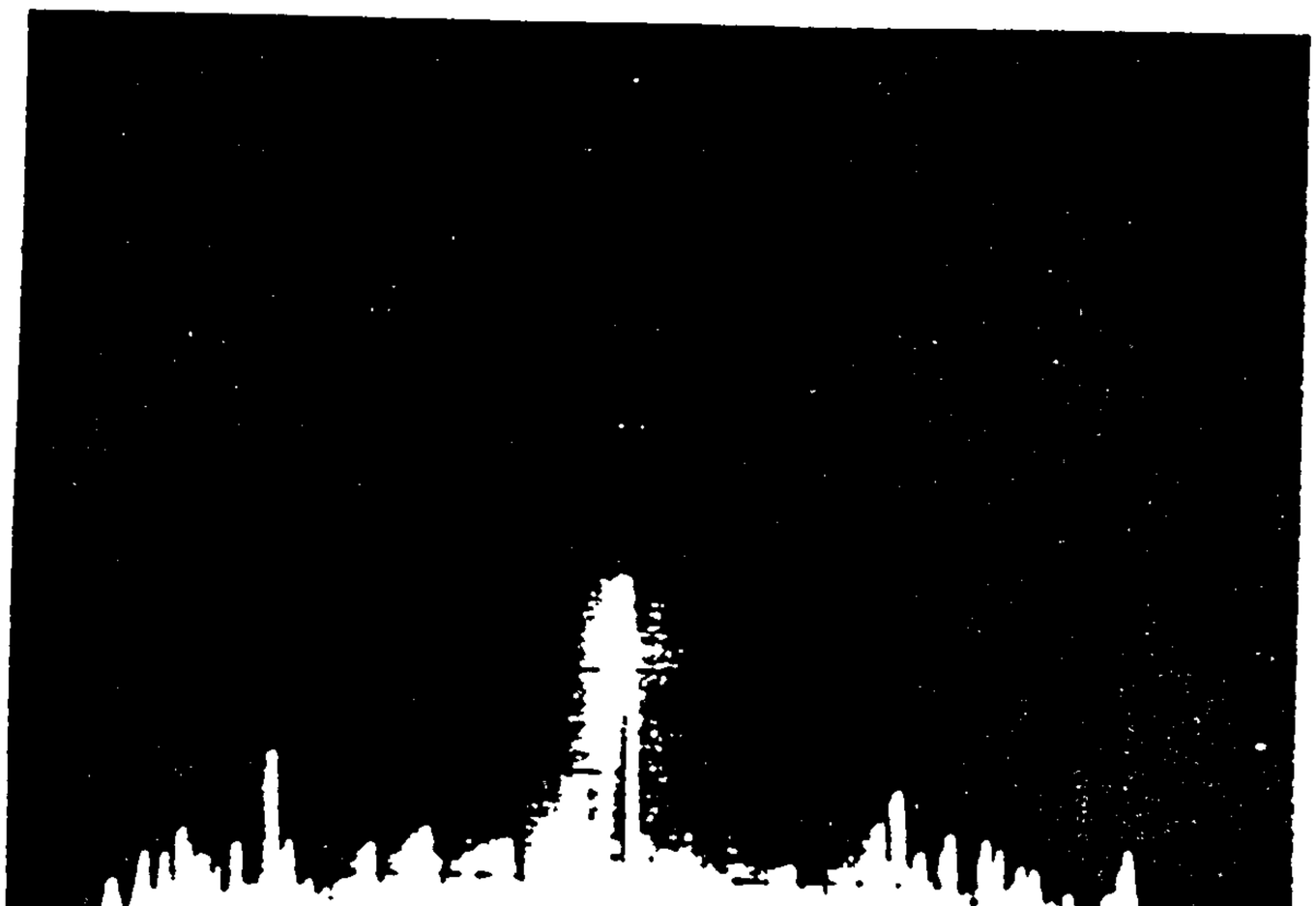

7 MHZ

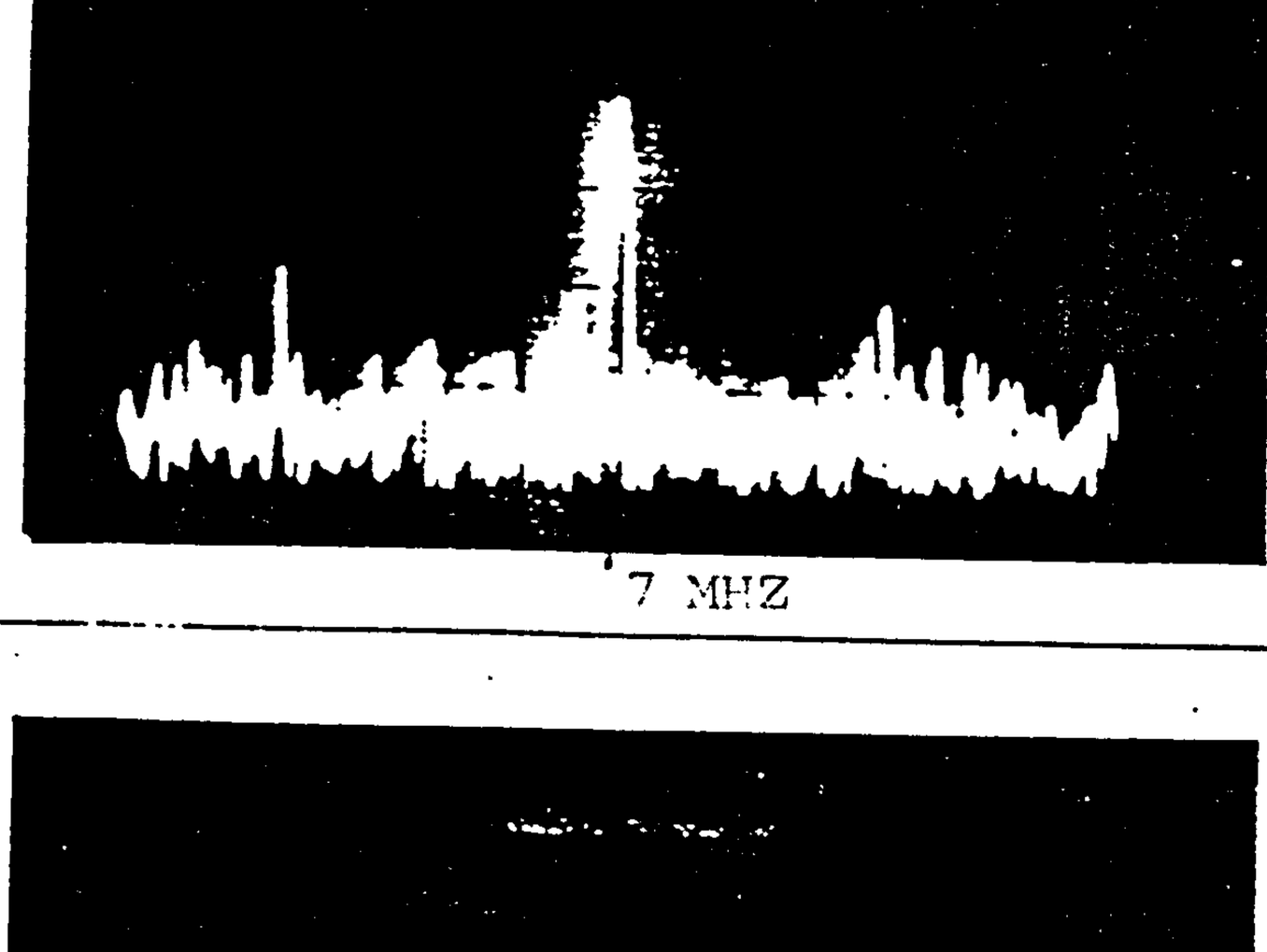

7 MHZ

Fig 10.29

S.CEREVISIAE, 4 HOURS AFTER STARTING INCUBATION
2 POINT ELECTRODES. H.P. SPECTRUM ANALYSER 8553B
CENTRE FREQUENCY 7.0 MHz. BANDWIDTH 0.3 KHz. SCAN 2 KHz/DIV.
GAIN 0.1μ V/DIV (LINEAR). SPECTRA AT 1 MIN. INTERVALS (APPROX).
15 APRIL 1983.

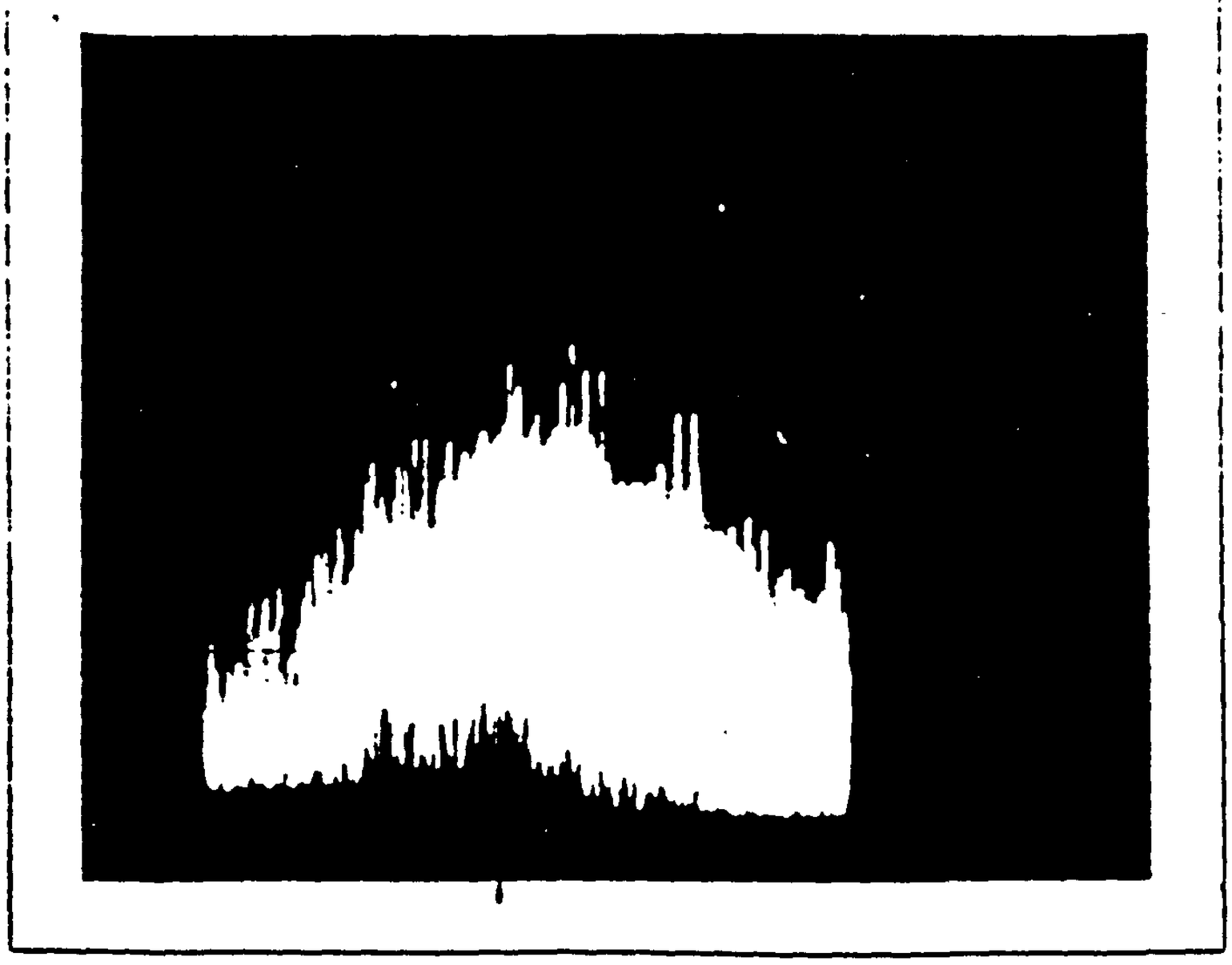

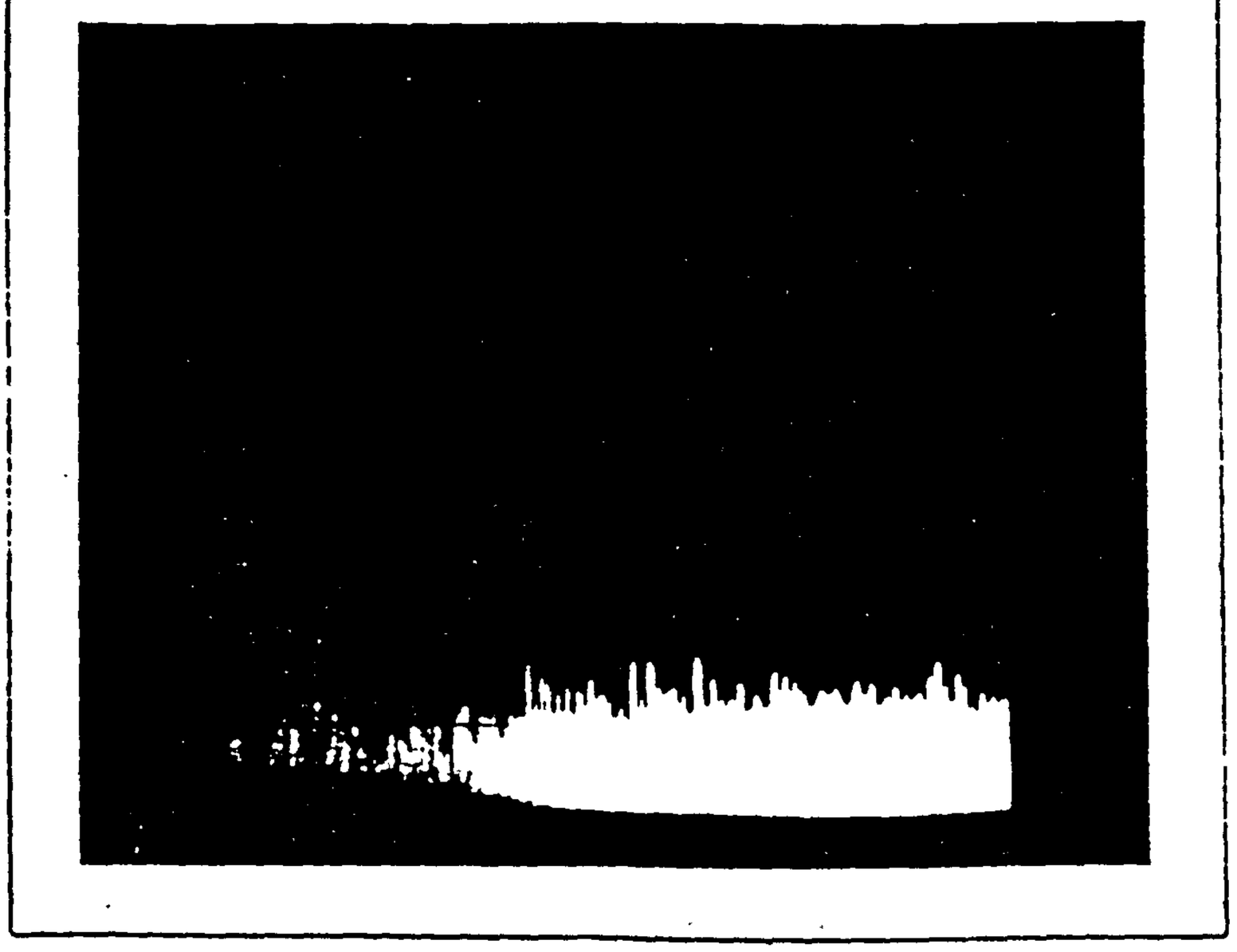

Fig. 10.30

S.CEREVISIAE, 4 HOURS AFTER STARTING INCUBATION.

2 POINT ELECTRODES, H.P. SPECTRUM ANALYSER 8553B

CENTRE FREQUENCY 8 MHz. BANDWIDTH 0.3kHz. SCAN 0.5 MHz/DIV.

SCAN RATE 0.5 SEC/DIV. GAIN 0.1μ V/DIV (LINEAR)

28 APRIL 1983.

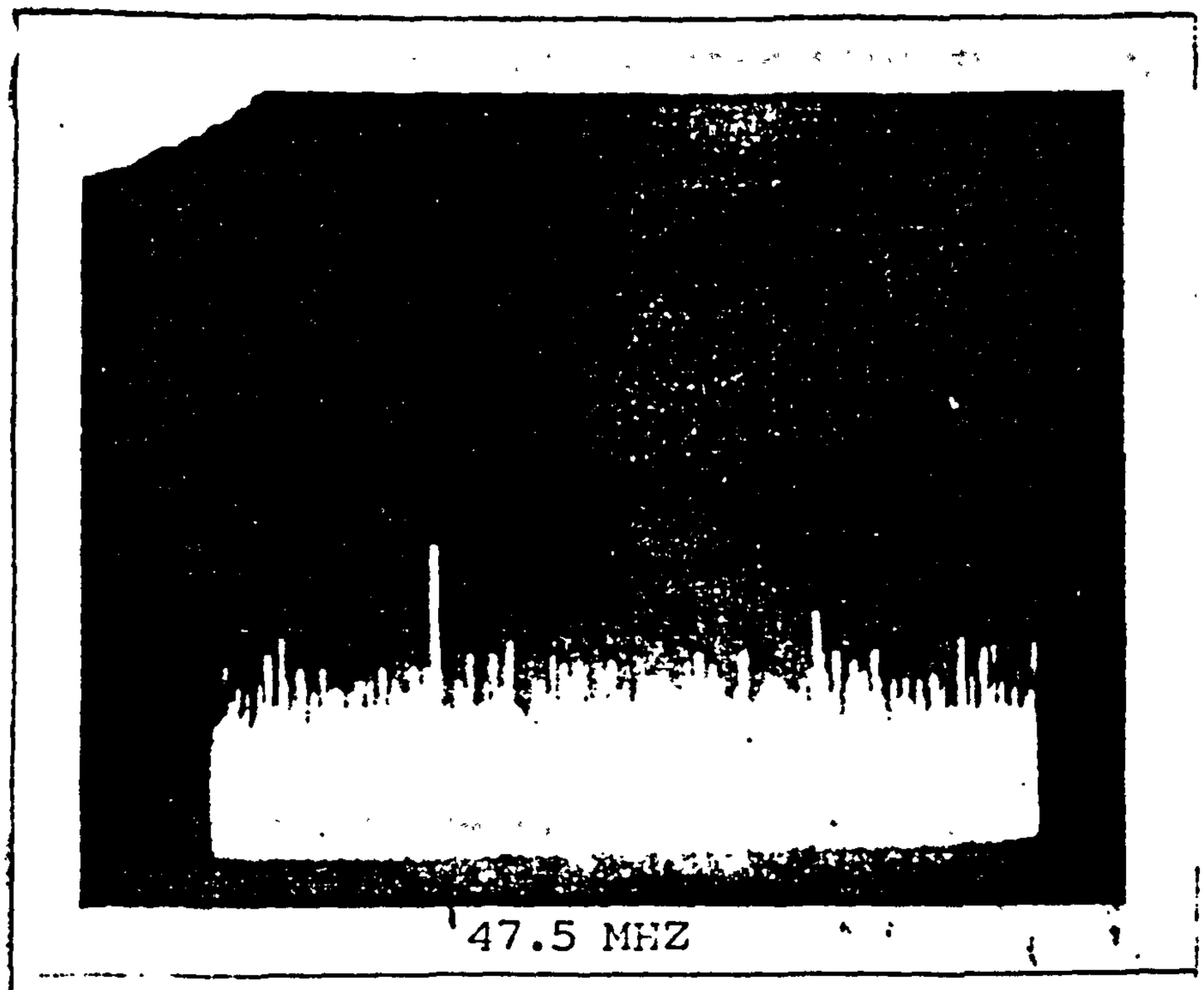

Fig 10.31
Centre frequency = 50 MHz
Scan Width = 1MHz/div.
Scan time = 0.5 sec/div.
Bandwidth = 0.3 kHz
Duration = 3 min.
Date : 3-6-83

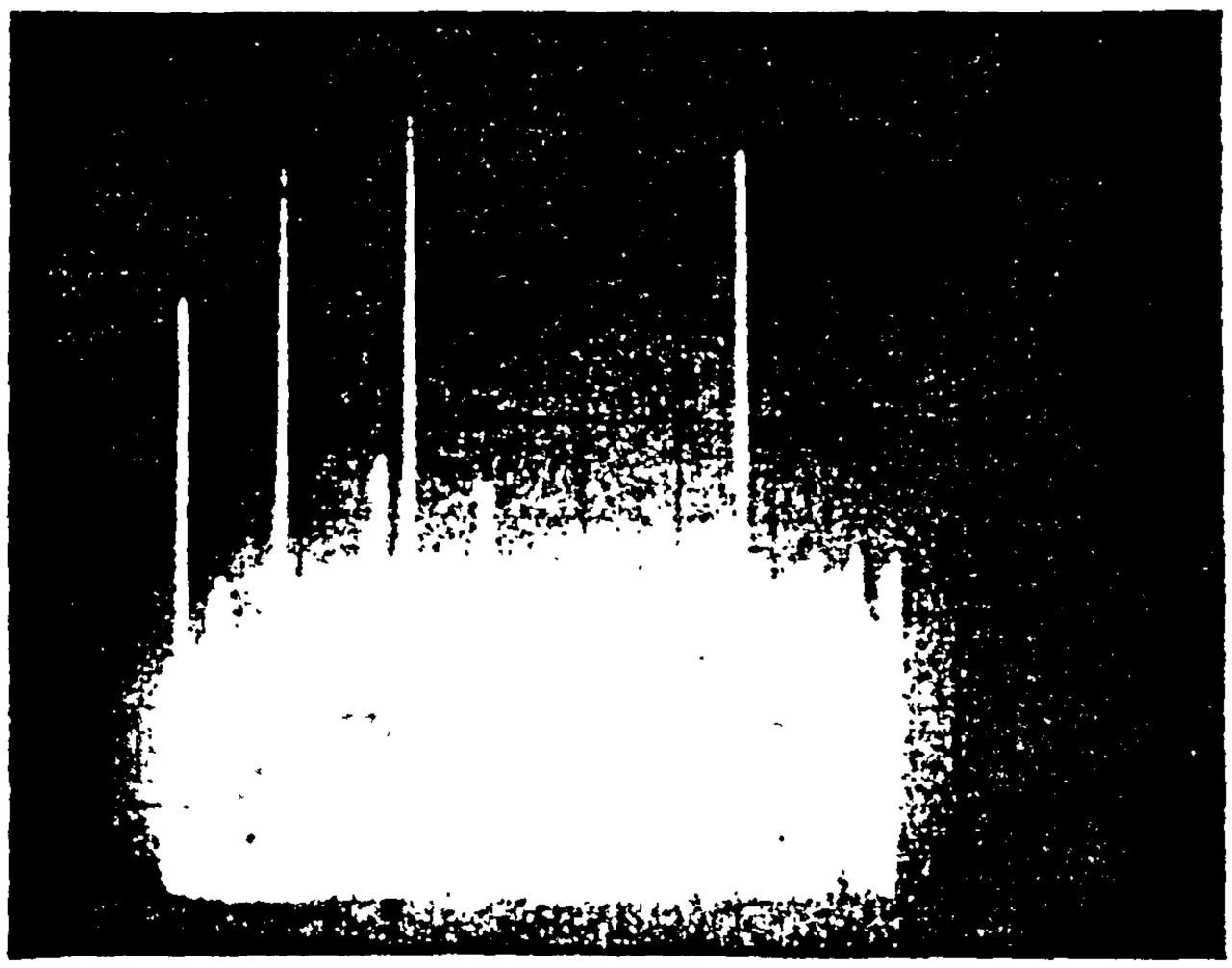

NO BROADCASTING SIGNAL
MATCH WITH THE EMITTED
SIGNAL BY CONNECTING
AN AERIAL IN PLACE
OF THE TEST CELL

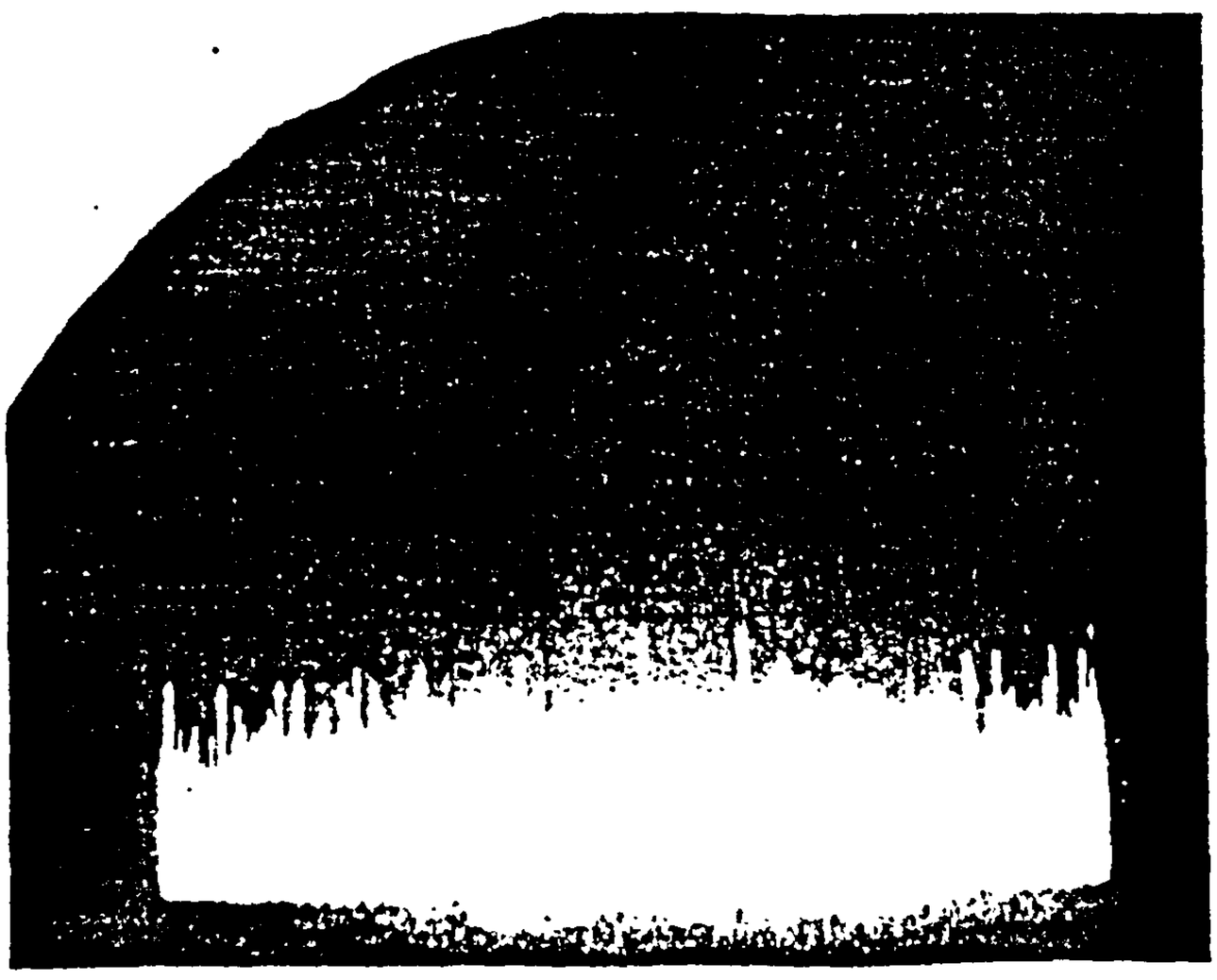

Noise Level

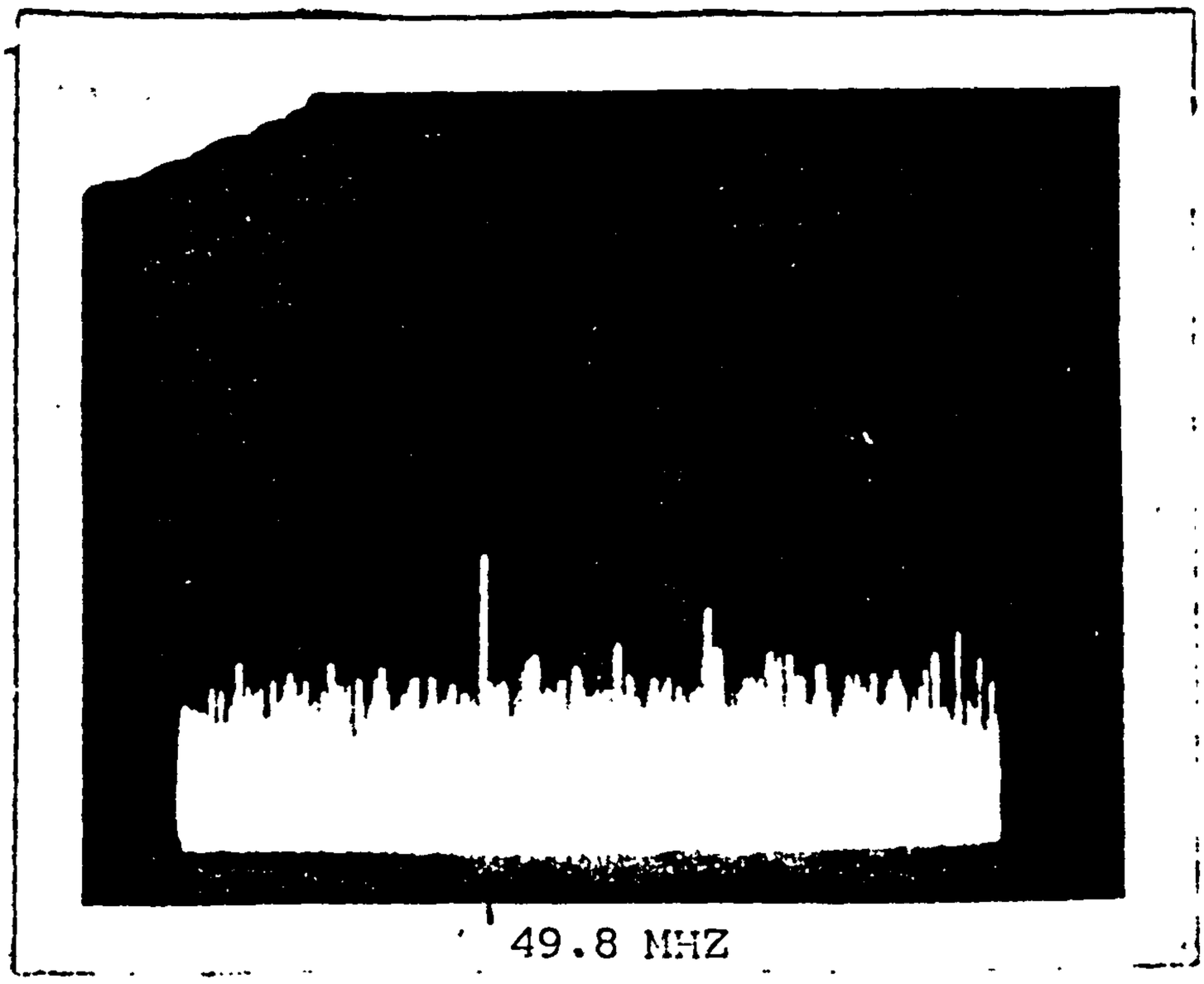

Fig 10.10.32

Centre frequency
= 50 MHz/div.

Scan width=0.1 MHz/div.

Scan time=0.5 sec/div.

Bandwidth=0.3 kHz

Duration = 3 min.

Date 6-6-83

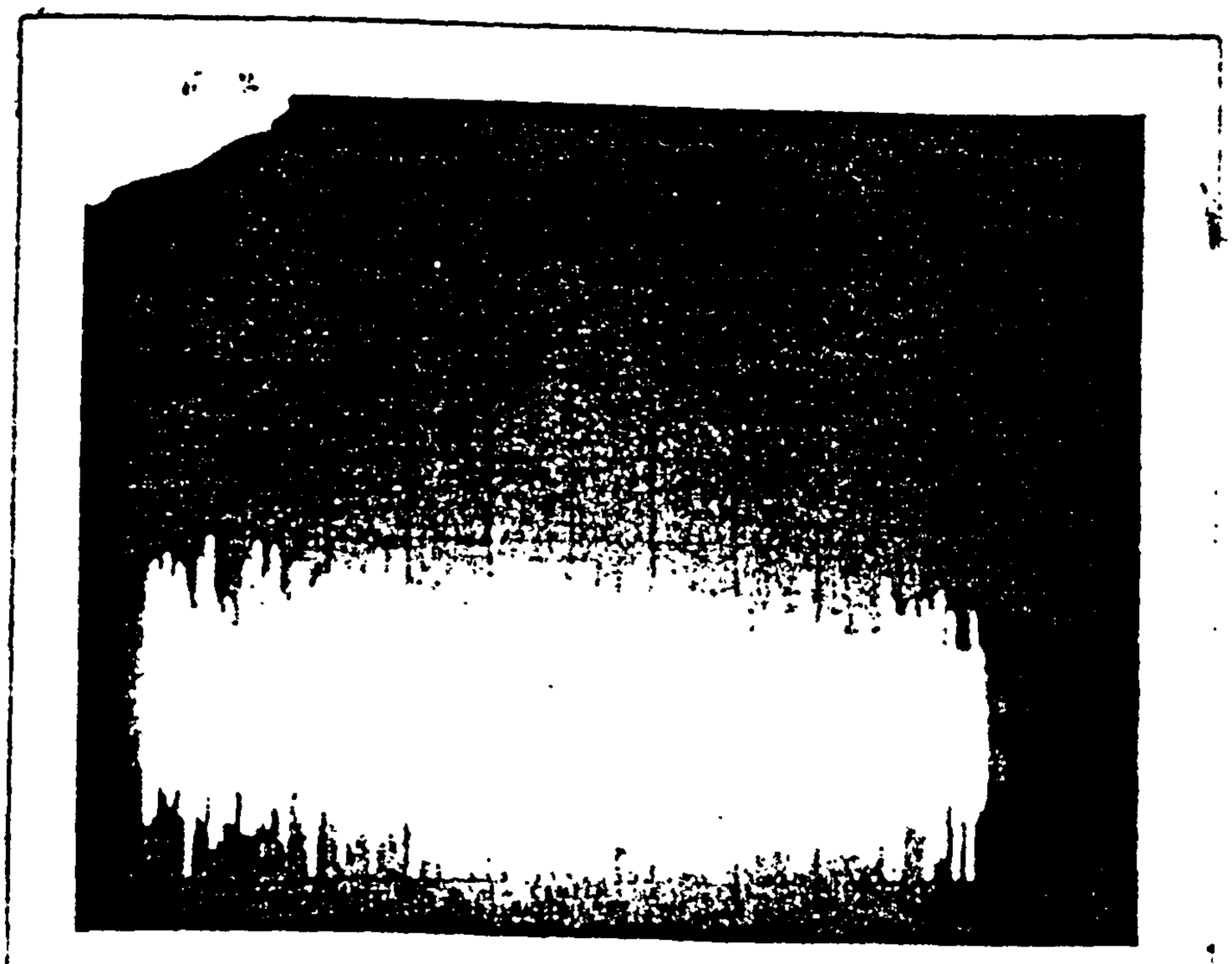

NO BROADCASTING SIGNAL WAS OBSERVED BY CONNECTING AN AERIAL IN PLACE OF THE TEST CELL

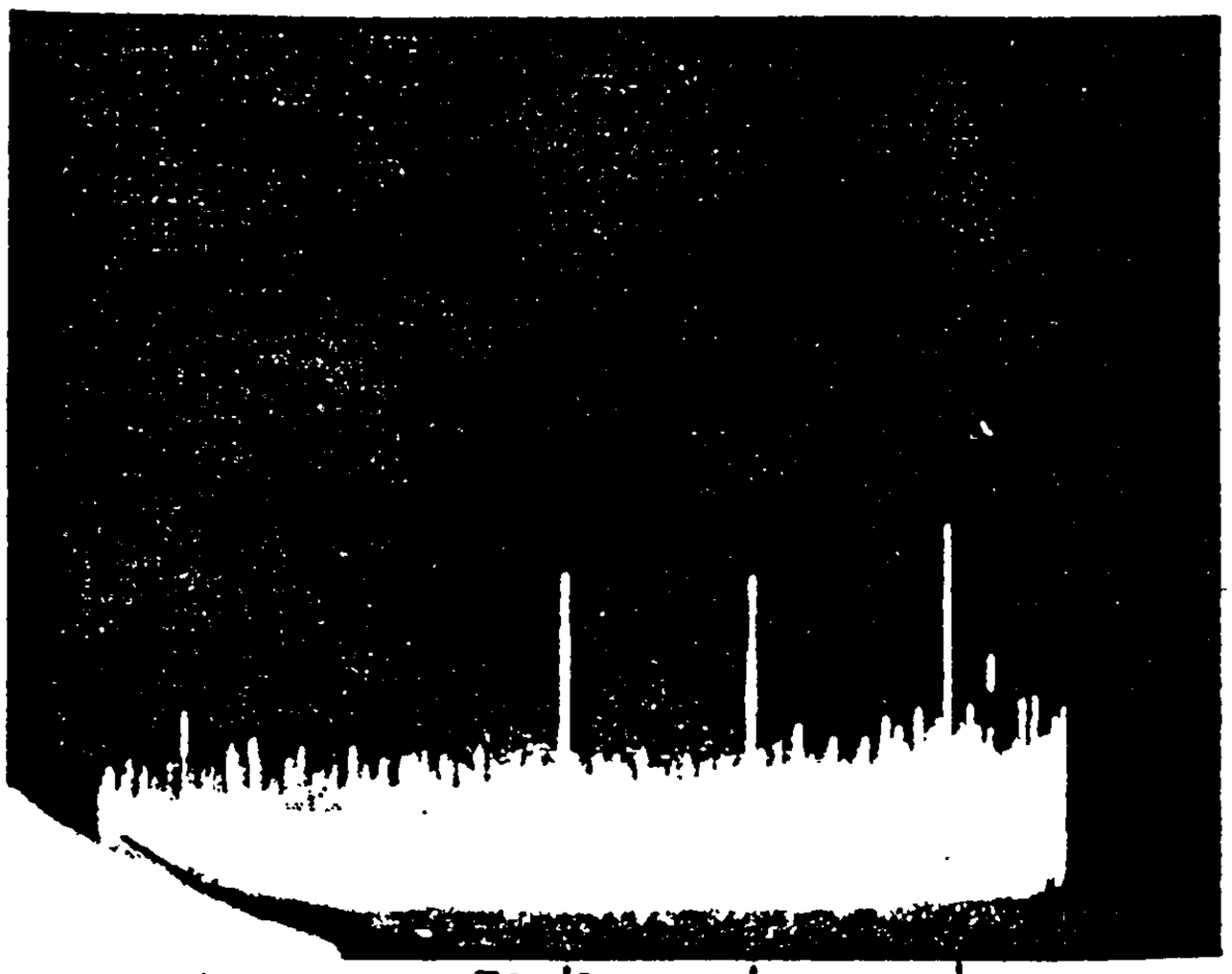

Fig 10.33
CF=72.28 MHZ/div.
SCW=1MHz/div.
SCT=1 sec/div.
BW=0.3kHz
Resistor=10 MΩ
and
Capacitance = 100PF
had removed the signal
Duration = 3 min.
26-6-83

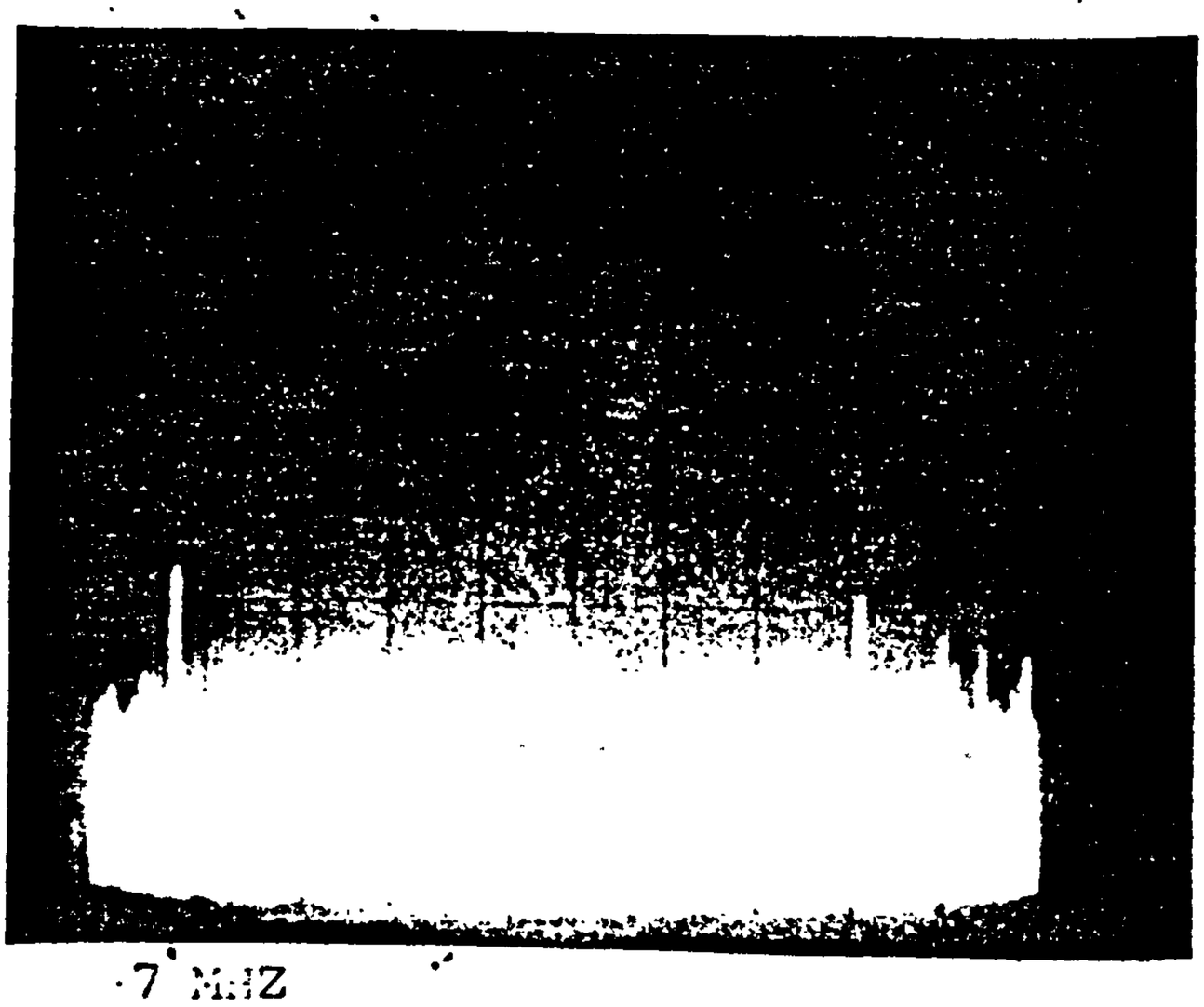

CF = 50 MHz
SCW = 10 MHz/div.
SCT = 0.5 sec./div.
BW = 0.3kHz
Ag/AgCl
electrodes
duration = 1 min
Date: 6-6-83

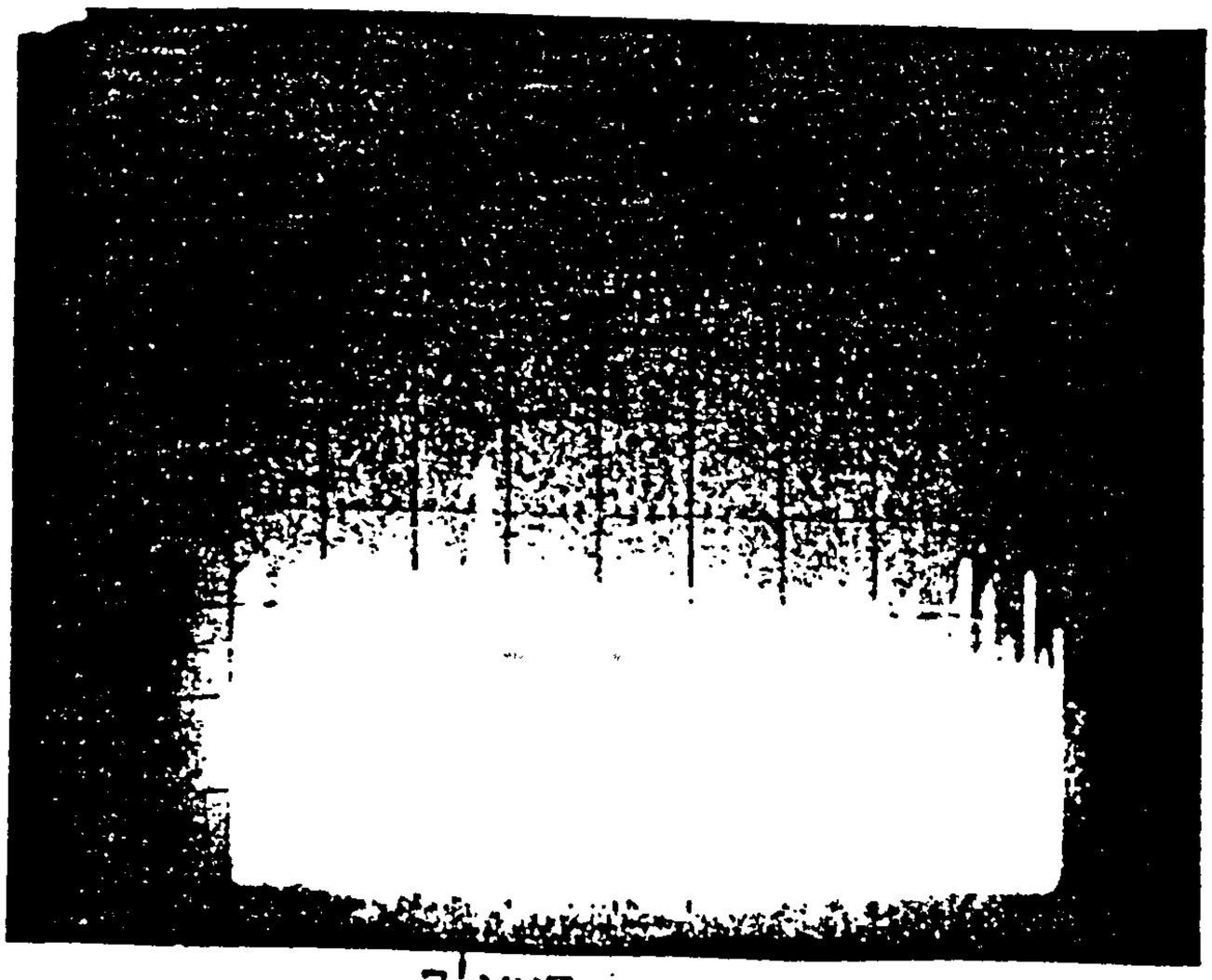

CF = 8MHz
SCW = 1MHz/div.
SCT = 0.5 sec/div.
BW = 0.3 kHz
Duration = 1 min
10-6-83

Fig 10.34
(a) Radio frequency emission from dividing yeast cells.

(b) Steps in the voltage-current characteristics of dividing yeast cells.

(c) Similar frequencies by measuring the change in reaction rate from subjecting partially inhibited lysozyme solution for 2h to the range of frequencies from 10KHz to 1GHz (Shaya and Smith, 1977). The cells weremicrococcus lysodeikticus and about half the size of the yeast cells.

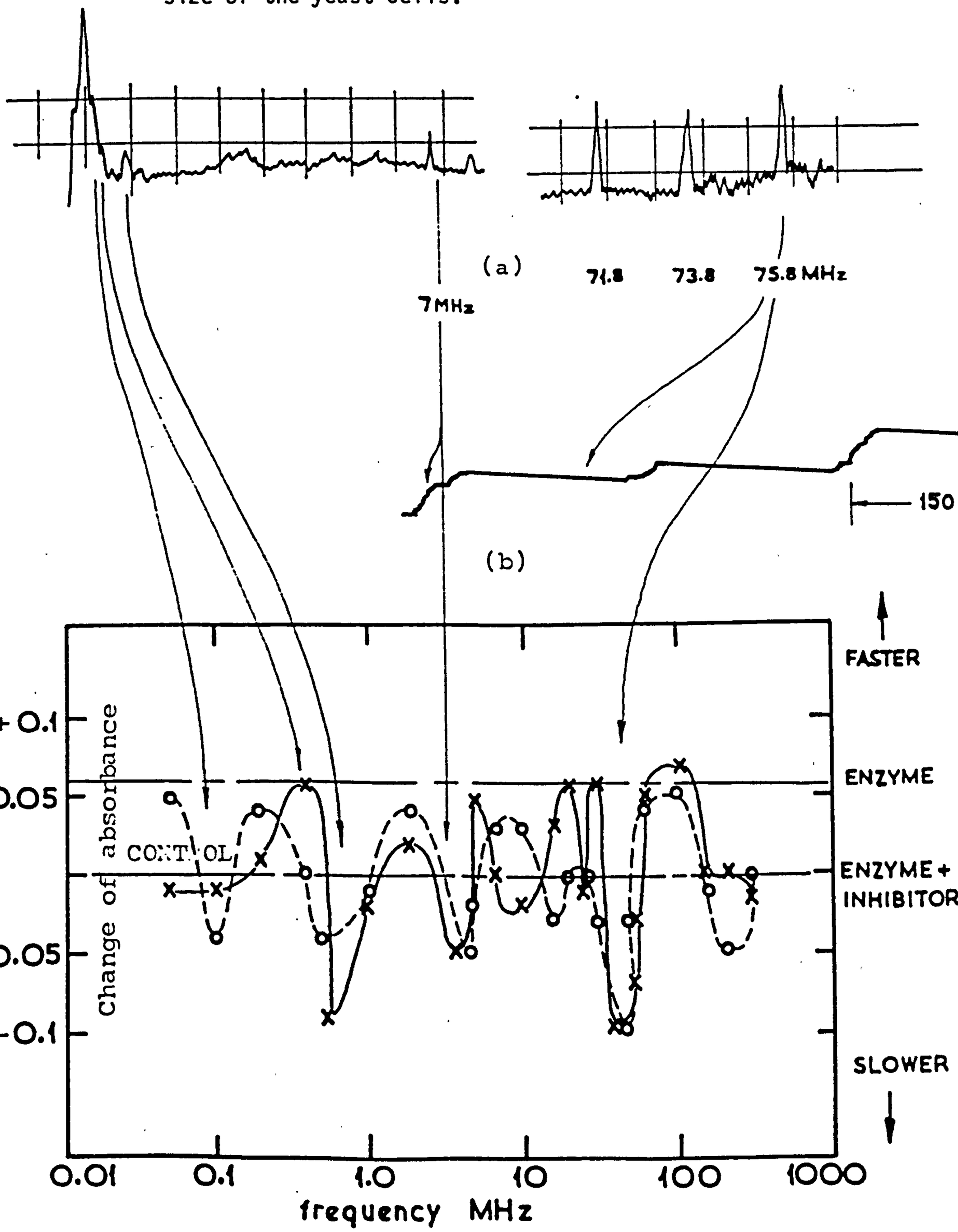

10.5 The effects of NMR on the sodium and potassium content of the bovine eye lenses through microwave modulation

Although most of the experiments were performed on the yeast cells, a few experimental observations were made on bovine eye lenses.

The effect of a range of frequencies of microwaves modulated under NMR conditions for magnetic isotopes (e.g. ^{23}Na, ^{39}K) in a positioned ambient magnetic field of the order of 1.9 gauss (190 μT) was investigated, as well as the duration of microwave irradiation. Dielectric measurements were also made on both actively metabolising lenses and lenses whose metabolism had been disrupted by ouabain in an ambient magnetic field of 0.5 gauss (50 μT).

Before performance of the experiments, the lenses were tested to determine the effect on potassium and sodium concentrations and weight increase of irradiation.

Microwave irradiation at a frequency of 960 MHz and other frequencies between 250 MHz and 2 GHz did not have any definite effect on the weight increase of lenses. There was no appreciable and consistent difference between the weight of the control and the weight of the irradiated lenses, whatever the period of irradiation (Figure 10.35).

Fig. 10.35

The effect of various periods of irradiation on the weight of Lenses at a frequency of 960MHz.

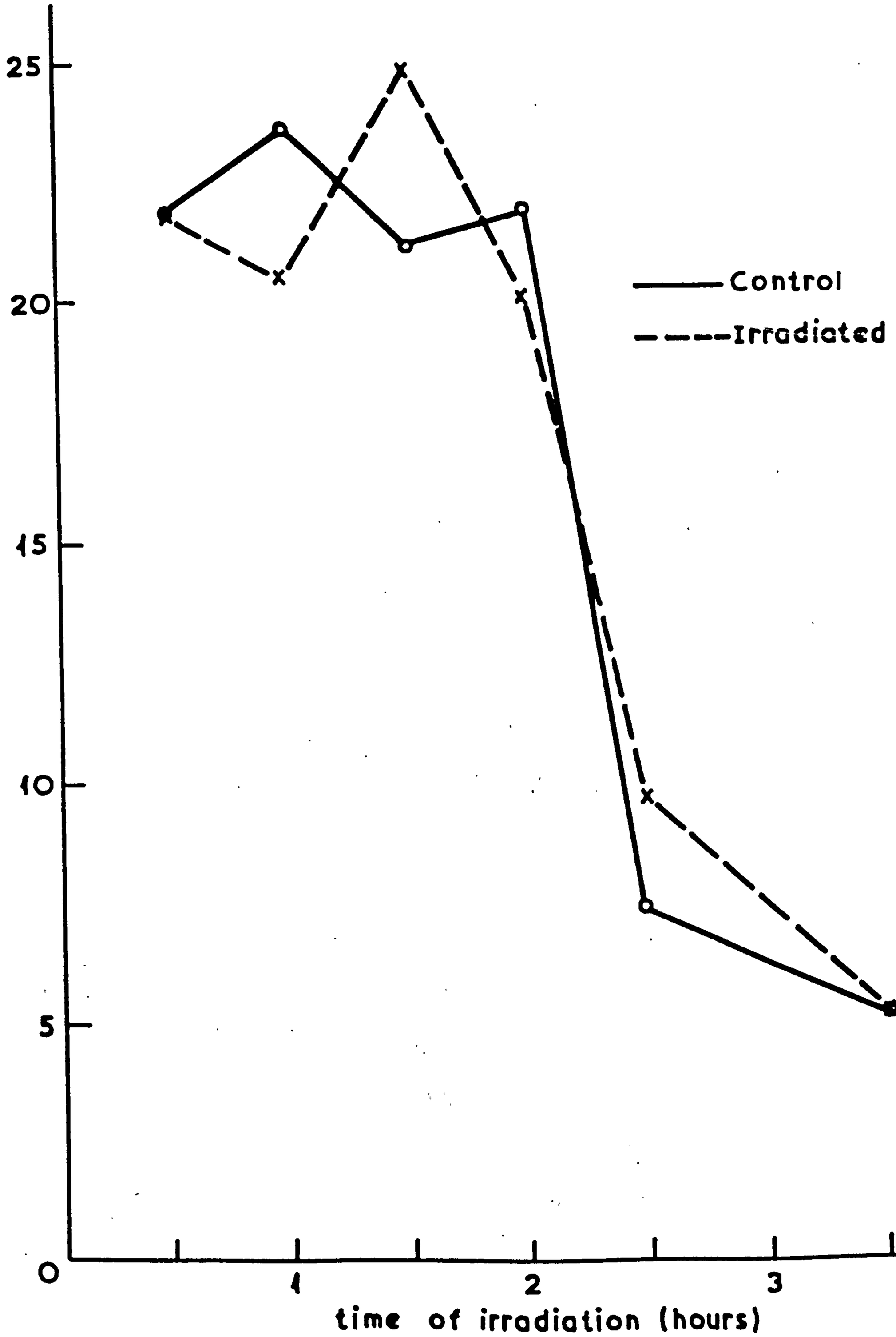

There was no consistent difference between the Na^+ concentration of control and irradiated lenses (Figure 10.36), though there was a difference in K^+ concentration, indicating a possible effect of microwave irradiation (Figure 10.37).

There was no appreciable effect on the weight increase of lenses, under either $^{23}Na^+$ or $^{39}K^+$ NMR conditions (Figures 10.38 and 10.39). However the application of NMR conditions does seem to have had some effect on the Na^+ and K^+ concentrations of lenses. Under NMR conditions for ^{23}Na, and between frequencies of 500 MHz and 960 MHz, the irradiated lenses showed a considerably higher Na^+ content than the control lenses (Figure 10.40). The only discrepancy in this observation was with the lens irradiated at 2 GHz, which had a lower Na^+ concentration than its control, a further investigation is needed in this region. Under NMR conditions for ^{39}K, the Na^+ concentration of irradiated lenses was still higher than that of the controls, but there was not nearly so much difference between the irradiated lenses and the controls as there was under ^{23}Na NMR conditions (Figure 10.41).

Under ^{39}K NMR, the irradiated lenses showed a decrease in ^{39}K concentration than the control lenses (Figure 10.42). Under NMR conditions for ^{23}Na resulted in a marked decrease in ^{39}K concentration (Figure 10.43).

The effect of ^{23}Na and ^{39}K NMR on Na^+ and K^+ concentrations are summarised in Figure 10.44, which shows the percentage changes of these magnetic isotopes between control and irradiated lenses at varying microwave frequencies. Finally

Fig. 10.36

The effect of various periods of irradiation on the sodium concentration of Lenses at a frequency of 960MHz.

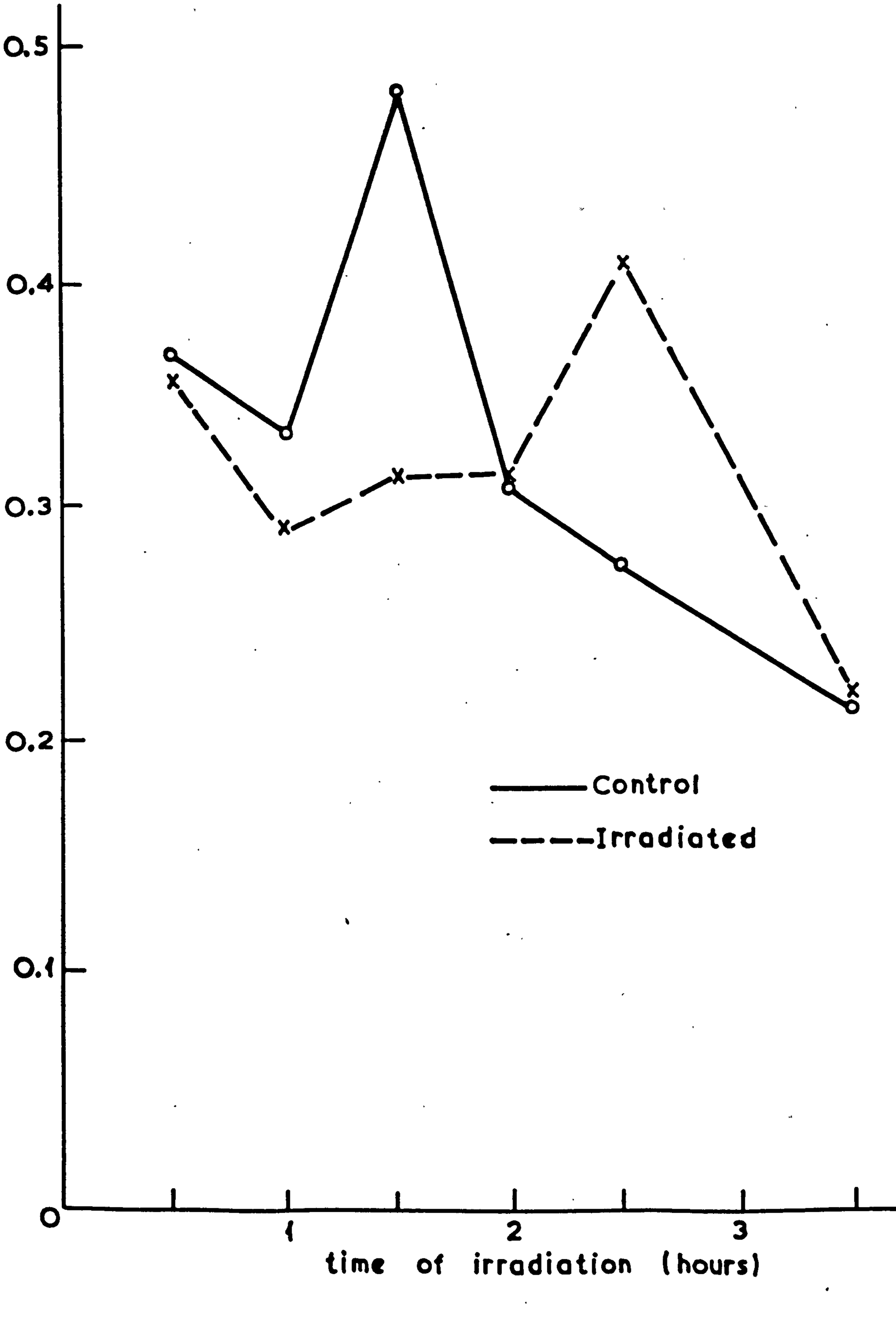

Fig. 10.37
The effect of various periods of irradiation on the Potassium concentration of Lenses at a frequency of 960MHz.

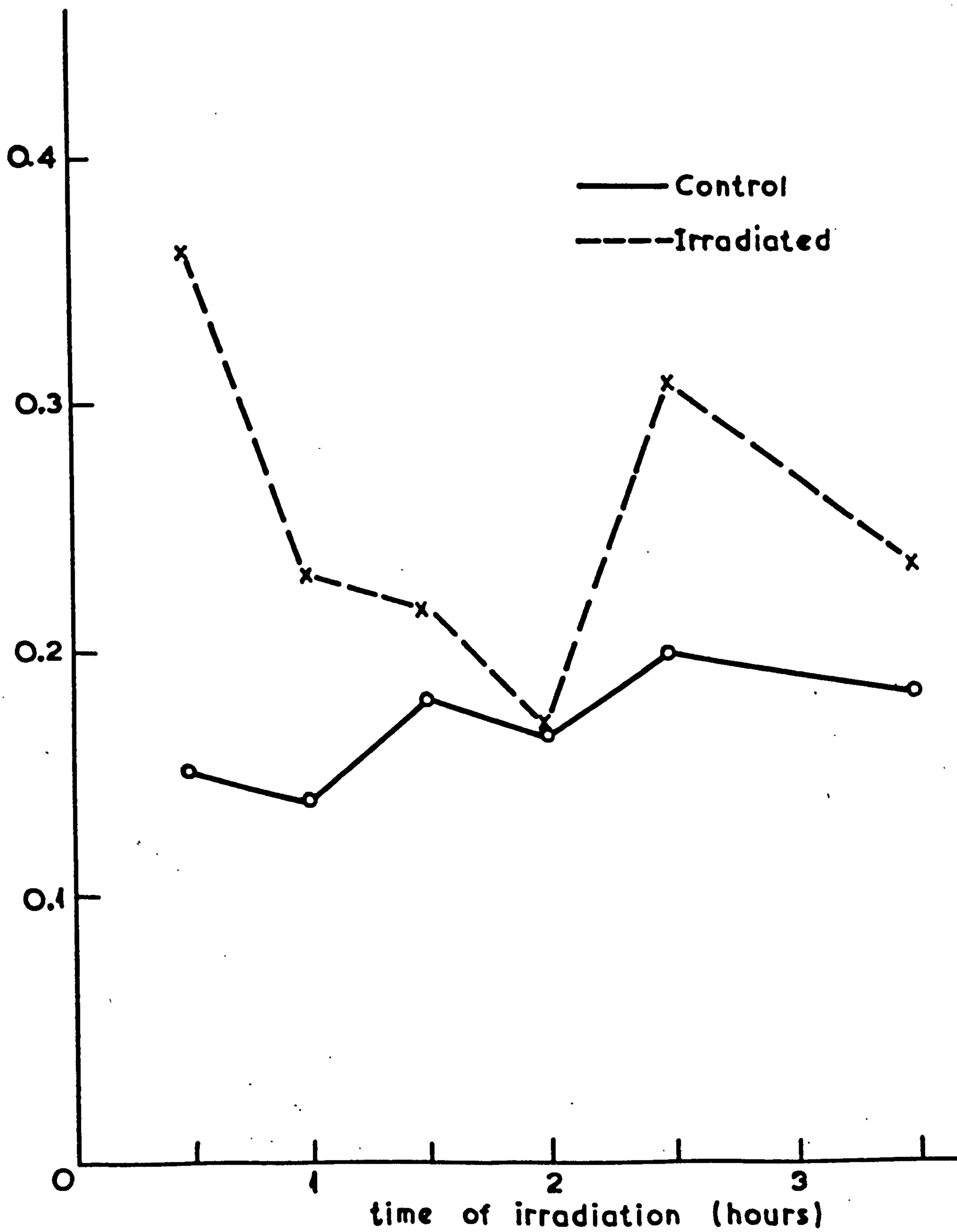

Fig. 10.38
The effect of various frequencies of Microwave Irradiation on the weight of a metabolising eye lense under NMR conditions for $^{23}Na^{+}$.

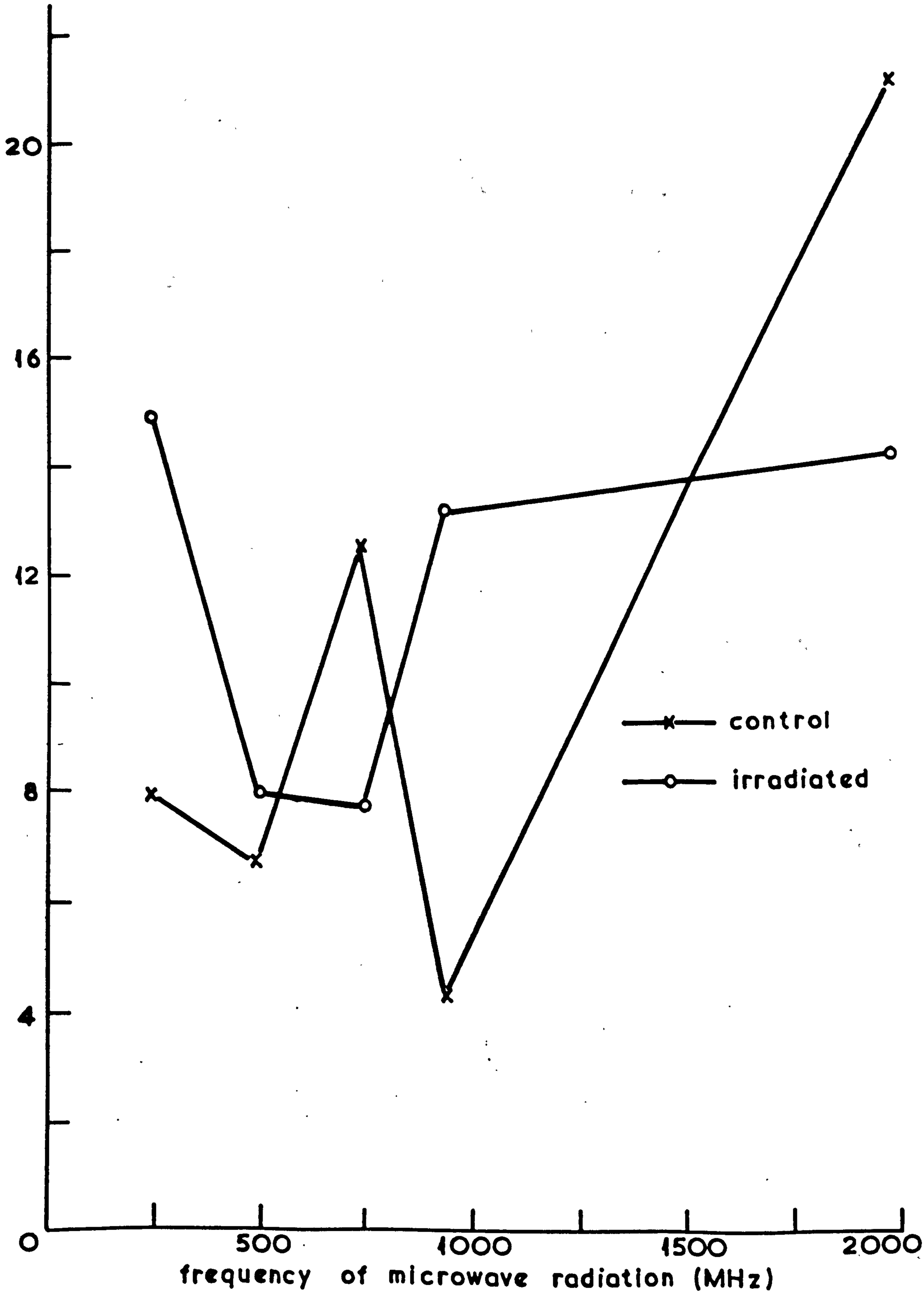

Fig. 10.39

The effect of various frequencies of Microwave Irradiation on the weight of a metabolizing eye lense under NMR conditions for $^{39}K^{+}$.

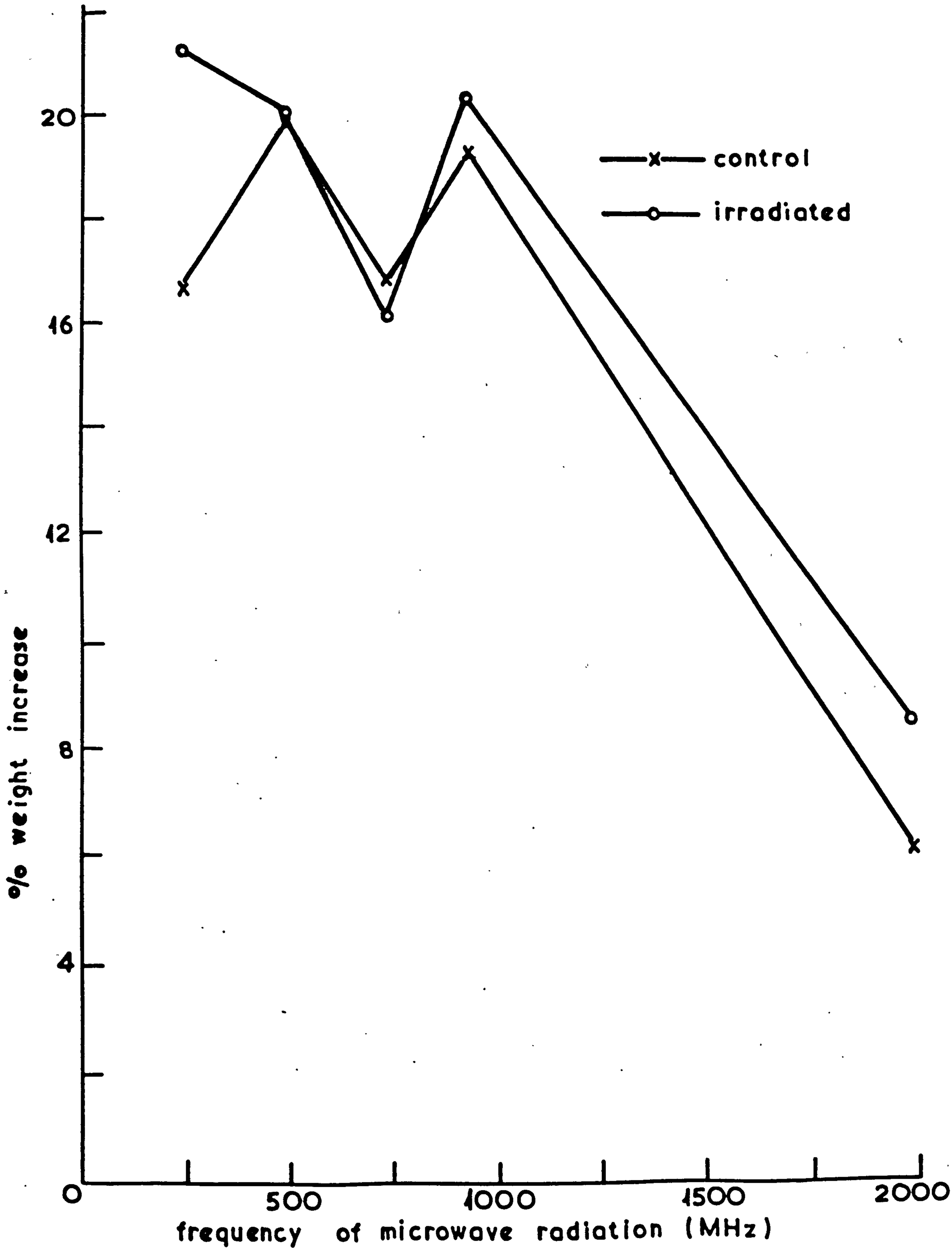

Fig. 10.40

The effect of various frequencies of Microwave Irradiation on the [Na^+] of a metabolising Bovine eye lense, under NMR conditions for $^{23}Na^+$.

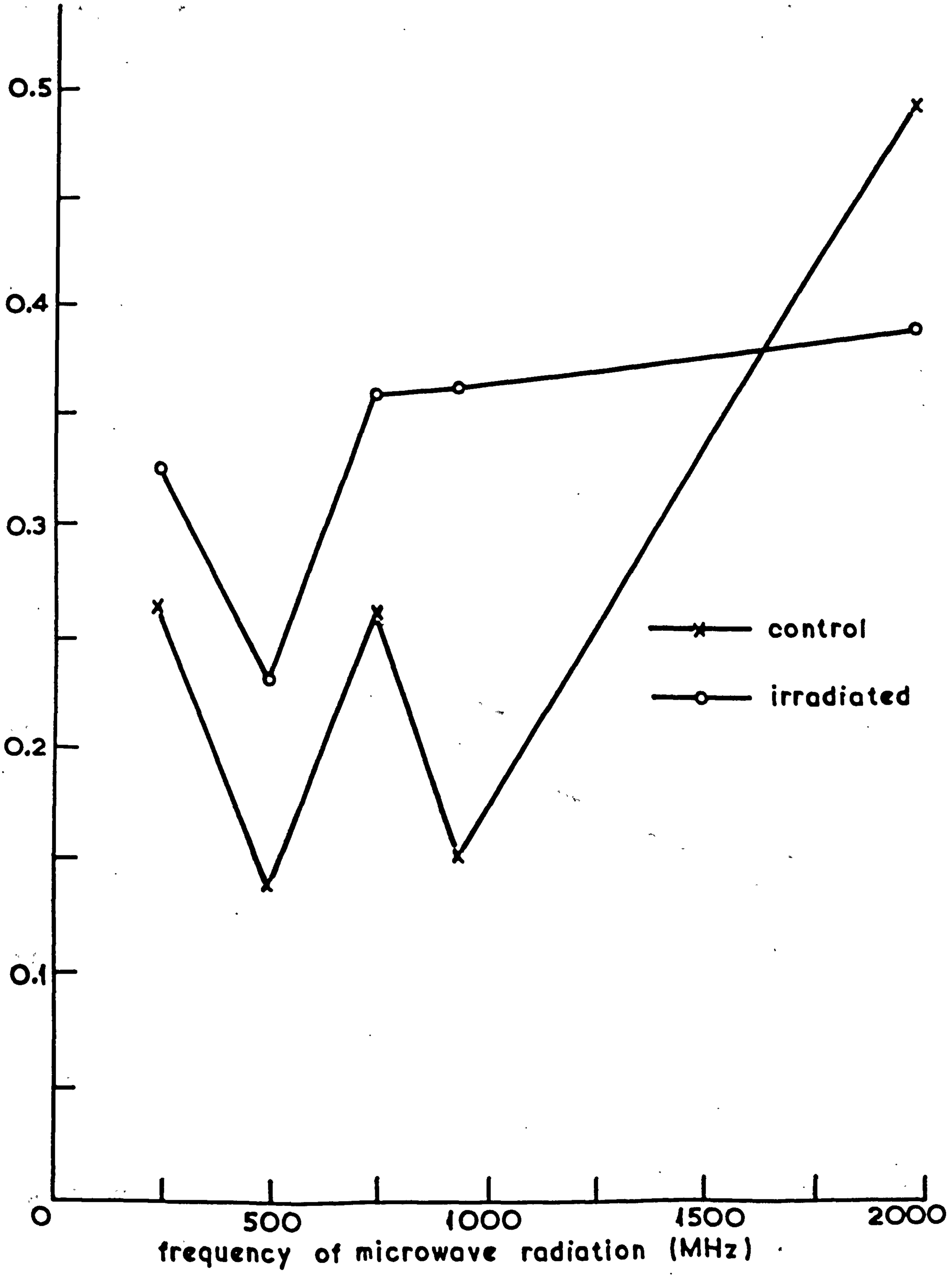

Fig. 10.41

The effect of various frequencies of Microwave Irradiation on the Na^+ of a metobolizing Bovine eye lense, under NMR conditions for $^{39}K^+$.

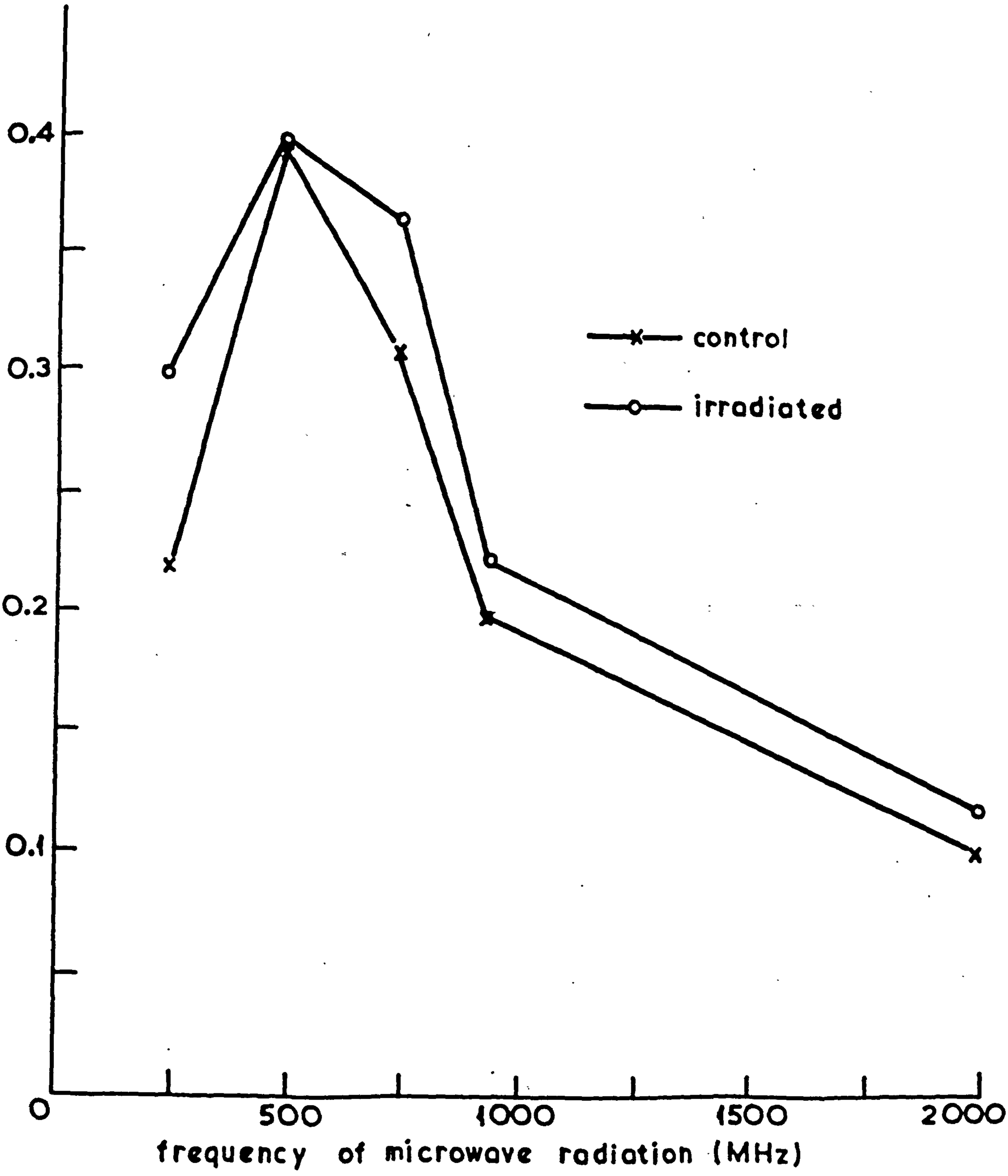

Fig. 10.42
The effect of various frequencies of Microwave Irradiation on the $[K^+]$ of a metabolising Bovine eye lense, under NMR conditions for $^{39}K^+$.

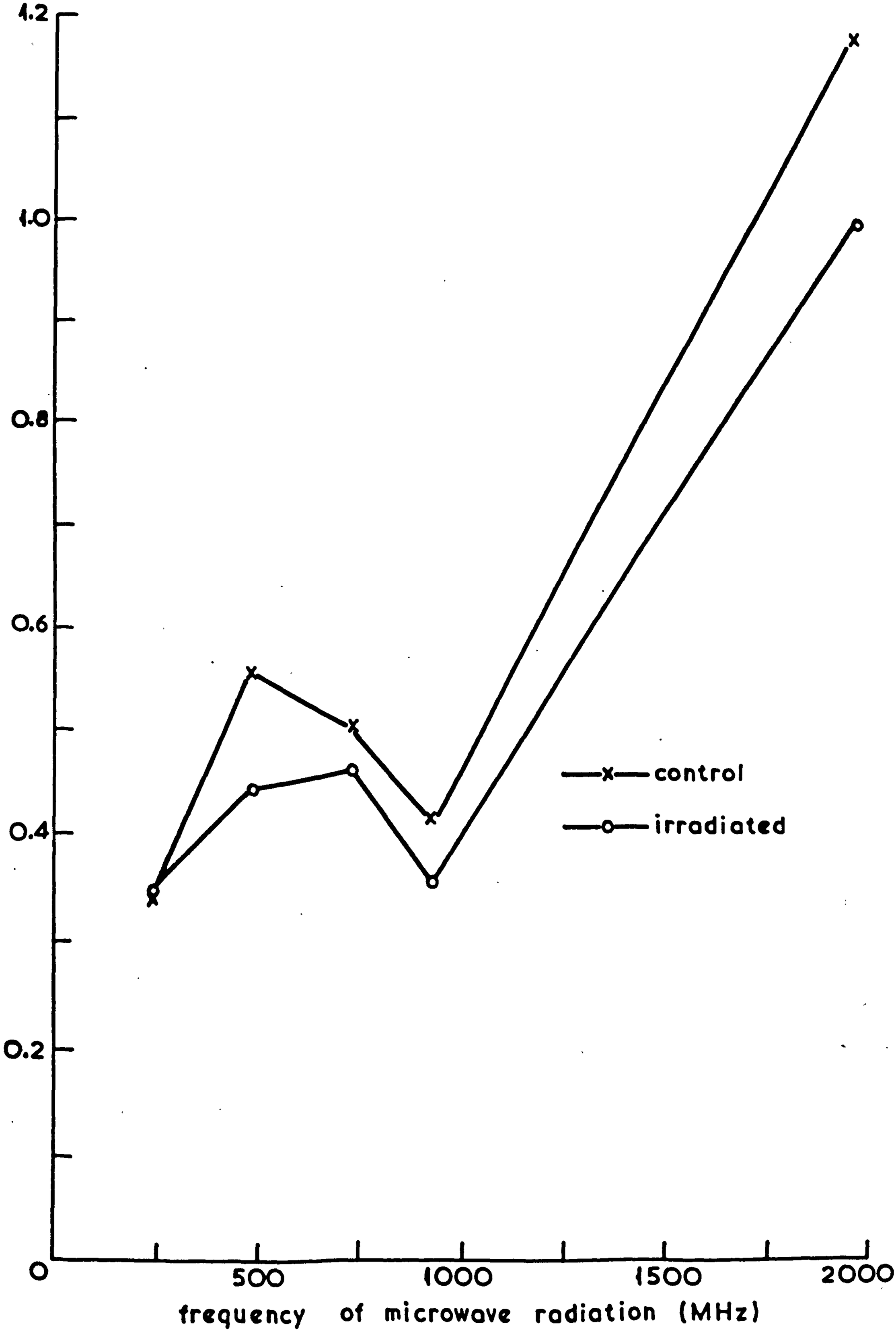

Fig. 10.43

The effect of various frequencies of Microwave Irradiation on the [K^+] of a metabolizing Bovine eye lense, under NMR conditions for $^{23}Na^+$.

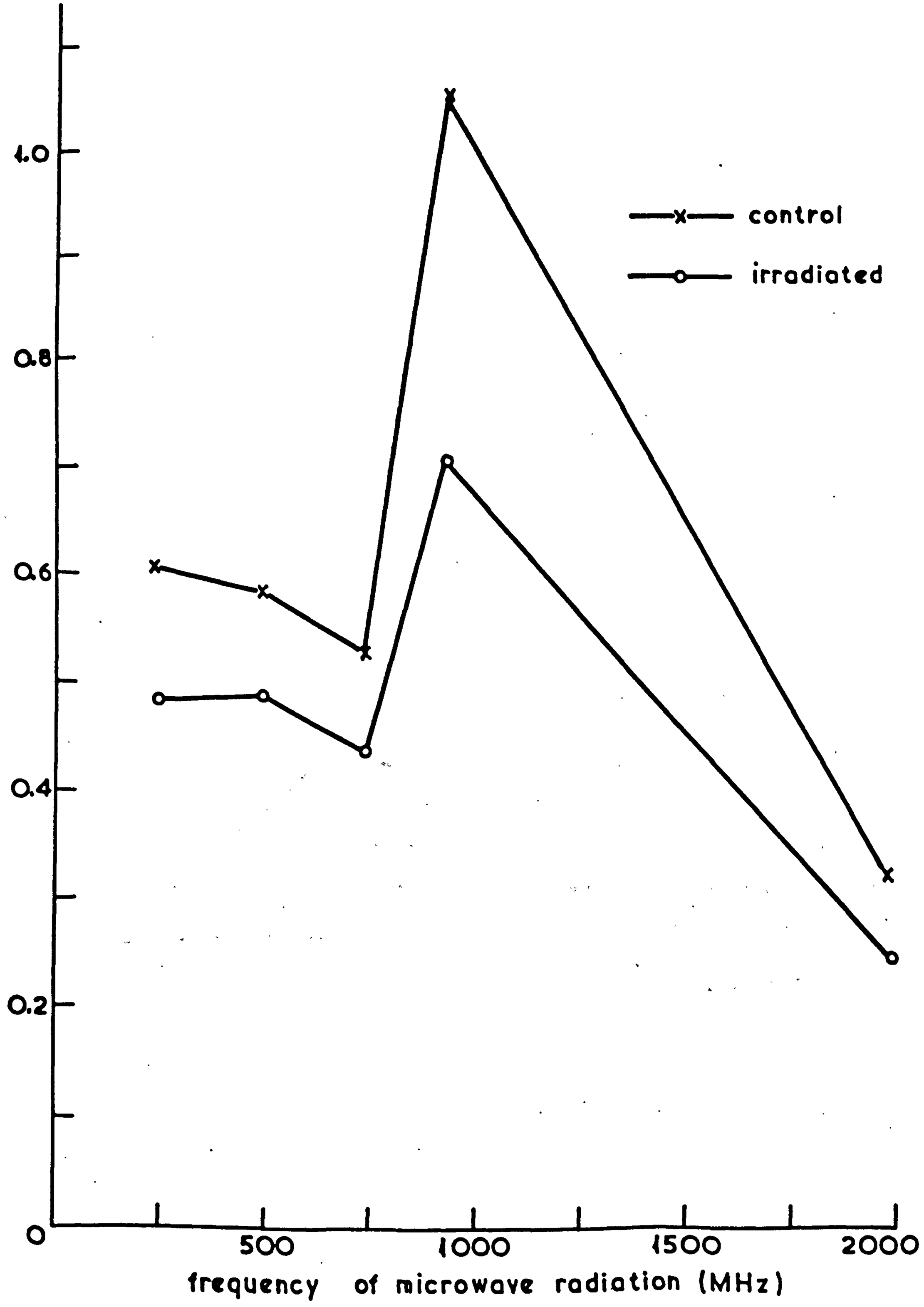

Fig. 10.44
A comparison of the % changes in $[Na^+]$ and $[K^+]$ under differing NMR conditions and frequency of microwave irradiation.

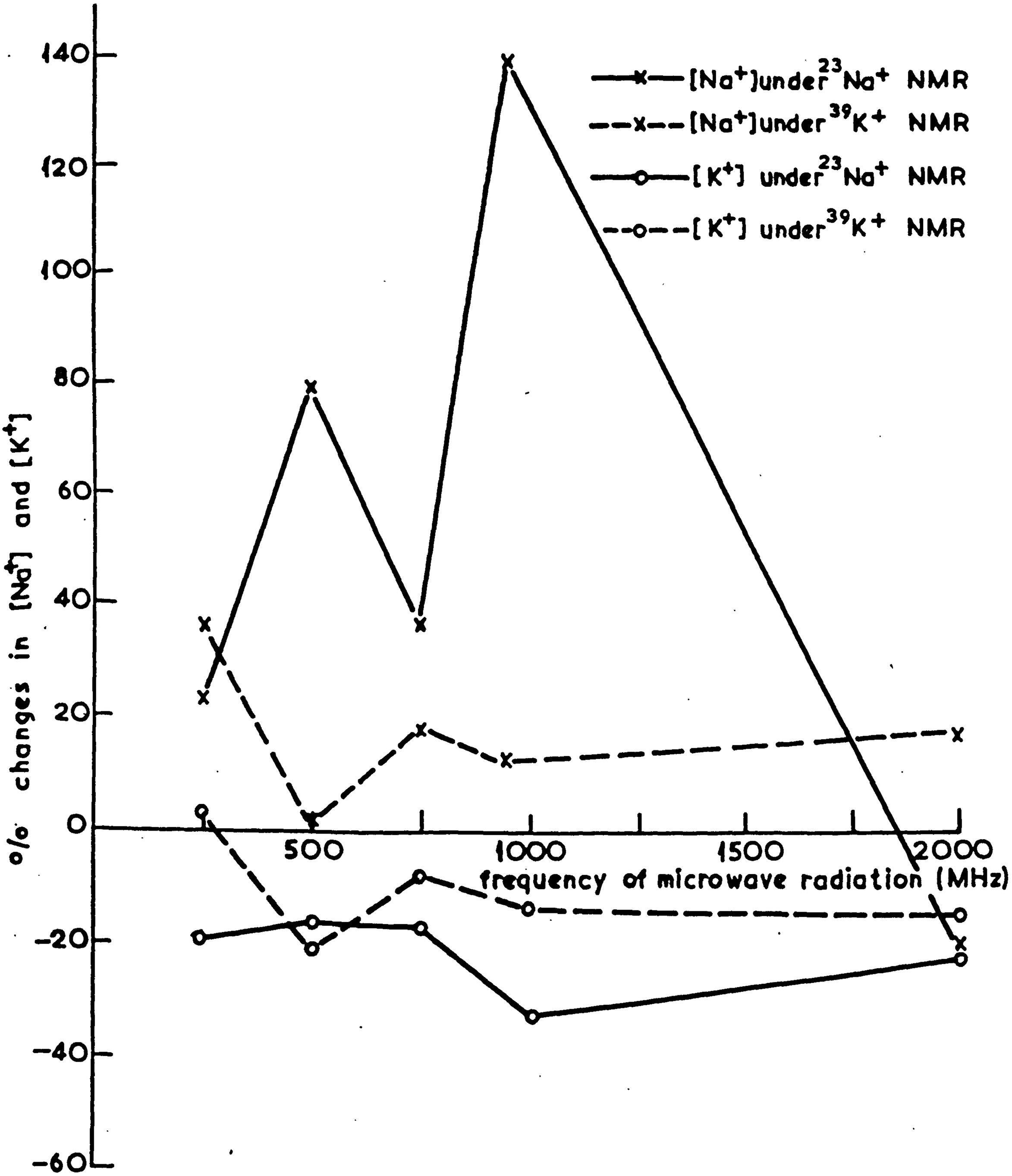

from the results recorded from these experiments, it must be concluded that the frequency of the microwave radiation has no easily-distinguishable effect on the weight increase or Na^+ and K^+ concentrations of lenses.

Figure 10.45 shows measurements comparing the dielectric properties in a geomagnetic field of actively metabolising lens tissue and lens whose metabolism had been disrupted by ouabain. The actively metabolising lens did show the anomalies of the above magnetic isotopes in the dielectric loss curve but not in the lens whose metabolism disrupted by ouabain.

Fig. 10.45
Detailed examination of the dielectric loss in the areas of NMR. a) A metabolising Bovine eye lens, b) the same but with a metabolic poison (Ouabain). Laboratory ambient field 0.5G (50μT), temperature 22°C.

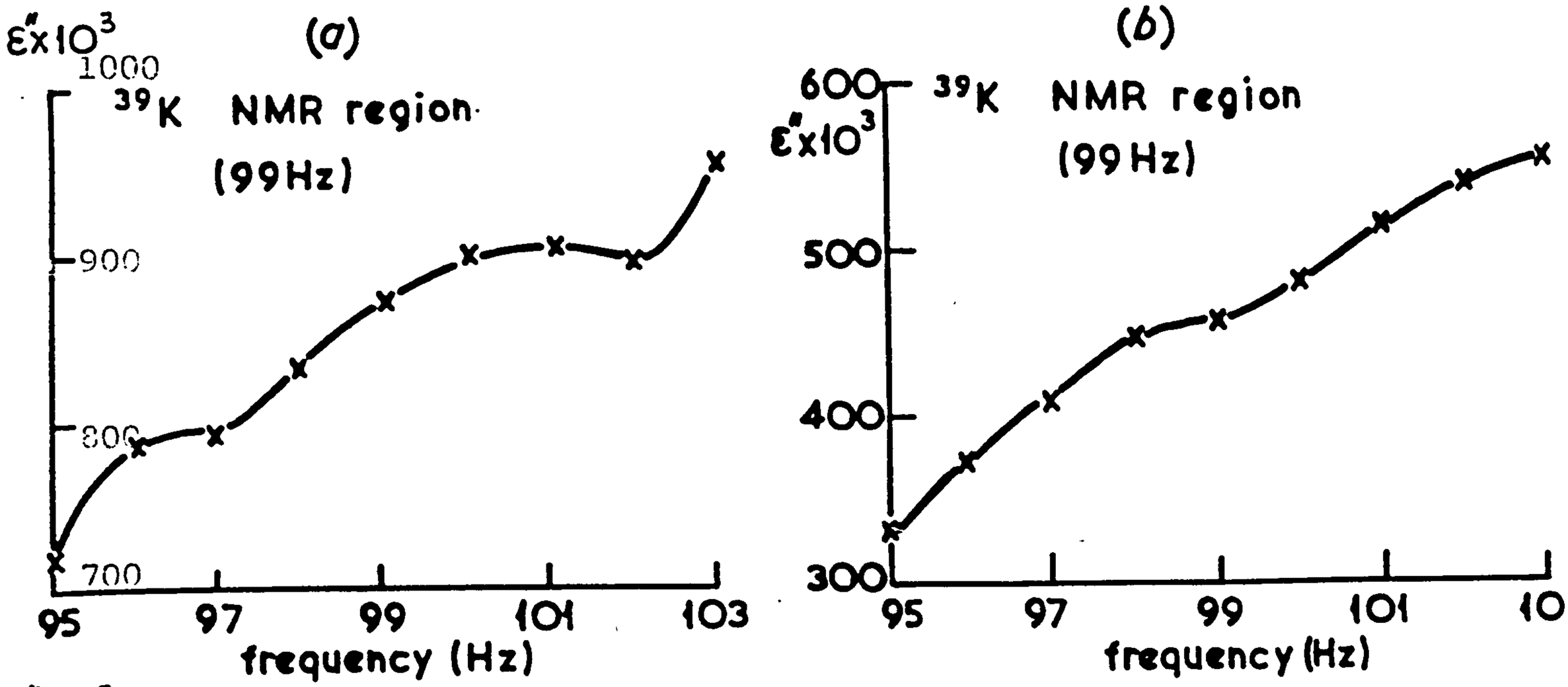

Fig. 10.45 continued

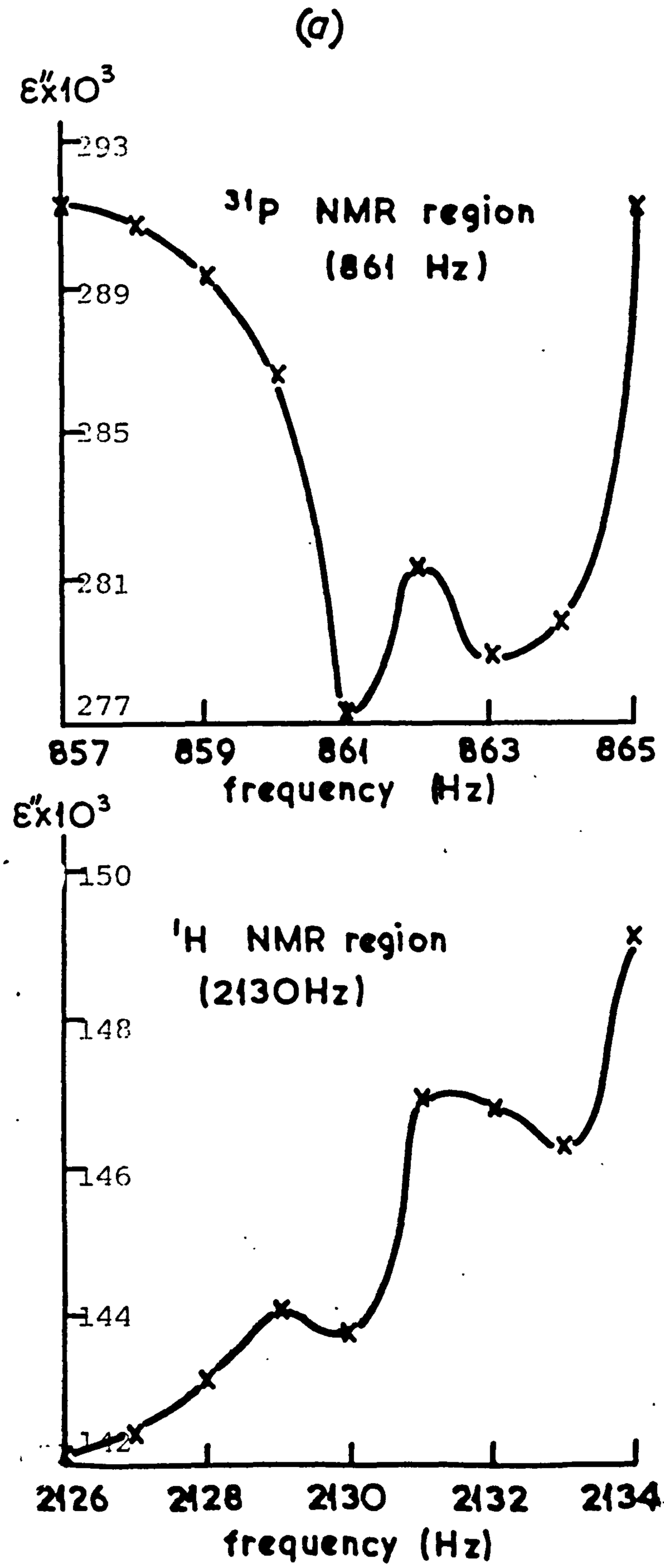

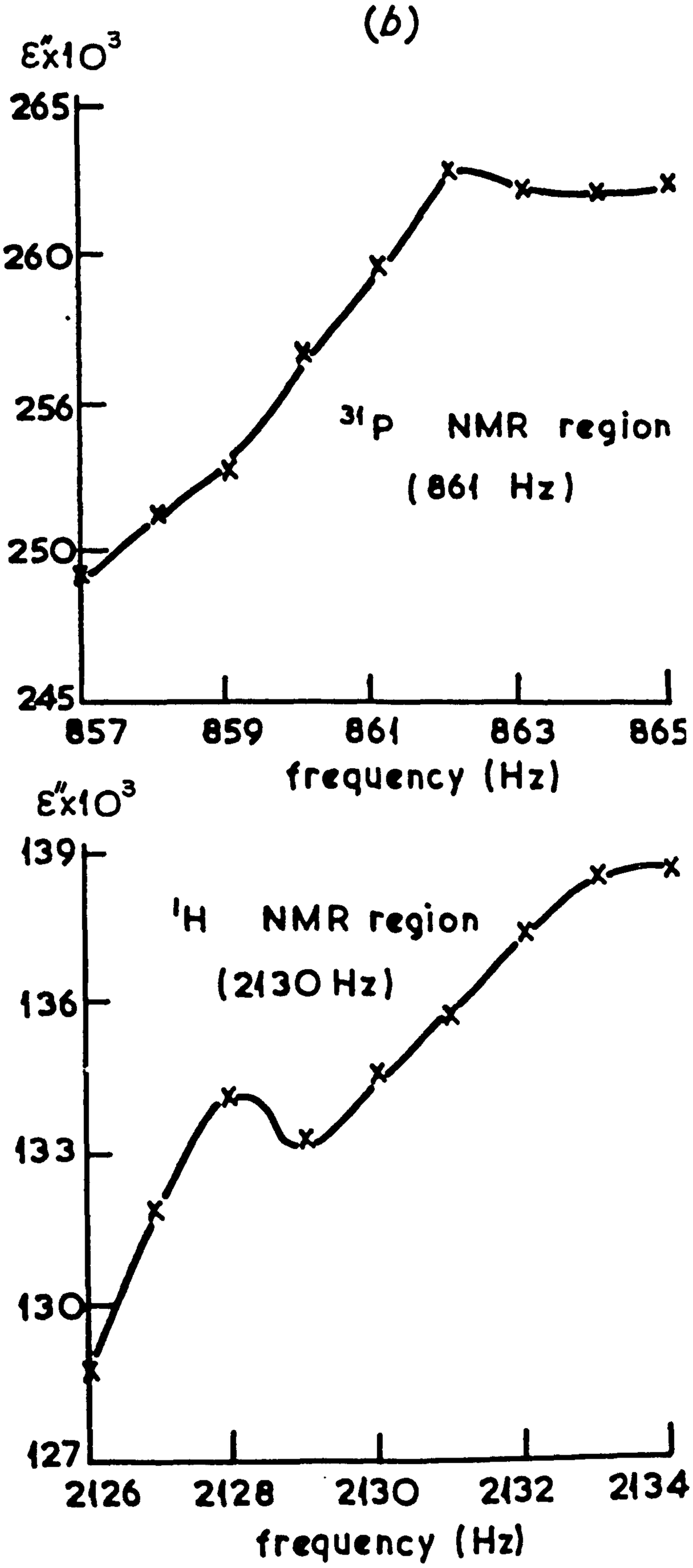

CHAPTER II DISCUSSION OF EXPERIMENTAL RESULTS

The experimental work described in this thesis started with the investigation of a suspected anomaly in the region of 2kHz noted in reported dielectrophoretic measurements. The possibility that it could be due to the NMR phenomenon, due to the interaction of the geomagnetic field was checked first. The experimental procedures and necessary equipment have been described (Chapter 9).

The rapid and simple process of dielectrophoresis when applied to suspension of cells shows that the collection of these bodies at the regions of highest field strength does readily reflect their total differential polarization, differential in the sense of directly comparing the difference between the total polarization of the cell and that of the medium in which it is suspended. This means that, if the neutral cell has a dielectric constant greater than that of the suspending fluid, then it will move to the electrode. If the dielectric constant of the cell is less than that of the fluid, the cell will be attracted less than the surrounding medium, resulting in a repulsive net force given by

$$F = -2\pi a^3 \varepsilon_o \tilde{\varepsilon}_1^* \left(\frac{\varepsilon_2^* - \varepsilon_1^*}{\varepsilon_2^* + 2\varepsilon_1^*}\right) \nabla |E|^2 \qquad (11.1)$$

In a nonuniform field the cell experiences a translational force. This occurs because under the influence of the nonuniform field it aquires a polarization and because the cell is neutral, the two charges on the body are in fact

equal and opposite. The fields operating on the two separated charges are unequal and this gives rise to net force. The result of such a polarization of a neutral high permittivity body in a nonuniform field is to bring about a force attracting the neutral body toward the region of stronger field. The "yield" was selected as the best descriptive dependent variable. It expresses the length of the stacks or chains of cells collected on the electrode in a given time. The experimental variation of the yield has been reported as a function of various physical and biological parameters. It was found to be linear with voltage over much of the range as is predicted from theory chapter 5 (Figure 10.2, page 150). Where the yield is given by:

$$Y = \frac{8\pi c v_1 r_2 a^4}{9\, r_1(r_2-r_1)} \left[\frac{2t\varepsilon_1^*(\varepsilon_2^* - \varepsilon_1^*)}{\eta(\varepsilon_2^* + 2\varepsilon_1^*)} \right]^{1/2} \qquad (11.2)$$

An increase in the voltage causes a stronger field at the electrodes. The dielectrophoretic force on each cell increases and hence more cells will be collected, at either electrode in a given time. Voltages up to 40 Vr.m.s. at frequencies from 100 Hz to 50 kHz were used.

According to equation (11.2) , it is predicted that the number of cells collected would vary directly with the square root of the time ($Y \propto t^{\frac{1}{2}}$). Experimental results were consistent with this up to the time of complete collection of the chamber contents by dielectrophoresis and by settling (Figure 10.4, page 152).

Although the theoretical parameters derived in chapter 5 were found to be consistent with the experimental results, the anomaly in the region of 2kHz remained in the same position irrespective of the variabilities in these parameters, which in turn demonstrates the genuiness of the interaction of the geomagnetic field with the biological cells under study.

Raising the magnetic field from 0.5 gauss to 1 gauss by bringing a permanent magnet near to the test sample, then taking measurements over the range 100 Hz to 50 kHz, and plotting the yield as a function of frequency, showed that the anomaly was no longer in the 2 kHz region but had shifted to 4.26 kHz. The procedure was repeated at various fields up to 5 gauss and it was found that the anomaly shifted in proportion to the steady magnetic field strength (Figure 10.5, page 153). The highest frequency at which 40 Vr.m.s. was available was 50 kHz, and this was the only limit to the maximum steady magnetic field tried. By taking an average of all values of frequency divided by the respective magnetic fields (Hz/gauss) and calculating the average yields, the anomaly appeared at 4.26 kHz (per gauss) which is exactly the proton (^{1}H) NMR condition (figure 10.6, page 154).

The likelihood that these effects are of a quantum nature is assessed by calculating the change in flux linkage through a typical yeast cell in these experiments.

Yeast cells suspended in the nutrient medium were microscopically observed, using an Olympus BHB413Ls phase - contrast microscope. These cells are near spherical, their dimensions are approximately 5 μm diameter. Magnetic flux is quantised in units of $\Phi_o = \frac{h}{2e} = 2.07 \times 10^{-15}$ Wb. The yeast cells are 5 μm in diameter giving an cross-sectional area of 20×10^{-12} m^2, and the corresponding field strength giving a magnetic flux linkage of one magnetic flux quantum per cell ($\Phi_o = B \times A$) is 10^{-4}T (1 gauss) or integer multiples of this. The effects at 0.5 gauss probably corresponded to pairs of yeast cells having twice the above area.

Magnetic flux is always quantised (Fröhlich, private communication). Bloch (1968) has considered the case of a thin super-conducting ring in a magnetic field. The rate of change of magnetic flux is proportional to the induced e.m.f. The units have been chosen so that the proportionality constant is unity. Hence

$$V = \frac{d\Phi}{dt} \qquad (11.3)$$

For a change of the flux Φ through the ring by the flux quantum ($n = \frac{2e\Phi}{h}$) one finds the circulating current I to exhibit a periodic dependence upon Φ. Denoting by τ the duration of a period, the rate of change of the flux is therefore

$$\frac{d\Phi}{dt} = \frac{nh}{2e\tau} \quad ,$$

and with the frequency given by $f = \frac{1}{\tau}$, one obtains from equation (11.3) for the dc voltage

$$V = \frac{nhf}{2e} \qquad (11.4)$$

which is in effect the Josephson relation for a superconductor.

There it can be seen from Figure 10.9, page 158 that for the results with an applied field of frequency 2.13 kHz, the proton NMR frequency in a laboratory ambient magnetic field of 50 μT (0.5 gauss) the onset of these effects appears at a strength of the steady magnetic field such that one quantum of magnetic flux (2.07×10^{-15} Wb) would link the cross-sectional area of a single biological cell or pair of cells, 100 μT or 50μT (1.0 gauss or 0.5 gauss) respectively in the case of 5 μm diameter yeast cells . Thus in this respect biological cells have analogous properties to a superconducting ring which in turn points to the cell membrane as the important entity.

The experiments were repeated on yeast cells which had been killed by exposing the freeze-dried powder to a TUV lamp (254 nm) overnight this inflicts damage to the membrane and the nucleus. The nucleus appeared granular as observed with a phase contrast microscope, and resulted in the cells being unable to reproduce themselves. The killed cells did not reflect any anomaly or peaks in the regions important to

the polarization (that is Maxwell-Wagner type interfacial bulk polarization mechanism) as for live ones, although they were less collected dielectrophoretically by the electrodes and the yield increased as a function of the applied voltage (Figure 10.3, page 151) . The absence of the peaks in their measured spectrum is due to the destruction of heterogeneous regions within the membrane giving rise to a Maxwell-Wagner type interfacial bulk polarization mechanism. However, the absence of the anomaly is due to the disruption of the active transport across the membrane by the killing process.

The anomalies have been found both in dielectrophoresis and dielectric loss for the Larmor precessions of ^{1}H, ^{31}P, ^{23}Na, ^{35}Cl, ^{39}K (Figure 10.10, page 159) given by

$$\omega = \gamma B_o \qquad (11.5)$$

Peaks in the dielectric loss curves were also observed by field conditions satisfying the electron spin resonance conditions (Figure 10.17, page 167) namely,

$$\nu/B_o = \frac{2\mu e}{h} = 2.8 \times 10^6 \text{ (Hz per gauss)} \qquad (11.6)$$

Live yeast cells killed at 121^{o}C in a pressure cooker did not show any signs of these anomalies in the dielectric loss curve (Figure 10.11, page 161) and the difference between the live cell and dead cell measurements were found to be large. No dispersion region occurred (Chapter 4) in the

ε' and ε'' curves or the general decrease in the dielectric loss. The absence of dispersion region caused by the non-existence of the dipole mpment in the case of dead cells. Because the permittivity of the substance is directly related to the dipole moment of its constituent molecules (see section 4.2), given by

$$\mu = 4\pi R^3 \varepsilon_o' \varepsilon_1' \frac{(\varepsilon_2' - \varepsilon_1')}{(\varepsilon_2' + \varepsilon_1')} E \qquad (11.7)$$

and its polarizability α therefore is

$$\alpha = \frac{3\varepsilon_o \varepsilon_1' (\varepsilon_2' - \varepsilon_1')}{(\varepsilon_2' + 2\varepsilon_1')} \qquad (11.8)$$

However, the measured permittivity and dielectric loss are due to the protons that have been dissociated from protein molecules for example. Such charges accumulate at the cell-medium interface and give rise to what appears to the experiment to be polarizability of the cell. It is seen as a measured dielectric constant characteristics of the suspension . Little loss (other than the dc loss component) occurs. On the other hand the absence of the anomalies in the killed cell measurements are due to the cell membranes may be made leaky by the process of killing them, thus the conductivity of the cell contents became same as that of the suspending medium. This would be the result of the cessation of active transport or ions diffusion through metabolic activity which in turn altering of the membrane polarizability. However,

the killed cell cross-sectional area is very much less than that of the live cell. Direct phase contrast microscope measurements confirm that the diameter of killed cell is reduced by autoclaving to a half, 2.5 μm, the live cell value. The flux quantum criterion would then preclude effect in the case of autoclaved yeast cells. However, no effect was observed at higher magnetic fields.

The magnitudes of the anomalies in Figure 10.10 page were found to be temperature dependent (Figures 10.12, 10.13, 10.14, pages 162, 163, 164.)
At a temperature of 4°C the cell is in a dormant or in the resting state, the activity of the cell in this state is extremely low; however, as the temperature is increased to 17°C the cell becomes slightly more active. As the temperature is further raised to 30°C the cell becomes extremely active the permittivity and dielectric loss both show a maximum at 30°C (Figure 10.16, page 166). This temperature which also corresponds with the temperature giving the maximum MGT of the yeast cell. The maximizing of the MGT and an increase in the dielectric properties of the cell is due to the presence of most of the magnetic isotopes at this temperature. As the temperature increased to 35°C most of these effects disappeared and both the MGT and the dielectric properties of the cell mostly returned to their original value. Presumably in such a case the effect of the temperature on the membrane permeability mechanism gave rise to the extensive chain of events that were observed in the most manifestations of metabolic activity. It

becomes clear in such a case that the direct effect of the temperature on the membrane permeability had caused a change in its functional-dynamic indices. On the other hand an increase in temperature causes an increase in the thermal motion, reducing the alignment of the permanent dipoles and hence reducing the orientational polarization. For this reason the dielectric properties of the cells decreases with rising temperature.

When the cell was grown under proton NMR conditions the MGT showed a slight shift from that for cell grown in the earth's magnetic field (Figure 10.15, page 165). The decrease in MGT for cell grown under proton NMR conditions caused by the energy fed in the membrane of the cell and this put the cell in an excited state where the chemical reaction rates are different. Since DNA replication is the only limiting factor for cell division to occur, these results suggest that NMR ^{1}H conditions speed up DNA replication in the cell, which in turn implies that the test cell was ready to divide at an earlier stage in the cell cycle compared with the cell at ambient field only (control).

Steps in the voltage-current characteristic (Figures 10.18, 10.19, 10.20, 10.21, 10.22, pages 170 - 176) and oscillation from dividing yeast cells (Figures 10.26, 10.27, 10.28, 10.29, 10.30, 10.31, 10.32, 10.33, pages 179 - 186) of a pearl-chain of yeast cells were found to occur for a few minutes around the time of cytokinesis as they were observed under phase contrast microscope. This indicates that the electrical control of activities represents another important

biological phenomenon. Membranes of biological systems usually have a thickness of about 10 nm across which an electrical potential difference of the order of 100 mV is maintained . This enormous field of about 10^7 V/m acts upon the membrane and its surroundings, which are therefore strongly polarized. This has long been recognized to play a role in nerve conduction. This could also play a role in cell reproduction. For the present purpose it may be pointed out that a section of the membrane oscillating with its displacements normal to the surface can represent an electric wave with a half wavelength ($\lambda/2$) equivalent to the thickness of the membrane (see section 3.1.1) and comprising an oscillating dipole. In such materials the elastic properties fix a velocity of sound V of the order of 1000 m/sec , indicating a frequency f of $f = \frac{V}{\lambda} \sim 1000 \times 10^8 \text{ sec}^{-1} = 10^{11}$ Hz. A typical membrane resting resistance for sodium and potassium are 150 kΩ and 1 kΩ respectively (Strong, 1973) This gives electrical vibrations with frequencies of the order of 10^{11} to 10^{12} (a typical membrane capacitance is 10^{-15}F indicating a frequency f of $f \simeq \frac{1}{CR}$) respectively. These electrical vibrations may be excited coherently and could cause sharp resonances in active biological membranes through chemical (metablic) processes when they are active and synchronised. Excitation of this type could have far-reaching consequences in biological systems, for they would lead to selective long-range interactions such as required to control growth. Control of chemical activity is, of course, in

many cases well understood in terms of relevant enzymes, which through their catalytic action regulate most biological chemical processes. Enzymes are proteins - they consist of a linear string of amino acids - which in globular proteins are folded in a very definite way. This structure of many enzymes has now been analyzed. They all contain an active group at which the respective chemical reaction can take place. This chemical reaction occurs only when the enzyme is in an activated state in the right place and at the right time. Clearly then it must be expected that particular physical properties within a cell will be dependent on the state or stage of growth. From the point of view of physics the processes are involved in nontrivial nonlinear effects that change with time and are maintained through constant energy supply. Measuring overall properties might thus yield a small effect, when in fact cells are active and synchronised, such an effect might be large but effective only during certain periods. In this manner a series of temporal changes could be programmed in a cell. For instance the possibility of switching on or off the collective oscillating mode through cellular metabolic processes might promote changes in the configuration of larger regions such as required in cell division.

The experimental observations made on bovine eye lenses indicated that microwave irradiation did not have any definite effect on the weight increase of lenses (Figure 10.35, page 190). There was no appreciable and consistent difference between the weight of the control and the weight of the irradiated lenses, whatever the period of irradiation. This suggests that the operation of the sodium pump is not

disturbed by the irradiation, and hence cellular water content remained unchanged. As described in section 3.1.2, heat can cause extrusion of excess sodium and removal of some water content of the lens. There was no consistent difference between the Na^+ concentration of control and irradiated lenses (Figure 10.36, page 192), though there was a difference in K^+ concentration (Figure 10.37, page 193). Though the period of irradiation does not seem to have any bearing on the K^+ concentration, it is noticeable that all the irradiated lenses showed a greater K^+ concentration than their controls . This suggests that the heating effect of the irradiation resulted in the recovery of the lost potassium or the take up of fresh potassium.

Under either ^{23}Na or ^{39}K NMR conditions there was no appreciable effect on the weight increase of lenses (Figures 10.38 and 10.39, pages 194 & 195). However, the application of NMR conditions does seem to have had some effect on the Na^+ and K^+ concentrations of lenses. Under NMR conditions for Na^+ and between frequencies of 500 MHz and 960 MHz, the irradiated lenses showed a considerably higher Na^+ content than the control lenses (Figure 10.40, page 196). The only anomaly in these observations occurred with the single lens irradiated at 2 GHz, a further investigation is needed in this region. Under NMR conditions for K^+, the Na^+ concentration of irradiated lenses was still higher than that of the controls

(Figure 10.41, page 197), but there was not nearly so much difference between the irradiated lenses and the controls as there was under Na^+ NMR conditions. This suggests that Na^+ NMR conditions facilitate the uptake of Na^+ ions by the lens to a greater extent than K^+ NMR conditions. Since a characteristic of cortical cataract formation is an increase in Na^+ NMR in the lens, this result indicates that NMR conditions may unblance the metabolism of the lens by facilitating the entry of Na^+, and hence cause the onset of cataract formation. As well as causing a definite increase in the Na^+ concentration, the application of Na^+ NMR also resulted in a marked decrease in K^+ concentration (Fig. 10.43, page 199). This would be expected, as a consequence of the increased uptake of Na^+ causing the extrusion of K^+ from the lens.

Under K^+ NMR, the much reduced increase in Na^+ concentration already mentioned was accompanied by a reduced decrease in K^+ concentration (Figure 10.42 page 198). Hence, K^+ NMR, has done so to a lesser extent than Na^+ NMR, and consequently has not caused the same degree of disruption to the metabolism of the lens. Finally the results of these experiments, showed consistently that the frequencies of the unmodulated microwave radiation used had no discernable effect on the weight increase or Na^+ concentration of lenses; only the modulation was effective, the microwaves merely providing the penetrating with transport of energy, with demodulation occurs with disipation of energy at the frequency

of modulation.

Measurements comparing the dielectric properties in a geomagnetic field of actively metabolising lens tissue and a lens whose metabolism had been disrupted by ouabain was investigated. The actively metabolising lens did show the anomalies of the above magnetic isotopes in the dielectric loss curve, however, the lens whose metablism was disrupted by ouabain did not show the anomalies in the NMR regions (Figure 45, page 202).

In connection with this inhibitor Kinsey and McGrady (1971) found that ouabain caused a relatively rapid fall in the anterior face potential in the rabbit lens from -40 to -20 mV , this was followed by a much slower change back towards zero. In the case of the toad eye lens, when ouabain was in contact with the anterior face Bentley and Candia (1971) found a similar decrease in the short-circuit current as measured by short circuiting the anterior and posterior lens faces; in contrast there was a negligible effect on the posterior face.From the above observations it can be concluded that ouabain caused a decrease in the ionic permeability of the magnetic isotopes across the membrane.

CHAPTER 12 CONCLUSION

Dielectrophoresis, the motion of an electrically neutral cell induced by a non-uniform electric field was found to be a useful technique for studying the interaction of electric and magnetic fields with the yeast cell suspended in liquid medium. The force and yield equations have been developed in Chapter 5. The force depends directly upon the first power of the volume and polarizability of the cell, but upon the square of the electric field intensity $|E|^2$. The latter emphasizes that dielectrophoresis is independent of the sign of the field direction. It can occur in an a.c. field.

The force and yield equations are general ones, capable of including frequency - dependent conduction or polarization mechanisms. The rate of dielectrophoretic collection by a point electrode is called the "yield". It was found to be strongly dependent upon the physiological state of the cell, the frequency of the applied a.c. electric field, the voltage , square root of the collection time and conductivity of the suspending medium. This confirmed the theoretical equations developed in Chapter 5. The resulting yield spectrum is complicated. In view of the frequency and conductivity effects observed with live cells, simple dielectric theory based on consideration only of static permittivity constants as for perfect insulators proved to be inadequate.

Although the experimental variation of the yield was found to be linear with voltage over much of the range (Figure 10.2, page 150) and directly proportional with the square root of time (Figure 10.4, page 152) as was predicted from theory chapter 5, the unexplained deviation in the region of 2kHz also seen in other workers dielectrophoretic yield results remained in the same position and showed magnetic and frequency dependence which satisfied NMR conditions, irrespective of variations in these parameters. This experimental result demonstrated the genuiness of the interaction of the geomagnetic field with the biological cell under study.

The procedure was repeated up to 5 gauss and it was found that the anomaly was shifting in proportions with the steady magnetic field strength (Figure 10.1, 10.5, pages 148 & 153). By taking an average of all values of frequency divided by the respective magnetic fields (^{Hz}/gauss) and calculating the average yeilds, the anomaly appeared at 4.26 kHz per gauss which is exactly the proton (^{1}H) NMR condition (Figure 10.6, page 154). The clear evidence that there is a threshold value of magnetic field strength below which no effect occurs, and the very sharp transition occurring at this point, suggest the possible existence of some quantum effect. The proton NMR frequency is 2.13 kHz in a laboratory ambient magnetic field of 50 μT (0.5 gauss). The onset of these effects appears with the strength of the steady magnetic field, such that one quantum of magnetic flux (2.07×10^{-15} Wb) would link the cross-sectional area of a single biological cell or pairs of cells, 100 μT or 50 μT

(1.0 gauss or 0.5 gauss) respectively in the case of 5 μm diameter yeast cell.

The magnetic isotopes ^{1}H, ^{31}P, ^{23}Na, ^{35}Cl and ^{39}K showed resonance features in the course of dielectrophoretic and dielectric measurements (Figure 10.10, page 159) as well as dielectric measurements on the bovine eye lens (Figure 10.45, page 202). These magnetic resonances were found to be absent on the killed yeast cell (Figures 10.3, 10.11, pages 161) and by the disturbing of the metabolism of the lens by ouabain. Modulating microwave frequencies in the range of 250 MHz to 2GHz with frequencies satisfying magnetic resonance conditions for ^{23}Na and ^{37}K showed an increase in the Na^+ content of the lens (Figure 10.40, page 196) and a decrease for K^+ content (Figure 10.42 page 198). The microwave irradiation by its own had no easily-discernible effect on the weight increase (Figure 10.35, page 190), or Na^+ concentration (Figure 10.36 page 192), however, had some effect on the K^+ concentration (Figure 10.37, page 193) indicated a possible effect of microwave irradiation.

The magnetic isotopes observed in Figure 10.10, page 159 , showed temperature dependence, such that as the temperature increased the presence of these isotopes became more evident (Figures 10.12, 10.13, 10.14, pages 162, 163, 164.)

The optimum temperature was found to be $30^{o}C$ which also corresponds with the temperature giving the maximum MGT of the yeast cell. At this temperature most of the magnetic isotopes showed their presence and the permittivity and loss curves showed a maximum (Figure 10.16, page 166). As the temperature was increased further, most of the magnetic isotope peaks disappeared and MGT and dielectric properties

returned to their original value.

Growing the cell in the ambient geomagnetic field and an applied alternating magnetic field of frequency such as to satisfy proton NMR conditions, the MGT changed by 25% Fig.10.15 Page 165 However, growing the cell under NMR conditions for other isotopes ^{39}K, ^{35}Cl, ^{23}Na, ^{31}P, the MGT showed only negligible shift from the ambient MGT by 3%.

Peaks in the dielectric loss curves were also obtained by satisfying the electron spin resonance conditions (ESR) (Figure 10.17,page 167).

Steps in the voltage current characteristic (Figures 10.18, 10.19, 10.20, 10.21, 10.22, pages 170 - 176) and a radio frequency emission at a level of 0.1 μV from a pearl-chain of yeast cells (Figures 10.26, 10.27, 10.28, 10.29, 10.30, 10.31, 10.32, 10.33, pages 179 - 186) were found to occur for a few minutes around the time of cytokinesis as observed under phase contrast microscopy. The cells were prepared for synchronous division and were collected between the electrodes by dielectrophoresis, it seemed to be essential to use an electrode at one micron or less. This is smaller than the cell diameter so that the cells collected in an annular manner around the gap mounted on a microscope slide. Steps and an emission were observed about 3 to 4 hours later at ambient temperature. The MGT is 4 hours. Shaya and Smith (1977) had observed the effects of similar frequencies by measuring the change in reaction rate resulting from produced subjecting partially inhibited lysozyme solution for 2h to the range of frequencies from 10 kHz to 1 GHz.

However, a slight shift in the peak position due to the difference in diameters of the yeast cell and MicrococcusLysodeikticus namely, 5 and 2.26 microns respectively (Figure 10.34, page 187) is to be expected.

Finally, all these effects were only observed on the live biological materials used in these experiments and not with dead cells under the conditions otherwise same in all aspects.

APPENDIX 13.1 MICROBIOLOGICAL TECHNIQUE

13.1.1 Concept of sterility and aseptic technique

Sterility results from the removal of all living microorganisms from an object by e.g. heating to red-heat, ultra-violet light, ionizing radiation, autoclave etc.

Objects remain sterile only so long as they remain uncontaminated. Aseptic technique is the method of working such that objects once sterilised (e.g. transfer loop (24 s.w.g. nichrome wire) used for the inoculations) are not contaminated by contact with unsterile objects or surfaces. Contamination results from, example, prolonged exposure to air, particularly if all dusty, contact with laboratory benches, skin, hair or clothing surfaces are likely coated with an unseen army of potentially contaminating microbes. Maintenance of sterility means, therefore, avoidance of contact . A further aim of aseptic technique is to avoid contaminating the experimenter and the environment with the culture that he is using.

13.1.1.1 Methods of achieving sterilisation

In studies of microorganisms it is necessary not only to grow organisms, but also to destroy them, or to inhibit the growth of some whilst promoting the growth of others. For the work described in this thesis sterility is achieved in the following ways:-

(a) TUV Cabinet

This cabinet used for sterilising pipettes and test cells used in experimental measurements. In this cabinet ultra-violet light used as a sterilising agent, producing peroxides in the medium, which in turn act as oxidizing agents. The most highly germicidal rays are those having wave length of the order of 254 nm. Ultra-violet light as a sterilising agent is limited, however, as its penetrating powers are low, it will only travel in an optical path and glass and water especially if containing suspended matter is able to filter off much of the incident radiation.

(b) Autoclave (Pressure Cooker)

This is used to sterilise the culture media and all equipment such as glassware that will withstand the high temperature ($\sim 121^{o}C$) . It is found extremely useful as large quantities of materials can be sterilised at one time. With this type of sterilisation steam at a pressure of 15 lb/sq.in. above atmosphoric pressure is at a temperature of $121^{o}C$ which is efficient to kill cells and spores within 15 minutes. Heat from steam is very penetrating as it will give up its latent heat of vaporisation on meeting a colder object, thereby rapidly raising its temperature. The sterilising procedure is carried out as follows:-

(1) Put some water in the pressure cooker sufficient just to cover its base by 1 inch.

(2) Place the object to be sterilised inside, put its cover on and wait until steam comes out of the head of the cooker.

(3) Place the small head weight in position and wait until a steam appears continuously from the small head weight, at this stage reduce the heating power to just enough to maintain sufficiently flow of steam, then wait for 15 minutes.

(4) After this, remove the pressure cooker from the heater and leave it to cool to ambient temperature (do not try to open the pressure cooker as soon as it is removed from the heating power, this is extremely dangerous due to the high pressure).

(5) Finally remove the object from the cooker and wash the cooker thoroughly so as to avoid growth of foreign organisms especially if the sterilised objects contained any kind of nutrient.

13.1.2 Aseptic transfer of microorganism cultures

Microorganism specimens and cultures may be kept in screw-capped sterilised bottles. The bottles most commonly used are:-

(a) "Bijou", holding about 7 ml.

(b) "Universal", holding about 25 ml.

The most satisfactory way to remove and hold the cap is by firm pressure between the little finger and palm of the right-hand (left-hand if left-handed) , so that the other fingers and thumb are free to manipulate a loop or pipette which can then transfer material to or from the opened bottle. If the cap is too tight, loosen slightly before attempting this.

As on all occasions when microorganism specimens or cultures are exposed to the atmosphere, this procedure should be carried out beside a bunsen flame, so that a current of air is flowing upwards and pass the culture, and particles containing bacterial or fungi are then less likely to fall into the open bottle. Similarly, the breath should be held, so as to avoid contamination of the cultures with droplets from the upper respiratory tract.

13.1.2.1. Sampling and transfer of microorganism cultures

The following procedural steps need to be carried out for sampling and transfer of microorganism cultures:-

(a) Sterilise transfer loop by heating near vertical to red-heat in bunsen flame, so that the whole length of the wire is heated to redness, thus ensuring complete sterilisation of the wire and the chuck of the handle.

(b) Allow the sterilised loop to cool thoroughly (10 sec) on a loop rest.

(c) Remove cap from mouth of the culture bottle and hold it between little finger and palm of the hand and flame its mouth briefly holding it near horizontal without spilling contents.

(d) Insert the sterile portion only of loop into open culture bottle and take up a loopful of sample.

(e) Transfer the loopful of inoculum of the culture sample taken to the microscope slide, petri dish of solid culture medium, fresh bottle of liquid culture medium as appropriate.

(g) Reheat inoculating loop to red-heat to re-sterilise it each time after use.

13.1.3 Culture of microorganism

If the colonial characteristics of an organism are to be examined, the Petri dish is an excellent container for the medium. The shallowness of the dish and the large surface area render macroscopic examination of colonies easy, and, if necessary, microscopic examination is possible.

13.1.3.1 Mapping out on solid media to give isolated colonies

When single cells of microorganisms are isolated on the surface of a nutrient medium solidified with agar and then incubated, all the progeny of a single cell pile up to give macroscopic colonies containing possibly 10^7 organisms. Such colonies are clones of genetically identical individuals (apart from rare spontaneous mutations) and often have a characteristic appearance - size, texture, colour, elevation, margin, etc. Colonial morphology is therefore an important aid in microorganism identification. It should be noted that for microorganisms which characteristically from clumps of cells, or mycelium, colonies will rarely arise from single cells. The maping out techniques is achieved by one of two methods:-

(a) Plate inoculation methods

To isolate single colonies, the medium in the Petri dish should be inoculated as follows:-

(1) Sterilise transfer loop by heating to red-heat. Allow to cool briefly. Take up a loopful of culture (aseptic precautions).

(2) Remove petri dish lid and hold it from top edges by thumb and first finger and keep the part facing the agar downwards.

(3) Gently map out loopful of culture over triangular area about $^{1}/5$ - $^{1}/10$ of agar medium surface (Figure 13.1.1). Care should be taken not to dig up agar surface. It may be found easier if the plate is held at such an angle that light is reflected from the surface of the medium thus enabling to see clearly the areas of the medium that have been inoculated. This inoculated area is called the inoculum well.

(4) Remove petri dish lid. Reflame transfer loop to resterilise.

During the mapping out procedure it is advisable for the transfer loop to be held at angle of 30^{o} degrees to the agar surface as it is shown in Figure 13.1.2 (viewed from side and above respectively). From Figure 13.1.2 (ii) it can be seen that the front edge only of actual loop is in contact with agar surface.

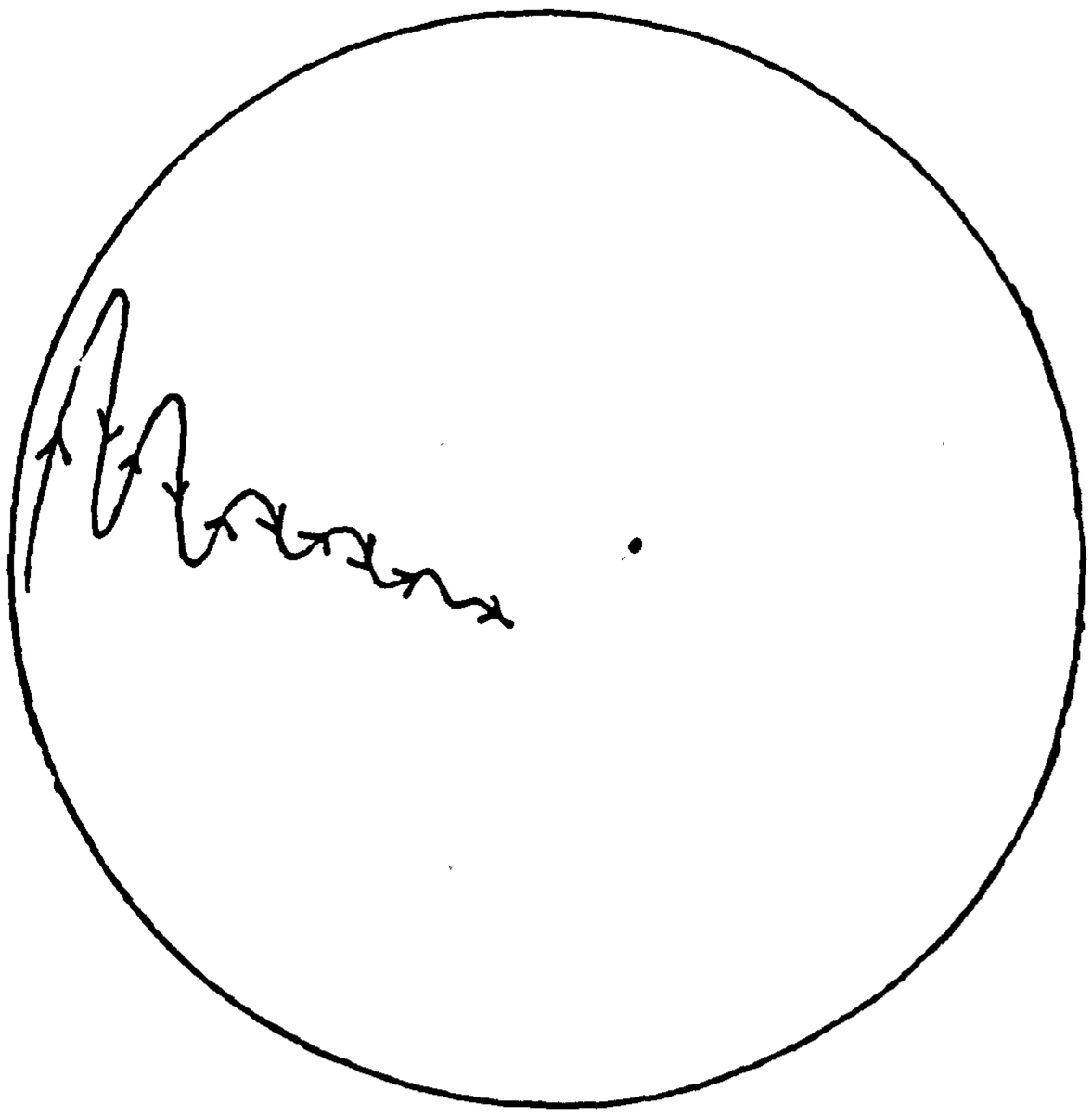

Fig. 13.1.1

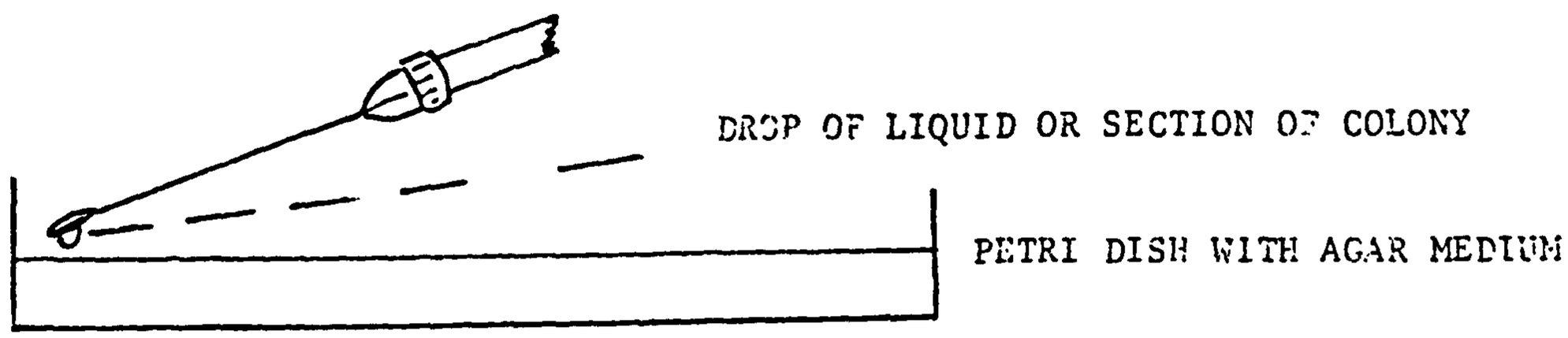

(i)

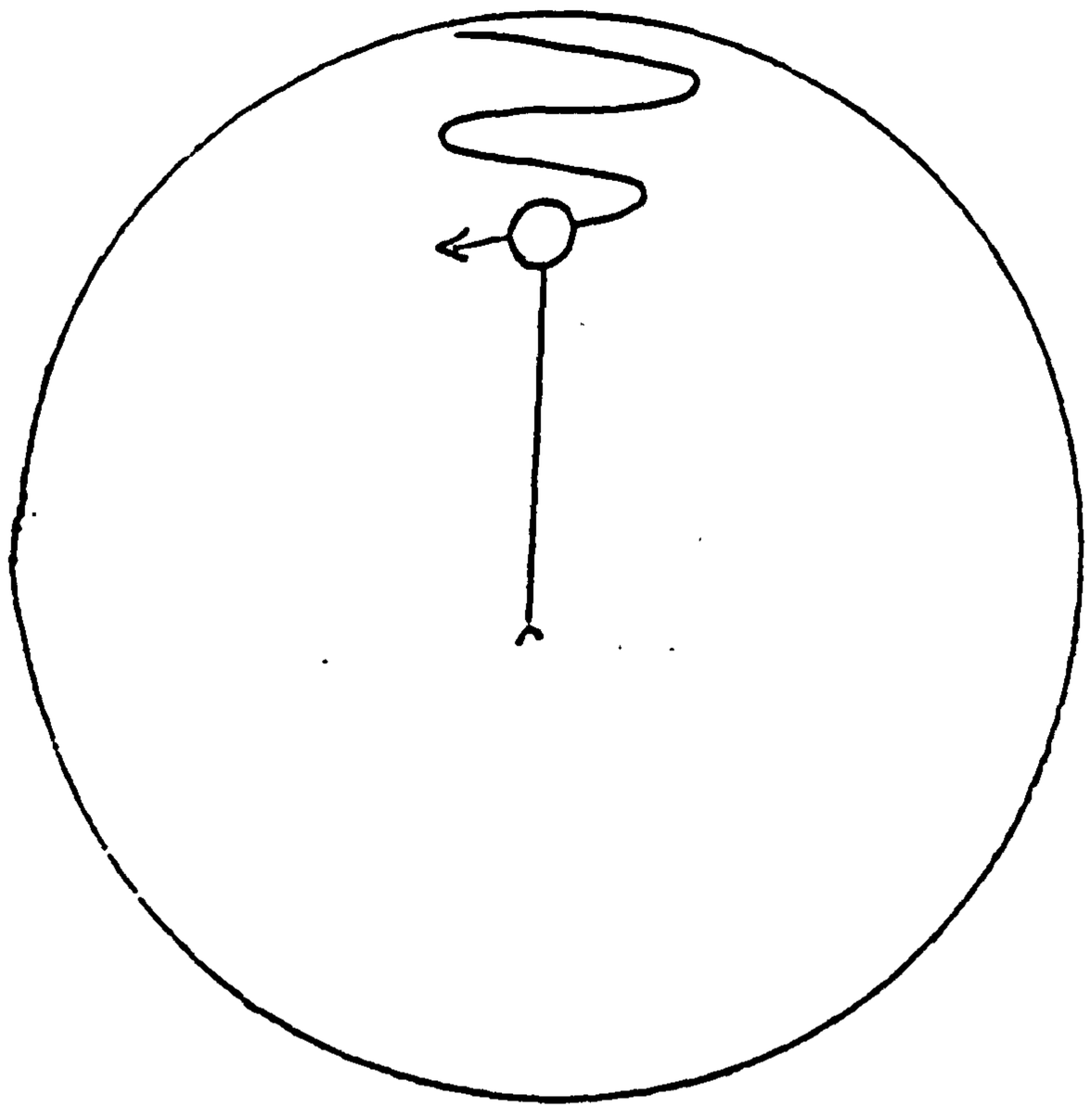

(ii)

Fig. 13.1.2. (i) View from side (ii) View from above.

(5) With transfer loop resterilised, allowed to cool a series of 5-6 parallel lines from the inoculum well out across the agar surface have been made (Figure 13.1.3). These are the primary inoculation lines. Replace the petri dish lid and resterilise the loop. Allow to cool.

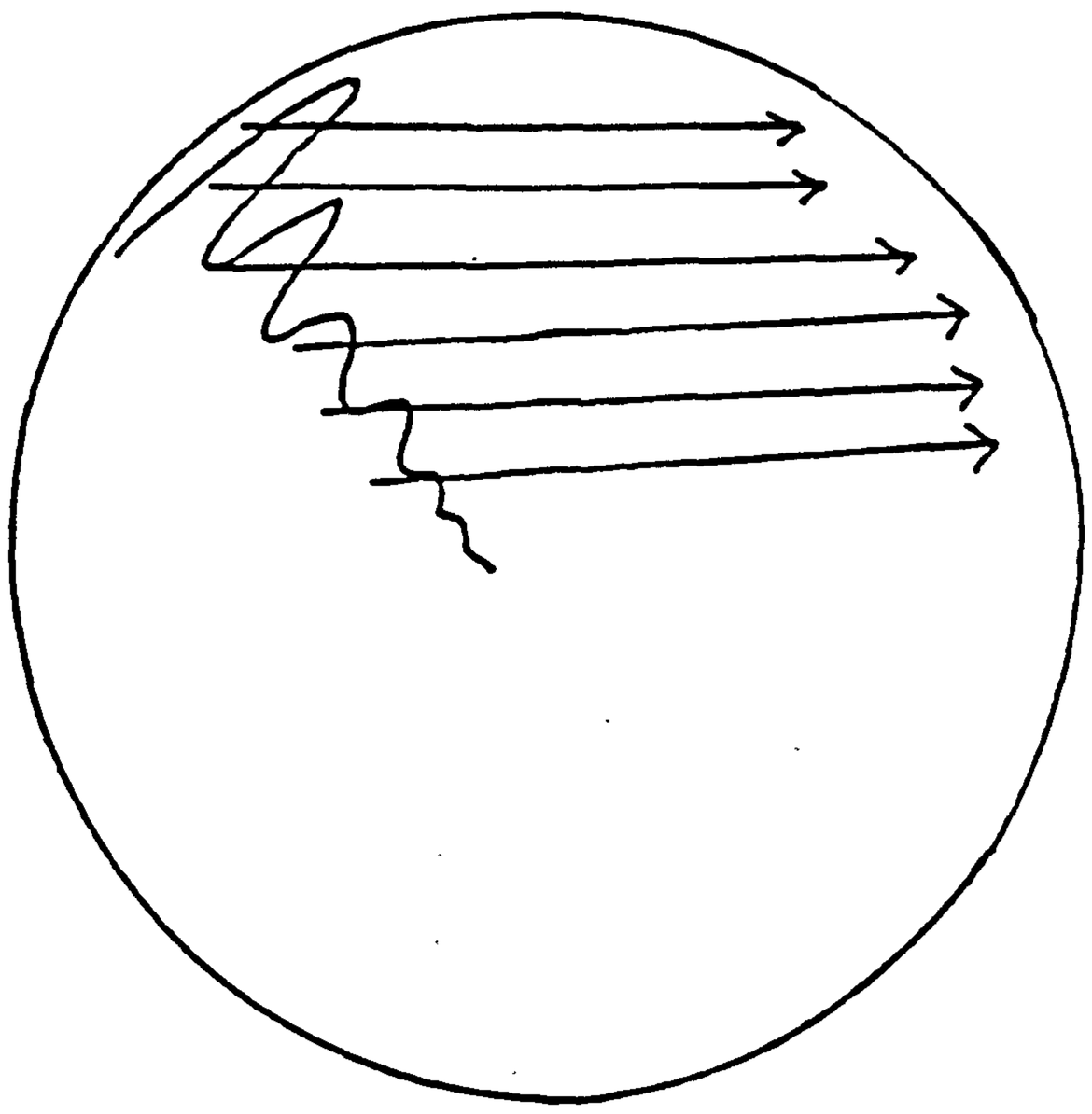

Fig. 13.1.3

(6) A series of secondary inoculation lines at right angles to primary lines are made (Figure 13.1.4). Replace petri dish lid, resterilise transfer loop, allow to cool.

(7) A series of parallel tertiary inoculation lines, avoiding both inoculum well and primary line areas are finally made (Figure 13.1.5) . Replace lid, resterilise loop and incubate at optimum temperature 30°C for example (yeast).

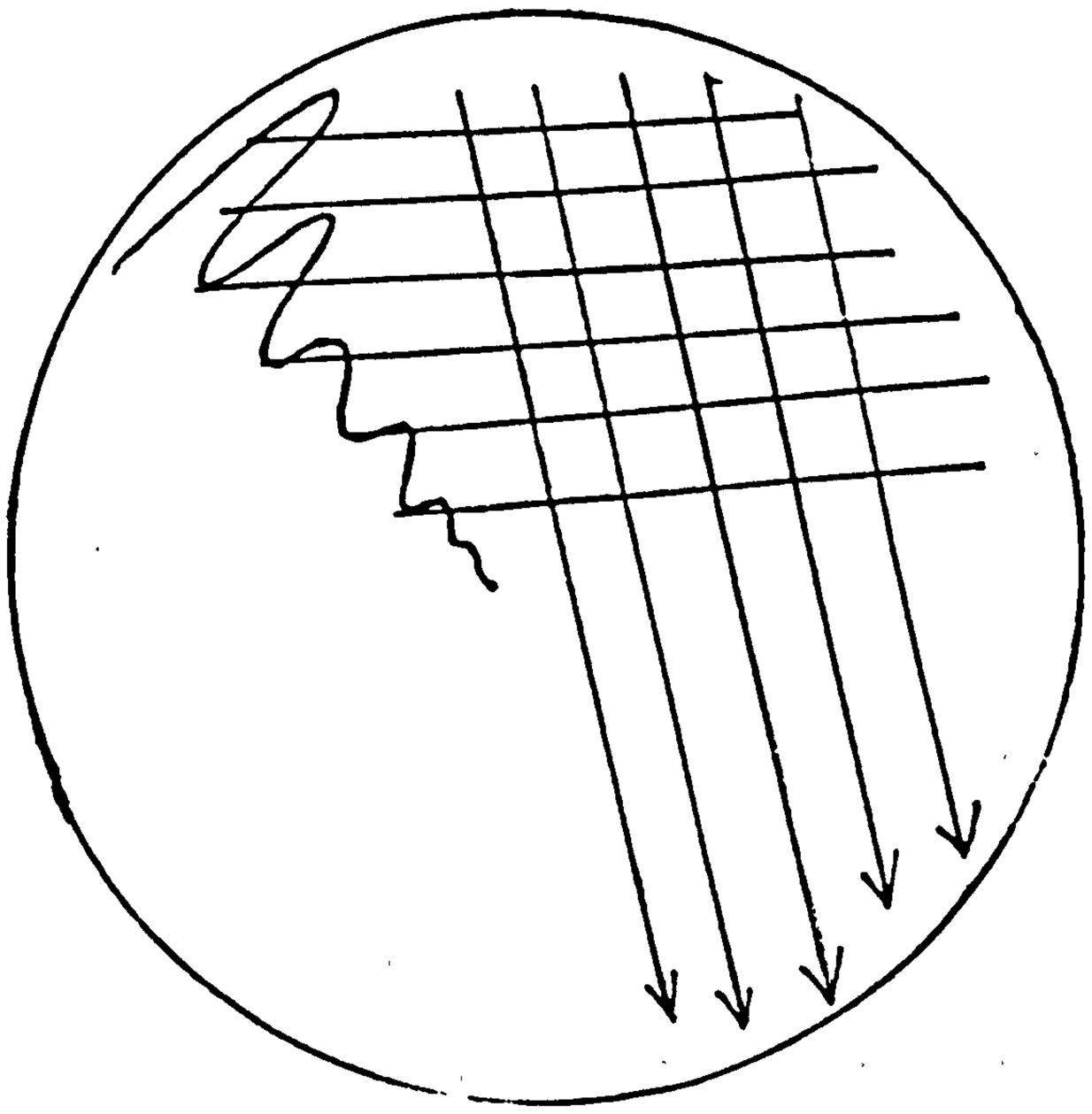

Fig. 13.1.4

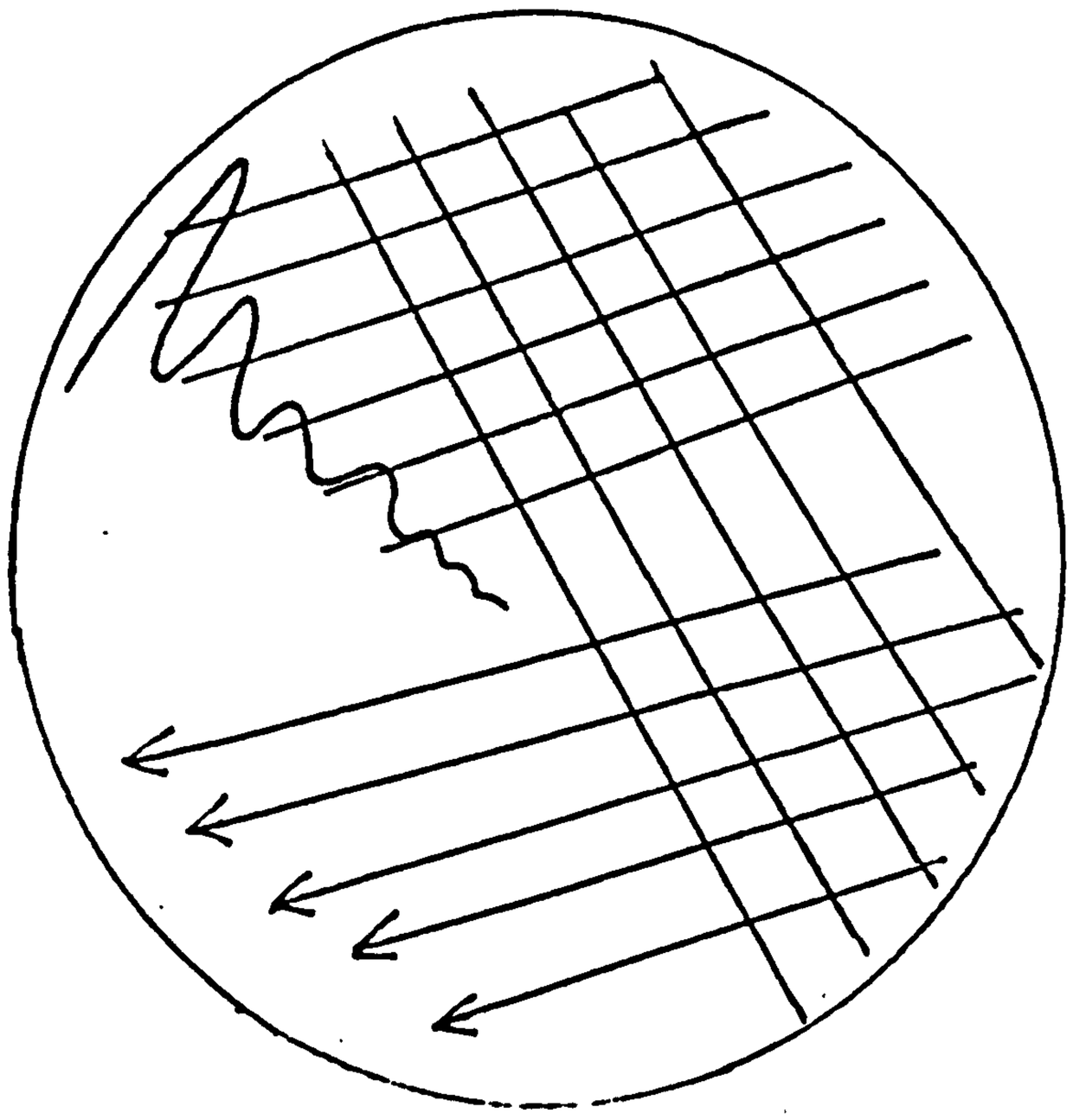

Fig. 13.1.5

(b) Bottle inoculation methods

Although many tests devised to differentiate organisms require a cultures on a solid media. It is not always necessary to grow an organism on a whole petri dish of medium, and slope cultures often suffice. 'Slopes' or 'slants' are bottles containing a small quantity of a gel nutrient medium that has been allowed to solidify with bottles slightly raised at one end as is shown in Figure 13.1.6.

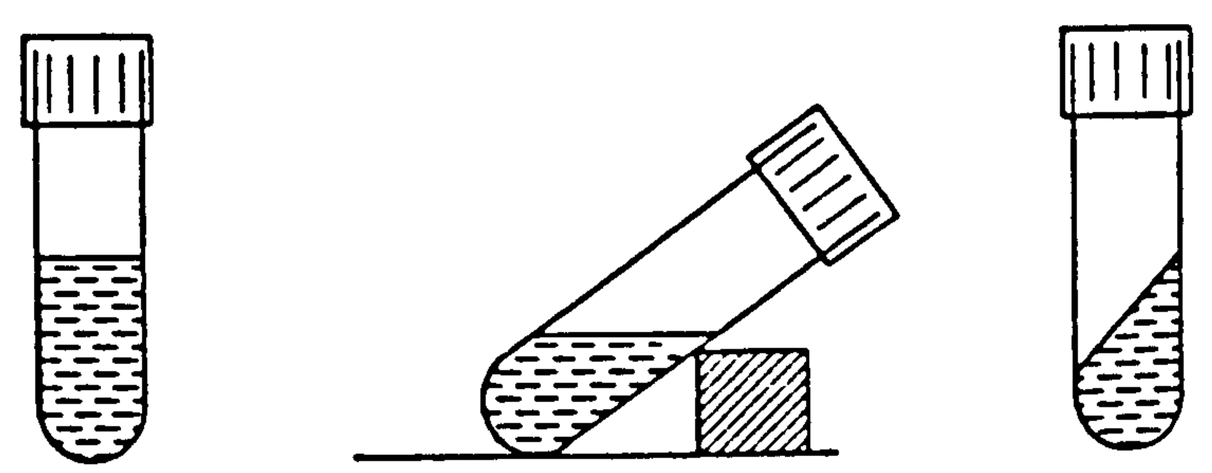

Fig. 13.1.6 Preparation of a slope molten agar medium.

It is essential to keep the medium free from contamination during inoculating procedure, and the following method should be adopted when inoculating one culture bottle from another.

(1) The two bottles are held in the left hand. The culture bottle is held between the thumb and first finger, the bottle to be inoculated between the first and second fingers (Figure 13.1.7). They are held in a near horizontal

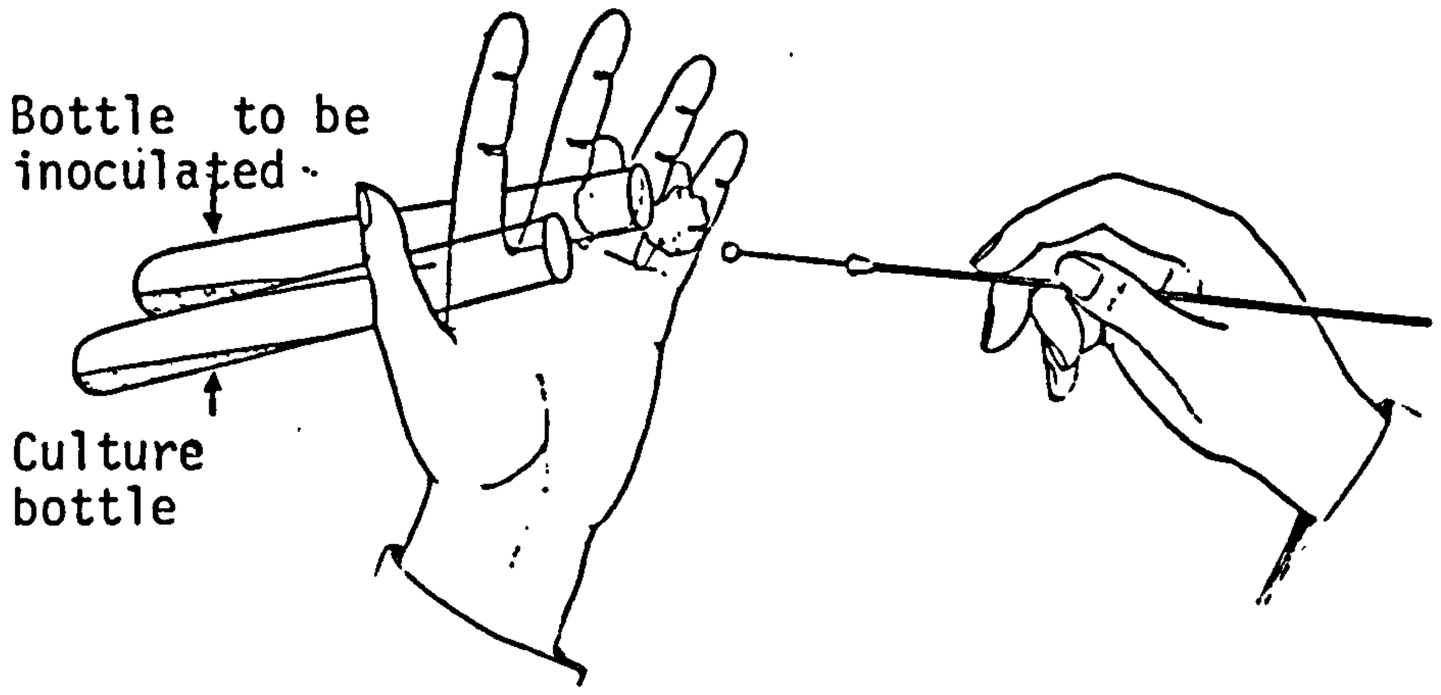

Fig. 13.1.7 Method of holding bottles and caps when inculating one bottle from another

position and close to the bunsen burner.

(2) With the right hand, the cap from the culture bottle is removed and placed between the second and third fingers; the cap from the inoculated tube is then removed and placed between the third and fourth fingers. The protruding end of the cap should be between the fingers.

(3) Using the right hand, flame the mouths of the bottles with the bunsen flame.

(4) Using a sterilised loop scrap a little of the growth from the culture, and line it over the surface of the uninoculated slope, still keeping the slopes in the near horizontal position.

(5) Sterilise the loop, place it on a loop rest, and again flame the mouths of the bottles.

(6) Replace the caps in the right order.

By keeping the bottles horizontal, and bringing the bunsen to them contamination from the air is minimized. In both methods, it is essential that the medium surface is dry so that discrete colonies are obtained.

13.1.4 Serial dilutions and plating technique

When estimates of cell numbers are based upon total cell counts it is obviously hazardous to assume that all the cells in the original inoculum are viable. This is not necessarily the case, particularly if the inoculum is taken from an old culture in which case the total number of cells will mostly far exceed the number of viable ones.

A technique commonly used to estimate the number of living cells in a culture is the dilution plating method.

(a) Serial dilutions of microorganism sample

When diluting liquids, for example, for microorganism count proceed as follows (aseptic technique used throughout):-

(1) Take a 0.1 ml sample of the preparation to be diluted using a sterile pipette. Eject this 0.1 ml sample into a 9.9 ml bottle of sterile dilution medium (this may vary, depending upon the organisms). Mixed thoroughly. This constitutes a 1 in 100 (i.e. 10^{-2}) dilution. Discard the

used pipette into decontaminating fluid.

(2) With a fresh sterile pipette take up a 0.1 ml sample of the 10^{-2} dilution and eject into a further 9.9 ml bottle of diluent. This step constitutes the 10^{-4} dilution.

(3) If an intermediate dilution is required (for example 10^{-3}, 10^{-5}) it is necessary to dilute the next lowest dilution by 10. In this case transfer 1 ml of the 10^{-2} dilution to a 9 ml, dilution bottle this gives 10^{-3} dilution (1 in 1000) etc. (Figure 13.1.8).

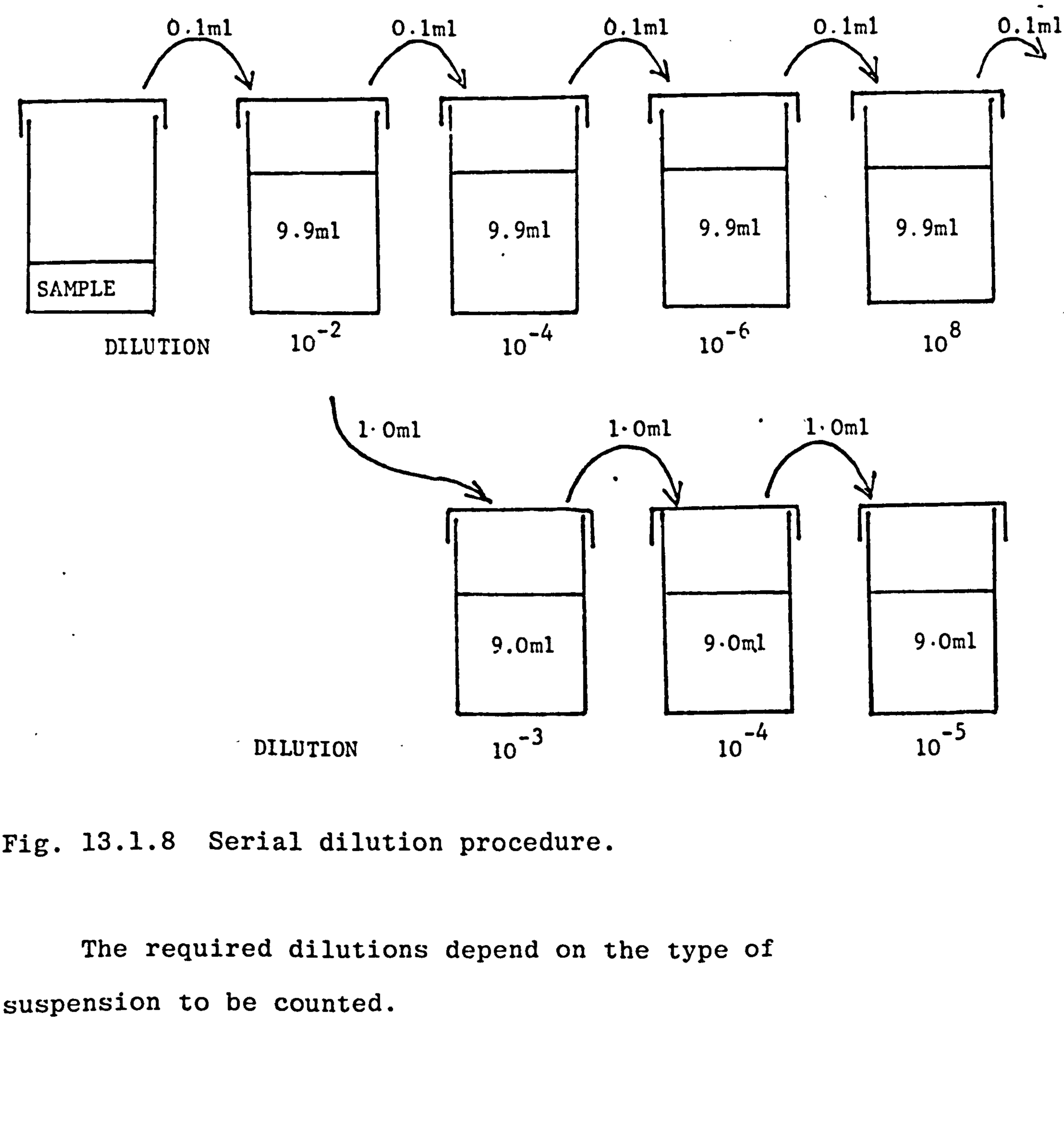

Fig. 13.1.8 Serial dilution procedure.

The required dilutions depend on the type of suspension to be counted.

(b) Plating out of microorganism suspension

This is achieved in the following way:-

(1) Using a sterile pipette, remove the required volume of suspension and transfer it to the surface of the agar plate. Care should be taken not to dig the end of the pipette into the plate. Replace the lid of the plate.

(2) Flame the glass spreader by dipping in the methylated spirit and passing it through a bunsen flame. Care should be taken not to set the container of spirit on fire; keep the lid on the container. Allow it to cool (10-15 secs).

(3) Gently, spread the sample on the surface of the agar, moving the spreader backwards and forwards whilst rotating the plate in order to completely cover the plate. Care need to be taken not to plough up the agar in the process. Return the lid to the plate and sterilise the spreader. Incubate the plate at appropriate temperature. The whole processes are shown in Figure 13.1.9.

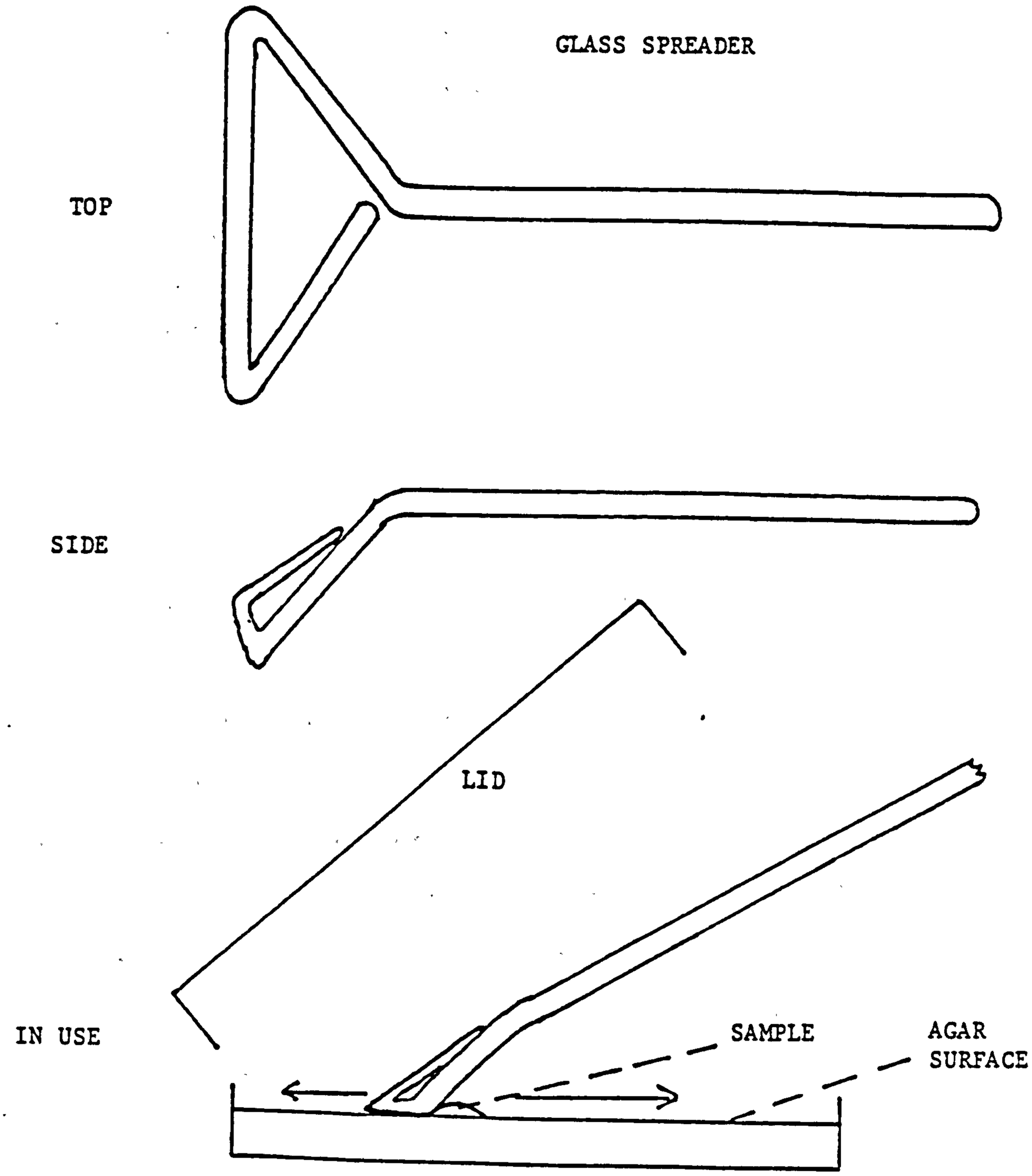

Fig. 13.1.9

An example of viable cell counts:-

Suppose a 0.1 ml sample of the 10^{-3} dilution transferred

on the surface of the agar plate. After spreading and incubating at 30°C for example 100 colonies had been counted. The number of organisms per ml in original culture is then calculated as follows:

$$\text{No. of organisms per ml} = 100 \times 10^3 \times \frac{1}{0.1} = 10^6 \text{ cells/ml}$$

13.1.5 Stock cultures

Although it is possible to purchase cultures of many microorganism it is always useful to have a small collection available for immediate use. Details of the collection should be catalogued in a book with the culture number, source and date of acquisition alongside the name of the species. Stock cultures are usually maintained on agar slopes which are labelled with the name of the species, catalogue number, the medium and date of last transfer. Most species can be kept alive for six to twelve months in a refrigerator on agar slopes media. Therefore, the stock cultures that are used for producing working cultures most be subcultured periodically.

13.1.6 Measuring the size of microorganisms

This is achieved with the aid of graduated reticule eyepiece and stage micrometer. When in position the scale on the reticule is superimposed on the image of the specimen when the observer looks down the microscope. The size,

diameter, length, or width of the specimen is measured in eyepiece units (EPU) . However the actual magnitude of each EPU is unknown and must be determined using a stage micrometer. This is a glass slide on which a scale of known dimensions is etched. A frequently used type has divisions of 0.1 mm (100 μm).

The stage micrometer is placed on to the microscope stage and the scale is found with the same eyepiece and objective used to measure the specimen originally, in our example high power x 40. When the eyepiece scale is superimposed on the scale of the stage micrometer it is seen that 39 EPU equals 1 slide division or 100 μm. Therefore

$$1 \text{ EPU} = \frac{100}{39} = 2.5 \ \mu m$$

The diameter of yeast cell measured 2 EPU long. That is

$$2 \text{ EPU} = 2.5 \times 2 = 5 \ \mu m$$

It is advisable to keep a note of the calculations as to save time on future occasions.

13.1.7 Equipments required for microbiological measurements

(a) Incubators:- are needed to grow cultures at known temperatures. Ideally several should be available to provide a range of temperatures for some investigations.

(b) Inoculating cabinets:- are highly desirable when any transfer of microorganism is being carried out. They protect the operator from the microorganism he is handling and also minimize contamination of the cultures from air-borne particles. There are two types of cabinets available either air drawn or blown over the culture. However, the author prefers an air drawn cabinet like the one used for the work described in this thesis. This is because air blown could cause some degree of contamination due to its non-sterility. The inoculating cabinet has especial importance when preparing petri dish agar medium. In this case the petri dishes lids can be left half off until the agar has solidified completely, the lids can then be slid over . This technique will prevent vapour condensation on the lids, this tends to happen if they are immediately covered after pouring the agar medium. This has another advantage, if in pouring the agar medium on to the petri dishes bubbles are formed due to pouring quickly so as to avoid contamination. The bubbles can be removed by touch with a transfer loop heated to red heat once before the agar medium solidifies.

(d) Microscopes:- are essential for observing microorganisms. It is useful to have phase - contrast facilities, they are found essential for microbiological studies.

Finally , the microbiological technique described above has fulfilled satisfactory most of the work presented in this thesis.

APPENDIX 13.2 THE PROCEDURE USED TO PREPARE Ag-AgCl ELECTRODE

The Ag-AgCl electrode is a practical electrode that approaches the characteristics of an ideal nonpolarizable electrode and can be easily prepared in the laboratory.

The behaviour of the Ag-AgCl electrode is governed by two chemical reactions. The first involves the oxidation of silver atoms on the electrode surface to silver ions in solution at the interface.

$$Ag \rightleftharpoons Ag^{+} + e^{-} \qquad (13.2.1)$$

The second reaction occurs immediately after the formation of Ag^{+} ions. These combine with Cl^{-} ions already in solution to form the ionic compound AgCl.

$$Ag + Cl^{-} \rightleftharpoons AgCl\downarrow \qquad (13.2.2)$$

AgCl is only very slightly soluble in water, so most of it precipitates out of solution onto the silver electrode and contributes to the silver chloride deposit. The rate of precipitation and of solution of the silver chloride determined by the solubility product (K_s). Under equilibrium conditions the ionic activities of the Ag^{+} and Cl^{-} ions are such that their product is the actual solubility product. Thus

$$a_{Ag^{+}} \times a_{Cl^{-}} = K_s \qquad (13.2.3)$$

The procedure used to prepare an Ag-AgCl electrode is shown in Figure 13.2.1.

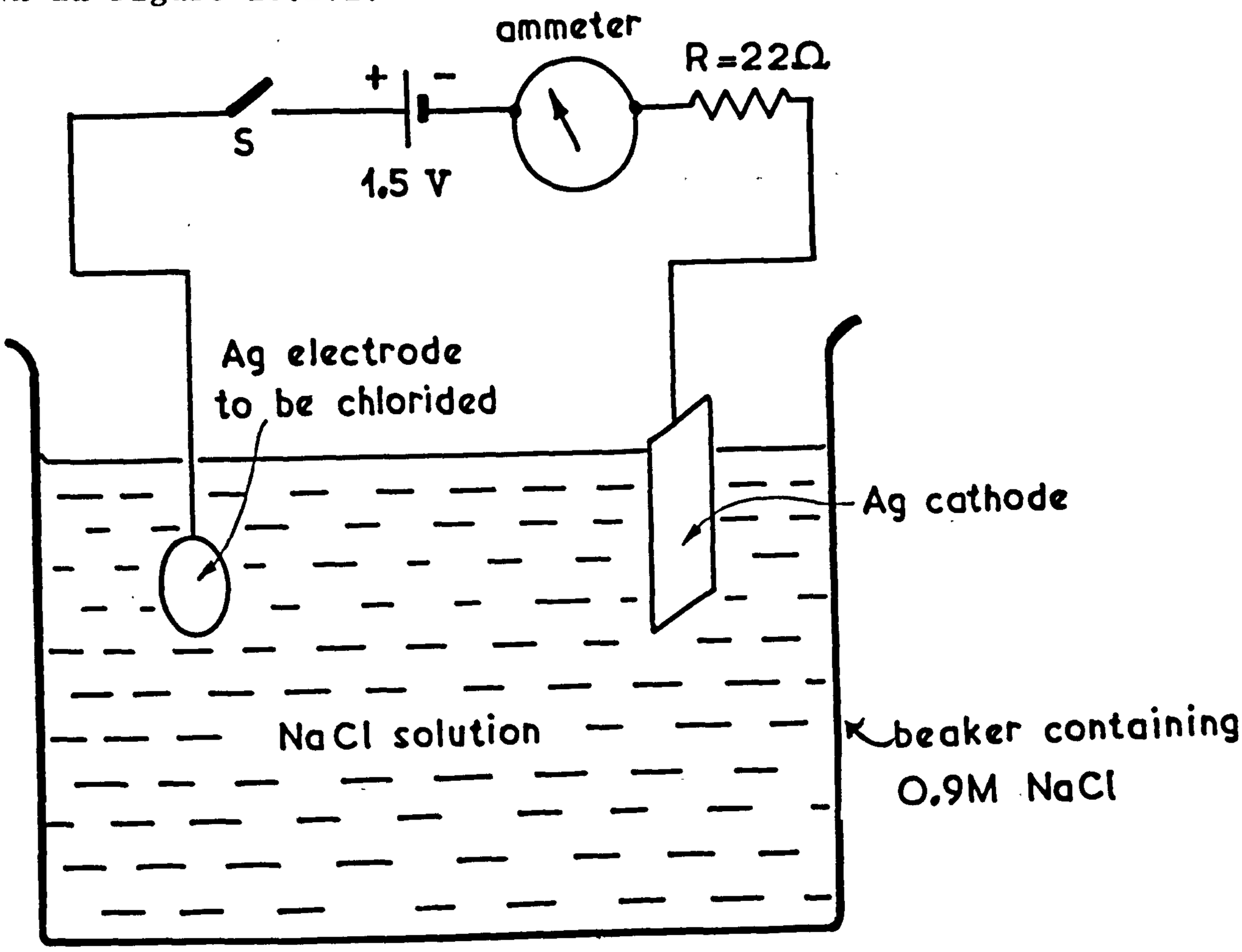

Fig. 13.2.1 Illustrates the electrolytic process for forming Ag-AgCl electrodes.

An electrochemical cell is made up in which the Ag electrode on which the AgCl layer is to be deposited serves as anode and another piece of Ag - having a greater surface area serves as cathode. A 1.5 V battery (or alternatively DC power supply) serves as energy source, and a series resistance limits rate of reaction. A milliammeter can be placed in the circuit to observe the current, which is proportional to the rate of reaction.

When the switch is closed, the reactions of (13.2.1) and (13.2.2) begin to occur and the current jumps to its maximum value. As the thickness of the deposited insulating AgCl layer increases, the rate of reaction decreases and the current drops according to the equation given below (Janz, 1968),

$$I = 100 \text{ mA } e^{\frac{-t}{10}} \qquad (13.2.4)$$

This situation continues, and the current approaches zero asymptotically. Theoretically, the reaction is not complete until the current drops to zero. In practice this never occurs because of other processes going on which also give a conduction current. The reaction can be stopped after a few minutes, once the current has reached a relatively stable low value usually of the order of 10 μA but depending on the type of the electrode under preparation.

APPENDIX 13.3

13.3.1 Preparation of the incubation medium

The bovine eyes were obtained from the Manchester abattoir. The tissue culture medium (199 T.C. 45) was prepared in the following way: a 10 g of the dried preparation was dissolved in 950 ml. of deionised water. A 200 mg of Crystamycin (a mixture of penicilin and streptomycin) was added, and the solution was passed through a 22 μ millipore filter. This was followed by 50 ml. of 1% sodium bicarbonate solution. The prepared medium was then stored at $4^{o}C$ for up to one month. The medium 199 T.C. 45 and composition strength (Croft, 1982) are given in table 3.

13.3.2 Dissection and incubation of the lenses (Carried out by the biochemistry department)

Twelve bovine eyes (six pairs) were collected from the abattoir each week, and stored in the refrigerator until the lenses were removed. The excess fatty material was cut away and the cleaned eyeball was placed in a clean petri dish. After trimming the excess fat, the eyeballs were sterilised by wiping them with a cotton swab which had been dipped in 1% W/V iodine in 75% ethanol. Throughout the disection plastic gloves were worn, and immediately after, the hands were washed. All glassware used in the preparation

TABLE 3

Inorganic salts	Mg/L	Vitamins	Mg/L
NaCl	6800.0	Aneurine hydrochloride	0.01
KCl	400.0	Riboflavine	0.01
$CaCl_2$	200.0	Pyridoxine	0.025
$MgSO_4.7H_2O$	200.0	Pyridoxal hydrochloride	0.025
$NaH_2PO_4.2H_2O$	150.0	Nicotinic acid	0.025
$Fe(NO_3)_3.9H_2O$	0.72	Nicotinamide	0.025
AMINO ACIDS		Calcium Pantothenate	0.01
l-Argenine hydrochloride	70.0	Inositol	0.05
l-Histidine hydrochloride	20.0	p-amino-benzoic acid	0.05
l-Lysine hydrochloride	70.0	Choline Chloride	0.5
dl-Phenylalanine	50.0	Ascorbic acid	0.05
dl-Methionine	30.0	d-biotin	0.01
dl-Serine	50.0	Folic acid	0.01
dl-Threonine	60.0	Menaphthone	0.01
dl-Leucine	120.0	Calciferol	0.01
dl-Isoleucine	40.0	Vitamin A Acetate	0.1
dl-Valine	50.0	α-Tocopherol phosphate	0.01
dl-Glutamic acid	150.0	Nucleic Acid Derivatives	
dl-Aspartic acid	60.0	Adenine hydrochloride	5.1
dl-Alanine	50.0	Guanine hydrochloride	0.3
l-proline	40.0	Xanthin	0.3
l-Hydroxyproline	10.0	Hypoxanthine	0.3
Gycine	50.0	Thymine	0.3
dl-Tryptophan	20.0	Uracil	0.3
l-Tyrosine	40.0	Adnylic acid	0.2
l-Cystine	20.0	Adenosine triphosphate	5.0
l-Cysteine hydrochloride	0.1	Ribose	0.5
Lipid Sources		Deoxyribose	0.5
Cholesterol	0.2	Miscellaneous	
Tween 80	5.0	Sodium acetate (hydrate)	84.0
		Glucose	1000.0
		Phenol red	10.0
		Glutathione	0.05
		l-Glutamine	100.0

of the incubation medium was autoclaved at 125°C and 15 lbs p.s.i. The scissors and forceps used in the dissection, and the culture vessels and glass rods were also sterilised by autoclaving.

For dissection an incision was made about 1 cm behind the cornea, using a sterilised scalpel. Then, using a pair of surgical scissors, a circular cut was made around the eyeball, giving a complete separation of the lens, cornea and iris from the vitreous body and retina. Using the scalpel any vitreous humour adhering to the lens was cut away and the Zonule fibres holding the lens in place were carefully cut. The lens was then lifted out using a glass loop. The aqueous humour which adhered to the lens was removed by carefully rolling the lens on a piece of filter paper. The lens was weighed, after which, it was placed in a culture vessel previously filled with 15 ml. of the incubation medium. The culture vessel was sealed using 'parafilm'. It was important that the lenses were irradiated as soon as they were removed from the eye, so that any changes in Na^+ and K^+ concentrations and weight, between control and irradiated lenses, could be attributed to microwave radiation, and not to incubation prior to irradiation. However, before any investigation into the effects of microwave radiation on the bovine eye lens was made, the effects of incubation on the weight and sodium, potassium concentration were studied first.

13.3.2.1 Measurement of the Na^+ content of the lens

After incubation of 48 hours and weighing, the lens was placed in a polythene centrifuge tube, and a 10 ml of 10% W/V trichloracetic acid was added. Using a glass rod the lens was ground up in the acid, and left for one hour. The protein precipitate was centrifuged down for 15 minutes at 10,000 r.p.m., using MSE 18 centrifuge. The supernatant was transferred to 50 ml graduated flask and made up to the tare mark with 10% W/V trichloracetic acid. The sodium content of the lens was then determined by flame photometry connected to a galvanometer.

Before determining the Na^+ content, a calibration graph was prepared. A series of standard solutions were prepared using "Analar" sodium chloride. NaCl (12.6 mg) was dissolved in 10% TCA (250 ml) to give solution 1. 25 ml of solution 1 was made up to 50 ml with 10% TCA to give solution 2. 25 ml of solution 2 was made up to 50 ml with 10% TCA to give solution 3. 25 ml of solution 3 was made up to 50 ml with 10% TCA to give solution 4.

The reading on the flame photometer was adjusted to give a deflection of 25 for solution 1. 10% TCA was used to give zero deflection on the galvanometer.

The four solutions had the following Na^+ concentrations, and gave the following readings on the galvanometer.

Solutions	$mgNa^+$/50 ml	Galvanometer reading
Solution 1	1.000	25
Solution 2	0.500	13
Solution 3	0.250	7
Solution 4	0.125	3

A graph was plotted of sodium concentration against galvanometer reading on the flame photometer Figure 13.3.1. This allowed the sodium content of the lenses to be determined, by reading from the calibration graph.

13.3.2.2 Measurement of the K^+ content of the lens

The same solutions were used as for the determination of their Na^+ content. The flame photometer was calibrated for potassium, using the potassium filter on the instrument. A series of standard solutions were prepared using "Analar" potassium chloride. KCl (47.75 mg) was dissolved in 10% W/V TCA (250 ml) to give solution 1. 25 ml of solution 1 was made up to 50 ml with 10% TCA to give solution 2. 25 ml of solution 2 was made up to 50 ml with 10% TCA to give solution 4. The reading of the flame photometer was adjusted to give a deflection of 50 for solution 1. 10% TCA was used to give zero deflection on the galvanometer.

The four solutions had the following K^+ concentrations, and gave the following readings on the galvanometer:

Solutions	mg K^+/50 ml	Galvanometer reading
Solution 1	5.0	50
Solution 2	2.5	24
Solution 3	1.25	12
Solution 4	0.625	6

Fl 13.3.1

Calibration curve for Sodium.

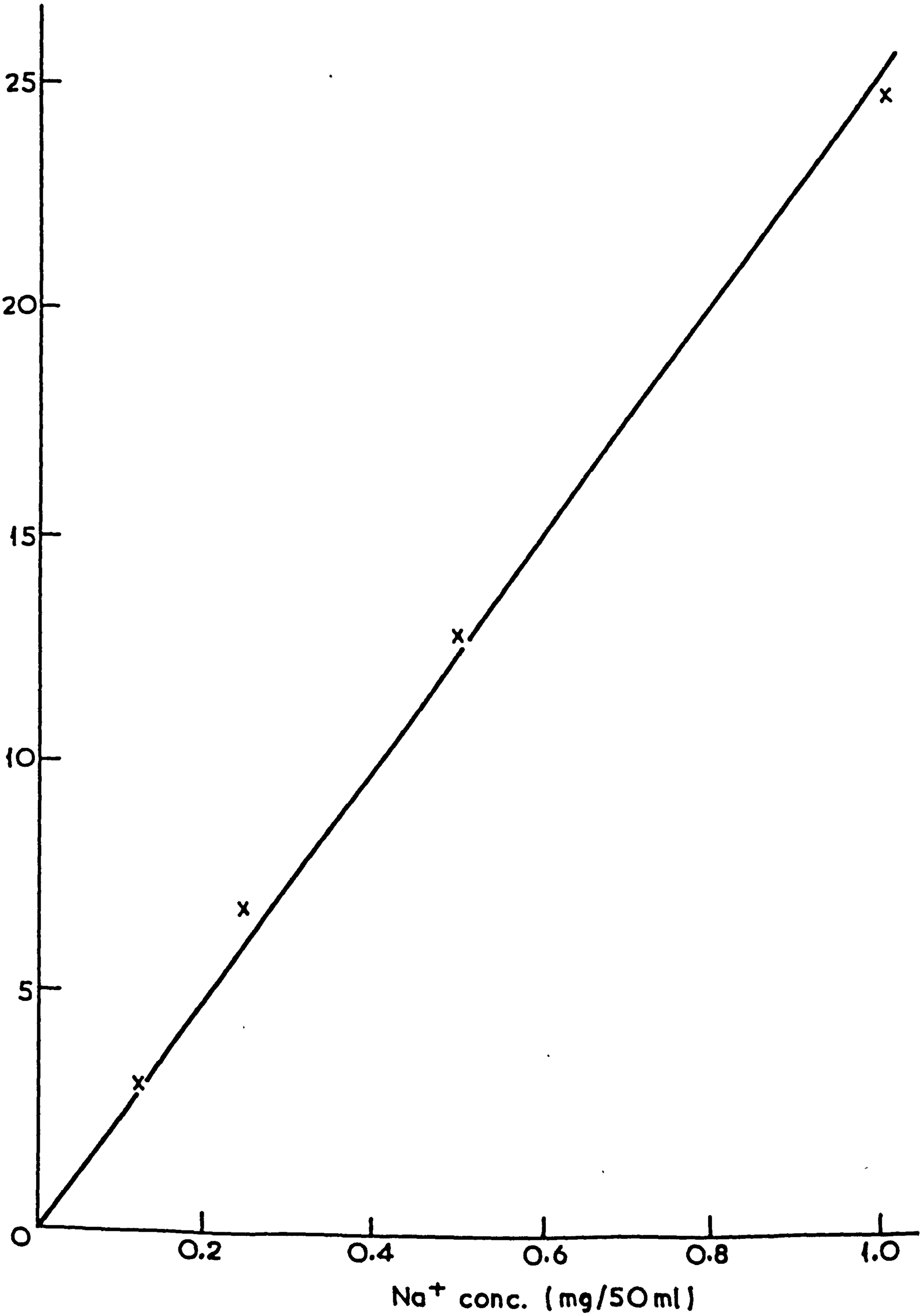

FI: 13.3.1 Continued

Calibration curve for Sodium.

(extrapolated to include higher galvanometer readings)

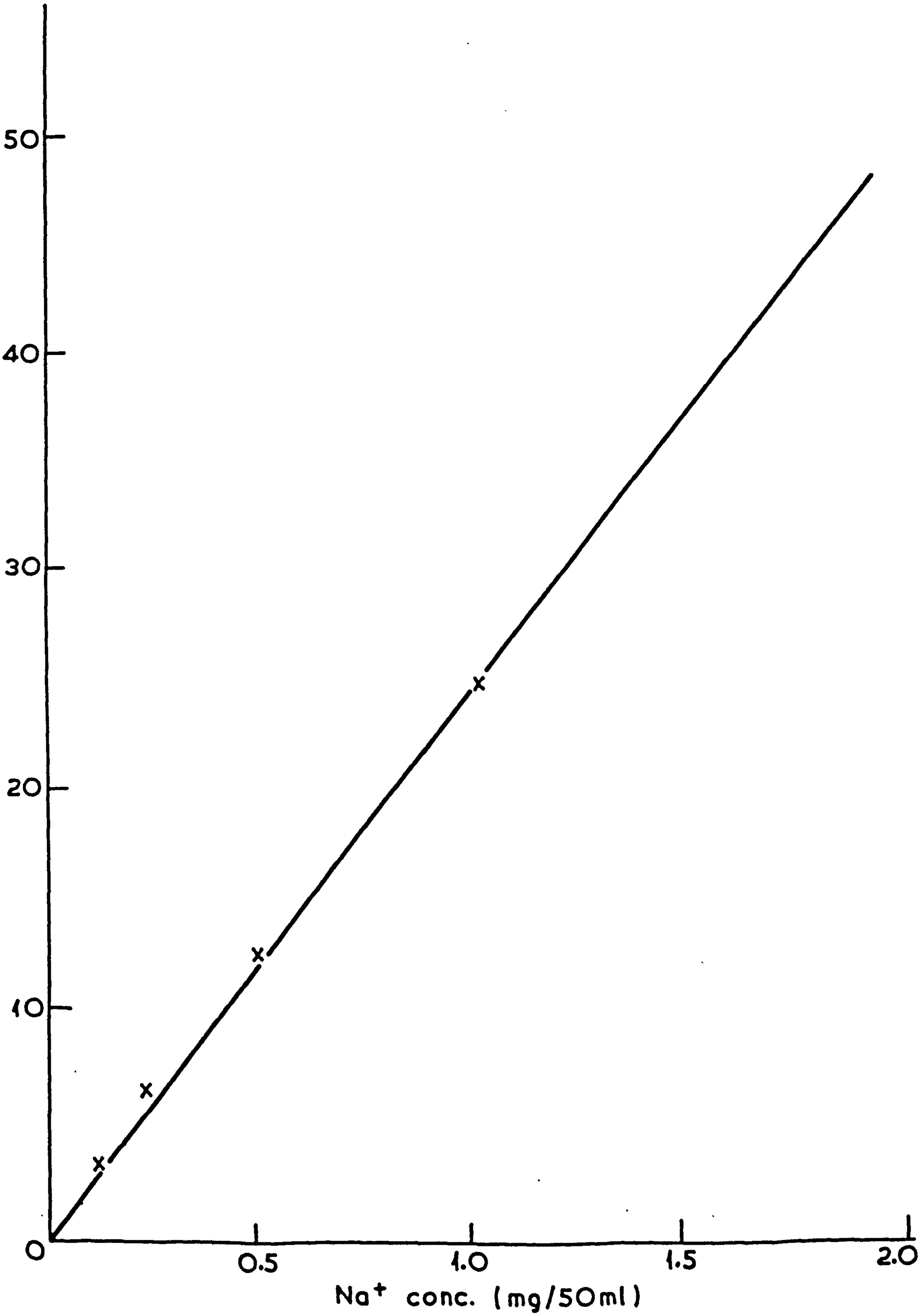

A graph was plotted from potassium concentration against the galvanometer reading on the flame photometer Figure 13.3.2. This allowed the potassium content of the lenses to be determined by reading from the calibration graph.

An example of calculation of Na^+ and K^+ concentration:

After O hours of incubation galvanometer reading for Na^+ = 7. From the calibration curve for $[Na^+]$ this is equal to O.2733 $mgNa^+$/50 ml solution. The weight of the wet lens = 2.O131 g. Therefore:

$$[Na^+] \text{ in mg/g wet lens} = \frac{O.2733}{2.O131} = O.316 \text{ mg/g}$$

wet lens.

PI 13.3.2

Calibration curve for Potassium.

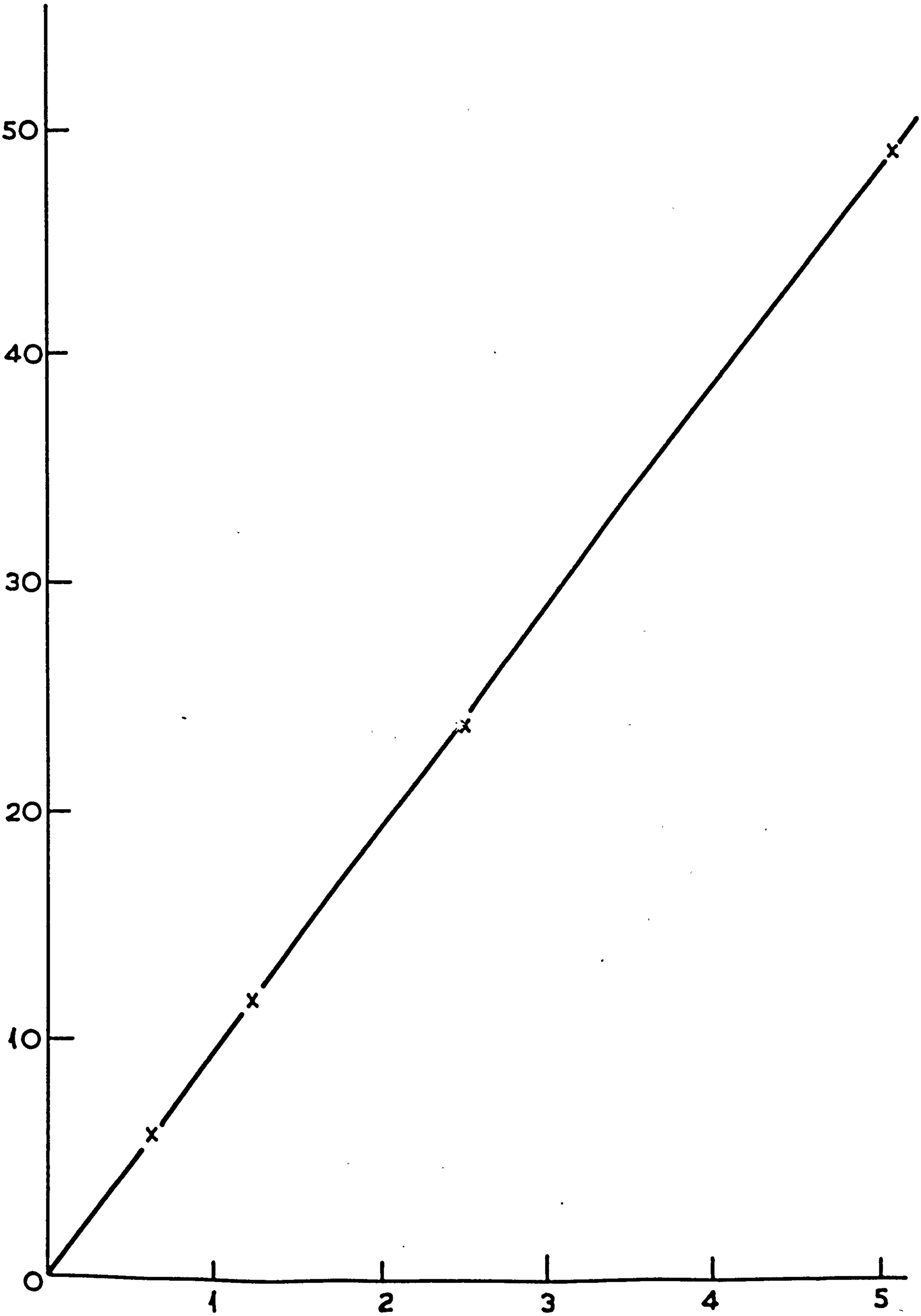

References

A Abragam, A., "The Principles of Nuclear Magnetism", Oxford: University Press (1961)

Alfidi, R.J., Radiology, 143, 82-175 (1982)

Amoore, J.E., Biochem.J. 72, 126-133 (1959)

Ahmed, N.A.G., Calderwood J.H, Fröhlich. H, Smith C.W., Phys. Lett. 53 A (2), 129-130 (1975).

Ahmed, N.A.G., Calderwood J.H, Fröhlich, H, Smith, C.W., Coll. Phen. 2, 155-166 (1976).

Ahmed, N.A.G., Smith C.W., Coll. Phen. 3, 25-33 (1978).

B Bangham, A.D., Ann. Rev. of Biochem. 4, 753-776 (1972)

Batholomew, J.W. and Mittwer, T., J. Bacteriol., 65, 272 (1953).

Baker, F.J., "Handbook of Bacteriological Technique", London, Butterworths (1962).

Brown, J.B., J. Mar. Biol. Assoc. UK 41 (1961)

Buchanan, T.J., Brit. J. Appl. Phys. 6, 64 (1952)

Bronner, F and Kleinzeller, A., (Eds) "Current Topics in Membranes and Transport", New York: Academic Press (1970)

Berliner, L.J., "Biological Magnetic Resonance". Vol. 1 (1978), Vol. 2 (1980) Vol. 3 (1981), London Plenum.

Baker, R.R., Science, 210, 555-557 (1980).

Buchachenko, A.L., "Chemical Polarization of Nuclei and Electrons", Moscow-Nauka, (1974).

Budinger, T.F., IEEE Trans. Nucl. Sci. NS 29, (5) 2821. (1979)

Brauner, L. and Diemer R., Planta 81 (2), 113 (1968).

Barmothy, M.F., Biological effects of magnetic fields. Vol. 1 (1964), Vol. 2 (1969), London Plenum.

Blakemore, R.P., Sci. 190, 377-379 (1975).

Bookman, M.A., Nature 267, 340-342 (1977).

Bloch, F., Phys. Rev. Lett, 21, 1241-1243 (1968).

C

Cole, K.S. and Cole R.H., J. Chem. Phys. 9, 341 (1941).

Cope, F.W., Microwave Power 11, 267-270 (1976)

Cope, F.W., Physiol. Chem. Phys. 5, 173-176 (1973).

Cope, F.W., Physiol. Chem. Phys. 3, 403-410 (1971).

Cleary, S.F., Health Phys. 25, 387-404 (1973).

Cohen, D., Physics Today 28, 34 (1975b).

Commoner, B., Proc. Nat. Acad. Sci. USA, 42, 710-8 (1956).

D

Davson,H., 'The Physiology of the Eye'. London, Churchill Livingstone (1972).

Dubrov, A.P., "Geomagnetic Field and Life", Plenum Press (1978).

Davidson, D.W. and Cole R.H., J. Chem. Phys. 18, 1417 (1950).

Dixey, R and Rein G., Nature 296, 253-256 (1982).

Debye, P., "Polar Molecules" (New York: The Chemical Catalogue Co.,) and Dover, New York (1947)

De Certaines, J., J. Nucl. Med. 23, 48-51 (1982).

Dubrov, A.P., Akad.Nauk, SSR 187(6), 1429 (1969)

Danielli, H., Regulatory Functions of Biological Membranes, London Elsevier (1968)

Duke-Elder, W.S., Ophthalmology, Henry Kimpton, London (1954).

E

Einstein, A., Phys. Z. 18, 121-128 (1917).

Ehrenberg, B., "Magnetic Resonance in Biological Systems", New York, Perganon (1967)

F

Fox, C.F. and Keith A. (Eds.). "Membrane Molecular Biology", Stamford: Sinauer (1972).

Falk, M. Hartman, K.A., Lord R.C., Am. Chem. Soc. 85, 387-391 (1963).

Feher, G., Phys.Rev. 103, 500-501 (1956)

Fröhlich, H., Nature 228, 1093 (1970).

Fröhlich, H., Coll. Phen. 1, 101-109 (1973).

Fröhlich, H., Phys. Lett. 51A, 21 (1975)

Fröhlich, H., "Makroskopishe Quanten Effectecte in Physik und Biologie. In.75.Jahre Quantentheorie". Akademieverlag-Berlin (1977).

Fröhlich, H., Advances in Electronics and Electron Phys. 53, 85-152 (1980).

Friedman, H. and Becker R.O., Nature 200, 626-630 (1963).

Friedman, H., and Becker R.O., Nat. 205, 1050-52 (1965).

Friedman, H and Becker R.O., Nature 213, 949-950 (1967)

G

Gould, J.L., Am. Sci. 68, 256-267 (1980).

Grant, E.H., Ann.N.Y. Acad. Sci. 125, Art. 2, 418 (1965a)

Guy, A.W., I.E.E.E. Trans. MTT 33, 492-498 (1975).

Gerencser, V., Nature, 10, 539-541 (1962).

H

Hasted, J.B., "Aqueous dielectrics", (ed) A.D. Buckingham, London Chapman and Hall (1973).

Holden, A., Bonds between atoms, Oxford:University Press (1971).

Hays, J.D. and Opdyke N.D., Science 158 3804, 1001-1011 (1967).

Hodgkin, A.L. and Huxley A.F., J. Physiol. 117, 501 (1952).

Harrop, P.J., "Dielectrics". London Butterworths (1971)

I

Ingram, D.J.E., "Free Radicals as Studied by Electron Spin Resonance", London Butterworths (1958)

Ingram, D.J.E., "Spectroscopy at Radio and Microwave Frequencies", London Butterworths (1967)

J

Jafary-Asl, A.H., Solanki, S., Aarholt, E. and Smith, C.W., J. Biol. Phys. 11, 15-22 (1983).

Jafary-Asl A.H., and Smith, C.W., Biological Dielectrics in Electric and Magnetic Fields (in press) (1983).

Jafary-Asl, A.H., Solanki, S., Aarholt E., and Smith, C.W., Dielectrics Society 1982 meeting, Pembroke College, Cambridge.

Jafary-Asl, A.H., Solanki, S., and Smith, C.W., Gordon Conference on Dielectric Phenomena 1982.

Johnson, B.D., Phys. Lett. 1, 251 (1962)

Josephson, B.D., Rev. Mod. Phys. 36, 216 (1964)

Josephson, B.D., Advan. Phys. 14, 419 (1965)

Johnson, C.C.and Guy, A.W., Proc. IEE 60,692 (1972)

Janz, G.J.and Ives, D.J.G., Ann N.Y. Acad. Sci. 148, 210-221 (1968).

K

Korn, E.D., Ann.Rev.Biochem. 38, 263-288 (1970)

Kittle, C., Introduction to Solid State Physics,
London, Wiley (1976).

Kip, S., "Electromagnetism" London McGraw-Hill (1963)

Kogan, A.B., Electrophysiology, Moscow Shkola
Vysshaya (1969).

Krylov, A.V., Akad. Nauk SSSR, Ser.Biol.No. 2, 221 (1961)

Kramer, P., Ann. NY Acad.Sci. 247, 155-65 (1975)

Kramer, P., J. Microwave Power 13, 239-49 (1978).

Keilmann, F., Grundler, W., and Fröhlich H.,
Phys. Lett. 62A, 463-466 (1977).

Kholodov, Y.A., Influence of magnetic fields on biological
objects. NTIS-JPRS 63038 (1974).

Koshland, D.E., Nect K.E., Ann.Rev.Biochem. 37, 359 (1968)

L

Lockwood, A.P.M., The membrane of animal cells,
London:Arnold (1971).

Lindegren, C.C., Symp.Soc.Expt.Biol. 6, 277 (1952).

Ling, C.N., "A physical theory of the living state",
Waltham, Blaisdell (1962).

Lipinski, B., Electronic Conduction Mechanoelectrical
Transduction in Biological Materials, Dekker (1982).

Lee, E.W., Magnetism, London Penguin (1963).

Lauterbur, P.C., Nature 242, 190 (1973).

Ladik, J ., et al., Phys. Rev., 188, 710 (1969).

Lavine, L.S., Science 175, 1118 (1972)

Liboff, R.L., Biophs. J. 5, 845-853 (1965).

Lindauer, M. and Martin H., J.Comp. Physiol.
122, 145-187 (1977).

Lovsund, P., Med. Biol. Eng. and Comp. 18, 758-764 (1980).

M

Mascarenhas, S., J. Electrostatics, 1, 141 (1975).

Marton, J.P., Phys.Chem. and Physic, 5, 259 (1973).

Mulay I.L. and Mulay, L.N., "Biological Effects of
Magnetic Fields". Vol. 1, Editor, M.F. Barnothy,
Plenum Press, New York (1964).

Michaelis, L., Fundamentals of Oxidation and Reduction.
In: Currents in Biochemical Research, ed. D.E. Green,
New York, Interscience Publishers (1946)

Mallard J.R. and Kent M., Nature (Lond), 204, 1192 (1966).

McAffee R.D., Biological Effects of Microwave Radiation,
Vol. 1, 25, Peyton, M.F. (Ed.), Plenum Press
New York (1961).

Magnusson, C.E., Am.J. Physiol, 29, 124-136 (1911).

Malinin G.I., Science 194, 844-846 (1976).

Maret G., Phys.Rev.Lett. 35, 397 (1975).

Marino A.A., Becker, R.O., Perry, F.S., and Reichmanis,M.,
Health Physics, 41, 267-277 (1981).

Moor, F.R., Science 196.1, 682-684 (1977).

Moor, R.L., Can. J. Microbiol. 25, 1145-1151 (1979).

Mulay I.L. and Mulay L.N., Nature 10, 1019 (1961).

N

Neumann, E., and Katchalsky A., Proc.Nat.Acad. Sci. USA, 69, 993 (1972).

New Scientist, 569, 18 June , 1970.

Negenkang, W., Physiol.Chem. and Physics, 2, 15-23 (1970).

O

Oatey, C., "Electric and Magnetic Fields", Cambridge: University Press (1976).

p Pethig, R., "Electronic and Power", 18 Oct p. 446 (1973)

Pethig, R., "Dielectric and Electronic Properties of Biological Materials". London, Wiley (1979)

Pethig, R., "Electronic Conduction in Biopolymers", (Ed.) B. Lipinski, Dekker (1982).

Pethig, R., Int. J. Quantum, 5?, 159-171 (1978).

Pethig, R. J.Mol.Biol. 141, 323 (1980)

Pethig, R., Int.J.Quantum, 22, 537 (1982).

Pethig, R. Phys.Med.Biol. 28, 31 (1983)

Pohl, H.A., and Pethig, R., J. Phys. E. 10, 190-193, (1977).

Pohl, H.A., J.Appl.Phys., 22, 869 (1951).

Pohl, H.A., J. Appl. Phys., 29, 1182 (1958).

Pohl, H.A., and Schwan , J.P., J.Appl.Phys., 30, 69 (1959).

Pohl, H.A. and Polymale C.E., J.Electrochem.Soc., 107, 383-390 (1960).

Pohl, H.A., and Crane J.S., J.Theor.Biol. 37, 15-41 (1972)

Pohl, H.A., Ann. N.Y. Acad.Sci. 238, 176-185 (1974)

Pohl, H.A., Conf. On "Organic and Biological Semoconductors". University of Nottingham, England, 23-25 September (1980).

Pohl, H.A., Int.J.Quant.Chem., Quant.Biol.Sympos. 1, 411-431 (1981).

Petrov, E.G., Int.J.Quant.Chem., 16, 133 (1979).

Purchell, E.M., Phys.Rev. 69, 681 (1946).

Piccardi, G., "Solar activity and Chemical Tests", Moscow, Neuka P. 141 (1971).

Pilla, A.A., Ann. N.Y. Acad.Sci., 238, 249 (1974).

Pressman, A.S., "Electromagnetic Fields and Life", Plenum Press (1970).

R

Rubin, L.F. and Barnett, K.C., Ann.N.Y.Acad.Sci., 141, 333-345 (1967).

Rothfield, L.I., "Structure and Function of Biological Membranes", London:Academic (1971)

Robinson, J.R. and Skou, H., Symp.Soc.Exp.Biol. 19, 237 (1965).

Rose, A.H., "Chemical Microbiology" (3rd ED.), London, Butterworths (1976).

Coelho, R., "Physics of Dielectrics", Elsevier (1979)

Rose, L.F. and Mattis, P.A., Science 153, 83-84 (1966).

Richardson, A.W., Arch.Phys.Med. 29, 765-769 (1948)

Rudden, C.N.R., and Wilson, J., A simplified approach to Solid State Physics, London, Butterworths (1971)

S

Smith, C.W., Coll.Phen. 3, 67-72 (1980).

Smith, C.W., J.Med.Eng and Tech., 6, 250-251 (1982).

Smith, C.W., Health Phys., 441 (1982)

Shaya, S.Y. and Smith, C.W., Coll.Phen. 2, 215 (1977)

Salhaney, J.M., Natl.Acad.Sci. USA, 72, 4966 (1975)

Samoilova, O.P., Biofizika 6, No. 1, 15-19 (1961)

Schwan, H.P., Adv.Biol.Med.Phys. 34, 147 (1957)

Shulman, R.G., Scien.Am. 248 Numb.1, 76-84 (1983).

Semm, Petal, Nature, 288, 607-608 (1980)

Szent-Györgyi, A., Nature 148, 157 (1941);

Science, 93, 609 (1941).

Sheppard, R., and Eisenbud, M., "Biological Effects of Electric and Magnetic Fields of Extremely Low Frequency , Univ. Press (1977).

T

Tulloch, D.S., "Physical Fundamentals of Materials Science, London Butterworths (1971).

Turby, F.K. and Goldzieher, J.W., Nature, London 182 (2), 1371 (1958).

Travkin, M.P., "Effect of Weak Magnetic Field on Plant Bioelectric Potentials", p. 76 Moscow (1971)

Ternberg, J.L. and Commoner, B., J.Am.Med.Ass., 183, (42) (1963)

V

Von Hippel, R., Dielectric Materials and Applications, M.I.T. Press (1954).

W

Williams, J.I., Micro-organisms, Mills and Boon Ltd. (1976)

Webster, J.G., Medical Instrumentation Application and Design, Boston Houghton: (1978)

Williams, R.J. and Weiter, Biological Effects of Non-Ionising Radiation 247 166-181 (1975)

Walcott, C. and Green, P.P., Science, 184, 180-182 (1974)

Z

Zaret, M.M., N.Y. State. J.Med. 74, 2032-48 (1974).